CBPF - CENTRO BRASILEIRO DE PESQUISAS FÍSICAS

Asymptotically Safe Unimodular Quantum Gravity

GUSTAVO PAZZINI DE BRITO

RIO DE JANEIRO
2020

GUSTAVO PAZZINI DE BRITO

Asymptotically Safe Unimodular Quantum Gravity

Thesis submitted to the Graduate Program at the Centro Brasileiro de Pesquisas Físicas in partial fulfillment of the requirements for the degree of Doctor in Science (Physics)

Supervisor: Prof. Dr. José Abdalla Helayël-Neto
Co-supervisor: Prof. Dr. Antônio Duarte Pereira Junior

RIO DE JANEIRO
2020

Dedicatória

Com muito pesar, eu não posso deixar de registrar que, no momento em que essa tese foi escrita, centenas de milhares de famílias brasileiras lamentam a perda de seus entes queridos. Um vírus que chegou ao país como uma ameaça, logo aliou-se às práticas fascistas daqueles que (des)governam esse país para tornar-se uma arma de extermínio contra as parcelas vulneráveis da população. Portanto, como uma tentativa singela de demonstração de solidariedade, eu gostaria de dedicar esse trabalho à todas as vítimas de um período que resulta não apenas de uma crise de saúde, mas, principalmente, de uma das maiores crises civilizatórias que já acometeram esse país.

Acknowledgments

During the time of my Ph.D. I had the support of many people that directly or indirectly contributed to the final form of this thesis. Here, I would like to express my gratitude to them.

First, I would like to thank my supervisor Prof. José Helayël-Neto for his guidance since I arrived at CBPF. His effort to offer high-level courses and to create an excellent collaborative environment among the students in his group had a great impact on me. Prof. Helayël is not only a great professor on scientific matters but also an example of character.

To my second supervisor Prof. Antônio Pereira, who gave me the opportunity to work on asymptotic safety. I am very grateful for his trust on share with me many interesting projects. I hope we can finish all of them and start several new ones! The interaction with Antônio was essential to define many important aspects of my scientific career.

During the time of my Ph.D. I had the opportunity to spend one year at Heidelberg University. I am very grateful to Prof. Astrid Eichhorn for receiving me in her research group. Her ideas on the interplay of gravity and matter in asymptotic safety were one of the main reasons why I decided to focus on this topic. Astrid, thank you for the opportunity to collaborate with you!

To Sebastião Alves Dias (Tião) for many interesting lectures on QFT! My acknowledgments to Tião are not restricted to his classes, but for his friendship during the years of CBPF. To Prof. Antonio Accioly, for his guidance during Master and the early stages of my Ph.D. studies. Also, I would like to thank my dear friend Emil for all the interesting conversations on the most diverse topics and for all the coffee-breaks.

I would like to thank Julio Hoff for his impact on the early stages of my scientific education and for various interesting discussions. I am very grateful to Denis Dalmazi for many interesting discussions on *TDiff* theories and unimodular gravity. I also would like to thank Alessandro for our friendship since I was an undergraduate student.

To my dear friends from Rio. The fellows from *sala Dirac*: Célio, Judismar, Yuri, Gabriel, Philipe, Fábio, Pedro Caneda, Pedro Malta and André (honorary member) for the numerous discussions on physics, politics and all that. Also, I would like to thank Laís, Vahid, Carlos and Anderson for their friendship during all these years. In special, I would like to thank Carlos for his help in my early days with *Mathematica*.

I would like to express my gratitude to Arthur for his collaboration in one of the projects related to this thesis. Also, I am indebted with Arthur and Rafael for proof-reading parts of this thesis.

To the members of my Ph.D. committee, I would like to acknowledge the careful reading of this material. In particular, I would like to thanks Gabriel Menezes and Denis Dalmazi for the various suggestions for the improvement of this thesis.

To the amazing quantum gravity group from Heidelberg: Aaron, Alessia, Arslan, Fleur, Johannes, Johanna, Marc, Martin, Masatoshi, Stefan and Tobias. In special, I would like to thank Marc for his valuable lessons on *Mathematica*, which was essential to the conclusion of this thesis.

I would like to thank my family for all their support. To my father, for all his love, friendship and unconditional support. To my mother, for her effort to be present in my life despite the physical distance. To my second parents: Neusa and Carlos (*in memorian*).

To my lovely wife, Fernanda, for being this amazing partner in my life! Her kindness and support were essential in many stressful moments during the development of this thesis. Thank you for making everything better!

I would like to thanks CNPq and CAPES for financial support during my Ph.D. To all the people involved in the maintenance of the public institutions for research and education in Brazil, which are essential for our development.

List of Publications

The following papers are associated with the content of this thesis:

- *"A link that matters: towards phenomenological tests of unimodular asymptotic safety"*,
  G.P. de Brito, A. Eichhorn and A.D. Pereira,
  JHEP **09** (2019) 100.

- *"Unimodular quantum gravity: Steps beyond perturbation theory"*,
  G.P. de Brito and A.D. Pereira,
  JHEP **09** (2020) 196.

- *"Asymptotic safety of unimodular $f(R, R_{\mu\nu}^2)$-gravity-matter systems"*,
  G.P. de Brito, A.D. Pereira and A.F. Vieira,
  arXiv: 2012.08904 [hep-th].

Publications on asymptotic safety that are not covered in this thesis:

- *"On the impact of Majorana masses in gravity-matter systems"*,
  G.P. de Brito, Y. Hamada, A.D. Pereira and M. Yamada,
  JHEP **08** (2019) 142.

- *"Asymptotic safety and field parametrization dependence in the f(R) truncation"*,
  G.P. de Brito, N. Ohta, A.D. Pereira, A. Tomaz and M. Yamada,
  Phys. Rev. D **98** (2018) 026027.

During the period of my Ph.D. I had the opportunity to work on parallel projects involving other topics, resulting in the following publications:

- "Quantum corrected gravitational potential beyond monopole-monopole interactions",
  G.P. de Brito, M.G. Campos, L.P.R. Ospedal and K.P.B. Veiga,
  Phys. Rev. D **98** (2020) 084015.

- *"Mass dimension one fermions at 1-loop"*,
  G.P. de Brito, J.M. Hoff da Silva and V. Nikoofard,
  Accepted for publication at European Physical Journal - Special Topics – arXiv: 1912.02912 [hep-th].

- *"Interesting features of a general class of higher-derivative theories of quantum gravity"*,
  A. Accioly, J. de Almeida, G.P. de Brito and W. Herdy
  Phys. Rev. D **98** (2018) 064029.

- *"Spin- and velocity-dependent nonrelativistic potentials in modified electrodynamics"*,
  G.P. de Brito, P.C. Malta and L.P.R. Ospedal,
  Phys. Rev. D **95** (2017) 016006.

- *"Renormalizability in D-dimensional higher-order gravity"*,
  A. Accioly, J. de Almeida, G.P. de Brito and G. Correia,
  Phys. Rev. D **95** (2017) 084007.

- *"Effective models of quantum gravity induced by planck scale modifications in the covariant quantum algebra"*,
  G.P. de Brito, P.I.C. Caneda, Y.M.P. Gomes, J. Guaitolini Junior and V. Nikoofard, *Adv. in High Energy Phys.* **2017** (2017) 1.

- *"Relating renormalizability of D-dimensional higher-order electromagnetic and gravitational models to the classical potential at the origin"*,
  A. Accioly, G. Correia, G.P. de Brito, J. de Almeida and W. Herdy,
  Mod. Phys. Lett A. **32** (2017) 1750048.

Abstract

In this thesis we investigate the asymptotic safety approach for quantum gravity. This approach relies on the possibility of a UV completion induced by means of fixed points in the renormalization group flow. In its standard version, asymptotically safe quantum gravity is constructed as a quantum theory for general relativity. In the present thesis we consider a different scenario, where the underlying classical theory corresponds to unimodular gravity, which is defined by a restriction on the determinant of the space-time metric. Under the appropriated assumptions, unimodular gravity and general relativity give rise to equivalent classical dynamics, however, the (in)equivalence at the quantum level remains unsettled. Using functional renormalization group techniques, we provide new results concerning the fixed point structure in the unimodular setting. Also, we discuss the impact of regulator induced contributions on the renormalization group flow obtained within the unimodular theory space. Based on the analysis of n-point connected correlation function, we provide strong arguments in favor of the equivalence between unimodular gravity and unimodular gauge, which is a particular gauge choice in the quantization of general relativity. Finally, by exploring the interplay between gravity and matter systems, we discuss the possibility of imposing phenomenologically motivated constraints in the unimodular theory space. Our results indicate that, due to the absence of the cosmological constant, the unimodular setting leads to more severe constraints in comparison the standard formulation of asymptotically safe quantum gravity.

Keywords: Quantum Gravity; Asymptotic Safety; Functional Renormalization Group; Unimodular Gravity; UV Fixed Points.

Resumo

Nesse trabalho investigamos o cenário de segurança assintótica para gravidade quântica. Essa abordagem está baseada na possibilidade de completude no regime UV por meio de pontos fixos no fluxo do grupo de renormalização. Na sua versão padrão, o cenário de gravidade quântica assintoticamente segura é construído a partir da quantização da relatividade geral. Nessa tese, consideramos uma versão alternativa com ponto de partida correspondente a uma teoria unimodular de gravitação, a qual é definida a partir de uma restrição sobre o determinante da métrica espaço-temporal. Partindo de hipóteses apropriadas, pode-se mostrar que gravidade unimodular e a relatividade geral descrevem classicamente a mesma física. No entanto, a (in)equivalência quântica entre as duas teorias permanece como uma questão em aberto. Utilizando métodos do grupo de renormalização funcional, apresentamos novos resultados em relação à estrutura de pontos fixos no cenário unimodular. Além disso, discutimos o impacto de contribuições induzidas por um efeito de regulador sobre o fluxo do grupo de renormalização na teoria unimodular. Com base em uma análise sobre de funções de correlação, apresentamos argumentos fortes em favor da equivalência entre gravitação unimodular e calibre unimodular, que corresponde a uma escolha de fixação de calibre na quantização da relatividade geral. Por fim, explorando a relação entre gravitação e setores de matéria, discutimos a possibilidade de se estabelecer vínculos fenomenológicos sobre o "espaço das teorias" unimodular. Os resultados apresentados aqui indicam que, devido a ausência da constante cosmológicas, o cenário unimodular produz vínculos mais severos em comparação com a formulação padrão de gravidade quântica assintóticamente segura.

Palavras-Chave: Gravidade Quântica; Segurança Assintótica; Grupo de Renormalização Funcional; Gravidade Unimodular; Pontos Fixos UV.

Notations and Conventions

List of abbreviations:

AS	Asymptotic Safety
ASQG	Asymptotically Safe Quantum Gravity
EAA	Effective Average Action
EFT	Effective field theory
EH	Einstein-Hilbert
FP	Fixed Points
FRG	Functional Renormalization Group
GR	General Relativity
IR	Infrared
QCD	Quantum chromodynamics
QFT	Quantum Field Theory
QG	Quantum Gravity
QGR	Quantum General Relativity
UQG	Unimodular Quantum Gravity
RG	Renormalization Group
SM	Standard Model
UG	Unimodular Gravity
UV	Ultraviolet
1PI	One-Particle Irreducible

List of symbols:

$g_{\mu\nu}$	Space-time metric
$\eta_{\mu\nu}$	Minkowski metric
$\delta_{\mu\nu}$	Euclidean metric
$R_{\mu\nu\alpha\beta}$	Riemann tensor
$R_{\mu\nu}$	Ricci tensor
R	Ricci Scalar
$C_{\mu\nu\alpha\beta}$	Weyl tensor
M_{Pl}	Planck mass
G_{N}	Newton coupling
Λ_{cc}	Cosmological constant
d	Space-time dimension
$h_{\mu\nu}$	Fluctuation field
h^{tr}	Trace of the fluctuation field
$\delta^{\alpha\beta}_{\mu\nu}$	Symmetrical identity
γ^{μ}	Gamma matrices
μ	Physical RG scale
k	FRG cutoff scale

We work with natural units such that $c = \hbar = 1$. In Sect. 1.1 we use Lorentzian conventions with signature $(-,+,+,\cdots)$. In the rest of this thesis we consider Euclidean signature. The Riemann tensor was defined according to $R^{\mu}{}_{\nu\alpha\beta} = \partial_\alpha \Gamma^{\mu}_{\nu\beta} + \Gamma^{\mu}_{\alpha\lambda}\Gamma^{\lambda}_{\nu\beta} - (\alpha \leftrightarrow \beta)$. Geometrical objects with an over-bar ($\bar{R}_{\mu\nu\alpha\beta}$, $\bar{R}_{\mu\nu}$, $\cdots$) are computed in terms of the background metric $\bar{g}_{\mu\nu}$. Once we decompose the full metric $g_{\mu\nu}$ in terms of $\bar{g}_{\mu\nu}$ and $h_{\mu\nu}$, the operations of raising and lowering indices are done with the background metric. For space-time integrals, we use the compact notation $\int_x = \int d^dx$. For the original results presented in this thesis we set our calculations to the four-dimensional case ($d = 4$). In some discussions we kept the dimension parameter d arbitrary. Finally, the symmetrical identity is defined as $\delta^{\alpha\beta}_{\mu\nu} = \frac{1}{2}(\delta^{\alpha}_{\mu}\delta^{\beta}_{\nu} + \delta^{\beta}_{\mu}\delta^{\alpha}_{\nu})$.

Contents

Introduction

According to our current understanding, nature organizes itself in terms of four fundamental interactions: strong, electromagnetic, weak, and gravitational. Quantum field theory (QFT) provides a very successful description of the first three ones. In special, the standard model (SM) of particle physics shows a remarkable, and even surprising, agreement with the experimental data collected in modern accelerators such as the LHC [1]. The SM, on the other hand, do not incorporate gravity, indicating that there is at least one missing piece in the understanding of fundamental interactions.

At the classical level, gravity has a very satisfactory description in terms of the theory of general relativity (GR). According to GR, gravity is nothing but a manifestation of the dynamics of space-time itself. In this setting, free particles move through geodesics in a space-time deformed by matter/energy content. Since its conception, GR was successfully confronted with many experiments [2], including the recent detection of gravitational waves and black-hole shadows [3, 4], providing the notable non-trivial tests of this theory in the strong-field regime. The presence of singularities in the solutions of Einstein's field equations in GR [5], however, indicates that this theory also has its limitations and fails to describe gravity at very small distance scales. This might suggest that quantum fluctuations could play an important role in the understanding of gravity, and the space-time itself, at the fundamental level.

The quest for a complete and consistent theory of quantum gravity remains as one of the major open problems in theoretical physics. In particular, the complete lack of direct experiments probing the quantum nature of gravity makes this task especially challenging [6]. The energy scale where quantum gravitational effects are expected to become important is of the order of the Planck mass ($\sim 10^{19}\,\text{GeV}$), while the current technology allows us to probe physics up to the electroweak scale ($\sim 10^2 - 10^3\,\text{GeV}$). Despite these limitations, in the past few decades, several attempts to quantize gravity were made, starting from multiple different premises and leading to a great variety of approaches [7,8]. Despite all the progress in various directions, none of the alternatives can be considered a full theory for quantum gravity (QG) so far.

Having in mind our experience with the other fundamental interactions, we might expect that QFT methods applied to GR should provide a natural framework for QG. For example, taking into account the "sum over histories" approach in QFT, our goal is to define a "functional integral over space-times" (geometries)[1]. A concrete (but not unique) realization of this task is achieved by a path integral over metric fluctuations around a fixed (non-dynamical) background [11]. This approach, sometimes referred to as covariant QG, defines a QFT where the metric fluctuation field plays the role of mediator of the gravitational interaction, namely, the graviton.

The naive application of the QFT toolbox in the covariant QG approach, however, is not completely satisfactory. In particular, the quantization of GR based in perturbative methods leads to non-renormalizable interactions due to the presence of vertices scaling with two derivatives [12–19]. In this case, the elimination of all possible ultraviolet (UV) divergences requires an infinite number of counter-terms, resulting in a lack of predictivity. A possible way to circumvent the problem of perturbative non-renormalizability is the introduction of higher-derivative (HD) terms in the action. In this case, there is an improved UV behavior of the graviton propagator, making the theory renormalizable at all orders in a perturbative expansion [20]. However, the price to be paid for renormalizability, in the perturbative level, is the appearance of an extra pole in the tree-level graviton propagator with negative residue, indicating unitarity violation[2].

As an alternative, covariant QG can be interpreted as an effective field theory (EFT) [29–31]. The ideas of EFT's have been extensively explored in particle physics and allow us to perform consistent computations, based on standard perturbative methods in QFT, even in the case of non-renormalizable theories [32]. Nevertheless, EFT's exhibit a limited range of validity and, therefore, allow us to answer only those physical questions characterized by energies below a cutoff scale. Theories involving such cutoff scales are said to be UV incomplete. In the case of QG, the cutoff scale is usually identified as the Planck mass. This framework allows us to compute QG contributions to physical processes with a typical energy scale below $\sim 10^{19}$ GeV. One of the most successful examples of the EFT approach to QG is the one-loop correction to the Newtonian potential first reported in the seminal papers by Donoghue [33,34]. Furthermore, during the last three decades, the EFT approach has been used to investigate QG contributions in several scattering processes (see, e.g., [35–37]).

The limitations of the covariant approach to QG built on top of standard perturbative methods suggest that, if we aim at constructing a fundamental theory within a QFT framework, some change of paradigm might be necessary. In the present thesis, we follow a route based on the concept of asymptotic safety (AS) [38, 39]. The basic idea of AS is to define a non-perturbative notion of renormalizability formulated in terms of a non-Gaussian UV fixed points (FPs) in the renormalization group (RG)

[1] Alternatively, we could also consider the canonical quantization of geometrical objects. This approach leads, for example, to the original formulation of loop quantum gravity [9, 10].

[2] For recent proposals to circumvent the unitarity problem in HD theories of QG, see [21–28].

flow [40–42]. In this approach, perturbative renormalizability is no longer considered a guiding principle in the definition of a meaningful QFT.

The notion of AS can be explored in parallel with the well-known concept of asymptotic freedom (AF). The latter one, first discovered in the context of Yang-Mills (YM) theories, describe interactions characterized by couplings that run towards a UV attractive Gaussian FP, i.e., a FP characterized by vanishing couplings. In this case, we say that theory becomes asymptotically free in the high-energy regime. The neighborhood of a Gaussian FP is the ideal regime to apply perturbation theory. In fact, the UV FP in the RG flow of YM theories is the key point for a consistent perturbative treatment of quantum chromodynamics (QCD) in the UV regime [43–45].

AS generalizes the concept of AF to the non-perturbative regime. An asymptotically safe theory is characterized by couplings running according to an RG trajectory ending in a non-Gaussian FP in the UV [42]. In this case, the theory remains interacting at the FP and UV completion is achieved by scale invariance in the high-energy regime. In order to ensure predictivity, we further demand a finite-dimensional critical surface associated to the UV FP. As a consequence, only a finite number of free parameters are necessary to parameterize UV complete trajectories. Furthermore, it is interesting to emphasize that any fundamental QFT has to admit a characterization in terms of asymptotically safe (or asymptotically free) RG trajectories.

The asymptotically safe quantum gravity (ASQG) approach puts together the concepts above discussed as a promising attempt to define a consistent, and UV complete, QFT describing the gravitational interaction. The existence of a non-Gaussian UV FP for gravity was first conjectured in a seminal work by Weinberg [42]. The earlier attempts to probe this conjecture was based on calculations done in $2 + \epsilon$ space-time dimensions [46–49], pointing towards the existence of a non-Gaussian FP for the gravitational interaction. Nevertheless, it is not clear if these results can be analytic continued to four dimensions. As a consequence, this research area was left aside until the development of more sophisticated techniques.

The current research on ASQG has been mostly done in terms of the functional renormalization group (FRG) techniques [50]. In general lines, the FRG provides an implementation of the Wilsonian picture of integrating field configurations in a "step-by-step way" [51] (see [52] for a recent review). It is achieved by the introduction of an infrared (IR) cutoff scale that suppresses the field configurations characterized by low-momentum. The central object in the FRG formulation is the effective average action (EAA) defined as a scale-dependent functional that interpolates between the bare action and the usual effective action (1PI generating functional) from quantum field theory. The most attractive feature of the FRG lies on the fact that the EAA satisfies an exact flow equation, the Wetterich equation [51]. Even though the use of approximations is necessary to extract quantitative information from the Wetterich equation, the FRG still provides an alternative framework to perform systematic QFT calculations beyond the usual perturbative methods.

Since the seminal paper by Reuter [50], the FRG has been systematically applied to the study and characterization of the RG flow in QG. Within a first approximation, a truncated EAA with the same functional form of the Einstein-Hilbert (EH) action has been used as an approximated solution for the Wetterich equation. This strategy allows for the computation of beta function for the Newton coupling and the cosmological constant. The resulting flow equation provides the first indication for a UV attractive fixed point in a legitimate four-dimensional setting. In the last two decades, a great number of investigations were done based within the FRG approach, and, by now, there are several indications pointing towards the consistency of the ASQG framework [53–94] (for recent reviews, see [38, 39, 52, 95]).

The RG approaches to QG, such as ASQG, not only provide a possible UV complete scenario within the QFT framework but also give a perspective on how to connect quantum aspects of gravity with low-energy phenomena accessible with current experimental technologies [96]. The RG works as a theoretical microscope that allows us to zoom in and out to probe different physical scales. In this sense, we can use RG trajectories to connect phenomena at the Planck scale down to the electroweak regime. This idea has been explored within the ASQG approach, providing indications that the existence of a gravitational UV FP might lead to interesting consequences on the running of SM-couplings. The most highlighted example is the prediction (within approximations) of the Higgs mass [97] close to the actual measured value two years before its observation in the LHC[3] [98, 99]. Investigations in the last few years also indicate the possibility of a post-diction for the top quark mass and also the top-quark mass difference [95, 96]. Furthermore, the AS scenario for QG might also help with a solution to the triviality problem in the Abelian gauge sector of the SM [100, 101].

From the RG perspective a theory is characterized by RG-trajectories in the space of all couplings compatible all the symmetries and degrees of freedom associated with the physical problem under investigation. Such a space is usually referred to as theory space. Within the standard formulation of ASQG, based on the quantization of GR, the theory space is constructed by the (infinite) set of operators compatible with diffeomorphism (*Diff*) symmetry, with the fundamental field being the space-time metric. In the thesis we explore a different choice, namely, the theory space defined by the quantization of unimodular gravity (UG) [102–109]. In this case, the space-time metric still plays the role of fundamental variable, however, with a configuration space restricted by a condition of fixed metric determinants. As a consequence of this re-

[3]We should emphasize that the "predicted" value for the Higgs from AS actually depends on the approximations under assumption. By now there are multiple calculations indicating that this value might vary in a range of a few GeV. Most importantly, a reliable method to estimate the errors resulting from these approximations is still missing.

striction, the underlying symmetry characterizing this theory space is reduced to the group of transverse diffeomorphism transformations (*TDiff*)[4].

UG is closely related to an observation made by Einstein in the early years of GR, namely, that by a convenient choice of coordinates we can set the metric determinant to one, leading to simplifications in the field equations of GR [110]. In such a case, we can simply view UG as a particular gauge in GR. In its modern formulation, UG is interpreted as an alternative theory where the determinant of the metric is fixed *a priori* and, therefore, not subject to any variation. One of the most attractive features of UG is the role played by the cosmological term. Since the determinant of the metric is not subject to any variation, the cosmological constant term in the unimodular version of the EH (uEH) action decouples from the dynamical field equations. On the other hand, it is possible to verify that a cosmological term re-appears at the level of the classical field equations as an integration constant. Nevertheless, this integration constant is not related to the usual cosmological term in the uEH action. This feature has attracted some attention to UG as a possible solution (or reinterpretation) of the cosmological constant problem[5] [103, 105, 107–109, 111–115]. The basic idea is that the cosmological term (an integration constant) in the dynamical field equation of UG does not receive quantum corrections from vacuum fluctuations[6].

At the classical level, UG turns out to be dynamically equivalent to GR. In fact, starting from the field equations derived from the uEH action we can reconstruct the usual Einstein's field equation for GR and, therefore, showing that both theories share the same classical solutions. In this sense, the only difference between UG and GR is the status of the cosmological term, an integration constant in the former, and a dynamical term in the latter. The (in-)equivalence at the quantum level turns out to be more subtle [115, 116, 118–127]. On the one hand, some calculations based on perturbative techniques indicate tree-level and 1-loop equivalent results [115, 121]. On the other hand, the inequivalence of both theories has been discussed in terms of formal manipulations at the level of path integrals [123].

The dispute regarding the quantum equivalence of GR and UG triggers the question on whether the AS program could be built on top of UG. While ASQG based as a quantum theory for GR has been extensively explored in the literature, only a few investigations were done in the unimodular counterpart. A few studies based on FRG

[4]Different versions of UG may be formulated in terms of different symmetry groups. For example, depending on how the unimodularity condition is imposed, the underlying symmetry might be characterized by one of the following choices: *TDiff*, Weyl-*TDiff* (*WTDiff*) or *Diff*. Along this thesis we focus in the *TDiff* formulation.

[5]It important to emphasize that the term "cosmological constant problem" is used to indicate more than one problem associated with the cosmological term in GR. In the present case, we are referring to the fine-tuning of the cosmological term in order to absorb quantum corrections proportional to the forth-power of a cutoff scale.

[6]See also [116,117] for a different point of view concerning the possibility of resolve the cosmological constant problem in the unimodular setting.

methods point towards the existence of asymptotically safe solutions in UG [125, 126, 128, 129]. Nevertheless, this area deserves further investigations.

In the present thesis, we further explore the theory space defined by UG. In this sense, we perform a systematic investigation based on FRG methods as a way to characterize the RG properties of UG beyond the standard perturbative regime. The analysis performed here was done in terms of two different approximation methods for the FRG, namely, the background approximation and the vertex expansion approach. In both cases, we present indications for UV FPs in the unimodular version of ASQG. Furthermore, by exploring the impact of graviton fluctuations in the running of SM-like couplings, we discuss the phenomenological viability of the unimodular ASQG scenario.

The present thesis is organized as follows: In chapter 1 we revise the basic theoretical aspects underlying the development of this thesis. In this sense, we discuss the concept of AS and the application of the FRG as a method to explore the RG flow in QG. In Chapter 2, we provide an introduction to unimodular (classical and quantum) gravity. Chapter 2 is also devoted to a systematic search for UV FPs in UG based on the background approximation for the FRG. In chapter 3, we investigate the RG flow of unimodular quantum gravity based in the vertex expansion approach for the FRG. We discuss some comparative aspects of the unimodular and the standard ASQG scenario. In chapter 4, we study the impact of graviton fluctuations in SM-like couplings. We explain how QG fluctuations might induce UV completion of SM couplings and we explore possible constraints on the unimodular theory space based on tests of phenomenological viability. In what follows, we draw our conclusion and present some further perspectives. A list of appendices collects some technical points that were not covered in the main text.

Chapter 1

Theoretical Foundations

1.1 Asymptotically Safe Quantum Gravity

1.1.1 Pushing the limits of fundamental physics

GR and QFT constitute the two main pillars supporting our understanding of nature at fundamental level. On the one hand, GR provides a very satisfactory description of the gravitational phenomena at large scales. In the context of GR, gravity is understood as a dynamical effect of space-time. In this sense, the gravitational field of a given object (e.g. a star or a planet) is nothing but the deformation caused by this object in the space-time. The interplay between geometry and matter/energy appears at the level of the Einstein's field equation,

$$R_{\mu\nu} - \frac{1}{2} g_{\mu\nu} R + \Lambda_{\rm cc}\, g_{\mu\nu} = 8\pi G_{\rm N}\, T_{\mu\nu}\,. \tag{1.1}$$

In this framework, the fundamental dynamical variable is the space-time metric $g_{\mu\nu}$. The energy-momentum tensor $T_{\mu\nu}$ acts as a source term and encodes the relevant information on how matter/energy impacts the geometry of space-time. The geometrical nature of gravity implies a universal behavior since the dynamical evolution of any physical (massive or not) object should be affected by deformations in the underlying space-time geometry. One of the consequences of this universal behavior was the prediction of the gravitational light-bending effect, considered as a benchmark in the experimental validation of GR [2].

Despite being a very successful description of gravity at large scale, GR also has its limitations. If we consider as an example the Schwarzschild metric, i.e., the outer solution of a spherically symmetric matter distribution (with mass M), the line element takes the form

$$ds^2 = g_{\mu\nu}dx^\mu dx^\nu = -\left(1 - \frac{r_\mathrm{S}}{r}\right)dt^2 + \left(1 - \frac{r_\mathrm{S}}{r}\right)^{-1} dr^2 + r^2 d\Omega\,, \tag{1.2}$$

where $d\Omega = d\theta^2 + r^2 \sin^2\theta d\phi^2$ is the solid angle element and $r_\mathrm{S} = 2MG_\mathrm{N}$ is the Schwarzschild radius. This solution indicates two potential singularity problems. The first one, at $r = r_\mathrm{S}$, does not characterize a physical problem, since the singularity can be removed by an appropriate choice of coordinates. The singularity at $r = 0$, on the other hand, turns out to be critical once it cannot be avoided by any change of coordinates. The most direct indication of the physical nature of this problem is the observation of a divergent Kretschmann scalar at $r = 0$,

$$R_{\mu\nu\alpha\beta}R^{\mu\nu\alpha\beta} = \frac{12\,r_\mathrm{S}^2}{r^6} \overset{r\to 0}{\to} \infty\ . \tag{1.3}$$

The ubiquitous presence of physical singularities in the solutions of the Einstein's field equation indicates that GR might breakdown at small scales (or, equivalently, large energies) [5, 130].

One of the most important changes of paradigms in the development of physics was the understanding that the rules describing nature at small scales are very different from our macroscopic experience, leading to the advent of quantum mechanics (QM). Furthermore, the combination of ideas from QM with the concepts from special relativity culminate in the foundation of QFT. In this framework, the central objects are fluctuating fields encoding the probabilistic nature of QM, while the relevant physical questions should be answered in terms of expectation values and correlation functions. QFT has been very successfully applied to the description of microscopic phenomena. In particular, QFT is the conceptual as well as technical basis for the SM of particle physics, showing an astonishing agreement between theoretical results and the experiments performed in modern colliders [1].

Nevertheless, the SM of particle physics also has its limitations. Possibly, the most evident limitation of the SM lies on the fact that it does not say anything about gravity. The probabilistic nature of QFT makes it hard to place the SM along with a geometrical description of gravity. In a semi-classical approach, we might consider the r.h.s. of the Einstein's field equation as the expectation value of the energy-momentum tensor associated with SM-fields, namely

$$R_{\mu\nu} - \frac{1}{2}g_{\mu\nu}R + \Lambda_\mathrm{cc}\, g_{\mu\nu} = 8\pi G_\mathrm{N}\,\langle T_{\mu\nu}^\mathrm{SM}\rangle\,. \tag{1.4}$$

However, this approach leads to some difficulties. In particular, it is not clear how to take all the back-reactions into account since, in this approximation, the space-time

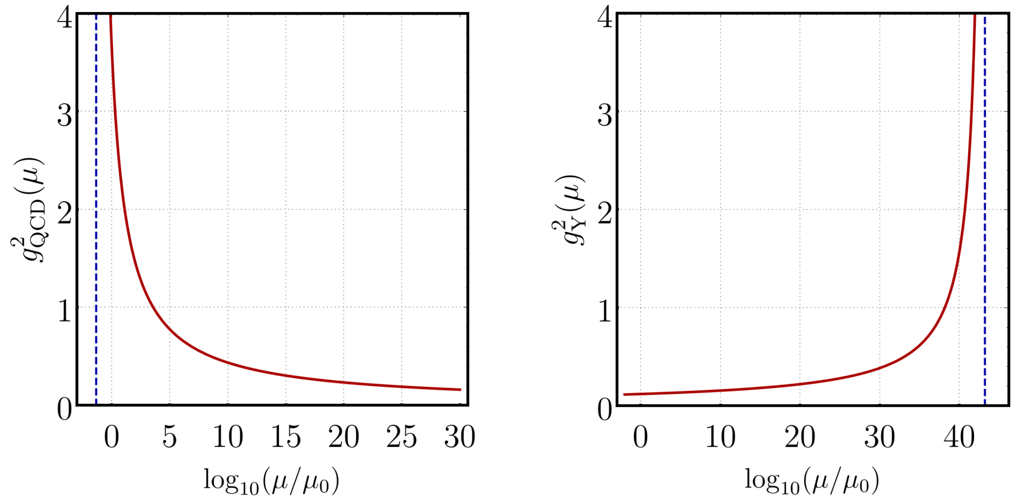

Figure 1.1: Running of the strong (left) and the hypercharge (right) gauge couplings, both evaluated at the 1-loop approximation. The vertical-dashed lines indicate the Laudau poles. We have used initial conditions $g_{\mathrm{QCD}}(\mu_0) = 1.17$ [134] and $g_{\mathrm{Y}}(\mu_0) = 0.35$ [135], with reference scale $\mu_0 = 173\,\mathrm{GeV}$.

geometry is only affected by the average of states in quantum superposition. This suggests that a consistent treatment of gravitating SM fields should also take into account the quantization of the gravitational degrees of freedom (see [131] for more details concerning this point).

Even disregarding gravity, the SM of particle physics seems to breakdown in extreme regimes. The incomplete nature of the SM can be observed by taking into account one of the most important lessons from QFT, namely, the running of coupling constants. As an example, consider the (1-loop) RG flow of the strong (g_{QCD}) and hypercharge (g_{Y}) gauge couplings [132, 133],

$$g^2_{\mathrm{QCD}}(\mu) = \frac{g^2_{\mathrm{QCD}}(\mu_0)}{1 + \frac{7}{16\pi^2} g^2_{\mathrm{QCD}}(\mu_0) \log(\mu^2/\mu_0^2)}\,, \tag{1.5a}$$

$$g^2_{\mathrm{Y}}(\mu) = \frac{g^2_{\mathrm{Y}}(\mu_0)}{1 - \frac{41}{96\pi^2} g^2_{\mathrm{Y}}(\mu_0) \log(\mu^2/\mu_0^2)}\,, \tag{1.5b}$$

where μ_0 indicate some reference energy scale. The running of the gauge couplings g_{QCD} and g_{Y} exhibit the failure of the SM, due to the appearance of Landau poles[1], at different regimes (see Fig. 1.1).

In the case of the strong gauge coupling, g_{QCD}, we first observe that at very high energy scales ($\mu \to \infty$) the coupling tends to zero. This is the phenomenon of asymptotic freedom [43–45], which indicates that quantum chromodynamics (QCD) can be

[1]A Landau pole correspond to a scale where the running of a given coupling diverges.

extended (as a perturbative theory) up to arbitrarily high energies. On the other hand, the running of the strong coupling hits a Landau pole when flowing towards the infrared regime (IR), indicating the breakdown of perturbative QCD at low energy scales [136]. The failure of perturbative methods to describe QCD in the IR constitute one of the main obstacles concerning our understanding from first principles of the confinement problem. The scale of breakdown of perturbative QCD (the Landau pole) is known as $\Lambda_{\rm QCD}$ and, at 1-loop approximation, it takes the form $\Lambda_{\rm QCD} = \mu_0\, e^{-\frac{7}{32\pi^2} g^2_{\rm QCD}(\mu_0)}$. Results from non-perturbative methods in QCD, however, seems to indicate that the Landau pole does not persist beyond perturbation theory [136]. Since in the present thesis we are mainly interested in the UV features of QFTs, we shall not come back to this point along the text.

The running of the hypercharge coupling indicates a problem in the other extreme of the RG-flow, i.e., in the UV regime. In this case, as one can observe from Fig. 1.1, the hypercharge coupling cannot be pushed to arbitrarily high energies since it would hit a Landau pole[2] at a finite energy scale ($\Lambda_{\rm pole} = \mu_0\, e^{\frac{41}{192\pi^2} g^2_{\rm Y}(\mu_0)}$) [137]. At first sight, this pathological behavior only indicates the breakdown of perturbative methods applied to the hypercharge sector. Nevertheless, there are indications that the Landau pole would persist even when non-perturbative methods are taken into account [138–140]. From an alternative perspective, the Landau pole can be avoided by tuning the hypercharge coupling at a reference energy scale to zero ($g_{\rm Y}(\mu_0) = 0$). In this case, however, the running of $g_{\rm Y}(\mu)$ (Eq. (1.5b)) enforce the hypercharge coupling to be zero along all the flow. This is known as the triviality problem [141]. For discussions concerning the Landau pole/triviality problem in the Higgs-Yukawa and quartic scalar sectors, see Refs. [142–152]

The arguments presented in this section provide (some) indications that the two main theories describing the known fundamental interactions in nature are not as fundamental as we would expect. Both GR and the SM of particle physics exhibit pathological features when confronted with extreme regimes. In special, the existence of singularities appears as a common problem and might suggest the existence of some missing ingredient shared both by gravity and the other microscopic interactions. In the present thesis we explore the point of view that a quantum treatment of the gravitational interaction is the missing piece (or, at least, one of the missing pieces) to our understanding of nature at a fundamental level.

1.1.2 Gravity from a QFT perspective

Taking into account our experience with the other microscopic interactions, a "natural" attempt to quantize gravity would be the application of QFT techniques to GR. In

[2] The Landau pole is already present in quantum electrodynamics (QED).

this sense, our goal is to promote the space-time metric, $g_{\mu\nu}$, from a classical dynamical variable to a quantum field. From a path integral perspective, the usual target is to compute expectation values based on the functional integral over field configurations, namely

$$\langle \mathcal{O}[g_{\mu\nu}]\rangle \sim \int \mathcal{D}g_{\mu\nu}\, \mathcal{O}[g_{\mu\nu}]\, e^{iS_{\mathrm{EH}}[g]}\,, \tag{1.6}$$

where $\mathcal{O}[g_{\mu\nu}]$ denotes an (idealized) observable and $S_{\mathrm{EH}}[g]$ is the EH action. This approach, however, is far from being straightforward. A quick look at the EH action

$$S_{\mathrm{EH}}[g] = -\frac{1}{16\pi G_{\mathrm{N}}}\int_x \sqrt{g}\,\left(2\Lambda_{\mathrm{cc}} - R(g)\right)\,, \tag{1.7}$$

revels very intricate non-linear terms involving non-polynomial combinations of the space-time metric. As a consequence, we observe that, in spite of being a classical field theory, GR exhibits a very different structure in comparison with the other known fundamental interactions. Therefore, we might expect that a quantization procedure directly in terms of the full metric tensor would require non-standard methods in QFT.

Rather than proceeding to a more radical approach, we can try to get some insight from a simplified regime of GR, namely, the linearized approximation (see, e.g., [8, 11, 153]). In this sense, let us consider metric fluctuations around a fixed (Minkowiskian) background

$$g_{\mu\nu} = \eta_{\mu\nu} + \sqrt{32\pi G_{\mathrm{N}}}\, h_{\mu\nu}\,, \tag{1.8}$$

where $\sqrt{32\pi G_{\mathrm{N}}}$ is just a convenient normalization factor. Note that, in this convention, the fluctuation field $h_{\mu\nu}$ has canonical mass dimension one. Expanding the EH according to (1.8) and keeping only those terms contributing to the linearized dynamics ($\mathcal{O}(h^2)$-terms at the level of action), leads to the following expression

$$S_{\mathrm{EH}}^{\mathrm{lin}}[h] = -\int_x \left(\frac{1}{2}\partial_\alpha h_{\mu\nu}\partial^\alpha h^{\mu\nu} - \frac{1}{2}\partial_\alpha h \partial^\alpha h + \partial_\mu h \partial_\nu h^{\mu\nu} - \partial_\mu h^{\mu\alpha}\partial^\nu h_{\nu\alpha}\right)\,. \tag{1.9}$$

This action is symmetric under linearized *Diff* transformation,

$$\delta_\epsilon h_{\mu\nu} = \partial_\mu \epsilon_\nu + \partial_\nu \epsilon_\mu\,, \tag{1.10}$$

where $\epsilon_\mu = \epsilon_\mu(x)$ is a vector field corresponding to the generator of *Diff* transformations. The linearized field equations obtained by varying (1.9) w.r.t. the fluctuation field take the form (in the de-Donder gauge[3]),

$$\Box h_{\mu\nu} = 0\,. \tag{1.11}$$

As one can see, the classical dynamics of the fluctuation field is governed by a standard wave equation. This is one of the most celebrated results from GR since it predicts the existence of gravitational waves, experimentally confirmed a few years ago by the LIGO-collaboration [3].

At the linearized level, GR resembles more similarities with field theories describing the other microscopic interactions. That is, the metric fluctuation field has a dynamical description in terms of a gauge-invariant action and, at first approximation, $h_{\mu\nu}$ satisfies a usual relativistic wave equation. This observation suggests that a possible QFT formulation of GR should treat the fluctuation field as the fundamental degree of freedom [8, 11, 38, 154], instead of the full space-time metric $g_{\mu\nu}$. From a path-integral perspective, we replace the formal expression (1.6) by a more treatable version in terms of the fluctuation field

$$\langle \mathcal{O}[g_{\mu\nu}] \rangle \sim \int \frac{\mathcal{D}h_{\mu\nu}}{V_{Diff}}\, \mathcal{O}[g_{\mu\nu}]\, e^{iS^{\text{fluct}}_{\text{EH}}[h;\bar{g}]}\,, \tag{1.12}$$

where[4] $S^{\text{fluct}}_{\text{EH}}[h;\bar{g}]$ denote the EH action written in terms of the fluctuation field $h_{\mu\nu}$ and a background metric $\bar{g}_{\mu\nu}$, and V_{Diff} (the volume of the symmetry group associated with *Diff* transformations) was introduced to factor out physically equivalent field configurations. The QFT approach based on the quantization of the fluctuation field around a fixed background is usually referred to as covariant QG. In this framework, $h_{\mu\nu}$ is typically called the graviton field. Furthermore, it is interesting to observe that the background metric used in the split (1.8) does not necessarily need to be the Minkowski one.

The covariant approach for QG is supported by some interesting results. As it was noticed by Weinberg, the unitary representation of the Poincaré group associated with massless spin-2 particles[5] naturally leads to a symmetric rank-2 tensor field transforming according to Eq. (1.10) [158]. This result was taken seriously by Deser, who showed the possibility of reconstructing the EH action from a "bottom-up" approach,

[3] Since the action is symmetric under a local field transformation, we can use this freedom to fix a gauge condition. In the present case, we consider the de-Donder gauge choice $\partial_\nu h^\nu{}_\mu - \frac{1}{2}\partial_\mu h = 0$.

[4] It is important to emphasize that $S^{\text{fluct}}_{\text{EH}}[h;\bar{g}]$ should not be confused with the linearized action $S^{\text{lin}}_{\text{EH}}[h]$. The former includes all orders in the fluctuation field, while the latter is truncated at $\mathcal{O}(h^2)$. This is an important difference since the functional integral should take into account all possible field configurations $h_{\mu\nu}$ and not only small fluctuations as in the linearized approximation.

[5] More precisely, the inhomogeneous transformation arising from the unitary representation of the Poincaré group involves a transversality constraint on the vector field. In this sense, the most "natural" symmetry transformation for massless spin-2 particles correspond to *TDiff* transformations [103, 155–157].

that is, starting from the linearized version of the EH action and including interactions according to an iterative procedure [159].

The QFT approach based on covariant QG allows us to extract some interesting physical results from tree-level scattering processes. The most usual example is the Newtonian gravitational energy (for two static bodies with masses m_1 and m_2) obtained by a simple Fourier integral over the non-relativistic (NR) limit of a scattering amplitude, $\mathcal{M}$, associated with a process of the type $1 + 2 \to 1' + 2'$, namely

$$U_{\text{Newton}}(r) = -\int \frac{d^3\vec{q}}{(2\pi)^3} \lim_{\text{NR}} \mathcal{M}(\vec{q})\, e^{i\vec{r}\cdot\vec{q}} . \tag{1.13}$$

In this case, a standard calculation leads to $\lim_{\text{NR}} \mathcal{M}(\vec{q}) = 4\pi G_{\text{N}} m_1 m_2 / \vec{q}^{\,2}$ (see, for instance [160]), resulting in the typical Newtonian potential

$$U_{\text{Newton}}(r) = -\frac{G_{\text{N}} m_1 m_2}{r} . \tag{1.14}$$

Another interesting example is the possibility of recover the gravitational light bending angle from a tree-level scattering process in QFT [161, 162].

While tree-level calculations based on the covariant approach for QG lead to a consistent physical result, the situation turns out to be more complicate once we take into account radiative corrections. In particular, the QFT treatment for GR based on standard perturbative methods leads to an undesirable UV behavior due to the appearance of non-renormalizable interactions. This issue can be easily observed by exploring the structure of the interactions in $S_{\text{EH}}^{\text{fluct}}$[6]

$$S_{\text{EH}}^{\text{fluct}} = \int_x \Big(\partial h\, \partial h + G_{\text{N}}^{1/2}\, h \partial h \partial h + G_{\text{N}}\, h^2 \partial h \partial h + G_{\text{N}}^{3/2}\, h^3 \partial h \partial h + \cdots \Big) . \tag{1.15}$$

From this schematic representation it is not difficult to see that the graviton propagator and the self-interaction vertices (in momentum space) exhibit UV scaling k^{-2} and k^2, respectively. As a consequence, a diagram containing L-loops (with I_h-graviton internal lines and V_h-vertices) involves integrals with UV behavior[7]

$$I_{\text{UV}} \sim \int (d^d k)^L \frac{(k^2)^{V_h}}{(k^2)^{I_h}} , \tag{1.16}$$

leading to the superficial degree of divergence

$$\omega_{\text{UV}} = d\, L + 2V_h - 2I_h = (d-2)L + 2 , \tag{1.17}$$

[6]Since the complicated tensorial structure of graviton self-interactions is not relevant for the present discussion, we consider a simplified schematic notation without showing the explicit indices.

[7]For the sake of this argument, it is interesting to keep the number of space-time dimensions arbitrary.

where we have used the topological relation $L-1 = I_h - V_h$. In the physical dimension $d = 4$, $\omega_{\rm UV}$ increases with L. In this case, we can conclude that at every order in the loop expansion new types of divergent terms will appear and, therefore, it is not possible to absorb all the UV divergences by a finite number of counter-terms. It is also interesting to observe that in the critical dimension $d = 2(= d_{\rm c})$, the superficial degree of divergence does not depend on the number of loops, meaning that 2-dimensional covariant QG is a perturbatively renormalizable QFT.

The power-counting argument indicates the qualitative behavior of UV divergences. In this sense, a precise statement concerning the failure of perturbative renormalizability requires a concrete calculation showing that the ill-desired UV divergences do not cancel by some mysterious fine-tuning. In this sense, a surprising result was obtained by 't Hooft and Veltman [12] by showing that the divergent part of the 1-loop effective action in QG is proportional to curvature squared invariants, namely

$$\Gamma^{\rm div}_{\text{1-loop}} \sim \frac{1}{\varepsilon} \int_x \sqrt{g} \left(c_1 \, R^2 + c_2 \, R_{\mu\nu} R^{\mu\nu} \right) \,, \tag{1.18}$$

where $\varepsilon = 4 - d$ is the usual parameter from dimensional regularization and c_1 and c_2 denote (finite) numerical coefficients. In the case of pure gravity (without cosmological constant) both R^2 and $R_{\mu\nu}R^{\mu\nu}$ vanish on-shell, therefore, the 1-loop effective action for QG (without matter and cosmological constant) turns out to be finite for on-shell field configurations. This situation, however, is not sustained by the inclusion of matter and the cosmological constant, since, in this case, the Einstein's field equation gives non-vanishing values for the curvature-squared terms [13–16]. Even in the case of pure gravity, the explicit calculation at 2-loops, first done by Goroff and Sagnotti [17, 18] (see also [19]), shows the existence of a divergent contribution like

$$\Gamma^{\rm div}_{\text{2-loop}} \sim \frac{1}{\varepsilon} \int_x \sqrt{g} \, R^{\mu\nu}{}_{\rho\sigma} R^{\rho\sigma}{}_{\alpha\beta} R^{\alpha\beta}{}_{\mu\nu} \,, \tag{1.19}$$

which does not vanish for on-shell field configurations and cannot be absorbed by the renormalization of couplings present in the bare action.

1.1.3 Safety beyond perturbation theory

Before introducing the concept of AS and explore its promising consequences to QG, it is useful to further explore the actual problems of the perturbatively non-renormalizable QFTs. The typical speech concerning non-renormalizable theories attribute the lack of physical meaning to the impossibility of eliminating the UV divergences by a suitable counter-term. Although this point of view is not wrong, it also not complete. As it was observed by Weinberg: "*... non-renormalizable theories are just as renormalizable as renormalizable theories, as long as we include all possible terms* *in the Lagrangian.*". In this sense, in a perturbative non-renormalizable theory we can still remove all the UV divergences provided that we start from a bare action of the form[8]

$$S_{\text{bare}}[\varphi_{\text{B}}] = \sum_{i=1}^{\infty} g_{\text{B},i}\, \mathcal{O}_i[\varphi_{\text{B}}]\,, \tag{1.20}$$

where $\{g_{\text{B},i}\}$ denotes the set of bare couplings and the sum is taken over the (infinite) set of all possible operators $\mathcal{O}_i[\varphi_{\text{B}}]$ compatible with the symmetries characterizing the physical system under investigation. While UV divergences can be removed by expressing $g_{\text{B},i}$ and φ_{B} in terms of renormalized quantities $g_{\text{R},i}$ and φ_{R}, predictivity is spoiled[9] since physical results depend on an infinite set of free parameters $g_{\text{R}} = \{g_{\text{R},i}\}$. The lack of predictivity can be better understood by observing that each renormalized coupling requires a renormalization condition, ultimately fixed by an experiment.

It is interesting to re-analyze the discussion of the previous paragraph translated to the RG-language[10]. As it is well known, the renormalized couplings run according to RG-flow equations, first introduced by Gell-Mann and Low [137], namely

$$\mu\partial_\mu \tilde{g}_{\text{R},i}(\mu) = \beta_i(\tilde{g}_{\text{R}})\,, \qquad (i = 1, 2, \cdots)\,, \tag{1.21}$$

where μ represents the RG scale and we have defined dimensionless couplings by $\tilde{g}_{\text{R},i} = \mu^{-\Delta_i} g_{\text{R},i}$ (Δ_i denotes the canonical mass dimension of $g_{\text{R},i}$). The RG-flow is an autonomous dynamical system and its solutions describe trajectories, parameterized by μ, in the theory space[11] (see, e.g. [38, 39]). In the case of non-renormalizable theories we have to deal with an infinite set of first-order differential equations and, therefore, an infinity set of initial conditions (determined by experiments) is required.

Perturbative renormalizability, however, should not be taken as a fundamental aspect of nature, it is just a practical guiding principle to define "acceptable" QFT's according to our technical limitations. The AS program replaces this guiding principle to a more general concept of renormalizability. As we have discussed in the previous paragraph, the crucial problem of (perturbatively) non-renormalizable is not the impossibility of extract finite physical results, but the lack of predictivity. In RG-language it translates to the need of infinitely many initial conditions to integrate the RG-flow

[8]Since the discussion performed here is not restricted to QG, we consider a generic field φ. The subscript "B" indicate bare quantities.

[9]It is important to emphasize that we are interested in theories that remains predictivity up to arbitrarily high-energies. Within the setting of EFTs, non-renormalizable theories are just as predictivity as the renormalizable ones [34].

[10]See Ref. [163] for a seminal review on RG. For comprehensive discussions on standard QFT textbooks see, e.g., [164–166].

[11]In this context, the theory space is defined by the set of operators $\{\mathcal{O}_i[\varphi]\}$ compatible with the underlying symmetries of the system. At the practical level it is useful to adopt the set of dimensionless systems $\tilde{g}_{\text{R}} = \{\tilde{g}_R^{(n)}\}$ as coordinates of the theory space.

equations. The idea of AS is to avoid this problem by demanding an additional physical principle, namely, scale invariance in the deep UV regime. More precisely, scale invariance in the UV regime is manifested by RG-trajectories flowing towards a FP [40–42].

A FP in the RG-flow is defined by a set of couplings $\tilde{g}^*_{\mathrm{R}} = \{\tilde{g}^*_{\mathrm{R},i}\}$ in which all the beta functions, $\beta_i(\tilde{g}_{\mathrm{R}})$, vanish simultaneously, i.e.

$$\beta_i(\tilde{g}^*_{\mathrm{R}}) = 0\,, \qquad (i = 1, 2, \cdots)\,. \tag{1.22}$$

QFTs characterized by a RG-trajectories that reach a FP in the UV regime are said to be UV-complete (or, safe). As it was argued by Weinberg [42], a physical process (with characteristic (single) energy scale E) can be quantified in terms of physical quantities (e.g. decay rates, cross-sections, etc), denoted as $\mathcal{P}$, of the form

$$\mathcal{P}(E, g_{\mathrm{R}}(\mu); X) = E^{[\mathcal{P}]}\,\mathcal{F}\left(\left\{g_{\mathrm{R},i}(\mu)/E^{\Delta_i}\right\}; X\right)\,, \tag{1.23}$$

where $[\mathcal{P}]$ denotes the canonical mass dimension of $\mathcal{P}$ and X represents a set of dimensionless kinematic variables (such as angles and energy ratios). The function $\mathcal{F}$ encodes non-trivial dependencies on the couplings and on the kinematic variables. Expressing the renormalized couplings $g_{\mathrm{R},i}(\mu)$ in terms of the corresponding dimensionless version $\tilde{g}_{\mathrm{R},i}(\mu)$, we find

$$\mathcal{P}(E, g_{\mathrm{R}}(\mu); X) = E^{[\mathcal{P}]}\,\mathcal{F}\left(\left\{(\mu/E)^{\Delta_i}\,\tilde{g}_{\mathrm{R},i}(\mu)\right\}; X\right)\,. \tag{1.24}$$

Identifying the RG-scale μ with the characteristic energy scale E, the explicit dependence w.r.t. E becomes a scaling factor, namely

$$\mathcal{P}(E, g_{\mathrm{R}}(E); X) = E^{[\mathcal{P}]}\,\mathcal{F}\left(\{\tilde{g}_{\mathrm{R},i}(E)\}; X\right)\,. \tag{1.25}$$

As a consequence, the non-trivial part of $\mathcal{P}$ is completely encoded in the function $\mathcal{F}\left(\{\tilde{g}_{\mathrm{R},i}(E)\}; X\right)$. If the set of dimensionless couplings $\{\tilde{g}_{\mathrm{R},i}(E)\}$ runs according to a safe trajectory, then the function $\mathcal{F}$ approaches a finite value in the UV regime[12], namely, $\mathcal{F}_* = \mathcal{F}\left(\tilde{g}^*_{\mathrm{R}}; X\right)$. In this sense, physical quantities defined on top of safe trajectories remain physically meaningful up to arbitrarily high energies.

Besides UV completion, a non-perturbative notion of renormalizability requires a solution to the problem of predictivity. Depending on the properties of the RG-flow, it can also be achieved by the requirement of a FP in the UV regime. The argument that leads to this conclusion can be better understood by analyzing the linearized flow around a FP. In this case, expanding the RG-flow in (1.21) around a FP solution g^*_{R},

[12]Note that it requires the implicit assumption that the FP value g^*_{R} should not be a pole in the function $\mathcal{F}$.

we find (for $i = 1, 2, \cdots$)

$$\mu\partial_\mu \tilde{g}_{\mathrm{R},i} = \sum_j \mathbf{M}_{ij}(\tilde{g}^*_{\mathrm{R}}) \left(\tilde{g}_{\mathrm{R},j} - \tilde{g}^*_{\mathrm{R},j}\right) + \mathcal{O}\left((\tilde{g}_{\mathrm{R}} - \tilde{g}^*_{\mathrm{R}})^2\right) \,, \tag{1.26}$$

where we have defined the stability matrix

$$\mathbf{M}_{ij}(\tilde{g}^*_{\mathrm{R}}) = \left.\frac{\partial \beta_i(\tilde{g}_{\mathrm{R}})}{\partial \tilde{g}_{\mathrm{R},j}}\right|_{\tilde{g}_{\mathrm{R}} = \tilde{g}^*_{\mathrm{R}}} \,. \tag{1.27}$$

The linearized flow admits the following solution

$$\tilde{g}_{\mathrm{R},i}(\mu) = \tilde{g}^*_{\mathrm{R},i} + \sum_{l=1}^{\infty} C_l \, V_i^{(l)} \, (\mu/\mu_0)^{-\theta_l} \,, \qquad (i = 1, 2, \cdots) \,. \tag{1.28}$$

Here, μ_0 is a reference scale, the C_l's denote integration constants and the pair $\{V_i^{(l)}, \theta_l\}$ is defined in terms of the eigenvalue equation $\sum_j \mathbf{M}_{ij}(\tilde{g}^*_{\mathrm{R}}) V_j^{(l)} = -\theta_l V_i^{(l)}$. The parameters θ_l's are known as critical exponents associated with the FP $\tilde{g}^*_{\mathrm{R}}$. The integration constants are determined in terms of initial conditions at the reference scale μ_0, namely

$$\tilde{g}_{\mathrm{R},i}(\mu_0) = \tilde{g}^*_{\mathrm{R},i} + \sum_{l=1}^{\infty} C_l \, V_i^{(l)} \,, \qquad (i = 1, 2, \cdots) \,. \tag{1.29}$$

At this point, the eventual lack of predictivity is encoded in the infinity set of initial conditions $\{\tilde{g}_{\mathrm{R},i}(\mu_0)\}$. Nevertheless, the arbitrariness of the initial conditions is subject to some properties of the eigenvalues of the stability matrix. In fact, if there a finite number of critical exponents such that $\mathrm{Re}(\theta_l) > 0$, here denoted by[13] $\{\theta_1, ..., \theta_N\}$, the linearized flow (Eq. 1.28) becomes[14]

$$\tilde{g}_{\mathrm{R},i}(\mu) = \tilde{g}^*_{\mathrm{R},i} + \sum_{l=1}^{N} C_l \, V_i^{(l)} \, (\mu/\mu_0)^{-\theta_l} + \sum_{l=N+1}^{\infty} C_l \, V_i^{(l)} \, (\mu/\mu_0)^{-\theta_l} \,. \tag{1.30}$$

In the UV limit, the first sum automatically vanishes since $\mathrm{Re}(\theta_l) > 0$. On the other hand, the second sum pushes $\tilde{g}_{\mathrm{R},i}(\mu)$ away from the FP once we approach the UV limit, unless we set $C_l = 0$ for $l \geq N+1$. This constraint on the integration constant feedback in (1.29), restricting the set of allowed initial conditions $\{\tilde{g}_{\mathrm{R},i}(\mu_0)\}$. In this sense, only a finite number of couplings need to be fixed by experiments, while the remaining ones become predictions of the RG-flow.

[13] Since we have the freedom to re-label the couplings and critical exponents, we can always assume that this subset involve the firsts eigenvalues. Moreover, in the complementary set of critical exponents $\{\theta_{N+1}, \theta_{N+2}, ...\}$ we assume $\mathrm{Re}(\theta_l) < 0$.

[14] The eigenvectors $V^{(l)}$ associated with critical exponents such that $\mathrm{Re}(\theta_l) > 0$ ($\mathrm{Re}(\theta_l) < 0$) are usually called relevant (irrelevant) directions.

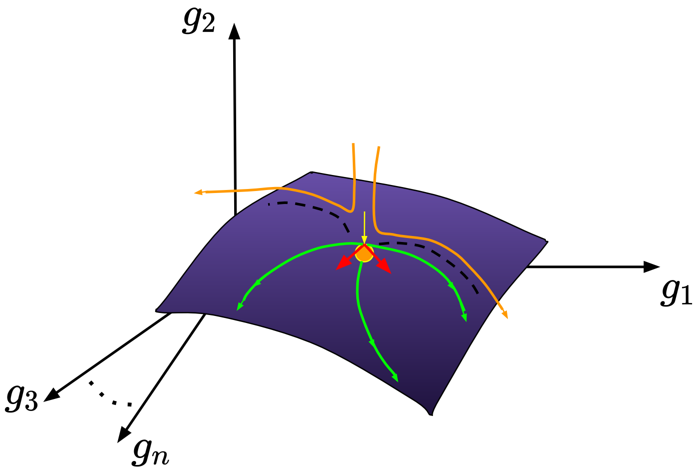

Figure 1.2: Illustration of an UV FP (yellow) with the associated UV critical surface. Trajectories starting from a point (orange) that does not belong the critical surface are repelled by the FP towards the IR. RG-trajectories connected to the FP (green) are completely embedded in the critical surface. The red arrows indicate the 2-relevant directions associated with the analysis of the linearized flow around the FP.

The conclusion of the above discussion can be extended beyond the regime of linearized flows. More generally, we define the concept of UV critical hyper-surface as the set of points in the theory space that can be connected to a UV FP through an RG-trajectory. Trajectories that do not belong to the critical hyper-surface are repelled by the FP in the UV. If the critical hyper-surface has finite dimension, then, UV complete RG-trajectories turn out to be characterized only by a finite number of free parameters. In this sense, safe RG-trajectories provide both UV-complete and predictive physical results (irrespective of any requirement regarding perturbative renormalizability). The situation described here is represented in Fig. 1.2

Given the elements discussed in this section, we can define an asymptotically safe theory in terms of the following requirements [42]:

i) the underlying RG-flow admits trajectories connected to a FP in the UV regime;

ii) there is a finite dimensional critical hyper-surface associated to this FP.

The concept of AS generalizes the usual property of AF appearing in the RG-flow associated with non-Abelian gauge theories. AF correspond to the special case of Gaussian FP's, namely, a FP characterized by vanishing couplings in the UV regime. AS, on the other hand, includes the possibility of non-Gaussian FP's, where at least one coupling remains interacting (non-vanishing) in the UV limit. Since the components of a non-Gaussian FP are not necessarily small, the study of AS usually requires techniques beyond perturbation theory.

The idea of AS has a special appeal for QG, since it might provide a UV complete and predictive framework for a QFT approach for gravity. The existence of a gravitational UV FP was conjectured by Weinberg [42]. The mechanism for such a FP was first discussed within a setup close to the critical dimension $d_{\rm c} = 2$, namely, using $d = 2 + \epsilon$ expansion. In this setting, the 1-loop beta function for the (dimensionless[15]) Newton coupling takes the form [42]

$$\beta_G^{\text{1-loop}} = (d-2)G + B\,G^2 = \epsilon\,G + B\,G^2\,. \tag{1.31}$$

At the critical dimension ($\epsilon = 0$) the beta function exhibit a Gaussian FP ($G^* = 0$) that might be either attractive ($B < 0$) or repulsive ($B > 0$) in the UV. The first case corresponds to an asymptotically free theory, while the second gives rise to a Landau pole. Away from the critical dimension (assuming $\epsilon > 0$), the Gaussian FP becomes UV repulsive irrespective of the sign of B. However, if $B < 0$[16], the RG-flow also exhibit a UV attractive non-Gaussian FP at $G^* = -\epsilon/B$ with corresponding critical exponent $\theta_G = \epsilon > 0$. Calculations performed using ϵ-expansion[17] approach, at least for pure gravity, point towards $B < 0$, providing an indication for AS in QG near the critical dimension $d_{\rm c} = 2$ [42].

The program of ASQG attempts at applying the ideas discussed along this section to the physical dimension $d = 4$. Unfortunately, in this case, a simple analytical extension based on the ϵ-expansion is not reliable and, therefore, more sophisticated methods are necessary to investigate the RG-flow in QG. In special, due to the non-renormalizability (in the perturbative sense) of the QFT approach for GR, the bare action in this setting should involve all possible operators compatible with the underlying *Diff* symmetry, namely[18]

$$\begin{aligned} S^{\rm bare}_{\rm QGR}[g] = &-\frac{1}{16\pi G_{\rm N}^{(\rm B)}}\int_x \sqrt{g}\,\left(2\Lambda_{\rm cc}^{(\rm B)} - R(g)\right) \\ &+ \sum_n \frac{1}{16\pi G_{\rm N}^{(\rm B)}}\int_x \sqrt{g}\,\alpha_n^{(\rm B)}\mathcal{O}_n(\nabla;\mathcal{R})\,, \end{aligned} \tag{1.32}$$

where $\mathcal{O}_n(\nabla;\mathcal{R})$ indicate higher-order operators constructed by appropriated contractions of curvature tensors (generically represented by $\mathcal{R}$) and covariant derivatives. In this case, the theory space for QGR is characterized by infinitely many couplings and, therefore, the search for a gravitational FP demand the investigation of the RG-flow involving more than just the Newton coupling.

[15]In d-dimensions the Newton coupling has canonical mass dimension $2-d$, therefore, its corresponding dimensionless version is defined as $G = \mu^{d-2}G_{\rm N}$

[16]The case $B > 0$ also lead to a non-Gaussian FP, however, with $G^* < 0$. This case is considered physically unacceptable.

[17]The value of B depends on the scheme of calculation. However, in all cases, the coefficient B turns out to be negative. See, e.g., Refs. [46–49].

[18]In this thesis, we adopt the nomenclature "quantum general relativity" (QGR) to designate a QFT approach for gravity involving all the operators compatible with *Diff* symmetry.

1.2 Functional Renormalization Group

1.2.1 The effective average action

From the Wilsonian point of view[19], the RG works as a theoretical microscope that allows us to resolve physics at different scales, by looking at effective descriptions characterized by effective parameters. In general, these parameters depend on the scale of resolution we are interested to deal with and the connection between different scales occurs via a RG transformation. From the perspective of the path integral quantization, this idea translates to a step-by-step integration procedure, where, instead of performing a functional integral over all field configurations, one integrates only modes characterized by some energy scale in a prescribed interval (usually referred as "momentum shell"). The successive integration of momentum shells defines the RG flow.

The functional renormalization group (FRG) is a practical realization of the Wilsonian ideas on renormalization [51], see also [172, 173][20]. In this framework, the central idea is the introduction of a regulator term to the Euclidean[21] path integral that suppresses modes with momenta[22] smaller than a cutoff scale k. The FRG regulator is defined in terms of the cutoff function[23]

$$\Delta S_k[\phi] = \frac{1}{2}\int_x \phi(x)\,\mathbf{R}_k(\Delta)\,\phi(x)\,, \tag{1.33}$$

with Δ representing a differential operator used to set a "momentum" scale. The regulator kernel, denoted as $\mathbf{R}_k(\Delta)$, is defined according to the following properties[24]

- For a fixed k, $\mathbf{R}_k(z)$ has to be monotonically decreasing in z.
- For a fixed z, $\mathbf{R}_k(z)$ has to be monotonically increasing with k.
- $\lim_{k\to 0}\mathbf{R}_k(z) = 0$, for all values of z.
- For $z > k^2$, $\partial_t\mathbf{R}_k(z)$ has to approach zero faster than $z^{-\alpha}$ (with $\alpha > 0$).
- $\mathbf{R}_k(0) = k^2$.

[19] By no means the intention of this section is to provide a self-contained discussion on the Wilsonian RG. For more elaborated discussions, see, e.g., [163, 164, 167–171].

[20] For comprehensive reviews on FRG, see Refs. [52, 171, 174–176].

[21] Starting from this point we move our discussion to the Euclidean setting. The use of Euclidean signature is a technical requirement of the FRG, since the appropriated definition of a "momentum shell" is only viable in the Euclidean setting. For a discussion concerning the analytical continuation (from Euclidean to Lorentzian signature) of FRG methods, see, e.g., Ref. [177].

[22] Despite we are using the term "momentum" as a label to field configurations, it does not correspond to a physical momentum scale in the usual sense. More generally, we use the term momentum in connection with the eigenvalue of some differential operator (e.g., the Bochner-Laplacian $\Delta = -\nabla^2$ in curved spaces) used to define a coarse-graining procedure.

[23] For the sake of simplicity, we consider an scalar field $\phi = \phi(x)$ as a working example. However, the discussion presented here can easily extended to other fields. See, e.g., [178–180].

[24] See, e.g., Ref. [38] for a discussion concerning these properties.

Except for this list of properties, the regular kernel can be chosen in an arbitrary way. Usually, we take the regulator kernel to be of the form $\mathbf{R}_k(z) = \mathcal{Z}_k R_k(z)$, where $\mathcal{Z}_k$ denotes a generalized wave-function renormalization factor that might carry some tensorial structure and $R_k(z)$ denotes the regulator function. For all the calculations presented in this thesis we have used the Litim's regulator defined as [181, 182]

$$R_k(z) = (k^2 - z)\theta(k^2 - z)\,, \tag{1.34}$$

with $\theta = \theta(x)$ being the Heaviside function. In some cases, we use the notation $R_k(z) = z\, r_k(z)$, where $r_k(z)$ is referred as shape-function.

Within the functional formalism, the FRG regulator is introduced by replacing the bare action $S[\phi]$ according to $S[\phi] \;\mapsto\; S[\phi] + \Delta S_k[\phi]$. In this case, we define the scale-dependent functional generator in the following way

$$Z_k[J] = \int \mathcal{D}\phi\; \mathrm{e}^{-S[\phi]-\Delta S_k[\phi]+\int_x J\cdot\phi}. \tag{1.35}$$

Due to the properties of the regulator kernel, the usual functional generator is recovered setting $k = 0$. In general, we define coarse-grained n-point correlation functions (in the presence of an external source J) as follows

$$\langle \phi(x_1)\cdots\phi(x_n)\rangle_k^J \;=\; \frac{\int \mathcal{D}\phi\, \phi(x_1)\cdots\phi(x_n)\, \mathrm{e}^{-S[\phi]-\Delta S_k[\phi]+\int_x J\cdot\phi}}{\int \mathcal{D}\phi\; \mathrm{e}^{-S[\phi]-\Delta S_k[\phi]+\int_x J\cdot\phi}}\,. \tag{1.36}$$

Since the cutoff function is defined as a quadratic form on the field ϕ, the introduction of such type of regulator basically affects the behavior the propagator. As an example, the propagator a free scalar field is modified according to

$$G(p) \sim \frac{1}{p^2} \quad\mapsto\quad G_k(p) \sim \frac{1}{p^2 + R_k(p^2)}\,. \tag{1.37}$$

As one can see, the FRG regulator acts as an effective (scale-dependent) mass term and, therefore, plays the role of an infrared regulator. At the level of the functional integral (1.35) the FRG regulator does not regularize the UV sector. As a consequence, the evaluation of the path integral (1.35) requires a supplementary UV regularization method. As we are going to see in the following, such a problem can be avoided by a proper definition of a coarse-grained effective action.

The main object in the FRG is the Effective Average Action (EAA) [51, 183] defined as a modified Legendre transform of the scale-dependent generating functional of connected correlation functions $W_k[J]$ ($= \ln Z_k[J]$), namely

$$\Gamma_k[\varphi] = \sup_J \left(\int_x J\cdot\varphi - W_k[J] \right) - \Delta S_k[\varphi]\,, \tag{1.38}$$

where $\varphi = \langle\phi\rangle_J$ denotes the mean-field. The definition of Γ_k is accompanied by the conjugation relations

$$\frac{\delta W_k[J]}{\delta J(x)} = \varphi(x) \qquad \text{and} \qquad \frac{\delta(\Gamma_k[\varphi] + \Delta S_k[\varphi])}{\delta\varphi(x)} = J(x)\,. \tag{1.39}$$

The EAA is a coarse-grained version of the usual effective action Γ in QFT, i.e., the generating functional of 1PI correlation functions. Due to the properties of the FRG regulator, the EAA interpolates between the microscopic (bare) action $\Gamma_{k\to\Lambda}[\varphi] = S_\Lambda[\varphi]$ (with Λ being a UV cutoff scale) and the effective action $\Gamma_{k\to 0}[\varphi] = \Gamma[\varphi]$ (see, e.g., [184]). For intermediate scales (finite k), the EAA provides an effective description of physics including quantum corrections originating from field configurations characterized by momentum larger than k.

1.2.2 The FRG equation

The most attractive feature concerning the definition of the EAA is the possibility of deriving an exact flow equation describing how Γ_k changes w.r.t. to the cutoff scale k. In this sense, we can translate the problem of solving a functional integral into a functional differential equation, the Wetterich equation[25] [51].

Since we are interested in a "differential equation" for Γ_k, let us start by acting with a scale derivative on both sides of Eq. (1.38). In this case, taking into account all possible sources of k-dependence we obtain[26]

$$\partial_t\Gamma_k[\varphi] = \sup_J\left(\int_x \partial_t J\cdot\varphi - \partial_t W_k[J]\right) - \partial_t(\Delta S_k[\varphi])\,. \tag{1.40}$$

Note that we are taking the mean-field φ as an independent variable. In this case, the external source J has to carry some k-dependence in order to compensate the k-independence of φ. The scale derivative acting on $W_k[J]$ can be written in the form

$$\partial_t W_k[J] = \tilde{\partial}_t W_k[J] + \int_x \frac{\delta W_k[J]}{\delta J(x)}\,\partial_t J(x)\,, \tag{1.41}$$

where $\tilde{\partial}_t$ denotes a scale derivative, but acting only on direct contributions from the regulator (i.e. keeping J fixed). Replacing the last expression in (1.40), we find

$$\partial_t\Gamma_k[\varphi] = \int_x \partial_t J(x)\,\underbrace{\left(\varphi(x) - \frac{\delta W_k[J]}{\delta J(x)}\right)\Bigg|_{J=J[\varphi]}}_{=0\text{ , due to (1.39).}} - \tilde{\partial}_t W_k[J] - \partial_t(\Delta S_k[\varphi]). \tag{1.42}$$

[25] Also known as flow equation or FRG equation or exact RG equation (ERGE).

[26] We define the "RG-time" according to $t = \log(k/k_0)$ (where k_0 is a reference scale). The scale derivative is defined as $\partial_t = k\partial_k$.

The second term, $\tilde{\partial}_t W_k[J]$, can be computed by taking into account $W_k[J] = \ln Z_k[J]$ along with the path integral representation (1.35), namely

$$\begin{aligned}\tilde{\partial}_t W_k[J] &= -\frac{\int \mathcal{D}\phi\, \partial_t(\Delta S_k[\varphi])\, \mathrm{e}^{-S[\phi]-\Delta S_k[\phi]+\int_x J\cdot\phi}}{\int \mathcal{D}\phi\ \mathrm{e}^{-S[\phi]-\Delta S_k[\phi]+\int_x J\cdot\phi}} \\ &= -\frac{1}{2}\int_{y,x} [\partial_t \mathbf{R}_k]_{x,y} \,\langle \phi(x)\phi(y)\rangle_k^J \,, \end{aligned} \tag{1.43}$$

where $[\partial_t \mathbf{R}_k]_{y,x} = \delta(y-x)\,\partial_t \mathbf{R}_k(\Delta_y)$ (with Δ_y acting only on fields with argument y). The last term in (1.42) can be written as

$$\partial_t(\Delta S_k[\varphi]) = \frac{1}{2}\int_{x,y} [\partial_t \mathbf{R}_k]_{y,x}\, \varphi(x)\, \varphi(y) = \frac{1}{2}\int_{x,y} [\partial_t \mathbf{R}_k]_{y,x} \,\langle \phi(x)\rangle_k^J \,\langle \phi(y)\rangle_k^J \,. \tag{1.44}$$

Putting together (1.42), (1.43) and (1.44), we find

$$\partial_t \Gamma_k[\varphi] = \frac{1}{2}\int_{x,y} [\partial_t \mathbf{R}_k]_{y,x}\, \mathbf{G}_k(x,y)\,, \tag{1.45}$$

where

$$\mathbf{G}_k(x,y) = \langle \phi(x)\phi(y)\rangle_k^J - \langle \phi(x)\rangle_k^J\, \langle \phi(y)\rangle_k^J = \frac{\delta^2 W_k[J]}{\delta J(x)\delta J(y)}\,, \tag{1.46}$$

represents the dressed propagator. The integral in the r.h.s. can be conveniently recast as a functional trace, namely

$$\int_{x,y} [\partial_t \mathbf{R}_k]_{y,x}\, \mathbf{G}_k(x,y) = \mathrm{Tr}\big[\mathbf{G}_k\, \partial_t \mathbf{R}_k\big]\,. \tag{1.47}$$

The conjugation relations (1.39) allow us to express the propagator $\mathbf{G}_k$ in terms of the 1PI 2-point function $\Gamma_k^{(2)}$ $(= \delta^2\Gamma_k/\delta\varphi\delta\varphi)$,

$$\mathbf{G}_k = \big(\Gamma_k^{(2)} + \mathbf{R}_k\big)^{-1}\,. \tag{1.48}$$

This equation is a coarse-grained version of the usual inversion relation $\mathbf{G}\cdot\Gamma^{(2)} = 1$ from standard functional methods in QFT. Finally, putting all these elements together we arrive at the flow equation describing the evolution of Γ_k,

$$\partial_t \Gamma_k[\varphi] = \frac{1}{2}\mathrm{Tr}\left[\big(\Gamma_k^{(2)} + \mathbf{R}_k\big)^{-1}\partial_t \mathbf{R}_k\right]\,, \tag{1.49}$$

which is the central element in the FRG.

The flow equation exhibits some important features that deserve further attention:

- A solution of the flow equation defines a trajectory, parameterized by k, in the

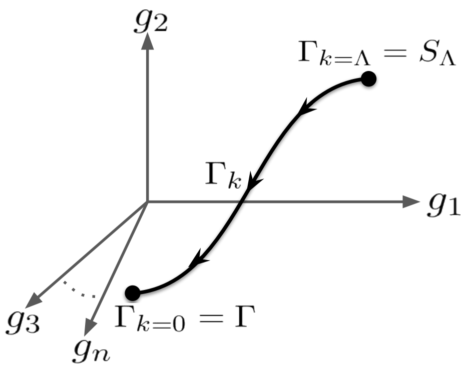

Figure 1.3: Sketch of the theory space. The trajectory represent the flow of the EAA.

theory space. In general terms, the theory space is an abstract functional space defined by the symmetries associated with the physical system we are interested to describe. The notion of theory space becomes more tangible by introducing a basis of operators $\{\mathcal{O}_n[\varphi]\}_{n=1,2,\cdots}$ compatible with the underlying symmetries. In this case, we expand Γ_k according to

$$\Gamma_k[\varphi] = \sum_n k^{-\Delta_n} g_{k,n}\, \mathcal{O}_n[\varphi]\,, \tag{1.50}$$

with $\{g_{k,n}\}_{n=1,2,\cdots}$ denoting a set of dimensionless couplings and Δ_n represents the canonical dimension of the operator O_n.. Within this basis, the dimensionless couplings play the role of coordinates in the theory space. Fig. 1.3 shows a pictorial representation of the theory space and an RG trajectory corresponding to the flow of Γ_k.

- Despite being introduced as an infrared regulator, at the level of the flow equation $\mathbf{R}_k$ also regularizes the UV sector. This follows as a consequence of the regulator insertion of the form $\partial_t \mathbf{R}_k$. Due to the requirement that $\partial_t \mathbf{R}_k$ should approach zero in a sufficiently fast way (for $z > k^2$), the regulator insertion suppresses UV modes in the functional trace appearing in the flow equation.

- The FRG equation exhibits a type of 1-loop structure. This can be realized by using the saddle point method to evaluate Γ_k within the perturbative 1-loop approximation. In this case, it is possible to show that (see, e.g., [38])

$$\Gamma_k^{\text{1-Loop}}[\varphi] = S[\varphi] + \frac{1}{2}\mathrm{Tr}\Big[\ln\big(S^{(2)} + R_k\big)\Big]\,, \tag{1.51}$$

where $S^{(2)} = \delta^2 S/\delta\varphi\delta\varphi$. By taking the scale derivative, we find

$$\partial_t \Gamma_k^{\text{1-Loop}}[\varphi] = \frac{1}{2}\mathrm{Tr}\left[\left(S^{(2)} + \mathbf{R}_k\right)^{-1} \partial_t \mathbf{R}_k\right] . \tag{1.52}$$

As one can observe, the 1-loop approximation for the EAA leads to a very similar flow equation in comparison with the FRG equation (1.49). The basic difference is the replacement of $S^{(2)}$ by $\Gamma_k^{(2)}$. The 1-loop structure of the flow equation (1.49) is usually represented in terms of the diagrammatic notation

$$\partial_t \Gamma_k^{\text{1-Loop}}[\varphi] = \frac{1}{2}$$ 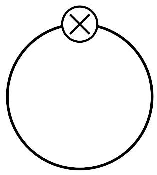 . (1.53)

It is important to emphasize that this diagrammatic representation should not be confused with the usual Feynman diagrams in perturbation theory. In the present case, the line correspond to the dressed G_k (not the tree-level one) and the cross indicates the regulator insertion of $\partial_t \mathbf{R}_k$.

- The FRG equation defines a local coarse-graining procedure. This notion of locality is associated with the fact that the scale derivative $\partial_t \Gamma_k^{\text{1-Loop}}[\varphi]$ is determined in terms of the EAA at the same scale k, without reference to the microscopic (bare) action. In this framework, the bare action only appears as a boundary condition at $k = \Lambda$.

1.2.3 Truncations methods

Despite being exact, we cannot count on any method to find exact solutions of the flow equation (2.38). In fact, finding a exact solution to the flow equation corresponds to resolve a QFT, a task that is not possible (with only a few exceptions of exactly solvable models). In this sense, to extract some relevant information from the FRG equation we have to adopt some kind of systematic expansion. Usually, the basic idea is to consider a truncation for the EAA, which is defined as an expansion in terms of a subset of operators compatible with the underlying symmetries, namely

$$\Gamma_k[\varphi] = \sum_{n \in \mathcal{T}} k^{-\Delta_n} g_{k,n}\, \mathcal{O}_n[\varphi] \,, \tag{1.54}$$

where $\mathcal{T}$ denotes a truncated set of labels. Typically, truncations involve only a finite number of terms, however, in some cases, it is also possible to extract relevant information from an infinite subset of operators compatible with the symmetries. The set of operators $\{\mathcal{O}_n\}_{n\in\mathcal{T}}$ defines a truncated theory space, with coordinates $\{g_{k,n}\}_{n\in\mathcal{T}}$.

At the practical level, we use the truncation method to compute approximated solutions to the flow equation. On the one hand, by acting with a scale derivative on (1.54), we find

$$\partial_t \Gamma_k[\varphi] = \sum_{n\in \mathcal{T}} k^{-\Delta_n} \left(\partial_t g_{k,n} - \Delta_n\, g_{k,n}\right) \mathcal{O}_n[\varphi]\,, \tag{1.55}$$

On the other hand, we can also use the truncation (1.54) to evaluate the trace in the r.h.s. of the flow equation. The crucial point is to project the result of this calculation in the same basis of operators defining the truncated theory space, namely

$$\frac{1}{2}\mathrm{Tr}\left[\left(\Gamma_k^{(2)} + \mathbf{R}_k\right)^{-1} \partial_t \mathbf{R}_k\right] = \sum_{n\in \mathcal{T}} k^{-\Delta_n} \mathcal{A}_n(g_k)\, \mathcal{O}_n[\varphi]\,, \tag{1.56}$$

where the coefficients $\mathcal{A}_n(g_k)$ can be computed in terms of the set of dimensionless couplings $g_k = \{g_{k,n}\}_{n\in\mathcal{T}}$. In general, the trace computation generates all possible terms compatible with the underlying symmetries, including operators that do not belong to the truncated theory space. In this sense, by projecting on the truncated theory space we simply remove all the contributions that are not part of the original truncation. By matching the coefficient of (1.55) and (1.56) we arrive at the following system of RG equations

$$\partial_t g_{k,n} = \Delta_n\, g_{k,n} + \mathcal{A}_n(g_k)\,, \qquad (\,\text{with}\, n \in \mathcal{T}\,). \tag{1.57}$$

In principle, this system of RG equations can be integrated, which allow us to reconstruct the RG trajectories describing the flow of the (truncated) EAA.

Even though the use of truncations is part of an approximation method, it is not associated with a perturbative expansion in the usual sense. Therefore, this strategy allows us to access non-perturbative aspects of QFTs. One of the difficulties concerning the use of truncation is the lack of a reliable method to control the systematic errors. Within the methods available in the literature, the best we can do is to check the self-consistency of a truncation by testing the stability of quantitative results against the inclusion of new operators. Although this idea does not provide a rigorous control of systematic errors, for a collection of physical systems where other non-perturbative techniques (e.g., lattice simulations, conformal bootstrap and so on) are applicable, the use of truncation methods indicates some level of reliability [185–187].

1.3 ASQG in the FRG framework

1.3.1 FRG equation in quantum gravity

The current research in ASQG is mostly based on the FRG as a tool to explore the RG-flow beyond standard perturbative calculations [50] (see also [38, 39]). As it was discussed in the previous section, the FRG provides a practical implementation of a coarse-graining procedure for Wilsonian renormalization. The basic idea is to modify the path integral over metric fluctuations by adding a cutoff function ΔS_k to the bare action, where the momentum scale k denotes an infrared regulator. In this context, we can define a scale-dependent generating functional of correlation functions,

$$\begin{aligned} Z_k[J,\eta,\bar{\eta};\bar{g}] = \int \mathcal{D}h_{\mu\nu}\mathcal{D}c^{\mu}\mathcal{D}\bar{c}_{\mu}\, \exp\bigg(&- S_{\text{QGR}}[h;\bar{g}] - S_{\text{g.f.}}[h,c,\bar{c};\bar{g}] \\ &- \Delta S_k[h,c,\bar{c};\bar{g}] + \int_x \sqrt{\bar{g}}\,(J^{\mu\nu}h_{\mu\nu} + \bar{\eta}_\mu c^\mu - \bar{c}_\mu \eta^\mu)\bigg)\,. \end{aligned} \tag{1.58}$$

where the fluctuation (bare) action $S_{\text{QGR}}[h;\bar{g}]$ is obtained by expanding (the Euclidean version of) $S^{\text{bare}}_{\text{QGR}}[g]$ around a fixed background metric $\bar{g}_{\mu\nu}$. As usually done in gauge-theories, we use the Faddeev-Popov method to perform the gauge-fixing procedure, resulting in additional functional integral over anti-commuting ghosts[27] (here denoted as c_μ and $\bar{c}_\mu$). The cutoff function involving both graviton and ghost fields is defined as a quadratic form

$$\Delta S_k[h,c,\bar{c};\bar{g}] = \frac{1}{2}\int_x \sqrt{\bar{g}}\, h_{\mu\nu}\, [\mathbf{R}_k^{hh}(\Delta)]^{\mu\nu\alpha\beta}\, h_{\alpha\beta} + \int_x \sqrt{\bar{g}}\, \bar{c}_\mu\, [\mathbf{R}_k^{\text{gh}}(\Delta)]^\mu{}_\nu\, c^\nu\,, \tag{1.59}$$

where $\mathbf{R}_k^{hh}(\Delta)$ and $\mathbf{R}_k^{\text{gh}}(\Delta)$ represent the regulator kernels. The argument of regulator kernels correspond to Laplacian operators defined on the background space.

The central object in the FRG is the effective average action, Γ_k, defined as a modified Legendre transform[28]

$$\Gamma_k[h,c,\bar{c};\bar{g}] = \int_x \sqrt{\bar{g}}\,(J^{\mu\nu}h_{\mu\nu} + \bar{\eta}_\mu c^\mu - \bar{c}_\mu\eta^\mu) - W_k[J,\eta,\bar{\eta};\bar{g}] - \Delta S_k[h,c,\bar{c};\bar{g}]\,, \tag{1.60}$$

where $W_k[J,\eta,\bar{\eta};\bar{g}] (= \log Z_k[J,\eta,\bar{\eta};\bar{g}])$ denotes a scale-dependent version of the usual Schwinger's generating functional. The most attractive feature of the FRG is that Γ_k

[27] For more details regarding the Faddeev-Popov method in QG, see App. A.

[28] It is important to emphasize that the argument of Γ_k correspond to the mean field obtained by taking derivatives of the Schwinger function w.r.t. the external sources. Nevertheless, we use the same notation both for the mean fields and the fluctuating fields appearing in the functional integral.

satisfies an exact flow equation with 1-loop structure [29]

$$\partial_t \Gamma_k = \frac{1}{2}\mathrm{Tr}\left(\left[\left(\Gamma^{(2)} + \mathbf{R}_k\right)^{-1} \right]_{hh} \partial_t \mathbf{R}_k^{hh} \right) - \mathrm{Tr}\left(\left[\left(\Gamma^{(2)} + \mathbf{R}_k\right)^{-1} \right]_{c\bar{c}} \partial_t \mathbf{R}_k^{\mathrm{gh}} \right). \tag{1.61}$$

1.3.2 A brief overview on the ASQG research program

Since the seminal work by Reuter, the FRG has been systematically used as a tool to investigate and characterize the RG-flow in QG. By now, there are many results in the literature pointing towards the existence of a UV FP in QG, providing indications that gravity might be consistently quantized as an asymptotically safe theory. In this section we present an overview of the current status of this research program[30].

The EH truncation:

The FRG was first applied to study the RG-flow in QG in a seminal paper by Reuter [50]. The basic idea was to adopt a simple truncation for Γ_k as a tentative solution for the FRG equation (Eq. (1.61)). At the practical level, Reuter used the EH-truncation (or EH-approximation) defined as a scale-dependent version of the (gauge-fixed) EH-action, i.e.

$$\Gamma^{\mathrm{trunc}}_{k,\mathrm{EH}}[h, c, \bar{c}\,; \bar{g}] = \frac{1}{16\pi G_{\mathrm{N},k}} \int_x \sqrt{g}\, \left(2\Lambda_{\mathrm{cc},k} - R(g)\right) + S_{\mathrm{g.f.}}[h, c, \bar{c}\,; \bar{g}]\,, \tag{1.62}$$

where $G_{\mathrm{N},k}$ and $\Lambda_{\mathrm{cc},k}$ denote, respectively, scale-dependent Newton's and cosmological constants. In this approximation, the gauge-fixing sector is assumed to have the same form as in the bare action. Plugging the EH-truncation as an *ansatz* in (1.61) and projecting both sides of the flow equation in the truncated subspace involving only the operators appearing in $\Gamma^{\mathrm{trunc}}_{k,\mathrm{EH}}$, we can extract the RG-flow of the dimensionless couplings G_k $(= k^{d-2} G_{\mathrm{N},k})$ and Λ_k $(= k^{-2}\Lambda_{\mathrm{cc},k})$,

$$\partial_t \Lambda_k = -2\Lambda_k + \frac{A_1 + 2B_1\,\Lambda_k + G_k(A_1 B_2 - A_2 B_1)}{2(1 + B_2 G_k)}\, G_k \coloneqq \beta_\Lambda(\Lambda_k, G_k)\,, \tag{1.63a}$$

$$\partial_t G_k = (d-2) G_k + \frac{B_1}{1 + B_2 G_k}\, G_k^2 \coloneqq \beta_G(\Lambda_k, G_k)\,. \tag{1.63b}$$

The coefficients A_1, A_2, B_1 and B_2 are computable quantities and depend on the dimensionless cosmological constant Λ_k and the space-time dimension d. It is important

[29]For more details on the derivation of the flow equation in QG, see, for instance, [38, 39].

[30]It should be emphasized that by no means the goal of this section is to provide a complete and self-contained overview of the literature. In this sense, we are going to cover only the results that are closely related to the content developed in the next chapters of this thesis. For updated reviews in ASQG, see e.g. [52, 95]. See also [38, 39, 188, 189] for pedagogical discussions.

to emphasize that these coefficients carry several scheme-dependencies (e.g., choice gauge, regulator, background, etc). Nevertheless, there are indications, based on explicit computations exploring various schemes in the EH-truncation, that the relevant qualitative properties are not severely affected by scheme variations. As an example, we show the explicit expressions computed in the Landau gauge, with Litim's-regulator (using type-Ib cutoff[31]) and employing the 4-sphere as the background. In this scheme, the coefficients A_i's and B_i's are given by

$$A_1 = \frac{3 + 7\Lambda_k - 16\Lambda_k^2}{3\pi(1 - 2\Lambda_k)(1 - 4\Lambda_k/3)}\,, \tag{1.64a}$$

$$A_2 = \frac{9 - 13\Lambda_k}{18\pi(1 - 2\Lambda_k)(1 - 4\Lambda_k/3)}\,, \tag{1.64b}$$

$$B_1 = \frac{-237 + 680\Lambda_k - 756\Lambda_k^2 + 368\Lambda_k^3}{72\pi(1 - 2\Lambda_k)^2(1 - 4\Lambda_k/3)}\,, \tag{1.64c}$$

$$B_2 = \frac{-48 + 97\Lambda_k - 42\Lambda_k^2}{108\pi(1 - 2\Lambda_k)^2(1 - 4\Lambda_k/3)}\,. \tag{1.64d}$$

With these expressions we can look for numerical solutions of the system[32]

$$\beta_\Lambda(\Lambda_k^*, G_k^*) = 0 \quad \text{and} \quad \beta_G(\Lambda_k^*, G_k^*) = 0\,, \tag{1.65}$$

resulting in a non-Gaussian FP at $(\Lambda_k^*, G_k^*) = (0.1307, 0.9786)$ with critical exponents $\theta_\pm = 2.3923 \pm 1.4221\, i$. Since $\mathrm{Re}(\theta_\pm) > 0$, such a FP is UV attractive for RG-trajectories lying in the $\Lambda_k \times G_k$ plane. In Fig. 1.4 we exhibit the portrait of the flow diagram obtained in the EH-truncation and containing UV complete trajectories for a variety of initial conditions[33].

Further evidences from extended truncations:

The EH-truncation provides a first hint, based on FRG techniques, towards a legitimate 4-dimensional FP in QG. However, it is natural to doubt whether this FP is a physical property of the RG-flow or just an artifact of a simple approximation. This questions have been investigated by several authors and, by now, there is a vast collection of results indicating that this FP is not a simple artifact of the EH-truncation.

[31] See Chap. 6 of Ref. [38] for the nomenclature of different cutoff choices.

[32] It interesting to mention that the fixed point solutions associated with the beta-function computed by Reuter [50] were first computed in Ref. [53].

[33] See Ref. [54] for a detailed discussion concerning the flow diagram in ASQG.

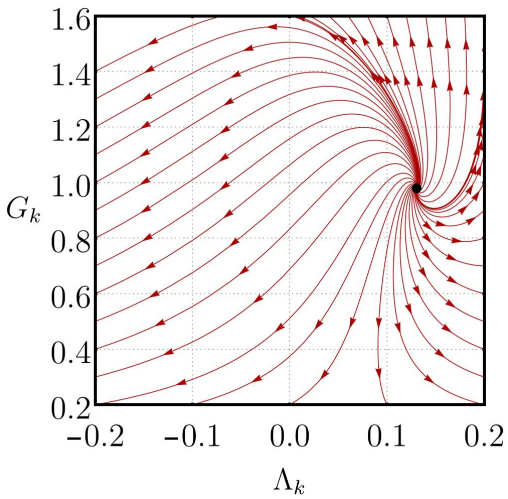

Figure 1.4: RG-flow obtained in the EH-truncation. The lines represent UV complete RG-trajectories for various IR initial conditions. In this plot, the arrows points towards the IR. The (black) dot indicate the UV FP at $(\Lambda_k^*, G_k^*) = (0.1307, 0.9786)$. We note that the spiraling behavior around the FP is a consequence of critical exponents with non-vanishing imaginary part.

Most of the search for suitable UV FPs beyond the EH-approximation consist in the use of extended truncation including higher-order curvature operators in the *ansatz* for Γ_k. In this sense, one direction that has been systematically investigated is the $f(R)$-approximation, defined by the following truncation[34]

$$\Gamma^{\text{trunc}}_{k,f(R)} = \int_x \sqrt{g}\, f_k(R)\,, \tag{1.66}$$

where $f_k(R)$ represent a scale-dependent function of the curvature scalar. In the case of polynomial truncations of the form $f_k(R) = \sum_{n=0}^{N_{\max}} k^{4-2n} g_{k,n}\, R^n$, Eq. (1.61) allow us to extract the RG-flow of the dimensionless couplings $\{g_{k,n}\}_{n=0,\cdots,N_{\max}}$. Calculations performed in terms of the Litim's regulator and using a maximally symmetric background (e.g. a 4-sphere), allows us to derive analytical beta functions for an arbitrary[35] $N_{\max}$ [58–60,73,90]. The structure of the beta function in the polynomial truncation allows us to search for UV FP within approximations involving several operators beyond the EH sector. In table 1.1, we summarize the progress on the investigation of FPs in the polynomial $f(R)$-truncation. In particular, the most remarkable result is the stabilization of the number of relevant directions against the inclusion of higher-order operators. As it was pointed out in Ref. [73,90], the critical exponents exhibit a "near-

[34] In most of the investigations of extended truncations the gauge-fixing is considered to be the same as in the EH-approximation, therefore, in these cases, we simply omit the gauge-fixing sector.

[35] Despite being analytical, the derivation of beta function in a polynomial $f(R)$-truncation requires the use of computer algebra systems (such as *Mathematica*). Therefore, arbitrariness of $N_{\max}$ is subject to computer limitations.

Ref.	Operators beyond EH	FP	# rel. dir.	$(\mathrm{Re}(\theta_1), \mathrm{Re}(\theta_2), \mathrm{Re}(\theta_3))$
[55]	$\sqrt{g}R^2$	✓	3	$(2.15, 2.15, 28.8)$
[60]	$\sqrt{g}R^2, \cdots, \sqrt{g}R^6$	✓	3	$(2.39, 2.39, 1.51)$
[59]	$\sqrt{g}R^2, \cdots, \sqrt{g}R^8$	✓	3	$(2.41, 2.41, 1.40)$
[73]	$\sqrt{g}R^2, \cdots, \sqrt{g}R^{34}$	✓	3	$(2.50, 2.50, 1.59)$
[90]	$\sqrt{g}R^2, \cdots, \sqrt{g}R^{70}$	✓	3	$(2.53, 2.53, 1.66)$

Table 1.1: Summary of results in the polynomial $f(R)$-truncation. The check-mark indicates the existence of suitable FPs within the truncation under investigation. These results point towards the existence of 3-dimensional critical surfaces. In the last column, we show the critical exponents associated with the relevant directions, exhibiting certain stability in the numerical values.

canonical" behavior, indicating that the critical exponents associated with higher-order operators are essentially determined in terms of the canonical mass dimension of these operators.

It is interesting to mention that the $f(R)$-approximation also has been investigated beyond the polynomial truncation. In particular, within the $f(R)$-truncation, it is possible to derive a flow equation for the dimensionless function $\tilde{f}_k(\tilde{R}) = k^{-4} f_k(k^2 \tilde{R})$ (where $\tilde{R} = k^{-2} R$). In this case, the flow equation takes the form

$$\partial_t \tilde{f}_k(\tilde{R}) = \mathcal{F}(\tilde{f}_k(\tilde{R}), \tilde{f}'_k(\tilde{R}), \tilde{f}''_k(\tilde{R}))\,. \tag{1.67}$$

In this context, the basic idea is to search for "fixed functions", $\tilde{f}_*(\tilde{R})$, defined as solutions of an ordinary differential equation of the form

$$\mathcal{F}(\tilde{f}_*(\tilde{R}), \tilde{f}'_*(\tilde{R}), \tilde{f}''_*(\tilde{R})) = 0\,. \tag{1.68}$$

This approach has been explored by some authors and provides further indications for AS beyond the polynomial truncation [68, 69, 79, 80].

Although the $f(R)$-truncation permits important tests regarding the existence of a gravitational FP, this approximation involve some issue that motivates other directions of investigation. In particular, the $f(R)$-truncation does not include operators constructed with more sophisticated contractions of geometrical objects. Assuming canonical power counting as a good guiding principle to define a truncation, we might expect that curvature squared operators like R^2, $R_{\mu\nu}R^{\mu\nu}$ and $R_{\mu\nu\alpha\beta}R^{\mu\nu\alpha\beta}$ play an important role in the RG-flow of QG[36]. At the practical level, computations involving curvature squared terms are rather complicated, in special, due to the impossibility

[36] In $d = 4$, the Gauss-Bonnet theorem allows express the invariant $R_{\mu\nu\alpha\beta}R^{\mu\nu\alpha\beta}$ as a combination of R^2 and $R_{\mu\nu}R^{\mu\nu}$.

of disentangle the running of the multiple coupling in a maximally-symmetric background. Despite this complication, some effort has been done concerning the search of UV FP based in a truncation of the type [57, 60, 62, 63, 72, 94]

$$\Gamma^{\text{trunc}}_{\mathcal{R}^2} = \Gamma^{\text{trunc}}_{k,\text{EH}} + \int_x \sqrt{g}\, \left(\alpha_k R^2 + \beta_k R^2_{\mu\nu} + \gamma_k R^2_{\mu\nu\alpha\beta}\right)\,. \tag{1.69}$$

Recent investigations based on calculations performed around an arbitrary background corroborate the results from $f(R)$-truncation pointing towards the existence of a suitable UV FP featuring a 3-dimensional critical surface [72, 94].

Further studies involving operators beyond the Ricci scalar were done [89], for example, by means of a truncation analogous to the $f(R)$-approximation, namely

$$\Gamma^{\text{trunc}}_{FZ} = \int_x \sqrt{g}\, \left(F_k(R^2_{\mu\nu}) + R\, Z_k(R^2_{\mu\nu})\right)\,. \tag{1.70}$$

In this case, investigations involving polynomial truncations for F_k and Z_k provide further indications for a UV FP with 3-relevant directions. Moreover, a highly non-trivial test for AS includes the Goroff-Sagnotti counter term as part of the truncation and gives further support to the aforementioned results [85].

Background approximation and the fluctuation approach:

The list of results above discussed were obtained by a specific approach usually referred as background approximation. In this case, the flow equation (Eq. 1.61) is explored in the regime of vanishing fluctuation fields, that is

$$\begin{aligned}\partial_t \bar{\Gamma}_k = \frac{1}{2}\text{Tr}\bigg(\Big[\big(\Gamma^{(2)} + \mathbf{R}_k\big)^{-1}\Big]_{hh} \partial_t \mathbf{R}_k^{hh} \bigg)\bigg|_{h,\,c,\,\bar{c}=0} \\ - \text{Tr}\bigg(\Big[\big(\Gamma^{(2)} + \mathbf{R}_k\big)^{-1}\Big]_{c\bar{c}} \partial_t \mathbf{R}_k^{\text{gh}} \bigg)\bigg|_{h,\,c,\,\bar{c}=0}\,,\end{aligned} \tag{1.71}$$

where $\bar{\Gamma}_k[\bar{g}] = \Gamma_k[0,0,0;\bar{g}]$ denotes the background EAA (bEAA). Nevertheless, the background approximation for the FRG exhibits some issues related with symmetry identities. In particular, in the background field approximations we typically use truncations that satisfy (the schematic equation)

$$\frac{\delta^2 \Gamma_k}{\delta h^2}\bigg|_{h,\,c,\,\bar{c}=0} = \frac{\delta^2 \bar{\Gamma}_k}{\delta \bar{g}^2} + \text{g.f. terms}\,. \tag{1.72}$$

However, this relation is known to be incompatible with the appropriate split Ward identities (or Nielsen identities) in the FRG (see, e.g., [190] for a recent discussion). This problem motivates complementary investigations with approaches beyond background approximation.

An alternative method of systematic investigation, usually called fluctuation approach, uses a vertex expansion as a way to extract approximated solutions from the FRG equation [190]. In this context, the basic idea is to derive flow equations for proper vertices

$$\Gamma_k^{(n;2m)}[\bar{g}] \sim \left.\frac{\delta^{n+2m}\Gamma_k}{\delta h^n \delta c^m \delta \bar{c}^m}\right|_{h,\,c,\,\bar{c}=0} . \tag{1.73}$$

Although less explored than the background approximation, in the last few years there was some important progress in the study of ASQG based in the fluctuation approach. Most of the computations in this direction make use of the (desired) property of background independence in order to set $\bar{g}_{\mu\nu}$ as the flat (Euclidean) metric $\delta_{\mu\nu}$. The updated results based on the fluctuation approach include the RG-flow of 2-, 3- and 4-point vertices associated with the graviton fluctuation fields [67,75,78,83,87,190]. These results provide further non-trivial evidence for a suitable gravitational FP with the same qualitative features obtained through the background approximation.

Quantum gravity-matter systems:

Up to now we have discussed evidence for a FP in pure gravity systems. Nevertheless, matter[37] exists and, therefore, a complete quantum theory for gravity should also be consistent with such degrees of freedom. The ASQG approach exhibits the attractive feature of being formulated in the same setting as we use to describe particle physics, namely, using QFT techniques. In this sense, the inclusion of matter in the ASQG scenario turns out to be straightforward and there are several works investigating the RG-flow within truncations involving gravitational and matter degrees of freedom [191–201].

The inclusion of matter is not only necessary, but, it could also provide consistency tests for QG candidates. In the ASQG framework, the first test to be considered concerns the impact of matter fields in the FP structure for gravity. In particular, do the indications for a gravitational FP, obtained for pure gravity, remain stable after the inclusion of matter? This question has a strong motivation from the beta function for YM theories. In the case of QCD, for example, the 1-loop beta function depends on the number of colored fermions (N_f) and scalars (N_s) in the following way [132,133]

$$\beta_{\mathrm{QCD}}^{\text{1-loop}} = -\left(11 - \frac{N_\mathrm{s}}{3} - \frac{2N_\mathrm{f}}{3}\right)\frac{g_{\mathrm{QCD}}^3}{16\pi^2} . \tag{1.74}$$

As we can observe, fermions and scalars contribute with the opposite sign in comparison with the pure YM contribution. As a consequence, if the number of fermions and/or

[37] Here, by "matter" we meant all the non-gravitational degrees of freedom, i.e. including gauge fields as part of the matter sector.

scalars is large enough, it can flip the overall sign of $\beta_{\rm QCD}^{\text{1-loop}}$, destroying the property of asymptotic freedom.

The possibility of such a mechanism in QG can be easily understood from the 1-loop beta function for the (dimensionless) Newton coupling in a setting of gravity minimally coupled to matter. Based on the scheme of calculation discussed in [193], we have

$$\beta_G^{\text{1-loop}} = 2G_k - \frac{G_k^2}{6\pi}(46 + 4N_{\rm v} - N_{\rm s} - 2N_{\rm f})\,, \tag{1.75}$$

with $N_{\rm v}$, $N_{\rm s}$ and $N_{\rm f}$ representing the number of vectors, scalar and fermions, respectively, coupled to gravity. The existence of a non-Gaussian UV FP G^* imposes the following constraint on the number of matter fields: $46 + 4N_{\rm v} - N_{\rm s} - 2N_{\rm f} > 0$. This inequality indicates that too many fermions and/or scalars can destroy the gravitational FP. The impact of matter in the ASQG scenario has been systematically explored (beyond the 1-loop approximation) in Ref. [193], testing the compatibility of several types of matter content with the existence of a gravitational UV FP. As an example, the results reported in Ref. [193] indicate that the matter content corresponding to the SM of particle physics is consistent with ASQG.

Investigations based in the fluctuation approach, on the other hand, leads to a different conclusion. As it has been argued in [195,196], graviton fluctuations dominate in the high-energy regime in such a way that the existence of a gravitational UV FP remains stable after the introduction of arbitrarily many matter fields, provided that the latter is sufficient weakly (self-)coupled in the UV.

The interplay gravity-matter also exhibits attractive features when explored in the other direction, i.e., concerning the impact of gravity in the matter sector [97, 100, 101, 202–226]. In this case, the impact of graviton fluctuations on the RG flow of matter couplings might help to impose phenomenological constraints on the gravitational theory. As we are going to discuss in mode detail in Chap. 4, this interplay potentially might help to bridge the gap between QG effects and experimental observations [97, 101, 210, 211, 215] (see [95, 96]for reviews).

Current challenges in ASQG:

Despite the considerable progress in the last two decades, mainly due to the use of FRG techniques, the AS program for QG still exhibits several intriguing questions. In the following, we present some of the challenges that deserve further attention. For a recent critical analysis of the ASQG research program, see [227, 228].

- **Euclidean *versus* Lorentzian signatures:** One of the most important problems in the research of ASQG is the use of Euclidean methods. In fact, the Wilsonian coarse-graining procedure embedded in the FRG is intrinsically related to the Euclidean notion of momentum shell. In non-gravitational relativistic QFTs one can usually proceed with Euclidean calculations and move to the Lorentzian setting through a Wick rotation. In QG this question is much more subtle since the Wick rotation is not a well-defined procedure in curved manifolds. In the gravitational setting, the causal structure inherited from the Lorentzian signature leads to important physical consequences, such as the existence of event horizons, which has no counterpart in the Euclidean case. Some steps towards the inclusion of causal structures in the AS program were done [66, 86, 197] by means of the Arnowitt-Deser-Misner (ADM) formalism, however, this is still far way from conclusive results.

- **Background independence:** In contrast with ordinary QFT, where the background field method is introduced as a convenient tool to perform gauge invariant calculations, in the QFT approach for QG the use of the background field method seems to be unavoidable. In fact, to define a coarse-graining procedure one has to introduce a non-dynamical covariant derivative (defined w.r.t. a background metric) used to distinguish slow modes and fast modes. This approach naturally raises the question of background independence in QG, which states that physical quantities should not depend on the choice of a particular background. Within the FRG framework, background independence is encoded in non-trivial split Ward identities emerging from the fact that the starting point for a functional quantization is a gravitational action depending on a single metric $g_{\mu\nu}$ [174, 190, 229–231]. For recent investigations taking into account the split Ward identities in QG see [65, 200, 232–238].

- **Propagating modes, unitarity and instabilities:** One important open issue in the AS program is the determination of propagating degrees of freedom in QG. As it is usually known from perturbative approaches, this question is not settled by simply fixing the field content of the theory. As an example, curvature squared gravity carries the same field content as in the EH action, however, it generates additional propagating modes due to higher-derivative contributions [20]. This point is deeply connected with the unitarity problem in perturbative curvature squared models[38]. Depending on the structure of the propagating modes, the unitarity problems is replaced by tachyonic instabilities. Within the non-perturbative setting this questions become much more complicated, since the analysis demands the knowledge of the full propagator (see [92, 239] for recent discussions). Up to this point, the AS program for QG does not provide any satisfactory answer to these questions.

[38] See [21–28] for recent proposals in this topic.

- **Controlled results and alternative methods:** As it was discussed in Sect. 1.2.3, the use of truncations is a practical way to access non-perturbative information from FRG equation. Nevertheless, the lack of control on the systematic errors involved in FRG truncations raises the question on how reliable are the results obtained with such a method. In non-gravitational theories the use of FRG truncations is usually confronted with other methods, providing further reliability [185–187]. In the QG framework, this strategy is not evident. The multiple approaches for QG are constructed on top of very different premises, making the comparison among them a very challenging task. In lattice approaches like causal/Euclidean dynamical triangulation (CDT/EDT) the search for a continuum limit, manifested as a second order phase transition, is a promising road for complementary evidence for AS in QG based on alternative non-perturbative methods [240–243]. Currently there is some effort to bridge the gap between these approaches based on the search of FP solutions in tensor models for QG [244] (usually interpreted as a dual representation of dynamical triangulation methods).

- **Physical observables in ASQG:** Even if one manages to solve the aforementioned theoretical problems (which are crucial for a self-consistent description), ultimately, a quantum theory for the gravitational interaction needs to be confronted with experimental tests. In QG, the search for direct observations is an extremely challenging task, since QG-effects are expected to be suppressed by positive powers of E/M_{Pl} (where E denotes the characteristic energy of a physical process and M_{Pl} denotes the Planck mass). In Chap. 4 we return to this point in more detail, where we discuss a possible link to observation based on the gravity-matter interplay. Furthermore, even the definition of a physical observable in QG is quite subtle. Actually, the difficulty appears already at the classical level, since the underlying *Diff* symmetry makes the notion of space-time point unphysical and implies that one cannot contruct local (gauge invariant) observable quantities[39].

[39]See [245–247] for more details concerning this point.

Chapter 2

Flowing in the Unimodular Theory Space

2.1 Unimodular Gravity

2.1.1 What is and why unimodular gravity?

GR has been established as a paradigm concerning the classical description of gravity. However, this is not the only viable classical theory. Starting from a slightly different premise, unimodular gravity (UG) also define a consistent setting to describe the gravitational interaction at the classical level. The difference between GR and UG lies in the definition of the configuration space associated with these theories. In UG, the space-time metric $g_{\mu\nu}$, the fundamental dynamical variable, is defined on top of a configuration space subject to the restriction[1] [102–108]

$$\det g_{\mu\nu}(x) = \omega(x)^2 \,, \tag{2.1}$$

where $\omega = \omega(x)$ is a non-dynamical function that defines a fixed volume form

$$\mathrm{Vol}_d = \omega(x)\; dx^0 \wedge \cdots \wedge dx^{d-1} \,. \tag{2.2}$$

UG is closely related to the unimodular gauge in GR. In the later, a convenient choice of coordinates allows us, locally, to fix the metric's determinant to be one [110]. In UG, however, the restriction to the metric's determinant is assumed *a priori*.

Classically, the dynamics of UG is encoded in the unimodular version of the EH action, i.e.

$$S_{\mathrm{UG}}[g_{\mu\nu}] = -\frac{1}{16\pi G_{\mathrm{N}}}\int_x \omega\, R(g) \,. \tag{2.3}$$

[1]Recall that we using Euclidean conventions. In this case, the metric's determinant is positive.

Taking the variation of $S_{\mathrm{UG}}[g_{\mu\nu}]$ w.r.t. to the dynamical metric $g_{\mu\nu}$, we find

$$\tilde{\delta} S_{\mathrm{UG}}[g_{\mu\nu}] = -\frac{1}{16\pi G_{\mathrm{N}}} \int_x \omega \, R^{\mu\nu} \, \tilde{\delta} g_{\mu\nu} \, . \tag{2.4}$$

Note that we have dropped out a boundary term of the form $g_{\mu\nu} \, \tilde{\delta} R^{\mu\nu}$. The notation "$\tilde{\delta}$" indicates that we are taking into account only variations that preserve the unimodularity condition (2.1). In general, the (unrestricted) variation of the metric's determinant gives $\delta(\det g_{\mu\nu}) = (\det g_{\mu\nu}) \, g^{\alpha\beta} \delta g_{\alpha\beta}$. Therefore, the unimodular-preserving functional variation is subject to the tracelessness condition

$$g^{\mu\nu} \, \tilde{\delta} g_{\mu\nu} = 0 \, . \tag{2.5}$$

In this sense, we can express $\tilde{\delta} g_{\mu\nu}$ as the traceless part of $\delta g_{\mu\nu}$, namely

$$\tilde{\delta} g_{\mu\nu} = \left(\delta^{\alpha\beta}_{\mu\nu} - \frac{1}{d} g_{\mu\nu} g^{\alpha\beta} \right) \delta g_{\alpha\beta} \, . \tag{2.6}$$

Plugging this expression in (2.4), the functional variation of the UG action can be recast in the following way

$$\tilde{\delta} S_{\mathrm{UG}}[g_{\mu\nu}] = -\frac{1}{16\pi G_{\mathrm{N}}} \int_x \omega \, \left(R^{\mu\nu} - \frac{1}{d} g^{\mu\nu} R \right) \, \delta g_{\mu\nu} \, . \tag{2.7}$$

The dynamical field equations for UG, in the absence of matter, can be readily obtained by equating the contribution inside the parenthesis to zero, resulting in the traceless part of the Einstein's field equation (in vacuum)

$$R_{\mu\nu} - \frac{1}{d} g_{\mu\nu} R = 0 \, . \tag{2.8}$$

An important difference between the formulations of GR and UG lies on the corresponding symmetry groups. As it is well known, GR is constructed using covariance under general coordinate transformations as a guiding principle. In such a case, GR is said to be symmetric under *Diff* transformations acting on the space-time metric according to

$$\delta_\epsilon g_{\mu\nu} = g_{\mu\alpha} \nabla_\nu \epsilon^\alpha + g_{\nu\alpha} \nabla_\mu \epsilon^\alpha \, , \tag{2.9}$$

In the case of UG, however, the situation is slightly different. Acting with δ_ϵ on the metric's determinant we have

$$\delta_\epsilon (\det g_{\mu\nu}) = 2 \, (\det g_{\mu\nu}) \nabla_\mu \epsilon^\mu \, . \tag{2.10}$$

The fixed determinant condition used to define UG requires $\nabla_\mu \epsilon^\mu = 0$, i.e., the generators of *Diff* are subject to a transversality condition. In this sense, the symmetry group of UG gravity is characterized by a subset of *Diff* transformations generated by transverse vectors. This subset of transformations defines the *TDiff* group. In order to distinguish the notation, we represent *TDiff* transformations as

$$\delta_{\epsilon_{\rm T}} g_{\mu\nu} = g_{\mu\alpha} \nabla_\nu \epsilon^\alpha_{\rm T} + g_{\nu\alpha} \nabla_\mu \epsilon^\alpha_{\rm T} \,, \tag{2.11}$$

where $\epsilon^\mu_{\rm T} = \epsilon^\mu_{\rm T}(x)$ denotes a transverse vector field subject to the condition $\nabla_\mu \epsilon^\mu_{\rm T} = 0$.

It is important to emphasize that UG should not be confused with the so-called *TDiff*-gravity [248]. Although both settings exhibit symmetry under transformations belonging to the *TDiff* group, the latter does not impose any restriction on the metric's determinant. As a consequence, in the case of *TDiff*-gravity there is an additional propagating degree of freedom in comparison with UG. Typically, *TDiff*-gravity is considered to be equivalent to scalar-tensor theories [248, 249].

There are various ways of implementing the unimodularity condition at the practical level and, depending on the choice, the underlying symmetry might be another one [122, 250]. A frequently used formulation is based on the change of variable $g_{\mu\nu} \mapsto \gamma_{\mu\nu}$ according to [120]

$$g_{\mu\nu} = (\omega^{-2} |\gamma|)^{-1/d} \gamma_{\mu\nu} \,, \tag{2.12}$$

where $\gamma_{\mu\nu}$ correspond to a tensorial density (a "densitized" metric) and we have defined $|\gamma| = \det \gamma_{\mu\nu}$. In such a case, it is not difficult to verify that the unimodularity condition $\det g_{\mu\nu} = \omega^2$ is satisfied irrespective of any restriction to the new dynamical variable $\gamma_{\mu\nu}$. Expressing the unimodular action in terms of $\gamma_{\mu\nu}$, we find

$$S_{\rm UG}[\gamma_{\mu\nu}] = -\frac{1}{16\pi G_{\rm N}} \int_x \omega^{(d-2)/d} \, |\gamma|^{-1/d} \left(R(\gamma) + \chi_d \left(|\gamma|^{-1} \, \nabla |\gamma| - 2\, \omega^{-1} \, \nabla \omega \right)^2 \right) , \tag{2.13}$$

where $\chi_d = (d-1)(d-2)/4d^2$. In addition to the symmetry under *TDiff* transformations, the UG action formulated in terms of $\gamma_{\mu\nu}$ also exhibit invariance w.r.t. Weyl transformations

$$\gamma_{\mu\nu} \;\mapsto\; \gamma'_{\mu\nu} = \Omega^2 \gamma_{\mu\nu} \,, \tag{2.14}$$

with $\Omega = \Omega(x)$ denoting a local dilation parameter. Accordingly, the symmetry group associated with this formulation of UG correspond to *WTDiff* (Weyl + *TDiff*). It is important to emphasize that the change of variables in Eq. (2.12) is non-invertible. Therefore, the equivalence between UG formulated in terms of $g_{\mu\nu}$ or $\gamma_{\mu\nu}$ is not guaranteed by field redefinition theorems. Classical and 1-loop results indicate that these two versions of UG are equivalent [122], however, we cannot say anything beyond such approximations.

The inclusion of matter follows the usual recipe, i.e., by adding a contribution $S_{\rm matter}[\Phi; g]$ (we denote by Φ a generic matter field multiplet) to the unimodular action. Taking the functional variation of $S_{\rm matter}[\Phi; g]$, we find

$$\tilde{\delta} S_{\rm matter}[\Phi; g] = \frac{1}{2} \int_x \omega\, \tilde{T}^{\mu\nu} \tilde{\delta} g_{\mu\nu} = \frac{1}{2} \int_x \omega \left(\tilde{T}^{\mu\nu} - \frac{1}{d} g^{\mu\nu} \tilde{T}^{\alpha}{}_{\alpha} \right) \delta g_{\mu\nu} \,, \tag{2.15}$$

where we have defined the energy-momentum tensor

$$\tilde{T}^{\mu\nu} = \frac{2}{\omega} \frac{\delta S_{\rm matter}}{\delta g_{\mu\nu}} \,. \tag{2.16}$$

The resulting field equation for UG in the presence of matter takes the form

$$R_{\mu\nu} - \frac{1}{d} g_{\mu\nu} R = 8\pi G_{\rm N} \left(\tilde{T}_{\mu\nu} - \frac{1}{d} g_{\mu\nu} \tilde{T}^{\alpha}{}_{\alpha} \right) \,. \tag{2.17}$$

The underlying symmetry w.r.t. *TDiff* transformations, however, does not guarantee covariant conservation of the energy-momentum tensor $\tilde{T}_{\mu\nu}$. In general, *TDiff* symmetry allows us to derive the weaker condition

$$\nabla_\mu \tilde{T}^{\mu\nu} = \nabla^\nu \Sigma \,, \tag{2.18}$$

with $\Sigma = \Sigma(x)$ denoting some scalar field [115]. In principle, this condition is interpreted as an energy diffusion process. Nevertheless, it is possible to restore the usual condition for energy-momentum conservation by observing that the field equation (2.17) remains invariant under the redefinition

$$\tilde{T}_{\mu\nu} \;\mapsto\; \tilde{T}'_{\mu\nu} = \tilde{T}_{\mu\nu} + g_{\mu\nu}\, \psi \,, \tag{2.19}$$

where $\psi = \psi(x)$ denote an arbitrary scalar function. We can use this arbitrariness in our favor to define an "improved" energy-momentum,

$$T_{\mu\nu} = \tilde{T}_{\mu\nu} - g_{\mu\nu}\, \Sigma \,, \tag{2.20}$$

such that it satisfies the usual equation energy-momentum conservation

$$\nabla_\mu T^{\mu\nu} = 0 \,. \tag{2.21}$$

In this sense, the energy-momentum conservation in UG appears as a subsidiary condition. In terms of $T_{\mu\nu}$, the field equation for UG reads

$$R_{\mu\nu} - \frac{1}{d} g_{\mu\nu} R = 8\pi G_{\mathrm{N}} \left(T_{\mu\nu} - \frac{1}{d} g_{\mu\nu} T^{\alpha}_{\ \alpha} \right) . \tag{2.22}$$

Despite of being defined over different configuration spaces, at the classical level, UG and GR are dynamically equivalent theories. Dynamical equivalence translates to the possibility of mapping the classical field equations from one theory to the other. On the one hand, starting from GR we can directly achieve Eq. (2.22) by projecting the Einstein's equation on its traceless part. On the other hand, starting from UG the situation is slightly more subtle. In such a case, it is convenient to recast (2.22) in the following way (for $d > 2$)

$$G_{\mu\nu} - 8\pi G_{\mathrm{N}} T_{\mu\nu} + \frac{d-2}{2d} g_{\mu\nu} \left(R + \frac{16\pi G_{\mathrm{N}}}{d-2} T^{\alpha}_{\ \alpha} \right) = 0 \,, \tag{2.23}$$

where $G_{\mu\nu} = R_{\mu\nu} - \frac{1}{2} g_{\mu\nu} R$ denotes the Einstein tensor. Acting with ∇^{μ} and using the contracted Bianchi $\nabla^{\mu} G_{\mu\nu} = 0$ along with the energy-momentum conservation (Eq. (2.21)), we find

$$\nabla_{\nu} \left(R + \frac{16\pi G_{\mathrm{N}}}{d-2} T^{\alpha}_{\ \alpha} \right) = 0 \,. \tag{2.24}$$

This equation can be easily integrated, resulting in

$$R + \frac{16\pi G_{\mathrm{N}}}{d-2} T^{\alpha}_{\ \alpha} = \frac{2d}{d-2} \Lambda_0 \,, \tag{2.25}$$

where Λ_0 denotes an integration constant (the multiplicative factor $2d/(d-2)$ has been introduced for convenience). Plugging this result back into Eq. (2.23), we recover the Einstein's field equations for GR,

$$R_{\mu\nu} - \frac{1}{2} g_{\mu\nu} R + \Lambda_0 g_{\mu\nu} = 8\pi G_{\mathrm{N}} T_{\mu\nu} \,. \tag{2.26}$$

It is interesting to observe that the reconstruction of the Einstein's field equations starting from UG makes explicit use of the subsidiary condition encoded in (2.21). If this condition was not taken into account, there would be an extra (diffusive) term in (2.26) [251–254], spoiling the dynamical equivalence between UG and GR.

One of the most interesting features of UG is the origin of the cosmological term in (2.26). In the case of GR, the cosmological constant appears as the vacuum energy contribution in the EH action. Since this term has a dynamical nature, due to the coupling with the metric's determinant, it appears in the Einstein's field equations. In UG the situation is quite different. In such a case, even if we include the vacuum energy contribution to the unimodular action, this term will not contribute to the dynamical field equation since the metric's determinant is fixed. In this sense, we usually say that the vacuum energy does not gravitate in UG. The "cosmological constant" Λ_0 appearing in (2.26), however, arises as a simple (arbitrary) integration constant and has nothing to do with any possible vacuum energy contribution eventually included in the unimodular action. The status of the cosmological constant in UG has been one of most important motivation for this formulation, since it could provide a natural solution to the "first cosmological constant problem"[2] [103, 105, 107–109, 111–115]. In the context of GR, such a problem appears as a fine-tuning in the cosmological constant term in order to match its observed value and, at the same time, compensate quantum correction proportional to the fourth-power of a cutoff scale. The "unimodular solution" simply lies on the decoupling of the vacuum energy. In such a case, the cosmological term appearing in (2.26) is unrelated to the vacuum energy and, therefore, no fine-tuning mechanism is required.

2.1.2 Unimodular quantum gravity

As it was discussed in the previous section, although UG features a different configuration space in comparison to GR, these theories are dynamically equivalent at the classical level. The quantum (in)equivalence between UG and RG, however, has not been established in a conclusive way [115, 116, 118–127]. At a first sight, the dynamical interaction terms appearing in UG exhibit a very different structure with respect to GR. As an example, if we consider a scalar field coupled to gravity, in the unimodular version, the (momentum independent) scalar potential does not couple directly to gravity. Based on this observation, there is no strong reason to believe that both settings describe equivalent quantum theories. In this sense, these theories might describe different quantum regimes, but with the same classical limit.

The computation of tree-level (on-shell) amplitudes involving the scattering of 3-, 4- and 5- gravitons indicates that UG and GR produce the same results, despite of the considerable differences in the structure of vertices and propagators [121]. Moreover, as it was pointed out in Ref. [115], the 1-loop effective action of UG takes the same functional form (up to an arbitrary constant term) as the 1-loop effective action of GR evaluated at unimodular metrics. As it was argued in Ref. [115], this result is sufficient to establish the equivalence between UG and RG at the level of 1-loop quantum equations of motion. These results, however, are not completely conclusive. Investigations based on the derivation of the path integral of UG starting from the Hamiltonian formalism indicates that those theories present different features at the quantum level [123].

[2] Actually, it is possible to argue that the "first cosmological constant problem" is more an aesthetic issue than a physical problem.

The lack of consensus concerning the quantum equivalence between UG and GR triggers the question on whether would be possible to construct an asymptotically safe theory starting from UG. Moreover, if viable, it is intriguing to explore whether the unimodular version of ASQG shares the same (physical) properties with the standard scenario constructed on top of GR. Conceptually, the unimodular and standard[3] versions of ASQG differ at the level of theory spaces, since they are defined in terms of different symmetry groups. A particularly important example is associated to the cosmological constant term. In the theory space defined by *Diff*-invariant operators, the "volume operator" which is associated with the cosmological constant corresponds to a direction in the theory space. Meanwhile, in the unimodular case, the volume operator is non-dynamical and, therefore, decouples from the underlying theory space.

A natural question concerning the quantization of UG is how to implement the unimodularity condition in the formulation of a quantum theory. In the framework of path integral quantization, the basic idea is to define a functional measure $\mathcal{D}g_{\mu\nu}$ (or $\mathcal{D}h_{\mu\nu}$, for the fluctuation field $h_{\mu\nu}$) restricted to unimodular metrics. At the practical level, there are multiple ways of implementing such a restriction. One possibility, commonly employed in the perturbative setting [120–122], relies on the use of $\gamma_{\mu\nu}$ (see Eq. (2.12)) as the fundamental "integration variable". Other possibilities include the use of Lagrange multipliers and Stückelberg (auxiliary) fields [116,123]. In the present thesis we follow the same strategy as in [125,126], which combines the background field method with the exponential parameterization for the metric. This parameterization, first introduced in the context of $2+\epsilon$ expansion [255–257], and later applied in the FRG framework [80,81,84,91,125,126,128,194,198,199,223,258–262], is defined in the following way[4]

$$g_{\mu\nu} = \bar{g}_{\mu\alpha}\,[\,\exp(\kappa\, h^{\cdot}_{\ \cdot})\,]^{\alpha}{}_{\nu} = \bar{g}_{\mu\nu} + \kappa\, h_{\mu\nu} + \sum_{n=2}^{\infty} \frac{\kappa^n}{n!} h_{\mu\alpha_1}\cdots h^{\alpha_{n-1}}{}_{\nu}\,, \tag{2.27}$$

where $\bar{g}_{\mu\nu}$ represents a background metric and we have defined $\kappa = (32\pi G_{\rm N})^{1/2}$. The main advantage of using the exponential parameterization is the fact that one can express the metric determinant as $\det g_{\mu\nu} = \det \bar{g}_{\mu\nu}\, {\rm e}^{h^{\rm tr}}$ (with $h^{\rm tr} = \bar{g}^{\mu\nu}h_{\mu\nu}$) and, therefore, the unimodularity condition can be easily implemented by combining $\det \bar{g}_{\mu\nu} = \omega^2$ with the tracelessness condition $h^{\rm tr} = 0$. From this perspective the functional quantization of UG translates into a path integral over traceless fluctuations.

While the standard ASQG scenario has been extensively explored in the literature, only a few number of works are dedicated to the unimodular theory space [125,126,128,

[3]To make clear distinction, we use the nomenclature "standard ASQG" as a reference to the usual AS scenario based in the quantization of *Diff*-invariant theories.

[4]See appendix B for more details concerning the exponential parameterization in QG.

129]. In Refs. [125, 128], the unimodular version of the EH (uEH) truncation, namely,

$$\Gamma_k^{\mathrm{uEH}} = -\frac{1}{16\pi G_{k,\mathrm{N}}} \int_x \omega\, R(g)\,, \tag{2.28}$$

was employed to extract the flow of the Newton coupling. The results obtained within the uEH truncation provide indications for UV FPs in the unimodular theory space. Later on, the unimodular version of the $f(R)$-truncation was investigated in Ref. [126], providing further indications for FP solutions in unimodular QG. In all these investigations, the unimodularity condition was implemented by means of the exponential parameterization above discussed. An alternative approach was adopted in [129], with a different formulation for UG involving a Stückelberg field[5], also showing indication for suitable FPs in UG.

An additional subtlety concerning the functional quantization of UG was pointed out in [115, 122]. In fact, when applying the Faddeev-Popov quantization procedure one usually identify the functional integral over the generators of a given gauge group as the volume factor of such a group. For example, in the usual QG gravity formulation based on the quantization of GR, the volume associated with the *Diff* group is usually expressed as

$$V_{Diff} = \int \mathcal{D}\epsilon^\mu\,, \tag{2.29}$$

where ϵ^μ denotes the generator of infinitesimal *Diff* transformations. In analogy, the naive expectation for the *TDiff* case is that one should identify V_{TDiff} with the functional integral

$$\int \mathcal{D}\epsilon^\mu_{\mathrm{T}}\,, \tag{2.30}$$

where $\epsilon^\mu_{\mathrm{T}}$ is the generator of infinitesimal *TDiff* transformations, which is defined according to the transversality condition $\nabla_\mu \epsilon^\mu_{\mathrm{T}} = 0$. Nevertheless, as it was pointed out in [115, 122], the integral (2.30) does not correspond to the volume factor of the *TDiff* group. The reason for that lies on the fact $\mathcal{D}\epsilon^\mu_{\mathrm{T}}$ cannot be treated as a metric independent object (due to the constraint $\nabla_\mu \epsilon^\mu_{\mathrm{T}} = 0$) and, as a consequence, cannot be factored out in the Faddeev-Popov procedure. In Ref. [115, 122], it was proposed that the appropriated definition of V_{TDiff} should include a functional determinant[6], namely

$$V_{TDiff} = \int \mathcal{D}\epsilon^\mu_{\mathrm{T}}\, \mathrm{Det}^{-1/2}(\Delta)\,, \tag{2.31}$$

[5] It is interesting to mention that the formulation used in [129] makes UG compatible with full *Diff* invariance.

[6] We use "Det" to distinguish functional determinants from the ordinary matrix determinants represented as "det".

where $\Delta = -\bar{\nabla}^2$. This definition is justified by noticing that volume of *TDiff* can be obtained by integrating over ϵ^μ with a functional Dirac delta $\delta(\nabla_\mu \epsilon^\mu)$. Combing this observation with the decomposition of a vector field in terms of its transverse and longitudinal components,

$$\epsilon^\mu = \epsilon^\mu_{\mathrm{T}} + \bar{\nabla}^\mu \chi\,, \tag{2.32}$$

where $\chi = \chi(x)$ denotes a scalar field, we can express the volume of the *TDiff* group according to

$$V_{TDiff} = \int \mathcal{D}\epsilon^\mu\, \delta(\nabla_\mu \epsilon^\mu) = \int \mathcal{D}\epsilon^\mu\, \delta(\bar{\nabla}_\mu \epsilon^\mu) = \int \mathcal{D}\epsilon^\mu_{\mathrm{T}} \mathcal{D}\chi\, \mathrm{Det}^{1/2}(\Delta)\, \delta(\Delta\chi)\,. \tag{2.33}$$

Note that we have used $\nabla_\mu \epsilon^\mu = \bar{\nabla}_\mu \epsilon^\mu$, which follows from the unimodularity condition. In the last equality we used $\mathcal{D}\epsilon^\mu = \mathcal{D}\epsilon^\mu_{\mathrm{T}} \mathcal{D}\chi\, \mathrm{Det}^{1/2}(\Delta)$, where the determinant arises as a Jacobian accounting for the change of variable $\epsilon^\mu \mapsto (\epsilon^\mu_{\mathrm{T}}, \chi)$. Recalling the property $\delta(\Delta\chi) = \mathrm{Det}^{-1}(\Delta)\, \delta(\chi)$, we find

$$V_{TDiff} = \int \mathcal{D}\epsilon^\mu_{\mathrm{T}} \mathcal{D}\chi\, \mathrm{Det}^{-1/2}(\Delta)\, \delta(\chi)\,, \tag{2.34}$$

Integrating the variable χ, with normalization $\int \mathcal{D}\chi\, \delta(\chi) = 1$, we recover the volume factor defined in (2.31).

Taking into account the volume factor (2.31) into the construction of a gauge-fixed (Euclidean) functional generator, one can express[7]

$$\begin{aligned} Z_{\mathrm{UG}}[J, \eta, \bar{\eta}; \bar{g}] = \int \mathcal{D}h_{\mu\nu} \mathcal{D}c^\mu \mathcal{D}\bar{c}_\mu\; \mathrm{Det}^{1/2}(\Delta)\; \exp\Bigg(&- S_{\mathrm{UQG}}[h; \bar{g}] \\ &- S_{\mathrm{g.f.}}[h, c, \bar{c}; \bar{g}] + \int_x \omega\, \left(J^{\mu\nu} h_{\mu\nu} + \bar{\eta}_\mu c^\mu - \bar{c}_\mu \eta^\mu\right) \Bigg)\,, \end{aligned} \tag{2.35}$$

where $S_{\mathrm{UQG}}[h; \bar{g}]$ is the unimodular version of $S_{\mathrm{QGR}}[h; \bar{g}]$ defined in the previous sections (see the discussion after Eq. (1.58)). Note that, in the present case, the (traceless) fluctuation field is defined according to the exponential parameterization in Eq. (2.27). For more detail concerning the gauge-fixing procedure in UG, see the App. A. Within the FRG framework, in addition to the cutoff function $\Delta S_k[h, c, \bar{c}; \bar{g}]$, the determinant $\mathrm{Det}^{1/2}(\Delta)$ coming from V_{TDiff} also requires regularization. Here, we adopt the following prescription

$$\mathrm{Det}^{1/2}(\Delta) \;\mapsto\; \mathrm{Det}^{1/2}(\Delta + R_k(\Delta))\,, \tag{2.36}$$

where $R_k(\Delta)$ is the FRG regulator. Using this prescription, we can define the scale-

[7] We use "UQG" as an abbreviation to unimodular quantum gravity.

dependent functional generator for UG according to

$$Z_{k,\mathrm{UG}}[J,\eta,\bar{\eta};\bar{g}] = \int \mathcal{D}h_{\mu\nu}\mathcal{D}c^{\mu}\mathcal{D}\bar{c}_{\mu}\ \mathrm{Det}^{1/2}(\Delta + R_k(\Delta))\ \exp\Bigg(- S_{\mathrm{UQG}}[h;\bar{g}] \\ - S_{\mathrm{g.f.}}[h,c,\bar{c};\bar{g}] - \Delta S_k[h,c,\bar{c};\bar{g}] + \int_x \omega\ (J^{\mu\nu}h_{\mu\nu} + \bar{\eta}_{\mu}c^{\mu} - \bar{c}_{\mu}\eta^{\mu})\Bigg). \quad (2.37)$$

Defining the EAA in the usual way (see Eq. 1.60), the standard derivation of the flow equation leads to

$$\partial_t\Gamma_k = \frac{1}{2}\mathrm{STr}\Big(\big(\Gamma^{(2)} + \mathbf{R}_k\big)^{-1}\partial_t\mathbf{R}_k\Big) - \frac{1}{2}\mathrm{Tr}\Big(\big[\Delta + R_k(\Delta)\big]^{-1}\partial_t R_k(\Delta)\Big). \quad (2.38)$$

The first term encode the usual traces (here represented with a condensed notation involving the super-trace[8]) composing the FRG equation in QG (see Eq. (1.61)). The second term in the r.h.s. correspond to an extra trace arising as a consequence of the determinant $\mathrm{Det}^{1/2}(\Delta + R_k(\Delta))$. Therefore, the flow equation in the case of UG picks up a contribution from the path integral measure. The consistency of such an extra trace can be checked by confronting the 1-loop approximation of the FRG equation[9] with calculations via other methods. In fact, if one neglects the extra trace in (2.38), the 1-loop determinants reported in [115, 122] are not properly matched by FRG calculations. It is important to remark that, due to the unimodularity condition, the extra trace does not contain any dependence on the fluctuation field $h_{\mu\nu}$. As a consequence, in the so-called background approximation calculations, such a term will contribute and quantitatively affects the results regarding the FP structure. However, for the computation of the flow of n-point functions, this term automatically drops since functional derivatives with respect to fluctuations give a vanishing result.

2.2 Novel Indications for Asymptotic Safety in the Unimodular Theory Space

2.2.1 Setting the stage

The possibility of AS formulated in terms of the unimodular theory space has been considerably less explored than the standard formulation as a quantum theory for GR. By now, most of the indications for UV FPs in the unimodular theory space comes from simple EH truncations [125, 128, 129], with exception of the unimodular version of the $f(R)$-approximation investigated in [126]. In this section, we explore further

[8]The super-trace, denoted as STr, is introduced as a way to account for the appropriate pre-factors that appear when we are tracing over fermionic fields.

[9]The 1-loop approximation of the FRG equation is obtained by replacing $\Gamma^{(2)}$ by $S^{(2)}$ in the r.h.s. of the flow equation.

indications for the existence of suitable FP solutions in the unimodular theory space. The novel aspects investigated in the remaining of this chapter can be summarized in the following way:

- In general, we have considered an extended truncation defined in terms of the arbitrary function $f_k(R, R^2_{\mu\nu})$. In principle, we have derived flow equations (using a spherical background) for generic function $f_k(R, R^2_{\mu\nu})$. Nevertheless, for practical calculations, including the search of FP solutions, we have considered particular projections on truncations of the type $f_k(R)$ and $F_k(R^2_{\mu\nu}) + R\, Z_k(R^2_{\mu\nu})$. In both cases we explore polynomial approximations, enlarging the truncated theory space previously considered in the literature of unimodular ASQG.

- In contrast with previous results presented in the literature, the investigation performed here includes the extra functional trace in the flow equation for UQG (see Eq. (2.38)), resulting from the appropriated treatment of the volume factor, V_{TDiff}, in the Faddeev-Popov procedure. Despite being formally necessary, the inclusion of the extra functional trace seems to keep the qualitative properties of the FP structure unchanged in comparison with previous results.

2.2.2 Defining a truncation, computing traces and all that

The starting point for any practical calculation based in the FRG technology is the definition of a truncation for the EAA. In what follows, we are going to explore the following truncation in the unimodular theory space

$$\Gamma^{\text{UG}}_{k,\text{trunc}} = \Gamma_{k,f}[g] + S_{\text{g.f.}}[h, c, \bar{c}; \bar{g}]\,, \tag{2.39}$$

where

$$\Gamma_{k,f}[g] = \frac{1}{16\pi G_{\text{N},k}} \int_x \omega\, f_k(R, R^2_{\mu\nu})\,, \tag{2.40}$$

where f_k is an RG scale-dependent arbitrary function of the Ricci scalar and the square of the Ricci tensor, $R^2_{\mu\nu} = R_{\mu\nu}R^{\mu\nu}$ (see [263] for 1-loop computation involving $f_k(R, R^2_{\mu\nu})$-term). For the analysis presented in this chapter, we take the gauge-fixing sector to be

$$S_{\text{g.f.}}[h, c, \bar{c}; \bar{g}] = \frac{1}{2\alpha} \int_x \omega\, \bar{g}^{\mu\nu} F^{\text{T}}_\mu[h; \bar{g}] F^{\text{T}}_\nu[h; \bar{g}] + \int_x \omega\, \bar{c}_\mu\, \mathcal{M}^\mu{}_\nu[h\,; \bar{g}]\, c^\nu\,, \tag{2.41}$$

where gauge condition $F^{\text{T}}_\mu[h; \bar{g}]$ has been defined in (A.6), with Faddeev-Popov operator $\mathcal{M}^\mu{}_\nu[h\,; \bar{g}]$ defined according to (A.15). Moreover, following the discussion of the previous section, we use a combination of the exponential parameterization (see Eq. (2.27)) along with $h^{\text{tr}} = 0$ as a practical way of implementing the unimodularity condition.

The results presented in this chapter were obtained within the background approximation for the FRG equation (see the discussion in Sect. 1.3.2). In this context, the basic idea is to use the truncation (2.39) as an approximated solution for the flow equation evaluated at vanishing fluctuation fields (see Eq. (1.71)). For the truncation that we are considering, the l.h.s. of Eq. (1.71) leads to

$$\partial_t \bar{\Gamma}^{\text{UG}}_{k,\text{trunc}} = \frac{1}{16\pi G_{\text{N},k}} \int_x \omega \, \left(-\eta_{\text{N}} \, f_k(\bar{R}, \bar{R}^2_{\mu\nu}) \, + \, \partial_t f_k(\bar{R}, \bar{R}^2_{\mu\nu}) \right) \,, \tag{2.42}$$

where we have defined the "background anomalous dimension" $\eta_{\text{N}} = -Z_{\text{N}}^{-1} \partial_t Z_{\text{N}}$, with $Z_{\text{N}} = (16\pi G_{\text{N},k})^{-1}$.

To extract relevant information from the FRG equation we still need to compute the functional traces in the r.h.s. of Eq. (1.71). This computation, however, is rather long and technical, but follows standard techniques used in the literature of covariant QG. For this reason, in the present thesis we shall only report few intermediary steps. For the reader interested in more details, we refer to similar calculations (in simpler examples) discussed in [38, 39, 264]. The first step towards the evaluation of the r.h.s. of Eq. (1.71) is to extract the Hessian matrix. In general lines, in order to compute $\Gamma^{(2)}_k$ we expand the truncation $\Gamma^{\text{UG}}_{k,\text{trunc}}$ up to second order in the fluctuation field and organize the resulting expression according to

$$\begin{aligned} \Gamma^{\text{UG}}_{k,\text{trunc}} = \bar{\Gamma}^{\text{UG}}_{k,\text{trunc}} &+ \int_x \omega(x) \, \Gamma^{(1)}_{k,A}[x\,;\bar{g}] \, \varphi^A(x) \\ &+ \frac{1}{2} \int_{x,y} \omega(x) \, \omega(y) \, \varphi^A(x) \, \Gamma^{(2)}_{k,AB}[x,y\,;\bar{g}] \, \varphi^B(y) + \mathcal{O}(\varphi^3) \,, \end{aligned} \tag{2.43}$$

where we have defined the "super-field" notation $\varphi = (h_{\mu\nu}, c_\mu, \bar{c}_\mu)$. The elements of the Hessian matrix can be identified as $\Gamma^{(2)}_{k,AB}[x,y;\bar{g}]$. Ideally, we would like to compute the Hessian in terms of an arbitrary background metric $\bar{g}_{\mu\nu}$, however, in such a case, the situation becomes extremely complicated. In particular, the inversion of the "regularized Hessian" $\Gamma^{(2)}_k + \mathbf{R}_k$ (which is necessary to compute the r.h.s. in (2.38)) is a very challenging task in the case of arbitrary background. To circumvent this problem, we restrict the background space to be a 4-sphere (S^4). In this case, the background Riemann's and Ricci's curvature tensors collapses to

$$\bar{R}_{\mu\nu\alpha\beta} = \frac{1}{12}(\bar{g}_{\mu\alpha}\bar{g}_{\nu\beta} - \bar{g}_{\mu\beta}\bar{g}_{\nu\alpha})\bar{R} \qquad \text{and} \qquad \bar{R}_{\mu\nu} = \frac{1}{4}\bar{g}_{\mu\nu}\bar{R} \,. \tag{2.44}$$

A direct consequence of this choice is that the action of background covariant derivatives on $\bar{R}_{\mu\nu\alpha\beta}$, $\bar{R}_{\mu\nu}$ and $\bar{R}$ leads to vanishing results.

Even though the choice of the 4-sphere as a background considerably simplifies the structure of the Hessian, the presence of off-diagonal contributions involving covariant derivatives makes the inversion of $\Gamma_k^{(2)} + \mathbf{R}_k$ complicated. The situation can be further simplified by taking into account the York decomposition [265],

$$h_{\mu\nu} = h_{\mu\nu}^{\mathrm{TT}} + \bar{\nabla}_\mu \xi_\nu + \bar{\nabla}_\nu \xi_\mu + \bar{\nabla}_\mu \bar{\nabla}_\nu \sigma - \frac{1}{4} \bar{g}_{\mu\nu} \bar{\nabla}^2 \sigma \,, \tag{2.45}$$

where $h_{\mu\nu}^{\mathrm{TT}}$ denotes a transverse ($\bar{\nabla}^\mu h_{\mu\nu}^{\mathrm{TT}} = 0$) and traceless ($\bar{g}^{\mu\nu} h_{\mu\nu}^{\mathrm{TT}} = 0$) symmetric tensor, ξ_μ represents a transverse vector ($\bar{\nabla}^\mu \xi_\mu = 0$) and σ is a scalar field. We note the absence of the trace mode due the unimodularity condition. After the York decomposition, we include wave function renormalization factors by refining the fields according to

$$h_{\mu\nu}^{\mathrm{TT}} \mapsto Z_{k,\mathrm{TT}}^{1/2} \, h_{\mu\nu}^{\mathrm{TT}} \,, \quad \xi_\mu \mapsto Z_{k,\xi}^{1/2} \, \xi_\mu \,, \quad \sigma \mapsto Z_{k,\sigma}^{1/2} \, \sigma \,, \tag{2.46a}$$

and

$$c_\mu \mapsto Z_{k,c}^{1/2} \, c_\mu \,, \quad \bar{c}_\mu \mapsto Z_{k,c}^{1/2} \, \bar{c}_\mu \,. \tag{2.46b}$$

As a consequence of this redefinition, the prescription that we use to define the regulator "kernels" produces anomalous dimensions $\eta_i = -Z_{k,i}^{-1} \partial_t Z_{k,i}$ coming from the regulator insertion $\partial_t \mathbf{R}_k$. Within the background approximation, the anomalous dimensions are fixed by the "RG-improved" prescription [74], namely

$$\eta_{\mathrm{TT}} = \eta_\sigma \coloneqq \eta_{\mathrm{N}} \qquad \text{and} \qquad \eta_\xi = \eta_c = 0 \,. \tag{2.47}$$

The Hessian in the "York basis" can be directly obtained from the quadratic form $\varphi^A(x) \, \Gamma_{k,AB}^{(2)}[x, y\,; \bar{g}] \, \varphi^B(y)$, where "super-field" is rewritten in the new basis according to $\varphi = (h_{\mu\nu}^{\mathrm{TT}}, \xi_\mu, \sigma, c_\mu, \bar{c}_\mu)$. For the truncation adopted in the present chapter (Eq. (2.39)), the Hessian matrix takes the form

$$\Gamma^{(2)} = \begin{pmatrix} \Gamma_{\mathrm{TT}}^{(2)} & 0 & 0 & 0 & 0 \\ 0 & \Gamma_\xi^{(2)} & 0 & 0 & 0 \\ 0 & 0 & \Gamma_\sigma^{(2)} & 0 & 0 \\ 0 & 0 & 0 & 0 & \Gamma_{c\bar{c}}^{(2)} \\ 0 & 0 & 0 & \Gamma_{\bar{c}c}^{(2)} & 0 \end{pmatrix} , \tag{2.48}$$

with components[10]

$$\Gamma_{\mathrm{TT}}^{(2)} = Z_{k,\mathrm{TT}} \left(f_k^{(0,1)} \left(\Delta_2 + (\gamma_2 - 1)\bar{R} \right) - f_k^{(1,0)} \right) \left(\Delta_2 + \frac{2\gamma_2 - 1}{2} \bar{R} \right) , \tag{2.49a}$$

[10]The Hessians reported here can also be extracted from [263].

$$\Gamma^{(2)}_{\xi} = \frac{2\,Z_{k,\xi}}{\alpha}\left(\Delta_1 + \frac{2\gamma_1 - 1}{2}\bar{R}\right)^2\,, \tag{2.49b}$$

$$\Gamma^{(2)}_{\sigma} = \frac{9\,Z_{k,\sigma}}{8}\left[\left(\Delta_0 + \frac{3\gamma_0 - 1}{3}\bar{R}\right)\mathbf{P}_f + \mathbf{Q}_f\right]\left(\Delta_0 + \frac{3\gamma_0 - 1}{3}\bar{R}\right)(\Delta_0 + \gamma_0\bar{R})^2\,, \tag{2.49c}$$

$$\Gamma^{(2)}_{c\bar{c}} = -\Gamma^{(2)}_{\bar{c}c} = -\sqrt{2}\,Z_{k,c}\left(\Delta_1 + \frac{2\gamma_1 - 1}{2}\bar{R}\right)\,, \tag{2.49d}$$

where we have defined

$$\mathbf{P}_f = f_k^{(2,0)} + \frac{1}{4}\bar{R}^2\,f_k^{(0,2)} + 4\,\bar{R}\,f_k^{(1,1)} + \frac{2}{3}f_k^{(0,1)}\,, \tag{2.50a}$$

$$\mathbf{Q}_f = \frac{1}{3}f_k^{(1,0)} + \frac{2}{9}\bar{R}\,f_k^{(0,1)}\,. \tag{2.50b}$$

Moreover, we adopt the compact notation

$$f_k^{(m,n)} = \frac{\partial^{m+n} f(\bar{R}, X)}{\partial\bar{R}^m\partial X^n}\,. \tag{2.51}$$

with $X = \bar{R}^2_{\mu\nu}$. The operators Δ_2, Δ_1 and Δ_0 were introduced as "interpolating" Laplacians, namely

$$\Delta_2 = \Delta_{\mathrm{L}_2} - \gamma_2\,\bar{R}\,, \qquad \Delta_1 = \Delta_{\mathrm{L}_1} - \gamma_1\,\bar{R}\,, \qquad \Delta_0 = \Delta_{\mathrm{L}_0} - \gamma_0\,\bar{R}\,. \tag{2.52}$$

where Δ_{L_2}, Δ_{L_1} and Δ_{L_0} correspond to the Lichnerowicz-Laplacian operators, defined (on spherical backgrounds) according to

$$\Delta_{\mathrm{L}_2} = \Delta + \frac{2}{3}\bar{R}\,, \qquad \Delta_{\mathrm{L}_1} = \Delta + \frac{1}{4}\bar{R}\,, \qquad \Delta_{\mathrm{L}_0} = \Delta\,, \tag{2.53}$$

where $\Delta = -\bar{\nabla}^2 = -\bar{g}^{\mu\nu}\,\bar{\nabla}_\mu\bar{\nabla}_\nu$ (referred as Bochner-Laplacian). We note that Δ_2, Δ_1 and Δ_0 were defined w.r.t. their action on transverse-traceless tensors, transverse vectors and scalars, respectively. The interpolating parameters were introduced such that $\gamma_2 = \gamma_1 = \gamma_0 = 0$ results in the Lichnerowicz-Laplacian and $\gamma_2 = 2/3$, $\gamma_1 = 1/4$ and $\gamma_0 = 0$ leads to the Bochner-Laplacian. In what follows, we are going explore both types of Laplacians as coarse-graining operators.

The use of the York decomposition requires the introduction of regulator "kernels" for each one of the York modes. In this case, we adopt the following prescription to the define the regulators [264]

$$\mathbf{R}_{k,\mathrm{TT}} = \Gamma^{(2)}_{\mathrm{TT}}|_{\Delta_2\to\Delta_2+R_k(\Delta_2)} \;-\; \Gamma^{(2)}_{\mathrm{TT}}\,, \tag{2.54a}$$

$$\mathbf{R}_{k,\xi} = \Gamma^{(2)}_{\xi}|_{\Delta_1\to\Delta_1+R_k(\Delta_1)} \;-\; \Gamma^{(2)}_{\xi}\,, \tag{2.54b}$$

$$\mathbf{R}_{k,\sigma} = \Gamma^{(2)}_{\sigma}|_{\Delta_0\to\Delta_0+R_k(\Delta_0)} \;-\; \Gamma^{(2)}_{\sigma}\,, \tag{2.54c}$$

$$\mathbf{R}_{k,c\bar{c}} = \Gamma^{(2)}_{k,c\bar{c}}|_{\Delta_1\to\Delta_1+R_k(\Delta_1)} \;-\; \Gamma^{(2)}_{k,c\bar{c}}\,. \tag{2.54d}$$

Within the background approximation, the flow equation written in terms of York variables takes the form

$$\begin{aligned}
\partial_t\bar{\Gamma}^{\mathrm{UG}}_{k,\mathrm{trunc}} = {} & \frac{1}{2}\mathrm{Tr}_{(2)}\left[\left(\Gamma^{(2)}_{\mathrm{TT}} + \mathbf{R}_{k,\mathrm{TT}}\right)^{-1}\partial_t\mathbf{R}_{k,\mathrm{TT}}\right] + \frac{1}{2}\mathrm{Tr}'_{(1)}\left[\left(\Gamma^{(2)}_{\xi} + \mathbf{R}_{k,\xi}\right)^{-1}\partial_t\mathbf{R}_{k,\xi}\right] \\
& + \frac{1}{2}\mathrm{Tr}''_{(0)}\left[\left(\Gamma^{(2)}_{\sigma} + \mathbf{R}_{k,\sigma}\right)^{-1}\partial_t\mathbf{R}_{k,\sigma}\right] - \mathrm{Tr}_{(1)}\left[\left(\Gamma^{(2)}_{c\bar{c}} + \mathbf{R}_{k,c\bar{c}}\right)^{-1}\partial_t\mathbf{R}_{k,c\bar{c}}\right] \\
& - \frac{1}{2}\mathrm{Tr}'_{(0)}\left[(\Delta_0 + R_k(\Delta_0))^{-1}\partial_t R_k(\Delta_0)\right] \;+\; \mathcal{T}^{\mathrm{Jacob.}}_{(1)} \;+\; \mathcal{T}^{\mathrm{Jacob.}}_{(0)}\,.
\end{aligned} \tag{2.55}$$

The first term in the third line corresponds to the extra functional traces arising from the appropriated treatment of the volume factor V_{TDiff}. The other two terms in the third line, $\mathcal{T}^{\mathrm{Jacob.}}_{(1)}$ and $\mathcal{T}^{\mathrm{Jacob.}}_{(0)}$, denote additional contributions coming from the Jacobian associated with the change of variables $h_{\mu\nu} \mapsto \{h^{\mathrm{TT}}_{\mu\nu}, \xi_\mu, \sigma\}$ [38]. These contributions manifest themselves as the additional traces

$$\mathcal{T}^{\mathrm{Jacob.}}_{(1)} = -\frac{1}{2}\mathrm{Tr}'\left[\left(\Delta_1 + R_k(\Delta_1) + \frac{2\gamma_1 - 1}{2}\bar{R}\right)^{-1}\partial_t R_k(\Delta_1)\right]\,, \tag{2.56a}$$

$$\begin{aligned}
\mathcal{T}^{\mathrm{Jacob.}}_{(0)} = {} & -\frac{1}{2}\mathrm{Tr}''\left[\left(\Delta_0 + R_k(\Delta_0) + \frac{1}{3}\bar{R}\right)^{-1}\partial_t R_k(\Delta_0)\right] \\
& - \frac{1}{2}\mathrm{Tr}''\left[\,(\Delta_0 + R_k(\Delta_0))^{-1}\,\partial_t R_k(\Delta_0)\right]\,.
\end{aligned} \tag{2.56b}$$

Finally, the "prime notation" Tr' (Tr'') indicates that we have to eliminate from the traces those contributions associated with the first (first and second) eigenvalues of the coarse-graining operator. The reason for that is the existence of field configurations ξ_μ

and σ satisfying (see, e.g., [38, 60])

$$\bar{\nabla}_\mu \xi_\nu + \bar{\nabla}_\nu \xi_\mu = 0 \qquad \text{and} \qquad \bar{\nabla}_\mu \bar{\nabla}_\nu \sigma - \frac{1}{4} \bar{g}_{\mu\nu} \bar{\nabla}^2 \sigma = 0\,, \tag{2.57}$$

which, therefore, do not contribute to the original fluctuation field $h_{\mu\nu}$. To remove these modes, at the practical level we define the "primed" trace according to

$$\mathrm{Tr}'^{\cdots\prime}_{(s)}\big[W(\Delta_s)\big] = \mathrm{Tr}_{(s)}\big[W(\Delta_s)\big] - \sum_{l \in M_s} D_l(s) W(\lambda_l(s)), \tag{2.58}$$

where $M_s = \{s, s+1, \cdots, m-1+s\}$ (m denotes the number of "primes"). In addition, $\lambda_l(s)$ represents the l-th eigenvalue of the "interpolating" Laplacian Δ_s defined on the 4-sphere and $D_l(s)$ denotes the degree of degeneracy associated with $\lambda_l(s)$. For the calculation presented here, the relevant expressions are given by

$$\lambda_l(s) = \frac{(l+3)\,l - s}{12}\, \bar{R} - \gamma_0\, \delta_{0,s}\, \bar{R} + \left(\frac{1}{4} - \gamma_1\right) \delta_{1,s}\, \bar{R}\,, \tag{2.59a}$$

$$D_l(s) = \frac{(2l+3)\,(l+2)!}{6\,l!} \delta_{0,s} + \frac{l\,(l+3)\,(2l+3)\,(l+1)!}{2\,(l+1)!} \delta_{1,s}\,, \tag{2.59b}$$

for $s = 0, 1$, which can be obtained by shifting the eigenvalues of the usual Bochner-Laplacian operators [38].

To compute the functional traces we use standard heat kernel techniques [266]. In general lines, a functional trace can be expanded in terms of heat kernel coefficients, namely (see, e.g. [38, 267–269])

$$\mathrm{Tr}_{(s)}\big[W(\Delta_s)\big] = \frac{1}{16\pi^2} \sum_{n=0}^{\infty} \int_x \sqrt{\bar{g}}\; Q_{2-n}[W]\; \mathrm{tr}\big[\mathbf{b}_{2n}(\Delta_s)\big], \tag{2.60}$$

with Q_n-functional defined according to

$$Q_n[W] = \frac{(-1)^k}{\Gamma(n+k)} \int_0^\infty dz\; z^{n+k-1}\, \frac{d^k W(z)}{dz^k}, \tag{2.61}$$

where k denotes some (arbitrary) positive integer satisfying the following restriction $n + k > 0$. Moreover, $\mathrm{tr}\big[\mathbf{b}_{2n}(\Delta_s)\big]$ denotes the trace of the (non-integrated) heat kernel coefficient $\mathbf{b}_{2n}(\Delta_s)$ associated with the coarse-graining operator Δ_s. For (4-dimensional) spherical backgrounds we can express

$$\mathrm{tr}\big[\mathbf{b}_{2n}(\Delta_s)\big] = c_s\, \bar{R}^n\,, \tag{2.62}$$

where c_s denote a numerical coefficient depending on the choice of coarse-graining operator. In table 2.1 and 2.2 we report the relevant c_s-coefficients for the analysis presented here[11].

s	$n=0$	$n=2$	$n=4$	$n=6$	$n=8$	$n=10$	$n=12$
0	1	$\frac{1}{6}$	$\frac{29}{2160}$	$\frac{37}{54432}$	$\frac{149}{6531840}$	$\frac{179}{431101440}$	$-\frac{1387}{201755473920}$
1	3	$\frac{1}{4}$	$-\frac{7}{1440}$	$-\frac{541}{362880}$	$-\frac{157}{2488320}$	$\frac{4019}{2299207680}$	$\frac{141853}{430411677696}$
2	5	$-\frac{5}{6}$	$-\frac{1}{432}$	$\frac{311}{54432}$	$\frac{109}{1306368}$	$-\frac{317}{12317184}$	$-\frac{6631}{4483454976}$

Table 2.1: c_s-coefficients associated with the Bochner-Laplacian as the coarse-graining operator. All the coefficients were computed within the 4-sphere background.

s	$n=0$	$n=2$	$n=4$	$n=6$	$n=8$	$n=10$	$n=12$
0	1	$\frac{1}{6}$	$\frac{29}{2160}$	$\frac{37}{54432}$	$\frac{149}{6531840}$	$\frac{179}{431101440}$	$-\frac{1387}{201755473920}$
1	3	$-\frac{1}{2}$	$\frac{19}{720}$	$-\frac{5}{18144}$	$-\frac{11}{2177280}$	$-\frac{19}{143700480}$	$-\frac{347}{67251824640}$
2	5	$-\frac{25}{6}$	$\frac{719}{432}$	$-\frac{23125}{54432}$	$\frac{101981}{1306368}$	$-\frac{952135}{86220288}$	$\frac{50728409}{40351094784}$

Table 2.2: c_s-coefficients associated with the Lichnerowicz-Laplacian as the coarse-graining operator. All the coefficients were computed within the 4-sphere background.

For the Litim's cutoff [181, 182] (see (1.34)), the Q_n-functionals can be computed analytically even for arbitrary form of the function $f_k(\bar{R}, \bar{R}^2_{\mu\nu})$. Due to specific properties of this choice of regulator, only a finite number of Q_n-functionals (with negative n) leads to non-vanishing results. As a consequence, the heat kernel expansion in (2.60) involves only a finite number of terms. In general, the result of the trace computation leads to very long expressions and, therefore, we shall not report explicit results here. In the next sections we discuss how to extract beta functions from two different types of polynomial projections.

[11] See, e.g., Ref. [38] for a discussion on how to compute the heat-kernel coefficients in a spherical manifold.

2.2.3 $f(R)$ – polynomial projection

In general, the result of the calculation described in the previous section leads to a flow equation of the form

$$\frac{1}{16\pi G_{\mathrm{N},k}}\left(-\eta_{\mathrm{N}}\, f_k(\bar{R},\bar{R}^2_{\mu\nu}) \,+\, \partial_t f_k(\bar{R},\bar{R}^2_{\mu\nu})\right) = \mathcal{F}(f_k, f_k^{(m,n)}, \eta_{\mathrm{N}}, \partial_t f_k, \partial_t f_k^{(m,n)})\,. \quad (2.63)$$

We note that the dependence on η_{N}, $\partial_t f_k$ and $\partial_t f_k^{(m,n)}$, in the r.h.s., come from the regulator insertion $\partial_t \mathbf{R}_k$. At the practical level, we are going to use polynomial truncations. Ideally, if we had performed all the calculations in a generic background, the most interesting choice of polynomial truncation (within the class of $f_k(R,R^2_{\mu\nu})$) would have the form

$$f_k(R,R^2_{\mu\nu}) = \sum_{n_1,n_2} \alpha_k^{(n_1,n_2)}\, R^{n_1}\,(R_{\mu\nu}R^{\mu\nu})^{n_2}\,. \quad (2.64)$$

where the $\alpha_k^{(n_1,n_2)}$'s denote scale-dependent couplings. By expanding both sides of Eq. (2.63) in powers of $\bar{R}$ and $\bar{R}^2_{\mu\nu}$, we should be able to extract the running of the couplings $\alpha_k^{(n_1,n_2)}$'s by comparing both sides of (2.63) order by order in the curvature invariants. Unfortunately, this task is not possible for a spherical background. In such a case, the invariant $\bar{R}^2_{\mu\nu}$ collapses to $\frac{1}{4}\bar{R}^2$ and, therefore, we can no longer disentangle the running of couplings $\alpha_k^{(n_1,n_2)}$ and $\alpha_k^{(m_1,m_2)}$, for all pairs (n_1,n_2) and (m_1,m_2) satisfying $n_1+2n_2 = m_1+2m_2$.

To circumvent this problem, without resorting to a generic background, one has to adopt a subclass of truncation. In this section, we consider the case corresponding to the $f(R)$-approximation, which can be directly obtained by neglecting the $R^2_{\mu\nu}$ dependence in our calculation. In particular, for practical computations we focus in the polynomial approximation

$$f_k(R) = -R + \sum_{n=2}^{N} k^{2-2n}\,\alpha_{k,n}\,R^n\,, \quad (2.65)$$

where the $\alpha_{k,n}$'s denote scale-dependent dimensionless couplings. The parameter N denotes a positive integer number that fixes the maximal order of the polynomial truncation. Note that we normalize the coefficient of the first term as -1 so that we recover the uEH truncation once we neglect higher-order powers of the curvature scalar. Moreover, we emphasize that the absence of a zeroth-order contribution is attributed to the fact that we are dealing with a unimodular truncation.

To extract the beta functions associated with the set of dimensionless couplings $\alpha_k = \{\alpha_{k,n}\}_{n=2,\cdots,N}$, we plug (2.65) into Eq. (2.63) and expand both sides of the flow equation up to order $\bar{R}^N$. In this case, Eq. (2.63) leads to the following structure

$$\frac{\eta_{\mathrm{N}}}{16\pi G_k}\,k^2\bar{R} + \frac{1}{16\pi G_k}\sum_{n=2}^{N} k^{4-2n}\left((2-2n-\eta_{\mathrm{N}})\,\alpha_{k,n}\; + \;\beta_\alpha^{(n)}\right)\bar{R}^n =$$

$$= \sum_{n=1}^{N}\left(\mathcal{A}_n(\alpha_k) + \mathcal{B}_n(\alpha_k)\,\eta_{\mathrm{N}} + \sum_{m=2}^{N}\mathcal{M}_{n,m}(\alpha_k)\,\beta_\alpha^{(m)}\right)k^{4-2n}\bar{R}^n\,, \tag{2.66}$$

where we have defined $\beta_\alpha^{(m)} = \partial_t \alpha_{k,n}$. At least for the Litim's cutoff, the coefficients $\mathcal{A}_n$, $\mathcal{B}_n$ and $\mathcal{M}_{n,m}$ can be computed analytically. By matching the contributions according to the power of the curvature scalar, we arrive at the RG equations

$$\beta_G = 2G_k\left[1 + \frac{8\pi G_k}{1-16\pi G_k\,\mathcal{B}_1(\alpha_k)}\left(\mathcal{A}_1(\alpha_k) + \sum_{m=2}^{N}\mathcal{M}_{1,m}(\alpha_k)\,\beta_\alpha^{(m)}\right)\right]\,, \tag{2.67a}$$

$$\beta_\alpha^{(n)} = (\eta_{\mathrm{N}} + 2n - 2)\,\alpha_{k,n} + 16\pi G_k\left(\mathcal{A}_n(\alpha_k) + \mathcal{B}_n(\alpha_k)\,\eta_{\mathrm{N}} + \sum_{m=2}^{N}\mathcal{M}_{n,m}(\alpha_k)\,\beta_\alpha^{(m)}\right)\,, \tag{2.67b}$$

with $n = 2, \cdots, N$. Note that we have used $\eta_{\mathrm{N}} = G_k^{-1}\beta_G - 2$ in (2.67a). We observe that the system of RG equations defined by (2.67a) and (2.67b) provides only an implicit results for the beta functions β_G and $\beta_\alpha^{(n)}$'s. In principle, we can solve (analytically) the system of equations in order to extract the explicit results for β_G and $\beta_\alpha^{(n)}$'s, however, this leads to very lengthy expressions and we shall not report them here.

Our primary interest in this chapter is the search of indications for UV FPs. Within the system of RG equations (2.67a) and (2.67b), we can look for FP solutions (denoted as G^* and α_n^*) that can be obtained from the following equations

$$2G^*\left(1 + \frac{8\pi G^*}{1-16\pi G^*\,\mathcal{B}_1(\alpha^*)}\mathcal{A}_1(\alpha^*)\right) = 0\,, \tag{2.68a}$$

$$(2n-4)\,\alpha_n^* \; + 16\pi G^*\big(\mathcal{A}_n(\alpha^*) - 2\,\mathcal{B}_n(\alpha^*)\big) = 0\,, \tag{2.68b}$$

with $n = 2, \cdots, N$. In Sect. (2.2.5), we report numerical FP solutions associated with various choices of N.

2.2.4 $F(R_{\mu\nu}^2) + R\,Z(R_{\mu\nu}^2)$ – polynomial projection

The $f(R)$-approximation was introduced in the previous section as a way to avoid a technical problem related to the used of a spherical background, namely, the fact that in such a background we can not distinguish the invariants $R^2_{\mu\nu}$ and R^2. In this section, we consider an alternative class of truncation characterized by the decomposition[12]

$$f_k(R, R^2_{\mu\nu}) = F_k(R^2_{\mu\nu}) + R\, Z_k(R^2_{\mu\nu})\,, \tag{2.69}$$

where $F_k(R^2_{\mu\nu})$ and $Z_k(R^2_{\mu\nu})$ denote scale-dependent functions of the invariant $R^2_{\mu\nu}$. This class of truncation was first introduced in [89] as an approach to include effects beyond the Ricci scalar. At a first sight one might suspect that, in the spherical background, the FZ-truncation would lead to the same result as in the $f(R)$-approximation, since both $F_k(\bar{R}^2_{\mu\nu})$ and $Z_k(\bar{R}^2_{\mu\nu})$ collapses to functions of $\bar{R}$. However, this is not the case as one can see from the Hessians corresponding to the $f(R)$- and FZ-truncations. As an explicit example, we consider here the Hessian associated with the transverse and traceless fluctuations, namely

$$\Gamma^{(2)}_{\mathrm{TT}}\big|_{f(R)} = -Z_{k,\mathrm{TT}}\, f^{(1)}_k \left(\Delta_2 + \frac{2\gamma_2 - 1}{2}\bar{R}\right)\,, \tag{2.70a}$$

$$\Gamma^{(2)}_{\mathrm{TT}}\big|_{FZ} = Z_{k,\mathrm{TT}} \left(\left(F^{(1)}_k + \bar{R}Z^{(1)}_k\right)\left(\Delta_2 + (\gamma_2 - 1)\bar{R}\right) - \bar{Z}_k\right)\left(\Delta_2 + \frac{2\gamma_2 - 1}{2}\bar{R}\right)\,, \tag{2.70b}$$

where we denote $f^{(1)}_k = \frac{df_k(\bar{R})}{d\bar{R}}$, $F^{(1)}_k = \frac{dF_k(X)}{dX}$, $Z^{(1)}_k = \frac{dZ_k(X)}{dX}$ and $\bar{Z}_k = Z_k(\bar{R}^2_{\mu\nu})$.

For practical computations we are going to restrict our attention to the case of a polynomial truncation defined by

$$F_k(R^2_{\mu\nu}) = \sum_{n=1}^{N_F} k^{2-4n}\, \rho_{k,2n}\, (R_{\mu\nu}R^{\mu\nu})^n\,, \tag{2.71a}$$

$$Z_k(R^2_{\mu\nu}) = -1 + \sum_{n=1}^{N_Z} k^{-4n}\, \rho_{k,2n+1}\, (R_{\mu\nu}R^{\mu\nu})^n\,, \tag{2.71b}$$

where $N_F = \lfloor N/2 \rfloor$ and $N_Z = \lfloor (N-1)/2 \rfloor$ (with $\lfloor \cdots \rfloor$ representing the floor function). Here we are going to denote as $\rho_k = \{\rho_{k,n}\}_{n=2,\cdots,N}$ the set of scale-dependent couplings associated with the FZ-truncation. To extract the system of RG equations associated with the dimensionless couplings G_k and $\rho_k = \{\rho_{k,n}\}_{n=2,\cdots,N}$ we follow the same procedure discussed in the $f(R)$-approximation. In such a case, replacing (2.71a) and (2.71b) into the l.h.s. and r.h.s. of Eq. (2.63), we find, respectively, the following

[12] We refer to such decomposition as FZ-truncation.

results

$$
\begin{aligned}
&\frac{1}{16\pi G_{\mathrm{N},k}}\left(-\eta_{\mathrm{N}}\, f_k(\bar{R},\bar{R}^2_{\mu\nu})\;+\;\partial_t f_k(\bar{R},\bar{R}^2_{\mu\nu})\right)\big|_{S^4} = \\
&\qquad = \frac{\eta_{\mathrm{N}}}{16\pi G_k}k^2\bar{R} + \frac{1}{16\pi G_k}\sum_{n=1}^{N_F}\frac{k^{4-4n}}{4^n}\left(\beta_\rho^{(2n)} + (2-4n-\eta_{\mathrm{N}})\rho_{k,2n}\right)\bar{R}^{2n} \\
&\qquad + \frac{1}{16\pi G_k}\sum_{n=1}^{N_Z}\frac{k^{2-4n}}{4^n}\left(\beta_\rho^{(2n+1)} - (4n+\eta_{\mathrm{N}})\rho_{k,2n+1}\right)\bar{R}^{2n+1}\,,
\end{aligned} \tag{2.72a}
$$

$$
\begin{aligned}
&\mathcal{F}(f_k, f_k^{(m,n)}, \eta_{\mathrm{N}}, \partial_t f_k, \partial_t f_k^{(m,n)})\big|_{S^4} = \\
&\qquad = \sum_{n=1}^{N}\left(\mathcal{A}_n(\rho_k) + \mathcal{B}_n(\rho_k)\,\eta_{\mathrm{N}} + \sum_{m=2}^{N}\mathcal{M}_{n,m}(\rho_k)\,\beta_\rho^{(m)}\right)k^{4-2n}\bar{R}^n\,.
\end{aligned} \tag{2.72b}
$$

The notation $(\cdots)|_{S^4}$ indicates the projections on spherical background. Once again, the basic idea is to match order by order in the curvature scalar $\bar{R}$, in this case, leading to system of RG equations

$$
\beta_G = 2G_k\left[1 + \frac{8\pi G_k}{1-16\pi G_k\,\mathcal{B}_1(\rho_k)}\left(\mathcal{A}_1(\rho_k) + \sum_{m=2}^{N}\mathcal{M}_{1,m}(\rho_k)\,\beta_\rho^{(m)}\right)\right]\,, \tag{2.73a}
$$

$$
\begin{aligned}
\beta_\rho^{(n)} &= (\eta_{\mathrm{N}} + 2n - 2)\,\rho_{k,n} \\
&+ 16^{1+\delta_n}\pi\, G_k\left(\mathcal{A}_n(\rho_k) + \mathcal{B}_n(\rho_k)\,\eta_{\mathrm{N}} + \sum_{m=2}^{N}\mathcal{M}_{n,m}(\rho_k)\,\beta_\rho^{(m)}\right)\,,
\end{aligned} \tag{2.73b}
$$

where $\delta_n = n/4$ for n even and $\delta_n = (n-1)/4$ for n odd. We note that despite of the similarities observed when we compare (2.67a) and (2.67b) with (2.73a) and (2.73b), the explicit expressions for the coefficients $\mathcal{A}$, $\mathcal{B}$ and $\mathcal{M}$ obtained within the FZ-truncation are considerably different from the ones obtained via $f(R)$-approximation. Finally, the FP solutions associated with the FZ-truncation satisfy the following equations

$$
2G^*\left(1 + \frac{8\pi G^*}{1-16\pi G^*\,\mathcal{B}_1(\rho^*)}\mathcal{A}_1(\rho^*)\right) = 0\,, \tag{2.74a}
$$

$$
(2n-4)\,\rho_n^* + 16^{1+\delta_n}\pi\, G^*\left(\mathcal{A}_n(\rho^*) - 2\mathcal{B}_n(\rho^*)\right) = 0\,, \tag{2.74b}
$$

where $n = 2, \cdots, N$.

2.2.5 Results and discussion

In this section, we present our results concerning the FP structure obtained within truncations previously defined. In general, the FP equations discussed in the previous sections (Eqs. (2.68a)-(2.68b) for the $f(R)$-approximation and Eqs. (2.74a)-(2.74b) for the FZ-truncation) are considerably complicated and requires the use of numerical techniques. Both in the case of $f(R)$- and FZ-approximations, we have employed the bootstrap method developed in Refs. [70, 73] as a systematic way to search numerical FP solutions. In this sense, we have developed and implemented a *Mathematica* routine to perform the numerical calculations within the truncations investigated here.

For the $f(R)$-approximation we have performed the search of FP solutions for polynomial truncations (see Eq. (2.65)) with N ranging from 1 to 20. The idea of computing FPs for a variety of values for N is motivated by two main reasons:

i) Firstly, it appears as a practical requirement related to the way the bootstrap method is implemented. Typically, search of numerical solutions within a truncation characterized by N requires inputs from the FP solutions associated with the case $N-1$.

ii) Secondly, the main goal of this analysis is not only to search for indications of FP solutions, but also to check their stability against the inclusion of further operators. In this sense, we can explore how the FP solutions (as well as the corresponding critical exponents) behave as a function of N.

In principle, the analysis performed here can be extended to $N > 20$, however, in this case, the implementation of the bootstrap strategy requires more sophisticated numerical methods and additional computational power. For the analysis performed here, $N \leq 20$ is sufficient to capture various qualitative features. It is interesting to mention that, in the case of standard ASQG, this analysis has been carried out within polynomial truncations involving terms up to R^{70} [90].

In Fig. 2.1, we exhibit our results for the FP values for some of the couplings (up to α_6^*) defined in the polynomial $f(R)$-truncation, as functions of N. For higher-order couplings, we find FP values characterized by $|\alpha_n^*| < 10^{-4}$ ($n = 7, 8, \cdots, 20$). In each one of the plots, we exhibit FPs evaluated by two different types of coarse-graining operators, namely, Bochner-Laplacian (blue/circle markers) and Lichnerowicz-Laplacian (red/square markers). The most notable feature in the plots exhibited in Fig. 2.1 lies on the stabilization of the FP values against the inclusion of new operators. As one can observe, after some oscillation for small truncations ($N \lesssim 7$), the FP coordinates for higher truncations stabilize around some specific values. In particular, we observe that, despite of the quantitative differences, the same qualitative picture is obtained for both types of coarse-graining operators. To complement our analysis concerning the FP structure for the $f(R)$-truncation, in Fig. 2.2 we exhibit FPs values normalized in a convenient way. For the "normalized FPs", here denoted as λ_n, we use a similar definition the one adopted in Ref. [73, 90], namely

$$\lambda_1 = \frac{G^*(N)}{G^*(N_{\max})} + 1 \qquad \text{and} \qquad \lambda_n = \frac{\alpha_n^*(N)}{\alpha_n^*(N_{\max})} + n\,, \tag{2.75}$$

where $G^*(N)$ and $\alpha_n^*(N)$ denote the FP values calculated within a truncation of order N, while $G^*(N_{\max})$ and $\alpha_n^*(N_{\max})$ stand for the FP values associated with the largest truncation under investigation (in the present case, $N_{\max} = 20$). The introduction of such normalized quantities is particularly useful to make clear the stabilization FP values against the truncation extensions.

The critical exponents exhibited in Fig. 2.3 indicate that the number of relevant directions (characterized by positive critical exponents) does not increase indefinitely, which is a crucial feature for ASQG. By looking at the critical exponents associated with the case of type I coarse-graining operator (Bochner-Laplacian), we observe two relevant directions for all the truncations under consideration (except for $N = 1$). For type II coarse-graining operator (Lichnerowicz-Laplacian), the situation is a bit more subtle. In this case, we note a variation on the number of positive critical exponents for small truncations ($N < 6$). However, with the inclusion of additional operators, the number of relevant directions seems to stabilize at two.

A remarkable feature of the results exhibited in Fig. 2.3 is the near-canonical behavior of the critical exponents. More precisely, the critical exponents obtained within the $f(R)$ truncation behave like $\theta_n \sim \Delta_n$, where $\Delta_n = 4 - 2n$ is the canonical scaling of an operator of the form R^n. The exception occurs for the two positive critical exponents, that are shifted away from the canonical scaling by a larger gap. The near-canonical behavior was already observed in the context of UQG based in the $f(R)$-approximation involving operators up to R^{10} [126]. Our findings not only indicate the stabilization of such results for higher-order truncations, but also include the extra trace mode in the flow equation (2.38), which was not considered in the previous analysis performed in the literature. Furthermore, it is interesting to mention that the near-canonical behavior of the critical exponents has been explored in great detail in the context of the standard formulation of ASQG [73, 90].

Now we turn our attention to the class of polynomial FZ-truncations. In such a case, the RG equations lead to larger expressions in comparison with the $f(R)$-approximation, and, as a consequence, it requires additional computational power than the previous case. For this reason, in the present case we explore the FP equations only up to a truncation where the highest-order operator correspond to $R(R_{\mu\nu}R^{\mu\nu})^7$ (i.e., $N_{\max} = 15$). Generally speaking, the search for FPs in the FZ-truncation follows the same strategy used in the $f(R)$-approximation. In this sense, we use the solutions

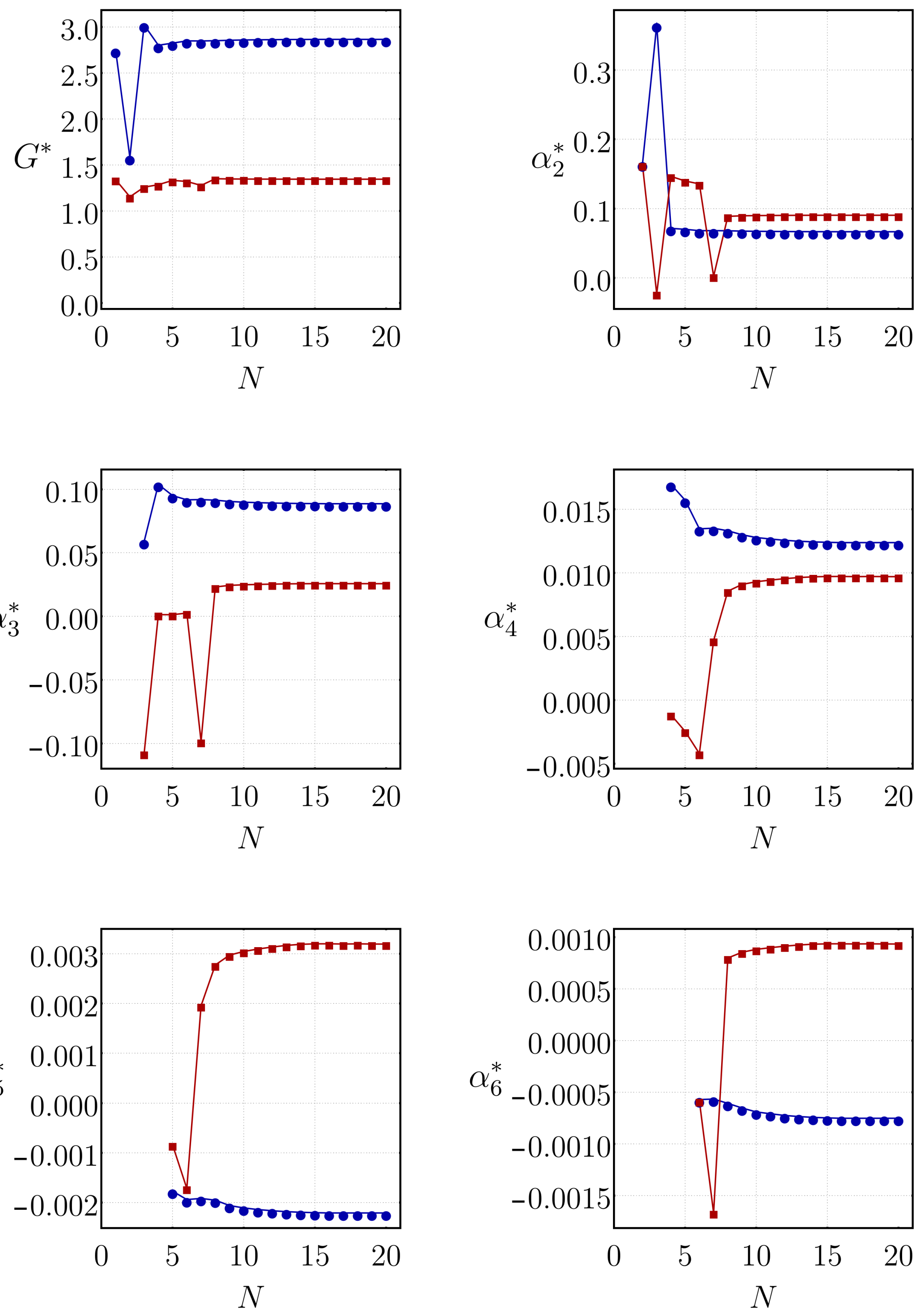

Figure 2.1: Fixed-point values for the couplings G_k, $\alpha_{k,2}$, $\alpha_{k,3}$, $\alpha_{k,4}$, $\alpha_{k,5}$ and $\alpha_{k,6}$ in the $f(R)$-truncation. The blue line (circle markers) indicates the Type I regularization (Bochner-Laplacian), whereas the red square indicates the Type II regularization (Lichnerowicz-Laplacian).

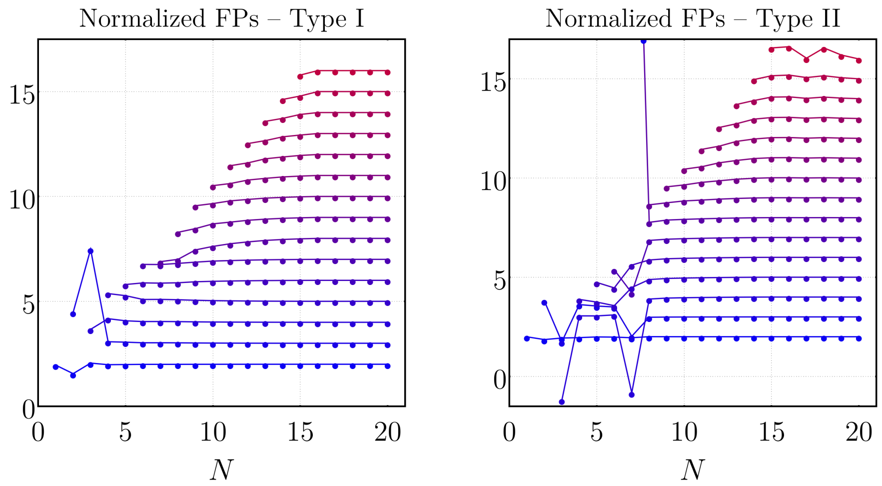

Figure 2.2: Normalized FPs in the $f(R)$-truncation. We use the normalization $\lambda_1 = \frac{G^*(N)}{G^*(N_{\max})} + 1$ and $\lambda_n = \frac{\alpha_n^*(N)}{\alpha_n^*(N_{\max})} + n$ (for $n > 1$). From bottom to top we show λ_1, λ_2, ..., λ_{15}. The left panel corresponds to results obtained via Bochner-Laplacian operator (type I), while the right panel shows the normalized FPs associated with the Lichnerowicz-Laplacian operator (type II).

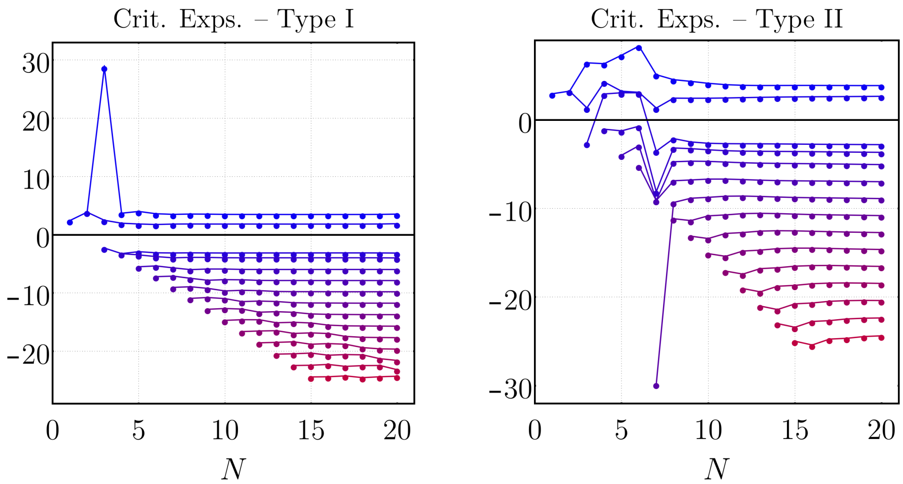

Figure 2.3: Critical exponents associated with the FP structure in the $f(R)$-approximation. The left panel corresponds to results obtained via Bochner-Laplacian operator (type I), while the right panel shows the results associated with the Lichnerowicz-Laplacian operator (type II).

obtained within a $(N-1)$-th truncation as the input for an algorithm to bootstrap FPs in a truncation of order N. It is interesting to emphasize that, even in the standard ASQG setting, the FZ-truncation has been considerably less explored than the $f(R)$ counterpart [89].

In Fig. 2.4, we report our findings for the FP values for some of the couplings (up to ρ_6^*) obtained within the FZ-truncation. As in the previous case, we exhibit the results for both types of coarse-graining operators. In addition, in Fig. 2.5 we exhibit the "normalized FP values". As one can observe, for Lichnerowicz-Laplacian operator (red/squared markers) our analysis leads to FP solutions for all the polynomial truncations up to $N_{\max} = 15$. In contrast, in the case of the Bochner-Laplacian coarse-graining operators, we only find suitable FP solutions up to the truncation characterized by $N = 9$. We attribute such a feature to a limitation in the numerical method used in the search of FPs.

Based on the critical exponents depicted in Fig. 2.6, our results for the FZ-truncation also point towards the existence of two relevant directions, for both types of coarse-graining operators. Despite of the stability on the number of relevant directions, the numerical values for the critical exponents suffer the same unstable behavior observed in the FP values (see. Fig. 2.4). At least for type I coarse-graining operator, despite of difficulties to extend our analysis to truncations higher than $N = 9$, the results exhibited in Fig. 2.6 (left) indicate that the critical exponents feature the same near-canonical behavior as we have discussed in the $f(R)$-approximation. Such behavior is less obvious in the case of type II coarse-graining operators. In this case, as one can see in Fig. 2.6 (right), some critical exponents behave according to the near-canonical scaling, however, for several choices of N we can observe points that exhibit considerable deviations from the canonical scaling of the operators involved in our truncation.

Our findings indicate that the unimodular FZ-truncation leads to less stable results in comparison with the $f(R)$-approximation. This result is in contrast with observations previously made in the standard ASQG setting. In particular, the systematic analysis performed in [89] indicates that the FZ-truncation exhibits a faster "convergence"[13] in comparison with the $f(R)$-approximation. Within the approximations considered here, our results indicate the opposite conclusion in the unimodular setting. So far, it is not clear what is the origin of such a difference. Nevertheless, there are some clues that could be confronted with further investigations:

- Exponential *versus* linear parameterization: The analysis performed here utilizes the exponential parameterization as a convenient way of implementing the unimodularity condition. On the other hand, previous calculations involving the FZ-truncation are based in the linear split [89]. The analysis performed in [91] (within the $f(R)$-approximation) indicates that the use of different choices field parameterization could lead to important differences in the FP structure.

- The use of spherical background: The choice of a spherical background in our calculation was motivated as a way to circumvent certain technical issues due to the presence of off-diagonal terms in the 2-point function $\Gamma^{(2)}$. For the $f(R)$-approximation, this choice is particularly interesting since it is self-consistent[14].

[13]Note that we are using the word "convergence" in a heuristic way. In this sense, there is no proof of mathematical convergence underlying such statements.

[14]The term "self-consistent" means that the spherical background already includes all the relevant contributions within this truncated theory space. The argument is based on the fact that we can

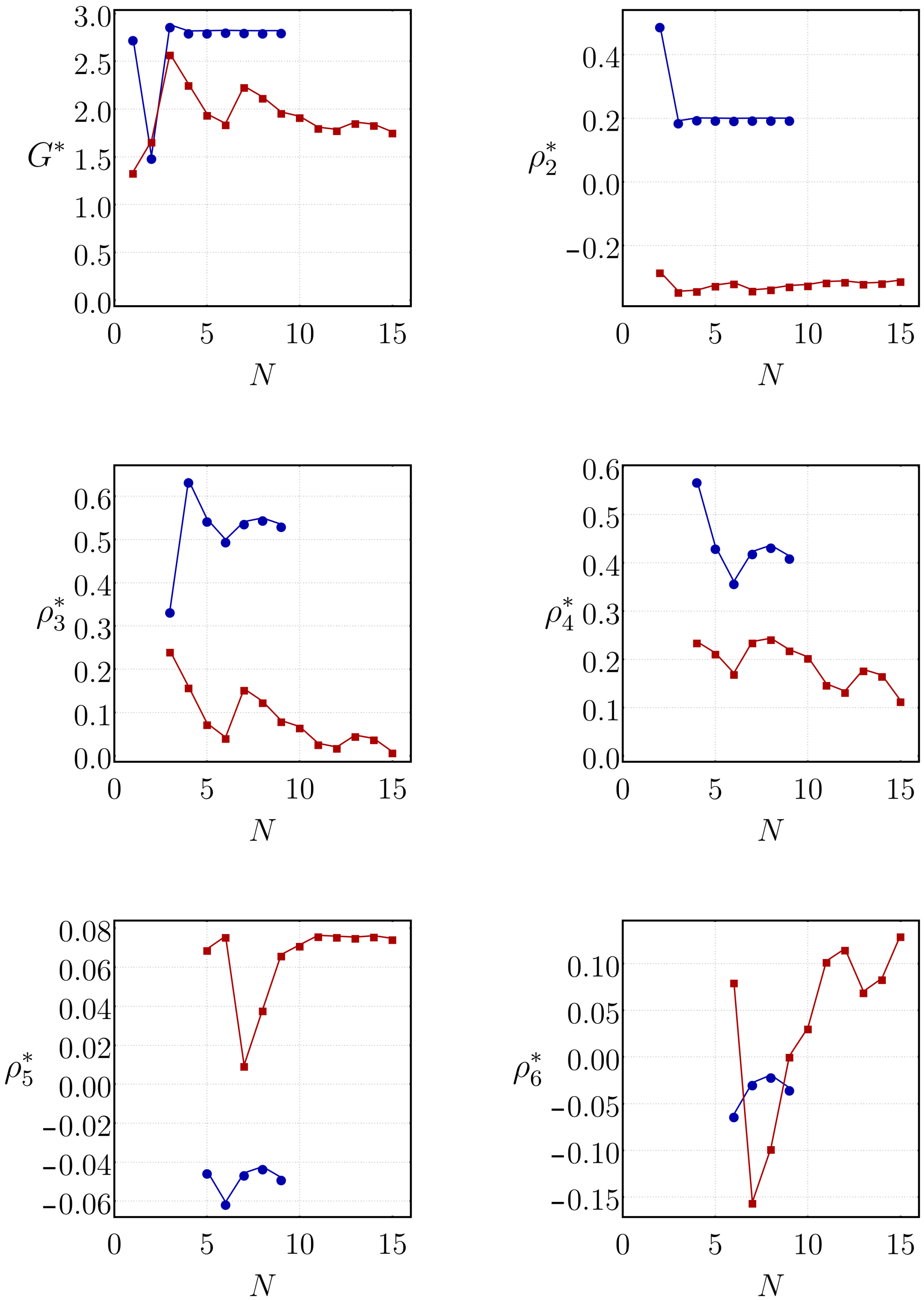

Figure 2.4: Fixed-point values for the couplings G_k, $\rho_{k,2}$, $\rho_{k,3}$, $\rho_{k,4}$, $\rho_{k,5}$ and $\rho_{k,6}$ in the FZ-truncation. The blue line (circle markers) indicates the Type I regularization (Bochner-Laplacian), whereas the red square indicates the Type II regularization (Lichnerowicz-Laplacian).

express the functional traces in the r.h.s. of the flow equation in terms of polynomial contributions in the Ricci scalar, plus contribution that vanishes on the set the spherical background.

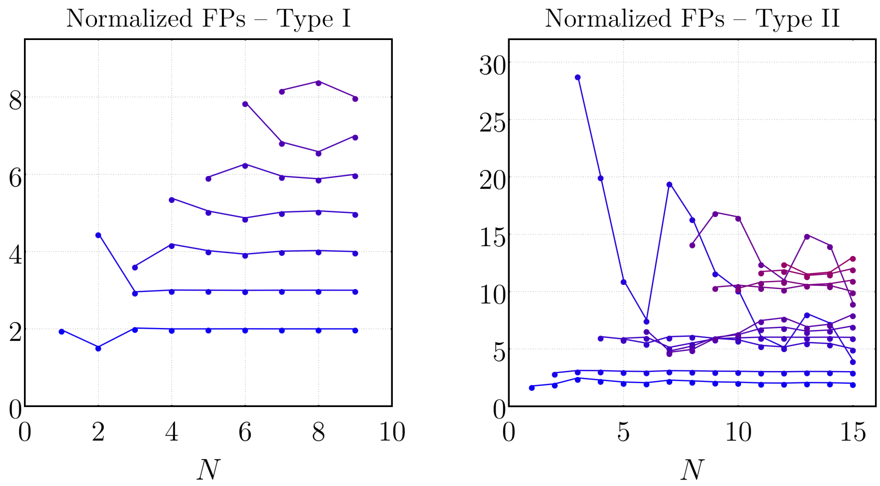

Figure 2.5: Normalized FPs in the FZ-truncation. We use the normalization $\rho_1 = \frac{G^*(N)}{G^*(N_{\max})} + 1$ and $\rho_n = \frac{\rho_n^*(N)}{\alpha_n^*(N_{\max})} + n$ (for $n > 1$). From bottom to top we show ρ_1, ρ_2, ..., ρ_7 (left-panel) and ρ_1, ρ_2, ..., ρ_{12} (right-panel). The left panel corresponds to results obtained via Bochner-Laplacian operator (type I), while the right panel shows the normalized FPs associated with the Lichnerowicz-Laplacian operator (type II).

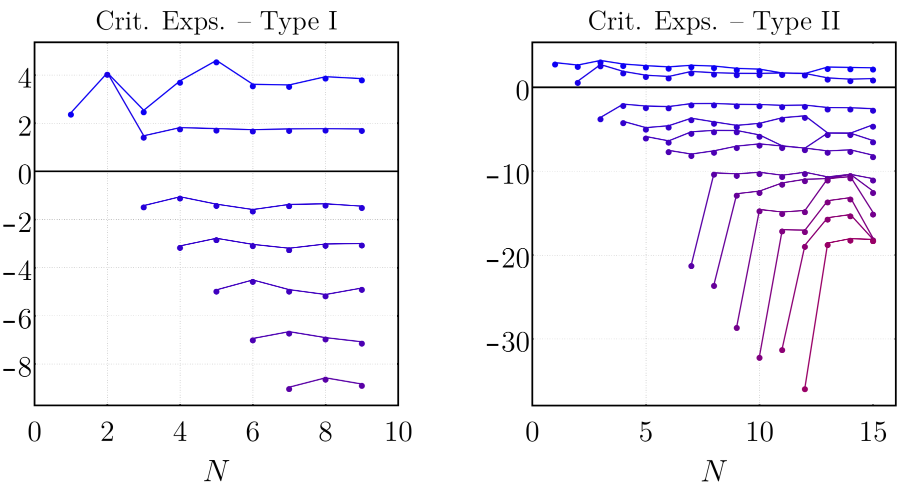

Figure 2.6: Critical exponents associated with the FP structure in the FZ-approximation. The left panel corresponds to results obtained via Bochner-Laplacian operator (type I), while the right panel shows the results associated with the Lichnerowicz-Laplacian operator (type II).

Nevertheless, this "self-consistency" is not valid for the FZ-truncation. As an example, an invariant of the form $R^{\mu}{}_{\nu}R^{\nu}{}_{\alpha}R^{\alpha}{}_{\mu}$, once projected on the sphere, generate spurious contributions to the beta function of the coupling associated with the operator $R\,R_{\mu\nu}R^{\mu\nu}$. As a hypothesis, one might consider that the existence of such spurious contributions could generate certain instabilities in the FP structure associated with the FZ-truncation. The validation of such reasoning requires calculations using a generic background, which goes beyond the scope of this thesis.

Chapter 3

Unimodular Quantum Gravity: Steps Beyond Perturbation Theory

3.1 Setting the stage

3.1.1 Symmetry identities and regulator effects

The notion of theory space, which is a fundamental concept in the FRG framework, is defined in terms of the configuration space and the underlying symmetries of the physical system under investigation. In UG, the configuration space is defined by metrics satisfying the unimodularity condition. Moreover, in this setting, the underlying symmetry is characterized by *TDiff* transformations, which follows from the invariance of the classical action, namely

$$\delta_{\epsilon_{\mathrm{T}}} S_{\mathrm{UG}}[g_{\mu\nu}] = 0\,. \tag{3.1}$$

As it is well known from the standard Faddeev-Popov procedure, the underlying gauge symmetry (*TDiff*) is broken by the introduction of a gauge fixing sector. Nevertheless, one can still keep track of original gauge symmetry by taking into account that the gauge-fixed system remains invariant under BRST transformations,

$$\delta_{\mathrm{BRST}}\big(S_{\mathrm{UG}}[g_{\mu\nu}] + S_{\mathrm{g.f}}[\varphi;\bar{g}]\big) = 0\,. \tag{3.2}$$

where $\varphi_A = (h_{\mu\nu}, \bar{c}_\mu\,, c^\mu\,, b_\mu)$ has been introduced as a "super-field" notation. Note that, in the gauge-fixing sector, we also introduced the Lautrup-Nakanishi field, b^μ, which is necessary to make the BRST symmetry valid for off-shell field configurations.

At the quantum level, the BRST symmetry translates into a functional identity involving the (full) effective action Γ, namely, the Slavnov-Taylor identity (STI)[1],

$$\frac{\delta\Gamma}{\delta Q}\cdot\frac{\delta\Gamma}{\delta\varphi}=0\,, \tag{3.3}$$

where Q denotes an extra source term introduced by its coupling with the BRST transformation of the field φ, i.e., by including $Q\cdot\varphi$ as part of the generating functional. Within the FRG framework, one can derive an analogous STI for the EAA, however, this is not obtained by the simple replacement $\Gamma\mapsto\Gamma_k$. In fact, the FRG regulator spoils BRST invariance since

$$\delta_{\mathrm{BRST}}\Delta S[\varphi;\bar{g}]\neq 0\,. \tag{3.4}$$

As a consequence the STI for Γ_k involves a soft-breaking contribution, resulting in the form [174, 190]

$$\frac{\delta\Gamma_k}{\delta Q}\cdot\frac{\delta\Gamma_k}{\delta\varphi}=\Upsilon_k[\varphi;\bar{g}]\,, \tag{3.5}$$

where $\Upsilon_k[\varphi;\bar{g}]$ is regulator-dependent term (that vanishes at $k=0$). This functional identity is usually referred to as modified STI (mSTI).

Besides the BRST symmetry, the covariant approach to QG brings a second type of local invariance, namely, split symmetry, which is associated with the use of the background field method. Split symmetry is defined by joint transformations,

$$\bar{g}_{\mu\nu}\mapsto\bar{g}_{\mu\nu}+\delta_{\mathrm{split}}\bar{g}_{\mu\nu}\qquad\text{and}\qquad h_{\mu\nu}\mapsto h_{\mu\nu}+\delta_{\mathrm{split}}h_{\mu\nu}\,, \tag{3.6}$$

such that the full metric remains invariant

$$g_{\mu\nu}\;\mapsto\;g_{\mu\nu}(\bar{g}+\delta_{\mathrm{split}}\bar{g}\,,h+\delta_{\mathrm{split}}h)=g_{\mu\nu}(\bar{g},h)\,. \tag{3.7}$$

For linear metric parameterization ($g_{\mu\nu}=\bar{g}_{\mu\nu}+\kappa\,h_{\mu\nu}$), split symmetry is manifested by the simple transformations $\delta_{\mathrm{split}}\bar{g}_{\mu\nu}=-\chi_{\mu\nu}$ and $\delta_{\mathrm{split}}h_{\mu\nu}=\kappa^{-1}\chi_{\mu\nu}$, with $\chi_{\mu\nu}=\chi_{\mu\nu}(x)$ being a local transformation parameter. For the non-linear metric parameterization, such as the exponential split (see Eq. (2.27)), the explicit form of $\delta_{\mathrm{split}}h_{\mu\nu}$ is more complicated. In this case, we denote $\delta_{\mathrm{split}}h_{\mu\nu}=\mathcal{N}_{\mu\nu}^{\alpha\beta}[h;\bar{g}]\chi_{\alpha\beta}$, which can be determined in an iterative way (see App. B).

The split symmetry allows us to derive a second type of functional identity that relates functional derivatives taken with respect to the background and fluctuation fields. This is usually known as Nielsen identity (NI) or split Ward identity and takes

[1] The "dot" is a compact notation to represent all indices contractions and space-time integration, i.e., $X\cdot Y=\int_x\omega\,X_A(x)Y^A(x)$.

the form

$$\frac{\delta\Gamma}{\delta\bar{g}_{\mu\nu}} - \mathcal{N}^{\alpha\beta}_{\mu\nu}[h;\bar{g}]\cdot\frac{\delta\Gamma}{\delta h_{\alpha\beta}} = \left\langle \frac{\delta S_{\text{g.f.}}}{\delta\bar{g}_{\mu\nu}} \right\rangle_k - \left\langle \mathcal{N}^{\alpha\beta}_{\mu\nu}[h;\bar{g}]\cdot\frac{\delta S_{\text{g.f.}}}{\delta h_{\alpha\beta}} \right\rangle_k . \tag{3.8}$$

The contribution on the r.h.s. encodes non-trivial information due to split symmetry-breaking caused by the gauge-fixing sector. In the FRG setup, the inclusion of a cutoff term $\Delta S_k[\varphi;\bar{g}]$ introduces a second source of symmetry-breaking[2], leading to a modified NI (mNI), namely [190, 231]

$$\frac{\delta\Gamma_k}{\delta\bar{g}_{\mu\nu}} - \mathcal{N}^{\alpha\beta}_{\mu\nu}[h;\bar{g}]\cdot\frac{\delta\Gamma_k}{\delta h_{\alpha\beta}} = \left\langle \frac{\delta S_{\text{g.f.}}}{\delta\bar{g}_{\mu\nu}} \right\rangle_k - \left\langle \mathcal{N}^{\alpha\beta}_{\mu\nu}[h;\bar{g}]\cdot\frac{\delta S_{\text{g.f.}}}{\delta h_{\alpha\beta}} \right\rangle_k + \Xi_k[\varphi;\bar{g}]\,, \tag{3.9}$$

where $\Xi_k[\varphi;\bar{g}]$ is a regulator-dependent contribution. As in the case of the mSTI, the regulator induced term vanishes at $k=0$.

In the background approximation, as we have considered in the calculations presented in Chap. 2, we typically consider truncations that are not compatible with the coarse-grained symmetry identities (3.5) and (3.9). In fact, the compatibility of the EAA with the appropriated symmetry identities, including modifications due to the FRG regulator, requires explicitly symmetry-breaking terms in Γ_k. In this sense, quantum symmetries (at $k=0$) require symmetry-breaking contributions at non-vanishing k. In this chapter, we perform some steps in this direction by including symmetry-breaking effects at the level of a truncation defined in the unimodular theory space. The results presented in this chapter are based on the recent publication [270].

3.1.2 Vertex expansion in UQG

The main purpose of this chapter is to investigate the RG flow of the graviton and Faddeev-Popov ghosts 2-point functions in UG. In this sense, we employ the strategy put forward in [67, 74] which is based on the vertex expansion approach for the FRG. The basic idea is to expand Γ_k in terms of its proper vertices. Schematically, the vertex expansion takes the form[3]

$$\Gamma_k[\varphi\,;\bar{g}] = \sum_n \frac{1}{n!}\int \Gamma^{(n)}_{k,A_1\cdots A_n}[\bar{g}]\,\varphi^{A_n}\,\cdots\,\varphi^{A_1}\,, \tag{3.10}$$

[2] Again, the gauge-fixing term treats the background and the fluctuations fields in such a way that such split symmetry is broken. Nevertheless, such a breaking comes in the form of a BRST-exact term. For the regulator, however, the split symmetry-breaking is explicit and not BRST exact.

[3] Each functional derivative "$\delta/\delta\varphi^A$" is associated to a space-time variable and the integral represents a collective integration over all such variables.

with vertices defined according to

$$\Gamma^{(n)}_{k,\,A_1\cdots A_n}[\bar{g}] = \frac{\delta^n \Gamma_k}{\delta\varphi^{A_1}\,\cdots\,\delta\varphi^{A_n}}\bigg|_{\varphi=0}\,. \tag{3.11}$$

Note that, besides the fluctuation field $h_{\mu\nu}$, the functional Γ_k also depends on the Faddeev-Popov ghosts c^μ and $\bar{c}_\mu$, as well as on the Lautrup-Nakanishi field b_μ. We note that, typically, the Lautrup-Nakanishi field is not included as part of the configuration space in FRG truncations in QG.

In order to define the truncated vertices we follow the same recipe employed in [194, 217]. The idea is to define a "seed" truncation $\hat{\Gamma}^{\text{seed}}_{\text{UG}}$ used to extract the tensorial structure that enters in the vertex expansion of the flow equation. In what follows we choose $\hat{\Gamma}^{\text{seed}}_{\text{UG}}$ to take the form

$$\hat{\Gamma}^{\text{seed}}_{\text{UG}}[h, c, \bar{c}, b; \bar{g}] = \hat{\Gamma}_{\text{uEH}}[g(h\,; \bar{g})] + \hat{\Gamma}_{\text{g.f.}}[h, c, \bar{c}, b\,; \bar{g}] + \hat{\Gamma}_{m^2}[h; \bar{g}]\,. \tag{3.12}$$

The first term, $\hat{\Gamma}_{\text{uEH}}$, includes only contributions that are invariant under the original *TDiff* symmetry. Our choice for $\hat{\Gamma}_{\text{uEH}}$ corresponds to the unimodular version of the Einstein-Hilbert (uEH) action in four dimensions,

$$\hat{\Gamma}_{\text{uEH}}[g(h\,; \bar{g})] = -\frac{1}{16\pi G_{\text{N}}}\int_x \omega\, R(g(h\,; \bar{g}))\,, \tag{3.13}$$

The argument $g(h\,; \bar{g})$ indicates that the full metric $g_{\mu\nu}$ is decomposed in terms of a background a $\bar{g}_{\mu\nu}$ and the fluctuation field $h_{\mu\nu}$. As we have discussed in the previous chapter, a convenient metric decomposition in UG is the exponential parameterization (see Eq. (2.27)).

The second term in (3.12) corresponds to the gauge-fixing sector obtained through the Faddeev-Popov procedure,

$$\hat{\Gamma}_{\text{g.f.}}[h, c, \bar{c}, b\,; \bar{g}] = \int_x \omega\, \bar{g}^{\mu\nu}\, b_\mu F^{\text{T}}_\nu[h\,; \bar{g}] - \frac{\alpha}{2}\int_x \omega\, \bar{g}^{\mu\nu}\, b_\mu b_\nu + \int_x \omega\, \bar{c}_\mu\, \mathcal{M}^\mu{}_\nu[h\,; \bar{g}]\, c^\nu\,. \tag{3.14}$$

As usual, α represents a gauge parameter. We use the transverse gauge condition defined in the App. A (see Eq. (A.6)). The Faddeev-Popov operator, $\mathcal{M}^\mu{}_\nu[h\,; \bar{g}]$, is defined according to Eq. (A.15). We refer to the App. A for comments on the Faddeev-Popov procedure in the unimodular setting.

The last term in (3.12) extends the truncated theory space to the sector of symmetry-breaking operators induced by the FRG regulator. As a first step in UG, we consider a simple mass-like term for the fluctuation field,

$$\hat{\Gamma}_{m_h^2}[h; \bar{g}] = \frac{m_h^2}{2}\int_x \omega\, \bar{g}^{\mu\alpha}\bar{g}^{\nu\beta} h_{\mu\nu} h_{\alpha\beta}\,, \tag{3.15}$$

where m_h denotes mass parameter. The inclusion of such a term is associated with a technical aspect related to the FRG type of regularization and, therefore, it should not be confused with a physical mass for the graviton. As we are going to see later, even if not present in the original truncation, this term is generated by the flow of the 2-point function $\delta^2\Gamma_k/\delta h^2$.

To extract the truncated vertices $\Gamma^{(n)}_{k,\,A_1\cdots A_n}$ from $\hat{\Gamma}^{\text{seed}}_{\text{UG}}$, we expand $\hat{\Gamma}_{\text{UG}}$ and $\hat{\Gamma}_{\text{g.f.}}$ up to order $\mathcal{O}(h^4)$ and $\mathcal{O}(h^2)$, respectively. For practical calculations we set the background metric to be flat $\bar{g}_{\mu\nu} = \delta_{\mu\nu}$. In this case, it is convenient to work in Fourier space. We note that higher-order terms in the fluctuation field do not give any contribution to the results presented in this chapter. The truncated vertices $\Gamma^{(n)}_{k,\,A_1\cdots A_n}$ are, then, obtained by dressing the "seed" vertices $\hat{\Gamma}^{(n)}_{A_1\cdots A_n}$ with tensor structures $[\mathcal{Z}_{k,\varphi}(p)^{1/2}]^B{}_A$. In such a case, we define

$$\Gamma^{(n)}_{k,\,A_1\cdots A_n}(\mathbf{p}) = [\mathcal{Z}_{k,\varphi_1}(p_1)^{1/2}]^{B_1}{}_{A_1}\cdots[\mathcal{Z}_{k,\varphi_n}(p_n)^{1/2}]^{B_n}{}_{A_n}\,\hat{\Gamma}^{(n)}_{B_1\cdots B_n}(\mathbf{p})\Big|_{G_{\text{N}}\mapsto k^{-2}G_k}\,, \tag{3.16}$$

with $\mathbf{p} = (p_1,\,\cdots,p_{n-1})$ (note that $p_n = -(p_1+\cdots+p_{n-1})$ due to momentum conservation). The relevant tensor structures are defined according to

$$[\mathcal{Z}_{k,h}(p)^{1/2}]^{\mu\nu\alpha\beta} = Z^{1/2}_{k,\text{TT}}\,\mathcal{P}^{\mu\nu\alpha\beta}_{\text{TT}}(p) + Z^{1/2}_{k,\xi}\,\mathcal{P}^{\mu\nu\alpha\beta}_{\xi}(p) + Z^{1/2}_{k,\sigma}\,\mathcal{P}^{\mu\nu\alpha\beta}_{\sigma}(p)\,, \tag{3.17a}$$

$$[\mathcal{Z}_{k,\bar{c}}(p)^{1/2}]^{\mu\nu} = [\mathcal{Z}_{k,c}(p)^{1/2}]^{\mu\nu} = Z^{1/2}_{k,c}\,\mathcal{P}^{\mu\nu}_{\text{T}}(p)\,, \tag{3.17b}$$

$$[\mathcal{Z}_{k,b}(p)^{1/2}]^{\mu\nu} = Z^{1/2}_{k,b}\,\mathcal{P}^{\mu\nu}_{\text{T}}(p)\,, \tag{3.17c}$$

where $Z_{k,\text{TT}}$, $Z_{k,\xi}$, $Z_{k,\sigma}$, $Z_{k,c}$ and $Z_{k,b}$ correspond to wave-function renormalization factors. In the graviton sector, we have used the projectors $\mathcal{P}_{\text{TT}}(p)$, $\mathcal{P}_{\xi}(p)$ and $\mathcal{P}_{\sigma}(p)$ defined on the York-basis (see App. C). Moreover, $\mathcal{P}_{\text{T}}(p)$ corresponds to the transverse projector acting on vector fields. The use of different pre-factors in the expansion of $\mathcal{Z}_{k,h}(p)^{1/2}$ account for possible symmetry-breaking effects induced by the FRG regulator. As a further step towards the inclusion of symmetry deformation contributions, we also redefine the mass parameter m_h^2, appearing in the graviton 2-point function, according to $m_h^2 \mapsto m^2_{k,\text{TT}}$, $m_h^2 \mapsto m^2_{k,\xi}$ and $m_h^2 \mapsto -\frac{1}{2}m^2_{k,\sigma}$ for the different tensorial sectors defined in terms of the projectors $\mathcal{P}_{\text{TT}}(p)$, $\mathcal{P}_{\xi}(p)$ and $\mathcal{P}_{\sigma}(p)$. The factor "$-1/2$" in the definition of $m^2_{k,\sigma}$ is just a convenient normalization for the 2-point function. In principle, the gauge-fixing parameter α is also allowed to run, therefore, we replace $\alpha \mapsto \alpha_k$.

Furthermore, in the present chapter we consider the following prescription for the

FRG regulator,

$$\mathbf{R}_{k,A_1A_2}(p) = [\mathcal{Z}_{k,\varphi_1}(p)^{1/2}]^{B_1}{}_{A_1}\,[\mathcal{Z}_{k,\varphi_2}(p)^{1/2}]^{B_2}{}_{A_2}\,\left(\hat{\Gamma}^{(2)}_{B_1B_2}(p_{\rm reg}) - \hat{\Gamma}^{(2)}_{B_1B_2}(p)\right)\,, \tag{3.18}$$

where we have defined $p^\mu_{\rm reg} = (1+r_k)^{1/2}p^\mu$ and $r_k = r_k(p^2)$ denotes the shape function. Here we consider the Litim's regulator $r_k(p^2) = (k^2/p^2-1)\theta(k^2/p^2-1)$ [181, 182].

3.2 Flow of the 2-point function

3.2.1 2-point functions, propagators and all that

The flow of the 2-point function $\Gamma_k^{(2)}$ can be obtained by acting with two functional derivatives w.r.t. φ on the FRG equation. In general, the flow equation for $\Gamma_k^{(2)}$ reads [184]

$$\partial_t\Gamma_k^{(2)} = -\frac{1}{2}\mathrm{STr}\Big(\mathbf{G}_k\,\Gamma_k^{(4)}\,\mathbf{G}_k\,\partial_t\mathbf{R}_k\Big) + \mathrm{STr}\Big(\mathbf{G}_k\,\Gamma_k^{(3)}\,\mathbf{G}_k\,\Gamma_k^{(3)}\,\mathbf{G}_k\,\partial_t\mathbf{R}_k\Big)\,, \tag{3.19}$$

where $\mathbf{G}_k = (\Gamma_k^{(2)} + \mathbf{R}_k)^{-1}|_{\varphi=0}$ denotes the dressed propagator. For the truncation we are considering here, we find the 2-point functions,

$$\begin{aligned}\frac{\delta^2\Gamma_k[\varphi]}{\delta h_{\mu\nu}(-p)\delta h_{\alpha\beta}(p)}\bigg|_{\varphi=0} &= Z_{k,\mathrm{TT}}\,(p^2+m^2_{k,\mathrm{TT}})\,\mathcal{P}^{\mu\nu\alpha\beta}_{\mathrm{TT}}(p)\\ &\quad + Z_{k,\xi}\,m^2_{k,\xi}\,\mathcal{P}^{\mu\nu\alpha\beta}_{\xi}(p) - \frac{1}{2}Z_{k,\sigma}\,(p^2+m^2_{k,\sigma})\,\mathcal{P}^{\mu\nu\alpha\beta}_{\sigma}(p)\,,\end{aligned} \tag{3.20a}$$

$$\frac{\delta^2\Gamma_k[\varphi]}{\delta h_{\mu\nu}(-p)\delta b_{\alpha}(p)}\bigg|_{\varphi=0} = \frac{1}{2i}Z^{1/2}_{k,\xi}Z^{1/2}_{k,b}\,\left(p^\mu\mathcal{P}^{\nu\alpha}_{\mathrm{T}}(p) + p^\nu\mathcal{P}^{\mu\alpha}_{\mathrm{T}}(p)\right)\,, \tag{3.20b}$$

$$\frac{\delta^2\Gamma_k[\varphi]}{\delta b_{\mu}(-p)\delta b_{\alpha}(p)}\bigg|_{\varphi=0} = -\alpha_k\,Z_{k,b}\,\mathcal{P}^{\mu\alpha}_{\mathrm{T}}(p)\,, \tag{3.20c}$$

$$\frac{\delta^2\Gamma_k[\varphi]}{\delta c_{\mu}(-p)\delta \bar{c}_{\alpha}(p)}\bigg|_{\varphi=0} = -\sqrt{2}\,Z_{k,c}\,p^2\,\mathcal{P}^{\mu\alpha}_{\mathrm{T}}(p)\,. \tag{3.20d}$$

Before we proceed with the main results of this chapter, let us add a brief remark concerning the running of the gauge-fixing parameter α_k. An interesting feature regarding the inclusion of Lautrup-Nakanishi fields in the FRG truncation is the possibility of extracting the flow of α_k directly in terms of the 2-point function $\delta^2\Gamma_k/\delta b^2$. In general, thanks to (3.19), the r.h.s. of the flow equation for $\delta^2\Gamma_k/\delta b^2$ involve 3- and 4-point vertices containing at least one functional derivative w.r.t. the Lautrup-Nakanishi field. However, vertices with this feature are not present in the truncation that we are considering. In such a case, the r.h.s. of for the flow equation for $\delta^2\Gamma_k/\delta b^2$ vanishes and, as a consequence, the running of α_k can be readily extracted from $\partial_t\left(\delta^2\Gamma_k/\delta b^2\right) = 0$, resulting in

$$\partial_t \alpha_k = \alpha_k\, \eta_b\,, \tag{3.21}$$

where we have defined $\eta_b = -Z_{k,b}^{-1}\partial_t Z_{k,b}$. Since $\partial_t\alpha_k$ is proportional to α_k itself, the Landau gauge choice $\alpha_k = 0$ turns out to be a partial FP. In this sense, we can set $\alpha_k = 0$ along the calculation without worrying of other values being generated by the flow. The running of α_k has been explored in Ref. [271], leading to the same conclusion in the standard ASQG setting based in the quantization of full diff-invariant theories.

At the practical level, the Landau gauge choice simplifies the analysis performed here. In particular, due to the choice $\alpha_k = 0$, the mass parameter $m^2_{k,\xi}$ and the wave-function renormalization factors $Z_{k,\xi}$ and $Z_{k,b}$ do not feedback in the flow of the graviton and ghost 2-point functions. This feature is a consequence of the form of the regularized graviton propagator which is,

$$\mathbf{G}^{\mu\nu\alpha\beta}_{k,hh}(p) = \frac{\mathcal{P}^{\mu\nu\alpha\beta}_{\mathrm{TT}}(p)}{Z_{k,\mathrm{TT}}\left(\left(1+r_k(p^2)\right)p^2 + m^2_{k,\mathrm{TT}}\right)} - \frac{2\,\mathcal{P}^{\mu\nu\alpha\beta}_{\sigma}(p)}{Z_{k,\sigma}\left(\left(1+r_k(p^2)\right)p^2 + m^2_{k,\sigma}\right)}\,, \tag{3.22}$$

in the Landau gauge. For this reason, in the present chapter, we focus our attention in the flow of $m^2_{k,\mathrm{TT}}$, $m^2_{k,\sigma}$, $Z_{k,\mathrm{TT}}$, $Z_{k,\sigma}$ and $Z_{k,c}$, with $\alpha_k = 0$. The other relevant propagator for the analysis performed here is the one associated with the ghost fields,

$$\mathbf{G}^{\mu\nu}_{k,c\bar{c}}(p) = -\frac{1}{\sqrt{2}\,Z_{k,c}\left(1+r_k(p^2)\right)p^2}\,\mathcal{P}^{\mu\nu}_{\mathrm{T}}(p)\,. \tag{3.23}$$

For the sake of completeness, we also include the dressed propagators involving the Lautrup-Nakanishi field

$$\mathbf{G}^{\mu\nu\alpha}_{k,hb}(p) = \frac{1}{\sqrt{2}\,i\,Z^{1/2}_{k,b}\,Z^{1/2}_{k,\xi}\left(1+r_k(p^2)\right)^{1/2}p^2}\left(\mathcal{P}^{\mu\alpha}_{\mathrm{T}}(p)\,p^\nu + \mathcal{P}^{\nu\alpha}_{\mathrm{T}}(p)p^\mu\right)\,, \tag{3.24a}$$

$$\mathbf{G}^{\mu\nu}_{k,bb}(p) = -\frac{m^2_{k,\xi}}{Z_{k,b}\left(1+r_k(p^2)\right)p^2}\,\mathcal{P}^{\mu\nu}_{\mathrm{T}}(p)\,. \tag{3.24b}$$

It is important to emphasize, however, that the $\mathbf{G}^{\mu\nu\alpha}_{k,hb}(p)$ and $\mathbf{G}^{\mu\nu}_{k,bb}(p)$ decouple from the calculation presented here due to the Landau gauge choice.

Besides this set of propagators, the results presented in this chapter also depends

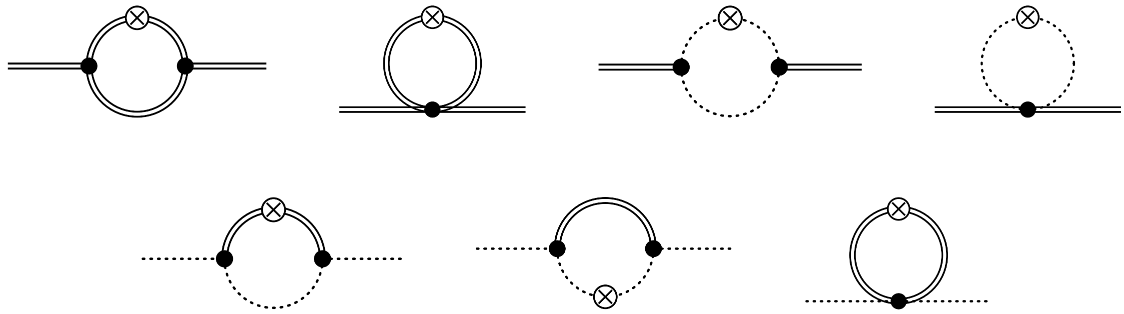

Figure 3.1: Diagrammatic representation corresponding to the r.h.s. of Eq. (3.19). The first row corresponds to the flow of the graviton 2-point function $\delta^2\Gamma_k/\delta h^2$. In the second row we include diagrams representing the flow of the ghost 2-point function $\delta^2\Gamma_k/\delta c\delta\bar{c}$. The double-line style corresponds to the graviton, while the Fadddeev-Popov ghosts are represented by dotted lines. The cross indicates the regulator insertion $\partial_t \mathbf{R}_k$.

on the evaluation of the 3- and 4-point vertices

$$\frac{\delta^3\Gamma_k}{\delta h^3}\,, \qquad \frac{\delta^4\Gamma_k}{\delta h^4}\,, \qquad \frac{\delta^3\Gamma_k}{\delta h\delta c\delta\bar{c}}\,, \qquad \frac{\delta^4\Gamma_k}{\delta h^2\delta c\delta\bar{c}}\,. \tag{3.25}$$

The expressions corresponding to these vertices are quite lengthy and, therefore, we shall not report the results explicitly.

3.2.2 Anomalous dimensions and symmetry-breaking masses

In the present section we report our results for the anomalous dimensions $\eta_{\mathrm{TT}} = -Z_{k,\mathrm{TT}}^{-1}\partial_t Z_{k,\mathrm{TT}}$, $\eta_\sigma = -Z_{k,\sigma}^{-1}\partial_t Z_{k,\sigma}$ and $\eta_c = -Z_{k,c}^{-1}\partial_t Z_{k,c}$ as well as the running of the mass parameters $m_{k,\mathrm{TT}}^2$ and $m_{k,\sigma}^2$. The basic idea is to use the flow equation (3.19) to express the 2-point running functions $\delta^2\Gamma_k/\delta h^2$ and $\delta^2\Gamma_k/\delta c\delta\bar{c}$ in terms of traces involving 3- and 4-point vertices extracted from our truncation for Γ_k. The traces contributing to the flow of the 2-point function can be represented in terms of the diagrams exhibited in Fig. 3.1.

To extract the anomalous dimension and the running of symmetry-breaking masses from Eq. (3.19), we apply the following projection rules

$$\eta_{\mathrm{TT}} = -\frac{1}{5\,Z_{k,\mathrm{TT}}}\left[\frac{\partial}{\partial p^2}\left(\mathcal{P}_{\mathrm{TT}}^{\mu\nu\alpha\beta}(p)\frac{\delta^2\partial_t\Gamma_k[\varphi]}{\delta h^{\mu\nu}(-p)\delta h^{\alpha\beta}(p)}\bigg|_{\varphi=0}\right)\right]_{p^2=0}\,, \tag{3.26a}$$

$$\eta_\sigma = \frac{2}{Z_{k,\sigma}}\left[\frac{\partial}{\partial p^2}\left(\mathcal{P}_{\sigma}^{\mu\nu\alpha\beta}(p)\frac{\delta^2\partial_t\Gamma_k[\varphi]}{\delta h^{\mu\nu}(-p)\delta h^{\alpha\beta}(p)}\bigg|_{\varphi=0}\right)\right]_{p^2=0}\,, \tag{3.26b}$$

$$\eta_c = \frac{1}{3\sqrt{2}\,Z_{k,c}} \left[\frac{\partial}{\partial p^2} \left(\mathcal{P}^{\mu\nu}_{\mathrm{T}}(p) \frac{\delta^2 \partial_t \Gamma_k[\varphi]}{\delta c^\mu(-p)\delta \bar{c}_\nu(p)} \bigg|_{\varphi=0} \right) \right]_{p^2=0} , \tag{3.26c}$$

$$\partial_t m^2_{k,\mathrm{TT}} = \eta_{\mathrm{TT}}\, m^2_{k,\mathrm{TT}} + \frac{1}{5\, Z_{k,\mathrm{TT}}} \left(\mathcal{P}^{\mu\nu\alpha\beta}_{\mathrm{TT}}(p) \frac{\delta^2 \partial_t \Gamma_k[\varphi]}{\delta h^{\mu\nu}(-p)\delta h^{\alpha\beta}(p)} \bigg|_{\varphi=0} \right)_{p^2=0} , \tag{3.27a}$$

$$\partial_t m^2_{k,\sigma} = \eta_\sigma\, m^2_{k,\sigma} - \frac{2}{Z_{k,\sigma}} \left(\mathcal{P}^{\mu\nu\alpha\beta}_{\sigma}(p) \frac{\delta^2 \partial_t \Gamma_k[\varphi]}{\delta h^{\mu\nu}(-p)\delta h^{\alpha\beta}(p)} \bigg|_{\varphi=0} \right)_{p^2=0} . \tag{3.27b}$$

The running of the corresponding dimensionless mass parameters ($\tilde{m}^2_{k,i} = k^{-2} m^2_{k,i}$) can be obtained by the simple formula $\partial_t \tilde{m}^2_{k,i} = -2\tilde{m}^2_{k,i} + k^{-2}\partial_t m^2_{k,i}$. The calculation for the anomalous dimensions and for the running of symmetry-breaking masses can be done by using the truncation defined in the previous section to evaluate the diagrams represented in Fig. 3.1. The explicit results for the η_i's and $\partial_t \tilde{m}^2_{k,i}$'s are reported in the App. C.

The anomalous dimensions resulting from the projection rules defined by Eqs. (3.26a), (3.26b) and (3.26c) lead to the following structure

$$\eta_{\mathrm{TT}} = (A_{\mathrm{TT}} + B^{\mathrm{TT}}_{\mathrm{TT}}\, \eta_{\mathrm{TT}} + B^{\sigma}_{\mathrm{TT}}\, \eta_\sigma + B^{c}_{\mathrm{TT}}\, \eta_c)\, G_k\,, \tag{3.28a}$$

$$\eta_\sigma = (A_\sigma + B^{\mathrm{TT}}_{\sigma}\, \eta_{\mathrm{TT}} + B^{\sigma}_{\sigma}\, \eta_\sigma + B^{c}_{\sigma}\, \eta_c)\, G_k \tag{3.28b}$$

$$\eta_c = (A_c + B^{\mathrm{TT}}_{c}\, \eta_{\mathrm{TT}} + B^{\sigma}_{c}\, \eta_\sigma + B^{c}_{c}\, \eta_c)\, G_k\,, \tag{3.28c}$$

where the coefficients A's and B's can be obtained by simple comparison of these expressions with Eqs. (C.1), (C.2) and (C.3). The anomalous dimensions in the r.h.s. appears as a consequence of the regulator insertion $\partial_t \mathbf{R}_k$ in the diagrams contributing to the flow of the 2-point function. The explicit expressions for the anomalous dimensions can be easily obtained by solving the linear system (3.28a), (3.28b) and (3.28c) for η_{TT}, η_σ and η_c.

Starting from the simplest situation, we first set $\tilde{m}^2_{k,\mathrm{TT}} = \tilde{m}^2_{k,\sigma} = 0$ in order to explore the behavior of the anomalous dimension in terms of the dimensionless Newton's coupling G_k. In Fig. 3.2, we plot the anomalous dimensions η_{TT}, η_σ and η_c as functions of G_k based on two different schemes: full and semi-perturbative. The full result is obtained by solving Eqs. (3.28a), (3.28b) and (3.28c) for η_{TT}, η_σ and η_c without any further approximation. The semi-perturbative calculation, on the other hand,

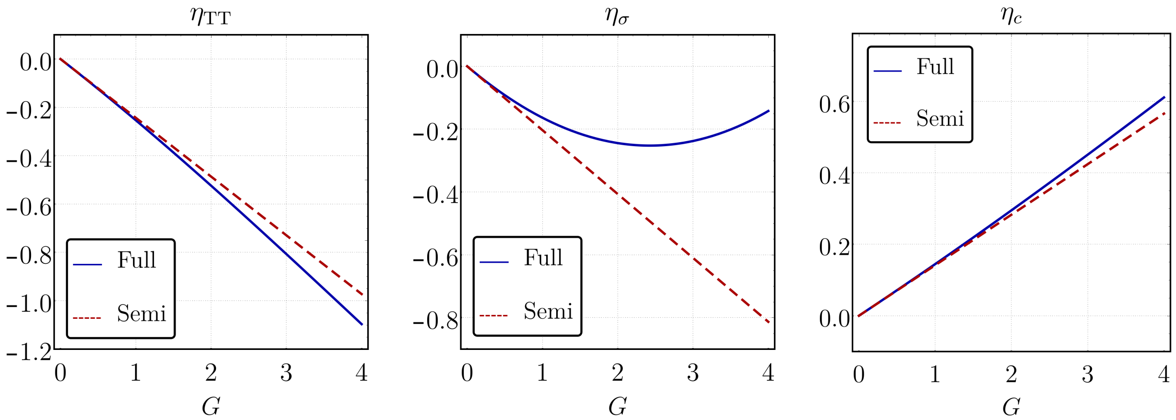

Figure 3.2: We show the anomalous dimensions $\eta_{\rm TT}$, η_σ and η_c, in terms of the dimensionless Newton's coupling, in the case corresponding to $m^2_{k,\rm TT} = m^2_{k,\sigma} = 0$.

corresponds to the anomalous dimension obtained by setting the η's to zero in the r.h.s. of (3.28a), (3.28b) and (3.28c). As we can observe in Fig. 3.2, for $\tilde{m}^2_{k,\rm TT} = \tilde{m}^2_{k,\sigma} = 0$, the full and semi-perturbative results exhibit very similar qualitative behavior both in the case of $\eta_{\rm TT}$ and η_c. Nevertheless, a different conclusion emerges from the calculation of η_σ. In this case, the full result shows a considerable deviation from the linear behavior obtained in the semi-perturbative approximation.

With the inclusion of the masses $m^2_{k,\rm TT}$ and $m^2_{k,\sigma}$, we investigate the viability of UV completion within the extended truncation. In this sense, here we look for FP solutions of the partial system of RG equations

$$\partial_t \tilde{m}^2_{k,\rm TT} = -(2-\eta_{\rm TT})\,\tilde{m}^2_{k,\rm TT} + f_{\rm TT}(\tilde{m}^2_{k,\rm TT}, \tilde{m}^2_{k,\sigma}, \eta_{\rm TT}, \eta_\sigma, \eta_c, G_k)\,, \tag{3.29a}$$

$$\partial_t \tilde{m}^2_{k,\sigma} = -(2-\eta_\sigma)\,\tilde{m}^2_{k,\sigma} + f_\sigma(\tilde{m}^2_{k,\rm TT}, \tilde{m}^2_{k,\sigma}, \eta_{\rm TT}, \eta_\sigma, \eta_c, G_k)\,. \tag{3.29b}$$

The explicit form of the functions $f_{\rm TT}$ and f_σ can be identified from Eqs. (C.4) and (C.5). Both $f_{\rm TT}$ and f_σ are non-vanishing for $G_k \neq 0$, which confirms that even if we set $\tilde{m}^2_{k,\rm TT} = \tilde{m}^2_{k,\sigma} = 0$ at some RG-scale k, symmetry-breaking mass terms would be generated due to graviton self-interactions. The partial system corresponding to Eqs. (3.29a) and (3.29b) is not closed, since, at this level, the Newton's coupling appears as an external parameter. Within this setting, we perform the search of FPs solutions for $\partial_t \tilde{m}^2_{k,\rm TT} = 0$ and $\partial_t \tilde{m}^2_{k,\sigma} = 0$, but treating possible FP values of the Newton's coupling, G^*, as free parameters. This strategy allows us to explore the FP properties of $m^2_{k,i}$'s and η_i's without relying in some specific expression (computed within an approximation scheme) for the running of the Newton's coupling.

In Fig. 3.3 we plot the FP values $(\tilde{m}^2_{\rm TT})^*$ and $-(\tilde{m}^2_\sigma)^*/2$ as functions of G^*. For the sake of comparison, we have considered three different schemes. The perturbative

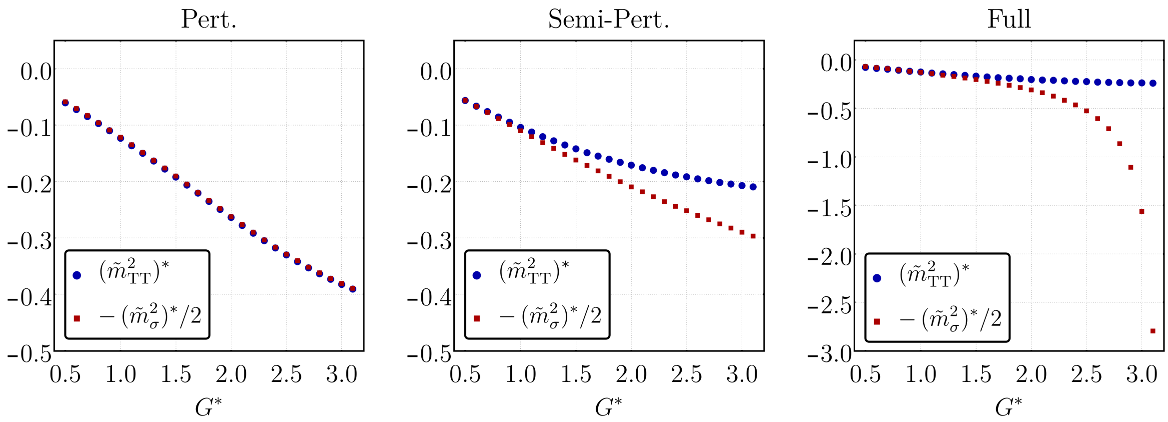

Figure 3.3: FP solutions for the partial system composed by Eqs. (3.29a) and (3.29b). In this case, the FP value of the dimensionless Newton's coupling, G^*, appears as an external variable.

approximation is obtained by setting the η's to zero in Eqs. (3.29a) and (3.29b). In this case, both $(\tilde{m}^2_{\rm TT})^*$ and $-(\tilde{m}^2_{\sigma})^*/2$ exhibit the same values along the range under consideration. The semi-perturbative regime is defined by setting the anomalous dimensions to zero in the functions $f_{\rm TT}$ and f_σ, but using the semi-perturbative expressions for $\eta_{\rm TT}$ and η_σ in the first term on the r.h.s. of Eqs. (3.29a) and (3.29b). Within this approximation we note that the separation between the FP values of $(\tilde{m}^2_{\rm TT})^*$ and $-(\tilde{m}^2_{\sigma})^*/2$ increases with G^*. Finally, the full result correspond to FP solutions of Eqs. (3.29a) and (3.29b) without further approximations. As one can observe, the FP value of $-(\tilde{m}^2_{\sigma})^*/2$ hits a pole around $G^* = 3.2$. On the other hand, $(\tilde{m}^2_{\rm TT})^*$ exhibit small variation along the range considered here. Furthermore, we note that $(\tilde{m}^2_{\rm TT})^*$ and $-(\tilde{m}^2_{\sigma})^*/2$ mostly coincide when G^* is small ($G^* \lesssim 1.5$).

In Fig. 3.4 we show the anomalous dimensions $\eta_{\rm TT}$, η_σ and η_c evaluated at the FP solutions of Eqs. (3.29a) and (3.29b). Comparing Figs. 3.2 and 3.4, we observe some clear differences regarding the behavior of the anomalous dimensions with and without setting the masses to zero. In particular, we note that the absolute values of $\eta^*_{\rm TT}$ and η^*_σ grow faster in the case where we take into account the regulator induced mass parameters, signaling that non-perturbative effects may become relevant for smaller values of G^* in comparison with the case $\tilde{m}^2_{k,i} = 0$. In addition, one can observe that η^*_σ becomes larger than 2 around $G^* \sim 3.2$. In connection to this point, it has been argued that there is a class of FRG regulators such that results with $\eta^* > 2$ becomes unreliable [195]. Since the regulator used in the present analysis belong to this class, one can argue that internal consistency for our results (with $\tilde{m}^2_{k,i} \neq 0$) requires G^* to be smaller than 3.2.

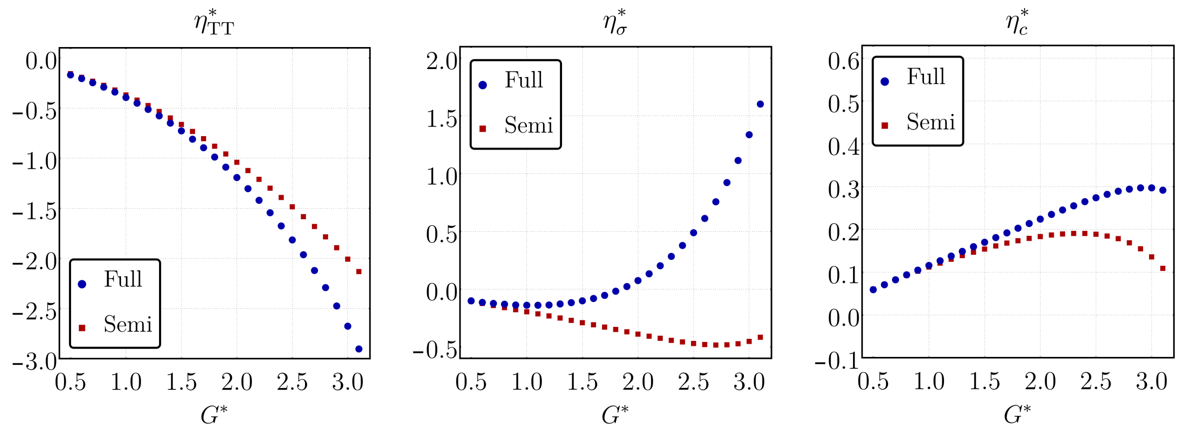

Figure 3.4: Anomalous dimensions $\eta_{\rm TT}$, η_σ and η_c evaluated at the FP solutions depicted in Fig. 3.3.

3.3 RG-flow and fixed points

3.3.1 Running of the Newton's coupling

Up to this point we have considered the FP values of the Newton's coupling as a free parameter. In this section, we explore the FP structure including explicit results for the beta function of the dimensionless coupling G_k. The running of G_k can be computed in several ways, each one corresponding to a different "avatar" of the Newton's coupling (see [200, 201] for a detailed discussion). The relation between different avatars are encoded in the mSTI and mNI [200, 201]. Here, following the simplest route, we extract the running of G_k from the background flow $\partial_t \Gamma_k[\varphi = 0; \bar{g}]$. In order to simplify the computations, the background is considered to be a 4-sphere. In such a case, the running of the dimensionless Newton's coupling can be obtained by the following expression

$$\partial_t G_k = 2\, G_k + 16\pi\, k^{-2}\, G_k^2 \times \left[\frac{\partial}{\partial \bar{R}} \left(\frac{\partial_t \Gamma_k[\varphi = 0; \bar{g}]}{V(S^4)} \right) \right]_{\bar{R}=0}, \tag{3.30}$$

where $V(S^4)$ stands for the volume of the 4-sphere. Using standard heat-kernel methods in order to compute the trace in the r.h.s. of (2.38) we arrive at the following structure for the running of G_k

$$\partial_t G_k = 2G_k + \frac{G_k^2}{24\pi} \Big(\mathcal{A}(\tilde{m}^2_{k,\rm TT}, \tilde{m}^2_{k,\sigma}) + \mathcal{B}_{\rm TT}(\tilde{m}^2_{k,\rm TT})\eta_{\rm TT} + \mathcal{B}_\sigma(\tilde{m}^2_{k,\sigma})\eta_\sigma + \mathcal{B}_c\, \eta_c \Big)\,. \tag{3.31}$$

The coefficients $\mathcal{A}(\tilde{m}^2_{k,\rm TT}, \tilde{m}^2_{k,\sigma})$, $\mathcal{B}_{\rm TT}(\tilde{m}^2_{k,\rm TT})$, $\mathcal{B}_\sigma(\tilde{m}^2_{k,\sigma})$ and $\mathcal{B}_c$ are scheme-dependent quantities that can be computed within the truncation defined in Sect. 3.1.2. In table 3.1 we present the explicit results for these coefficients in terms of two types of regularization schemes distinguished by the choice of coarse-graining operators, namely, using

	$\mathcal{A}(\tilde{m}^2_{k,\mathrm{TT}}, \tilde{m}^2_{k,\sigma})$	$\mathcal{B}_{\mathrm{TT}}(\tilde{m}^2_{k,\mathrm{TT}})$	$\mathcal{B}_\sigma(\tilde{m}^2_{k,\sigma})$	$\mathcal{B}_c$
Type I	$-\frac{30\,(3+2\,\tilde{m}^2_{k,\mathrm{TT}})}{3\,(1+\tilde{m}^2_{k,\mathrm{TT}})^2} + \frac{4}{1+\tilde{m}^2_{k,\sigma}} - 19$	$\frac{5\,(4+3\,\tilde{m}^2_{k,\mathrm{TT}})}{3\,(1+\tilde{m}^2_{k,\mathrm{TT}})^2}$	$-\frac{1}{1+\tilde{m}^2_{k,\sigma}}$	6
Type II	$-\frac{10\,(7+10\,\tilde{m}^2_{k,\mathrm{TT}})}{(1+\tilde{m}^2_{k,\mathrm{TT}})^2} + \frac{4}{1+\tilde{m}^2_{k,\sigma}} - 10$	$\frac{5\,(4+5\,\tilde{m}^2_{k,\mathrm{TT}})}{(1+\tilde{m}^2_{k,\mathrm{TT}})^2}$	$-\frac{1}{1+\tilde{m}^2_{k,\sigma}}$	0

Table 3.1: Explicit coefficients $\mathcal{A}(\tilde{m}^2_{\mathrm{TT}}, \tilde{m}^2_\sigma)$, $\mathcal{B}_{\mathrm{TT}}(\tilde{m}^2_{\mathrm{TT}})$, $\mathcal{B}_\sigma(\tilde{m}^2_\sigma)$ and $\mathcal{B}_c$ for two types of coarse-graining operators. Here, we use the nomenclature "type I" to designate the case where the coarse-graining operator corresponds to the Bochner-Laplacian $\Delta_{\mathrm{B}} = -\bar{\nabla}^2$. The nomenclature "type II" corresponds to the choice of Lichnerowicz-Laplacian defined as $\Delta_{\mathrm{L}} = -\bar{\nabla}^2 + \alpha \bar{R}$ (with $\alpha = 2/3$, $\alpha = 1/4$ and $\alpha = 0$, respectively, for transverse-traceless tensors, transverse vectors and scalars) on spherical backgrounds.

Bochner (type I) and Lichnerowicz (type II) Laplacians (see Chap. 2). The calculation that leads to the explicit coefficients reported in table 3.1 follows the same ideas discussed in the previous chapter and, therefore, we will not provide further details here. It is important to remark that $\partial_t G_k$ involves (via anomalous dimension contributions) the avatars of the Newton's coupling extracted from 3- and 4-graviton vertices and graviton-ghost vertices. We take as an additional approximation the identification of all these avatars with a single coupling G_k.

We should emphasize the difference between the investigation performed here and previous results in asymptotically safe UG (see chapter 2 and references therein). The main difference lies on the fact that previous computations in this setting were done within the background approximation. In such a case, the 2-point function $\delta^2\Gamma_k/\delta h^2|_{\varphi=0}$ is identified with $\delta^2\Gamma_k/\delta \bar{g}^2|_{\varphi=0}$ (plus gauge-fixing contributions). Within this approximation, the anomalous dimensions arising from the regulator insertion $\partial_t \mathbf{R}_k$ is fixed according to the prescription,

$$\eta_{\mathrm{TT}} = \eta_\sigma = -2 + G_k^{-1}\partial_t G_k \qquad \text{and} \qquad \eta_c = 0\,, \tag{3.32}$$

sometimes referred as "RG-improved" anomalous dimensions [74]. Furthermore, the background approximation does not include regulator induced masses. In this sense, the results presented here involve two steps beyond the background approximation:

i) we have computed the anomalous dimensions η_{TT}, η_σ and η_c using the derivative expansion;

ii) the truncation considered here includes symmetry deformation effects parameterized by the masses $m^2_{k,\mathrm{TT}}$ and $m^2_{k,\sigma}$.

Another important difference with respect to previous investigations in the literature of asymptotically safe UG is the inclusion of an extra trace in the flow equation (see

	G^*	θ	$\eta^*_{\rm TT}$	η^*_σ	η^*_c
1-Loop – Type I	3.35	2	0	0	0
1-Loop – Type II	1.98	2	0	0	0
"RG-Improv." – Type I	2.67	2.50	-2	-2	0
"RG-Improv." – Type II	1.32	3.00	-2	-2	0
η's from D.E. – Type I	3.18	2.14	-0.86	-0.23	0.48
η's from D.E. – Type II	1.77	2.23	-0.46	-0.23	0.26

Table 3.2: FP structure associated to the case $\tilde{m}^2_{k,\rm TT} = \tilde{m}^2_{k,\sigma} = 0$. Here we report results obtained using both types of coarse-graining operators and for the different approximations concerning the anomalous dimensions.

Eq. (2.38)), accounting for the appropriate treatment of the volume factor associated with the *TDiff* symmetry group.

3.3.2 Fixed point structure

In what follows we explore the FP structure for UG by taking into account the running of the Newton's coupling discussed in the previous section. In view of a better understanding concerning the impact of the anomalous dimensions and the symmetry-breaking mass parameters, it is useful to consider some intermediary approximations.

Let us start with the case where the masses $m^2_{k,\rm TT}$ and $m^2_{k,\sigma}$ are set to zero along the flow. In this case, G_k is the only essential coupling within the truncated theory space under investigation. As a consequence, the relevant properties concerning the truncated RG flow is encoded in the simple equation

$$\partial_t G_k = \beta_G(G_k)\,, \tag{3.33}$$

where the beta function $\beta_G(G_k)$ corresponds to the r.h.s. of (3.31) (using the anomalous dimensions $\eta_{\rm TT}$, η_σ and η_c reported in Sect. 3.2.2 and setting $\tilde{m}^2_{k,\rm TT} = \tilde{m}^2_{k,\sigma} = 0$). In Fig. 3.5 we show the beta function $\beta_G(G_k)$ for the two types of regularization schemes considered here. For the sake of comparison we also include the 1-loop and the "RG improved" closure where, instead of using the anomalous dimensions reported in the in Sect. 3.2.2, we use the prescriptions $\eta_{\rm TT} = \eta_\sigma = \eta_c = 0$ and $\eta_{\rm TT} = \eta_\sigma = -2 + G_k^{-1}\partial_t G_k$ and $\eta_c = 0$, respectively. In all cases we observe a UV attractive interacting FP for the dimensionless Newton's coupling. The numerical values for the FPs and critical exponents (see table 3.2) are, as usual, scheme and approximation dependent. However, by looking at Fig. 3.5 we observe the same qualitative features in all the approximations under investigation.

The results presented in Sect. 3.2.2 provide indications that the approximation $\tilde{m}^2_{k,\rm TT} = \tilde{m}^2_{k,\sigma} = 0$ is not self-consistent, in the sense that, even if not included in the original truncation, the symmetry-breaking masses would be generated by the flow

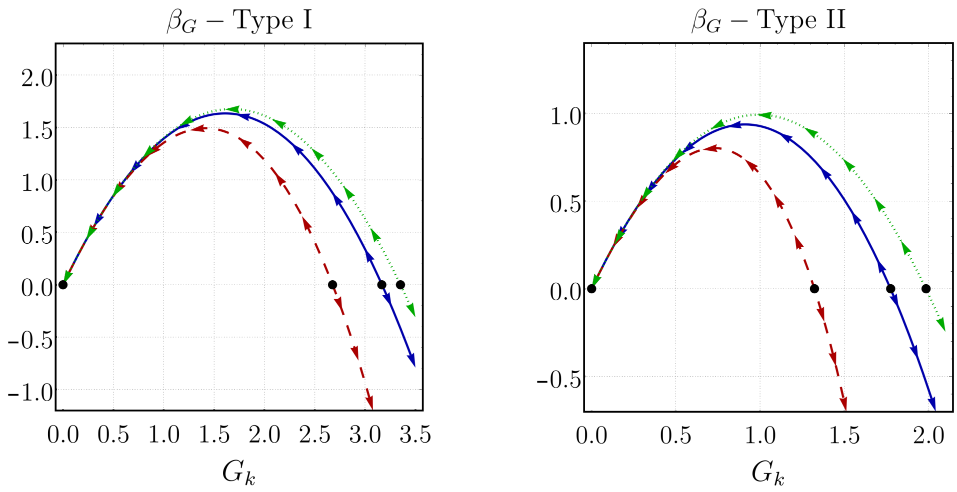

Figure 3.5: Beta function of the dimensionless Newton's coupling in the case $\tilde{m}^2_{\rm TT} = \tilde{m}^2_\sigma = 0$. The plot on the left (right) corresponds to the type I (II) coarse-graining operator. The blue (continuous) line corresponds to the case where the anomalous dimensions were replaced by the results reported in the Sect. 3.2.2. The red (dashed) and green (dotted) lines represent "RG improved" and 1-loop closure, respectively. Conventionally, the arrows point towards the infrared.

equations. Here, we consider the full system describing the RG flow in truncated theory space including G_k, $\tilde{m}^2_{k,\rm TT}$ and $\tilde{m}^2_{k,\sigma}$. In table (3.3), we summarize our findings for the FP structure. The corresponding anomalous dimensions and critical exponents are shown in tables 3.4 and 3.5, respectively. In order to understand the impact of the anomalous dimensions, besides the full closure involving the η_i's computed via derivative expansion, we also include results corresponding to the 1-loop approximation ($\eta_{\rm TT} = \eta_\sigma = \eta_c = 0$). The results obtained here can be summarized in the following way:

- Confronting the results exhibited in table 3.2 and 3.3 we observe that the inclusion of symmetry-breaking masses shifts G^* towards smaller values in comparison with the case where $\tilde{m}^2_{k,\rm TT} = \tilde{m}^2_{k,\sigma} = 0$.

- At 1-loop, we observe FP values with $(\tilde{m}^2_{\rm TT})^* \approx -\frac{1}{2}(\tilde{m}^2_\sigma)^*$, in agreement with the analysis presented in Sect. 3.2.2 (see Fig. 3.3).

- Within the full closure, the FP values of $(\tilde{m}^2_{\rm TT})^*$ and $-\frac{1}{2}(\tilde{m}^2_\sigma)^*$ exhibit a considerable difference, in special, for the type I regularization scheme.

- We also observe substantial differences concerning the FP values for the different avatars of the graviton anomalous dimensions, $\eta^*_{\rm TT}$ and η^*_σ. In particular, we note that η^*_σ change the sign according with the type of coarse-graining operators.

The critical exponents reported in table 3.5 provide indications that the three couplings under investigation, G_k, $\tilde{m}^2_{k,\rm TT}$ and $\tilde{m}^2_{k,\sigma}$, constitute UV relevant directions. At

	G^*	$(\tilde{m}^2_{\rm TT})^*$	$-(\tilde{m}^2_\sigma)^*/2$
1-Loop & $m^2_{k,i} \neq 0$ – Type I	2.30	−0.30	−0.30
1-Loop & $m^2_{k,i} \neq 0$ – Type II	1.75	−0.22	−0.22
Full Closure – Type I	2.23	−0.19	−0.37
Full Closure – Type II	1.52	−0.15	−0.19

Table 3.3: FP structure in the truncated theory space defined by G_k, $\tilde{m}^2_{k,\rm TT}$ and $\tilde{m}^2_{k,\sigma}$. We report results obtained using both types of coarse-graining operators. The "1-Loop" closure correspond to the case where we set $\eta_{\rm TT} = \eta_\sigma = \eta_c = 0$. We use the nomenclature "Full Closure" to designate FP solutions involving anomalous dimensions computed via derivative expansion.

	$\eta^*_{\rm TT}$	η^*_σ	η^*_c
Full Closure – Type I	−1.43	0.24	0.25
Full Closure – Type II	−0.72	−0.08	0.18

Table 3.4: Anomalous dimensions evaluated at the FP solutions exhibited in table 3.3.

a first sight, this result suggests that the RG flow of the symmetry-breaking masses would also require initial conditions determined by experimental observations. However, $\tilde{m}^2_{k,\rm TT}$ and $\tilde{m}^2_{k,\sigma}$ appear as technical artifacts related with the method used to implement the Wilsonian renormalization. Therefore, the symmetry-breaking masses do not present any direct physical meaning and we should not expect initial conditions on $\tilde{m}^2_{k,\rm TT}$ and $\tilde{m}^2_{k,\sigma}$ coming from experiments. Ideally, a consistent treatment of the FRG equation should also take into account mSTI's and mNI's controlling gauge and split symmetries in a coarse-grained way. In this sense, we expect that those symmetry identities should provide further constraints along the RG flow, eliminating the necessity of experiments to determine initial conditions associated with couplings arising from regulator induced effects. A full treatment involving the mSTI and mNI, however, goes beyond the scope of this thesis.

3.3.3 Flow diagram in unimodular gravity

The results presented in the previous section provide indications for a suitable UV FPs in simple truncations defined in the unimodular theory space. Here, we complement this analysis by exploring the RG flow diagram in UG. For simplicity, we consider an approximated slice of truncated theory space characterized by the single mass approximation

$$\tilde{m}^2_{k,\rm TT} \mapsto \tilde{m}^2_{k,h} \qquad \text{and} \qquad \tilde{m}^2_{k,\sigma} \mapsto -2\tilde{m}^2_{k,h}\,. \tag{3.34}$$

The use of such an approximation is a convenient choice to avoid three dimensional plots. Nevertheless, it is interesting to remark that the flow diagram in the theory space

	θ_1	θ_2	θ_3
1-Loop & $m_{k,i}^2 \neq 0$ – Type I	$1.99 - 1.37\,i$	$1.99 + 1.37\,i$	2.0
1-Loop & $m_{k,i}^2 \neq 0$ – Type II	$1.89 - 0.65\,i$	$1.89 + 0.65\,i$	2.0
Full System – Type I	$3.15 - 1.18\,i$	$3.15 + 1.18\,i$	1.75
Full System – Type II	$2.56 - 0.92\,i$	$2.56 + 0.92\,i$	2.07

Table 3.5: Critical exponents associated with the FP solutions reported in table 3.3.

defined by couplings G_k, $\tilde{m}_{k,\mathrm{TT}}^2$ and $\tilde{m}_{k,\sigma}^2$ exhibits the same qualitative properties as the results presented in this section. Within the single mass approximation, we define the running of the mass parameter $\tilde{m}_{k,h}^2$ by projecting the flow of the graviton 2-point (at vanishing momentum) function in the TT sector (see Eq. (3.27a)). In this case, we arrive at the flow equation

$$\begin{aligned}\partial_t \tilde{m}_{k,h}^2 = &- (2 - \eta_{\mathrm{TT}})\, \tilde{m}_{k,h}^2 + \frac{G_k\,(-620 - 1160\,\tilde{m}_{k,h}^2 + (91 + 145\,\tilde{m}_{k,h}^2)\,\eta_{\mathrm{TT}})}{1296\pi\,(1 + \tilde{m}_{k,h}^2)^3} \\ &+ \frac{G_k\,(100 + 880\,\tilde{m}_{k,h}^2 + (1 - 110\,\tilde{m}_{k,h}^2)\,\eta_\sigma)}{6480\pi\,(1 - 2\tilde{m}_{k,h}^2)^3} - \frac{G_k\,(110 - 7\eta_c)}{540\pi}\,.\end{aligned} \tag{3.35}$$

In Fig. 3.6 we plot the RG flow diagram in UQG in the plane defined by $\tilde{m}_{k,h}^2 \times G_k$. Notably, the flow diagram represented in Fig. 3.6 exhibits remarkable similarities in comparison with the typical phase portrait in the standard ASQG setting, with the identification $\tilde{m}_{k,h}^2 = -2\Lambda_k$ (see Fig. 1.4 in Chap. 1). It is important to emphasize that the similarities between the flow diagrams for unimodular and standard ASQG do not necessarily imply the physical equivalence between these theories. In particular, the identification $\tilde{m}_{k,h}^2 = -2\Lambda_k$ does not take into account the different status of $\tilde{m}_{k,h}^2$ and Λ_k. As we have discussed in the previous section, in unimodular ASQG, the symmetry-breaking masses arise as an artifact induced by the FRG regulator. In this case, we expect that the symmetry identities (mSTI and mNI) could provide strong constraints such that the inclusion of symmetry-breaking terms does not require additional initial conditions to be fixed by experiments. In contrast, in the context of standard ASQG, the flow of the cosmological constant is not expected to be constrained by any symmetry identity, therefore, requiring initial conditions fixed by experimental data.

3.4 Unimodular gravity versus unimodular gauge

3.4.1 Unimodular gauge

The unimodular gauge (sometimes also referred as physical gauge) has been used in the full *Diff* version of ASQG as a convenient choice [81, 198, 259]. In the full *Diff*

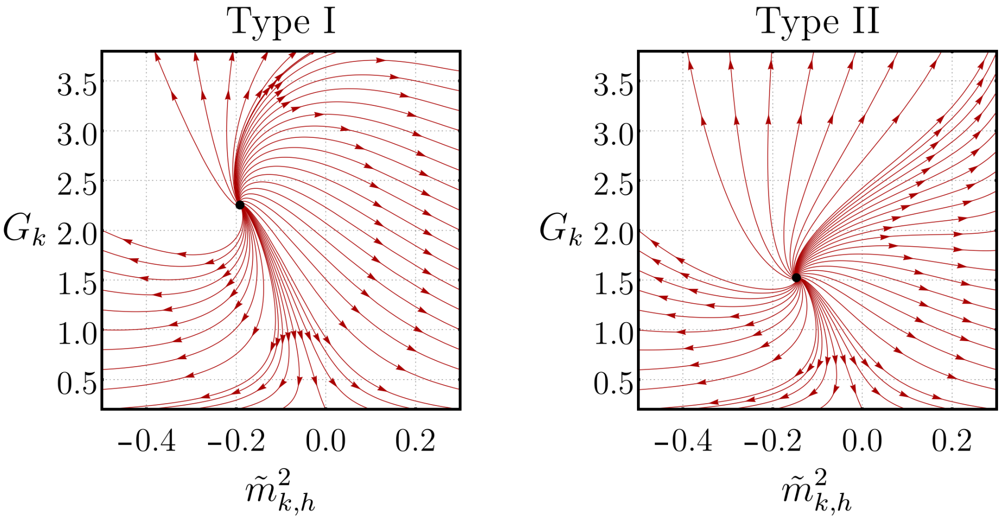

Figure 3.6: Flow diagram of UQG in the single mass approximation. The RG trajectories correspond to numerical solutions of Eqs. (3.31) and (3.35). As usual, the arrows point towards the infrared. In the single mass approximation, we found FP solutions $((\tilde{m}_h^2)^*, G^*)_{\text{Type I}} = (-0.19, 2.25)$ and $((\tilde{m}_h^2)^*, G^*)_{\text{Type II}} = (-0.15, 1.52)$, with corresponding critical exponents $\theta_\pm^{\text{Type I}} = 3.21 \pm 1.25\, i$ and $\theta_\pm^{\text{Type II}} = 2.58 \pm 0.94\, i$.

setting we usually work with a gauge fixing sector defined in terms of the function

$$F_\mu[h\,;\bar{g}] = \bar{\nabla}^\nu h_{\mu\nu} - \frac{1+\beta}{4}\,\bar{\nabla}_\mu h^{\text{tr}}\,, \tag{3.36}$$

where β is a gauge parameter. In the present section, we denote $h_{\mu\nu}$ as the full fluctuation field without the tracelessness condition. The unimodular gauge is characterized by a combination of the exponential parameterization ($g_{\mu\nu} = \bar{g}_{\mu\alpha}[e^{\kappa\, h^{\cdot}_{\;\cdot}}]^\alpha{}_\nu$) with the limit $\beta \to -\infty$. This limit imposes a constant trace-mode $h^{\text{tr}} = \text{const.}$, which, together with the exponential parameterization, implies a kind of unimodular restriction on the full metric $g_{\mu\nu}$. In this sense, it is interesting to investigate whether the RG flow associated with the unimodular gauge produces equivalent results in comparison with the unimodular theory space explored along this thesis. In what follows, we present some simple arguments in favor of this equivalence. It is important to emphasize that all the statements performed here are valid at the level of the FRG truncation that we are considering.

To perform practical calculations in the unimodular gauge, we follow the same strategy to define a truncation as discussed in Sect. 3.1.2. In the present case, we start from the "seed" truncation[4]

$$\hat{\Gamma}^{\text{seed}}_{\text{QGR}}[h,c,\bar{c},b;\bar{g}] = \hat{\Gamma}_{\text{EH}}[g(h\,;\bar{g})] + \hat{\Gamma}_{\text{g.f.}}[h,c,\bar{c},b\,;\bar{g}]\,, \tag{3.37}$$

We use the label "QGR" to indicated that we working in the theory space defined from the quantization of GR. The $\hat{\Gamma}_{\text{EH}}[g(h\,;\bar{g})]$ contribution is the usual Einstein-Hilbert truncation

$$\hat{\Gamma}_{\text{EH}}[g(h\,;\bar{g})] = \frac{1}{16\pi G_{\text{N}}}\int_x \sqrt{g}\,\left(2\Lambda_{\text{cc}} - R(g(h\,;\bar{g}))\right)\,. \tag{3.38}$$

In contrast to UG, in the present case, the inclusion of the cosmological constant terms is justified by the fact that the metric determinant is not restricted *a priori*. For the gauge-fixing sector, we consider the truncation

$$\begin{aligned}\hat{\Gamma}_{\text{g.f.}}[h,c,\bar{c},b\,;\bar{g}] = &\int_x \sqrt{\bar{g}}\;\bar{g}^{\mu\nu}\,b_\mu F_\nu[h\,;\bar{g}] - \frac{\alpha}{2}\int_x \sqrt{\bar{g}}\,\bar{g}^{\mu\nu}\,b_\mu b_\nu \\ &+ \int_x \sqrt{\bar{g}}\,\bar{c}_\mu\,\mathcal{M}^\mu{}_\nu[h\,;\bar{g}]\,c^\nu\,.\end{aligned} \tag{3.39}$$

Since the starting point here correspond to the full *Diff* invariant setting, in the present case the Faddeev-Popov ghost is not subject to the transversality condition as in the case of UG. Following the recipe discussed in Sect. 3.2.2, the dressed vertices are defined according to

$$\Gamma^{(n)}_{k,\,A_1\cdots A_n}(\mathbf{p}) = [\mathcal{Z}_{k,\varphi_1}(p_1)^{1/2}]^{B_1}{}_{A_1}\cdots[\mathcal{Z}_{k,\varphi_n}(p_n)^{1/2}]^{B_n}{}_{A_n}\,\hat{\Gamma}^{(n)}_{B_1\cdots B_n}(\mathbf{p})\Big|_{\substack{G_{\text{N}}\mapsto k^{-2}G_k \\ \Lambda_{\text{cc}}\to k^2\Lambda_k}}\,, \tag{3.40}$$

with slightly different dressing functions, namely

$$\begin{aligned}[\mathcal{Z}_{k,h}(p)^{1/2}]^{\mu\nu\alpha\beta} = &\;Z^{1/2}_{k,\text{TT}}\;\mathcal{P}^{\mu\nu\alpha\beta}_{\text{TT}}(p) \,+\, Z^{1/2}_{k,\xi}\;\mathcal{P}^{\mu\nu\alpha\beta}_{\xi}(p) \\ &+ Z^{1/2}_{k,\sigma}\;\mathcal{P}^{\mu\nu\alpha\beta}_{\sigma}(p) \,+\, Z^{1/2}_{k,\text{tr}}\;\mathcal{P}^{\mu\nu\alpha\beta}_{\text{tr}}(p)\,,\end{aligned} \tag{3.41a}$$

$$[\mathcal{Z}_{k,\bar{c}}(p)^{1/2}]^{\mu\nu} = [\mathcal{Z}_{k,c}(p)^{1/2}]^{\mu\nu} = Z^{1/2}_{k,c_{\text{T}}}\;\mathcal{P}^{\mu\nu}_{\text{T}}(p) \,+ Z^{1/2}_{k,c_{\text{L}}}\;\mathcal{P}^{\mu\nu}_{\text{L}}(p)\,, \tag{3.41b}$$

$$[\mathcal{Z}_{k,b}(p)^{1/2}]^{\mu\nu} = Z^{1/2}_{k,b_{\text{T}}}\;\mathcal{P}^{\mu\nu}_{\text{T}}(p) + Z^{1/2}_{k,b_{\text{L}}}\;\mathcal{P}^{\mu\nu}_{\text{L}}(p)\,. \tag{3.41c}$$

The modification in the dressing functions account for the inclusion of the trace mode h^{tr} and for the longitudinal sector of the Faddeev-Popov and Lautrup-Nakanishi fields.

[4]For simplicity, here we shall not include the regulator induced masses. In this sense, we compare the RG flow in the unimodular gauge with the case of UG with $m^2_{\text{TT}} = m^2_\sigma = 0$. The discussion and conclusions presented here, however, can be extended to include the symmetry-breaking masses in both settings.

3.4.2 On the equivalence between UG and unimodular gauge

In the present section, we focus in the equivalence between UG and unimodular gauge at the level of n-point correlation functions around flat background[5]. In this sense, the main result of this section can be summarized by the following equation (with $n > 1$)

$$\langle \varphi_{A_1}(p_1) \cdots \varphi_{A_n}(p_n) \rangle_k^{\text{conn.}} = \langle \varphi_{A_1}(p_1) \cdots \varphi_{A_n}(p_n) \rangle_k^{\text{conn.}}|_{\text{UG}} + \mathcal{O}(\beta^{-1}) \,, \tag{3.42}$$

where $\langle \cdots \rangle_k^{\text{conn.}}|_{\text{UG}}$ denotes the correlation function evaluated in UG. Taking Eq. (3.42) to be valid, in the limit corresponding to the unimodular gauge ($\beta \to -\infty$) we verify that both settings lead to the same correlation functions. In the remaining of this section we present the arguments that lead to Eq. (3.42).

The crucial point to justify Eq. (3.42) is the observation that, in the large-$|\beta|$ limit, the dressed propagators associated with the truncation defined by $\hat{\Gamma}^{\text{seed}}_{\text{QGR}}$ deviate from the propagators obtained in UG by $\mathcal{O}(\beta^{-1})$ contributions, namely

$$\mathbf{G}_k^{\mu\nu\alpha\beta}(p) = \mathbf{G}_{k,hh}^{\mu\nu\alpha\beta}(p)|_{\text{UG}} + \mathcal{O}(\beta^{-1}) \,, \tag{3.43a}$$

$$\mathbf{G}_{k,c\bar{c}}^{\mu\nu}(p) = \mathbf{G}_{k,c\bar{c}}^{\mu\nu}(p)|_{\text{UG}} + \mathcal{O}(\beta^{-1}) \,, \tag{3.43b}$$

$$\mathbf{G}_{k,hb}^{\mu\nu\alpha}(p) = \mathbf{G}_{k,hb}^{\mu\nu\alpha}(p)|_{\text{UG}} + \mathcal{O}(\beta^{-1}) \,, \tag{3.43c}$$

$$\mathbf{G}_{k,bb}^{\mu\nu}(p) = \mathbf{G}_{k,bb}^{\mu\nu}(p)|_{\text{UG}} + \mathcal{O}(\beta^{-1}) \,. \tag{3.43d}$$

For the sake of simplicity, we introduce the compact notation

$$[\mathbf{G}_k(p)]^A{}_B = [\mathbf{G}_k^{\text{UG}}(p)]^A{}_B + \mathcal{O}(\beta^{-1}) \,. \tag{3.44}$$

As a direct consequence, in the limit corresponding to the unimodular gauge, we observe the decoupling of the trace mode h^{tr} as well as of the longitudinal components of c^μ, $\bar{c}_\mu$ and b_μ. Notably, this result turns out to be sufficient to establish the equivalence between UG and unimodular gauge. The basic idea is to express the connected correlation functions $\langle \varphi_{A_1}(x_1) \cdots \varphi_{A_n}(x_n) \rangle_k^{\text{conn.}}$ in terms of "tree-level" functional relations involving contractions of the dressed propagators and n-point vertices $\Gamma^{(n)}_{k,\,A_1 \cdots A_n}(\mathbf{p})$

[5]More precisely, in terms of coarse-grained connected correlation functions obtained taking functional derivatives of the scale-dependent Schwinger functional $W_k[J]$.

(with $n \geq 3$). As an example, we take the 3-point (connected) correlation function

$$\begin{aligned}\langle \varphi_{A_1}(p_1)\varphi_{A_2}(p_2)\varphi_{A_3}(p_3)\rangle_k^{\text{conn.}} &= \\ &= [\mathbf{G}_k(p_1)]^{B_1}{}_{A_1}\,[\mathbf{G}_k(p_2)]^{B_2}{}_{A_2}\,[\mathbf{G}_k(p_3)]^{B_3}{}_{A_3}\,\Gamma^{(3)}_{k,\,B_1B_2B_3}(p_1,p_2,p_3)\,.\end{aligned} \tag{3.45}$$

Using Eq. (3.44) to express the dressed propagator, we find

$$\begin{aligned}\langle \varphi_{A_1}(p_1)\varphi_{A_2}(p_2)\varphi_{A_3}(p_3)\rangle_k^{\text{conn.}} &= \\ &= [\mathbf{G}_k^{\text{UG}}(p_1)]^{B_1}{}_{A_1}\,[\mathbf{G}_k^{\text{UG}}(p_2)]^{B_2}{}_{A_2}\,[\mathbf{G}_k^{\text{UG}}(p_3)]^{B_3}{}_{A_3}\,\Gamma^{(3)}_{k,\,B_1B_2B_3}(p_1,p_2,p_3) + \mathcal{O}(\beta^{-1})\,.\end{aligned} \tag{3.46}$$

By looking at the structure of the dressed propagators in UG, it is not difficult to convince ourselves of the following properties

$$\mathbf{G}^{\mu\nu\alpha\beta}_{k,hh}(p)|_{\text{UG}} = \mathbf{G}^{\mu\nu\lambda\rho}_{k,hh}(p)|_{\text{UG}}\,\mathcal{P}^{\alpha\beta}_{1-\text{tr},\lambda\rho}(p) = \mathcal{P}^{\mu\nu}_{1-\text{tr},\lambda\rho}(p)\,\mathbf{G}^{\lambda\rho\alpha\beta}_{k,hh}(p)|_{\text{UG}}\,, \tag{3.47a}$$

$$\mathbf{G}^{\mu\nu\alpha}_{k,hb}(p)|_{\text{UG}} = \mathbf{G}^{\mu\nu\lambda}_{k,hb}(p)|_{\text{UG}}\,\mathcal{P}^{\alpha}_{\text{T},\lambda}(p) = \mathcal{P}^{\mu\nu}_{1-\text{tr},\lambda\rho}(p)\,\mathbf{G}^{\lambda\rho\alpha}_{k,hb}(p)|_{\text{UG}}\,, \tag{3.47b}$$

$$\mathbf{G}^{\mu\nu}_{k,bb}(p)|_{\text{UG}} = \mathbf{G}^{\mu\lambda}_{k,bb}(p)|_{\text{UG}}\,\mathcal{P}^{\nu}_{\text{T},\lambda}(p) = \mathcal{P}^{\mu}_{\text{T},\lambda}(p)\,\mathbf{G}^{\lambda\nu}_{k,bb}(p)|_{\text{UG}}\,, \tag{3.47c}$$

$$\mathbf{G}^{\mu\nu}_{k,c\bar{c}}(p)|_{\text{UG}} = \mathbf{G}^{\mu\lambda}_{k,c\bar{c}}(p)|_{\text{UG}}\,\mathcal{P}^{\nu}_{\text{T},\lambda}(p) = \mathcal{P}^{\mu}_{\text{T},\lambda}(p)\,\mathbf{G}^{\lambda\nu}_{k,c\bar{c}}(p)|_{\text{UG}}\,, \tag{3.47d}$$

where $\mathcal{P}_{1-\text{tr}}$ denotes to the traceless projector (see App. C). More compactly, we have

$$[\mathbf{G}_k^{\text{UG}}(p)]^A{}_B = [\mathbf{G}_k^{\text{UG}}(p)]^A{}_C\,\mathbf{P}^C{}_B(p) = \mathbf{P}^A{}_C(p)\,[\mathbf{G}_k^{\text{UG}}(p)]^C{}_B\,. \tag{3.48}$$

The "projector" $\mathbf{P}^A{}_B(p)$ corresponds to $\mathcal{P}_{1-\text{tr}}$ if contracted with indices associated with the fluctuation field $h_{\mu\nu}$ and stands for the transverse projector $\mathcal{P}_\text{T}$ if contracted with indices associated with Faddeev-Popov or Lautrup-Nakanishi fields. Thanks to Eq. (3.48), the 3-point correlation function can be written as

$$\begin{aligned}\langle \varphi_{A_1}(p_1)\varphi_{A_2}(p_2)\varphi_{A_3}(p_3)\rangle_k^{\text{conn.}} &= \\ &= [\mathbf{G}_k^{\text{UG}}(p_1)]^{B_1}{}_{A_1}\,[\mathbf{G}_k^{\text{UG}}(p_2)]^{B_2}{}_{A_2}\,[\mathbf{G}_k^{\text{UG}}(p_3)]^{B_3}{}_{A_3} \\ &\quad\times \mathbf{P}^{C_1}{}_{B_1}(p_1)\mathbf{P}^{C_2}{}_{B_2}(p_2)\mathbf{P}^{C_3}{}_{B_3}(p_3)\,\Gamma^{(3)}_{k,\,C_1C_2C_3}(p_1,p_2,p_3) + \mathcal{O}(\beta^{-1})\,.\end{aligned} \tag{3.49}$$

By construction, the contraction of $\mathbf{P}^A{}_B(p)$ with n-point vertices essentially project out the trace mode h^{tr} and the longitudinal components of c^μ, $\bar{c}_\mu$ and b_μ. Since the truncation defined by $\hat{\Gamma}^{\text{seed}}_{\text{QGR}}$ differs from the one discussed in Sect. 3.1.2 due to the presence of such modes, we can identify

$$\mathbf{P}^{B_1}_{A_1}(p_1)\,\cdots\,\mathbf{P}^{B_n}_{A_n}(p_n)\,\Gamma^{(n)}_{k,\,B_1\cdots B_n}(\mathbf{p}) = \Gamma^{(n)}_{k,\,A_1\cdots A_n}(\mathbf{p})|_{\mathrm{UG}}\,. \tag{3.50}$$

In such a case, the r.h.s of (3.49) can be expressed in terms of propagators and vertices extracted from the unimodular truncation $\hat{\Gamma}^{\mathrm{seed}}_{\mathrm{UG}}$,

$$\begin{aligned}
&\langle\varphi_{A_1}(p_1)\varphi_{A_2}(p_2)\varphi_{A_3}(p_3)\rangle^{\mathrm{conn.}}_k = \\
&\quad= [\mathbf{G}^{\mathrm{UG}}_k(p_1)]^{B_1}_{\ \ A_1}[\mathbf{G}^{\mathrm{UG}}_k(p_2)]^{B_2}_{\ \ A_2}[\mathbf{G}^{\mathrm{UG}}_k(p_3)]^{B_3}_{\ \ A_3}\,\Gamma^{(3)}_{k,\,B_1B_2B_3}(p_1,p_2,p_3)|_{\mathrm{UG}} + \mathcal{O}(\beta^{-1})\,.
\end{aligned} \tag{3.51}$$

and, therefore

$$\langle\varphi_{A_1}(p_1)\varphi_{A_2}(p_2)\varphi_{A_3}(p_3)\rangle^{\mathrm{conn.}}_k = \langle\varphi_{A_1}(p_1)\varphi_{A_2}(p_2)\varphi_{A_3}(p_3)\rangle^{\mathrm{conn.}}_k|_{\mathrm{UG}} + \mathcal{O}(\beta^{-1})\,.$$

Although the argument presented here was based in the particular case of the 2-point correlation function, the same reasoning can be used to demonstrate Eq. (3.42) for larger values of n. The case $n = 2$ can be easily verified since the 2-point (connected) correlation functions correspond to the dressed propagators itself, namely

$$\begin{aligned}
\langle\varphi_{A_1}(p_1)\varphi_{A_2}(p_2)\rangle^{\mathrm{conn.}}_k &= [\mathbf{G}_k(p)]_{A_1A_2} \\
&= [\mathbf{G}^{\mathrm{UG}}_k(p)]_{A_1A_2} + \mathcal{O}(\beta^{-1}) \\
&= \langle\varphi_{A_1}(p_1)\varphi_{A_2}(p_2)\rangle^{\mathrm{conn.}}_k|_{\mathrm{UG}} + \mathcal{O}(\beta^{-1})\,.
\end{aligned}$$

Up to this point, our argument is sufficient to establish the equivalence of UG and unimodular gauge at a fixed RG scale k. To complete the discussion, we still need to demonstrate that such equivalence is preserved along the RG flow. For the dressed propagator, for example, it depends on the equivalence of the anomalous dimensions computed in both settings. In such a case, explicit computations based on the truncation $\hat{\Gamma}^{\mathrm{seed}}_{\mathrm{UG}}$ lead to the following results

$$\eta_{\mathrm{TT}} = \eta_{\mathrm{TT}}|_{\mathrm{UG}} + \mathcal{O}(\beta^{-1})\,, \tag{3.52a}$$

$$\eta_{\sigma} = \eta_{\sigma}|_{\mathrm{UG}} + \mathcal{O}(\beta^{-1})\,, \tag{3.52b}$$

$$\eta_{c_{\mathrm{T}}} = \eta_{c}|_{\mathrm{UG}} + \mathcal{O}(\beta^{-1})\,, \tag{3.52c}$$

In the limit corresponding to the unimodular gauge we obtain the same anomalous dimensions as in the case of UG.

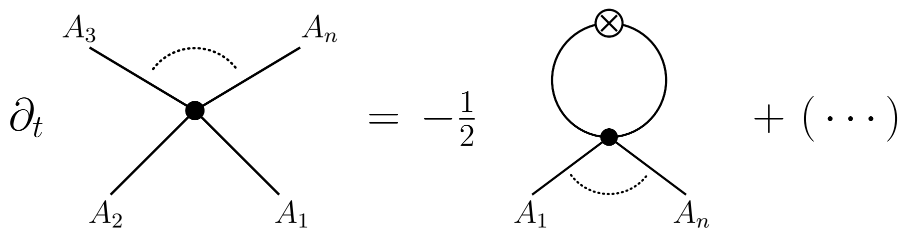

Figure 3.7: Simplified diagrammatic representation of the flow equation for the n-point vertex $\Gamma^{(n)}_{k,A_1\cdots A_n}(\mathbf{p})$. Here we have used $(\cdots)$ to denote that there are other diagrams contributing to the flow equation.

To complete the discussion, we still need to show that

$$\mathbf{P}^{B_1}_{\ A_1}(p_1)\cdots\mathbf{P}^{B_n}_{\ A_n}(p_n)\,\partial_t\Gamma^{(n)}_{k,B_1\cdots B_n}(\mathbf{p}) = \partial_t\Gamma^{(n)}_{k,A_1\cdots A_n}(\mathbf{p})|_{\mathrm{UG}} + \mathcal{O}(\beta^{-1})\,, \tag{3.53}$$

is compatible with the vertex expansion of the FRG equation. In such a case, the basic idea is to use the flow equation for the n-point vertex, schematically represented as

$$\partial_t\Gamma^{(n)}_k = -\frac{1}{2}\mathrm{STr}\Big(\mathbf{G}_k\,\Gamma^{(n+2)}_k\,\mathbf{G}_k\,\partial_t\mathbf{R}_k\Big) + (\cdots)\,, \tag{3.54}$$

where $(\cdots)$ denote additional traces involving contractions of the dressed propagator $\mathbf{G}_k$, the regulator insertion $\partial_t\mathbf{R}_k$ and vertices $\Gamma^{(m)}_k$ (with $3 \leq m \leq n+1$). Diagrammatically, Eq. (3.54) is represented by Fig. 3.7. Contracting the flow equation (3.54) with $\mathbf{P}^{B}_{\ A}(p)$, in the r.h.s. we obtain projected external lines, but keeping unprojected internal legs contracted with the dressed propagator $\mathbf{G}_k$. Thanks to Eqs. (3.44) and (3.48), in the limit $\beta \to -\infty$ the internal lines also become projected on the subspace defined by $\mathbf{P}^{B}_{\ A}(p)$. With this observation, all the diagrams contribution to the flow of the projected vertices $\mathbf{P}^{B_1}_{\ A_1}(p_1)\cdots\mathbf{P}^{B_n}_{\ A_n}(p_n)\,\Gamma^{(n)}_{k,B_1\cdots B_n}(\mathbf{p})$ can be fully expressed in terms of propagators and vertices defined in the theory space associated with UG. In this case, we can conclude that in the limit $\beta \to -\infty$ both $\mathbf{P}^{B_1}_{\ A_1}(p_1)\cdots\mathbf{P}^{B_n}_{\ A_n}(p_n)\,\Gamma^{(n)}_{k,B_1\cdots B_n}(\mathbf{p})$ and $\Gamma^{(n)}_{k,A_1\cdots A_n}(\mathbf{p})|_{\mathrm{UG}}$ satisfy the same flow equations, justifying Eq. (3.53) and completing our argument in favor of the equivalence between unimodular gauge and UG.

Chapter 4

Exploring the Gravity-Matter Interplay in the Unimodular Setting

4.1 A link that matters: connecting quantum gravity with particle physics

One of the greatest challenges in QG is the current impossibility of direct experimental observations of its effects. From a simple dimensional analysis, one typically expects that QG effects on physical processes with characteristic energy E are power-law suppressed by $(E/M_{\rm Pl})^{\#}$, where $M_{\rm Pl}$ is the Planck mass and # denotes some positive number. As a consequence, direct probes of QG remain far away from the current technology. The LHC, for example, is limited to characteristic energies of order TeV, leading to a suppression factor $E_{\rm LHC}/M_{\rm Pl} \sim 10^{-16}$.

Although the requirement of internal and mathematical consistency plays an important (and necessary) role in the search for a viable quantum theory of gravity, it is not completely satisfying from the physical point of view. In this chapter, we explore the possibility of determining phenomenological constraints on QG candidates by means of the interplay of gravity with matter systems. A consistent description of the microscopic d.o.f. in nature should account both for gravity and matter. In a QFT setting, this can be achieved in a relatively simple way, since matter degrees of freedom have a satisfactory description in terms of quantum fields. The key point for observational tests based on the gravity-matter interplay is that the properties at the Planck scale regime might actually determine some aspects of the matter sector at low energies. In this sense, we can look for constraints in the Planck scale regime by demanding consistency with observations, for example, in particle physics experiments.

Naively, the idea of connecting particle physics experiments at TeV scale with QG effects seems to be incompatible with the principle of separation of scales in nature. This principle basically states that an effective macroscopic description decouples from microscopic d.o.f.. As example, an effective description in fluid dynamics does not make explicit reference to microscopic degree of freedom. However, macroscopic parameters, such as the viscosity, depend on microscopic details. In this spirit, one can argue that, despite of QG effects being suppressed in physical processes at the TeV scale, the couplings in the SM might carry some information coming from a more fundamental description involving d.o.f. at the Planck scale.

A particularly interesting class of SM couplings is the one associated with (canonically) marginal operators. Below the Planck scale, where QG fluctuation are highly suppressed, marginal couplings exhibit a logarithmic running. As a consequence, changes of $\mathcal{O}(1)$ at the Planck scale is connected with changes of $\mathcal{O}(1)$ at the TeV scale. Within the AS scenario, this observation allows us to set constraints on the structure of UV FPs based on particle physics observations. In special, the study of the impact of QG fluctuations on the renormalization properties of canonically marginal couplings in the SM open de possibility of two indirect observational consistency tests:

- Induced UV completion: As we have discussed in Chap. 1, the appearance of Landau poles in the Abelian gauge sector of the SM provides an indication that new physics might be necessary [137–140]. The problem also appears in the Higgs-Yukawa sector [142–149] . In this sense, we hope that QG fluctuations might resolve such problems inherent to SM of particle physics. In the ASQG scenario, the mechanism that hopefully leads to a resolution of this problem also dictates upper bounds in the IR values of these couplings. Ideally, if we manage to perform precision computations in gravity-matter systems, we would be able to test the compatibility of such theoretical results with experimental observations in particle physics.

- Predicting (or post-dicting) SM parameters: Despite of providing a very successful description of particle physics, the SM exhibits the undesired feature of a large number of free parameters to be adjusted by experiments. Hopefully, the values of these free parameters could emerge as predictions from a more fundamental microscopic description, possibly including QG effects. In the ASQG program, the requirement of a finite number of UV relevant directions could lead to predictive values for (some) canonically marginal couplings in the SM [95, 96]. In this setting, there are indications, based on simple approximations, pointing out towards the possibility of computing the correct values[1] for the Higgs mass [97] and the Top-Botton mass difference [210, 215] as a consequence of the FP structure in ASQG. The comparison of theoretically predicted values (if computed with high precision) with the observed ones in particle physics experiments should work as a "smoking-gun" criterion to select phenomenologically viable QG models.

[1] At least in terms of order of magnitude.

The underlying mechanism supporting these possibilities in ASQG can be qualitatively understood through a simple example by looking at the 1-loop beta function for the Yukawa coupling [209],

$$\beta_y^{\text{1-Loop}} = \frac{5}{16\pi^2}\, y^3\,, \tag{4.1}$$

where y is the coupling associated with a Yukawa interaction $\sim i\phi\,\bar{\psi}\psi$. The only FP in the RG flow of the Yukawa coupling is the Gaussian one $y^* = 0$, which, due to the positive coefficient of the y^3 term in $\beta_y^{\text{1-Loop}}$, has a UV repulsive nature. In such a case, unless we set $y = 0$ along all the RG flow (triviality problem), the Yukawa coupling hits a Landau pole at some finite RG scale.

In the case of the Higgs-Yukawa interactions in the SM, the Landau pole obtained from usual perturbative calculations turns out to be located beyond the Planck scale and, therefore, we might expect that QG effects could change the picture. The key idea is that graviton fluctuations add new terms to the beta function of the Yukawa coupling and, depending on the properties of such contributions the RG might present different features in the UV regime. To explore such a possibility in more detail, let us parameterize the leading order (in the Yukawa coupling) gravitation contribution to $\beta_y^{\text{1-Loop}}$ according to [209]

$$\Delta\beta_y^{\text{Grav}} = -f_y\, y\,, \tag{4.2}$$

where f_y depends on the details of the graviton propagator and gravity-matter vertices. By adding this contribution to Eq. (4.1), we find

$$\beta_y^{\text{1-Loop+Grav}} = \frac{5}{16\pi^2}\, y^3 - f_y\, y\,. \tag{4.3}$$

The physical picture basically depends on the sign of f_y. If $f_y \leq 0$, the situation does not change in comparison with the case without gravity. In such a case, the only FP is the Gaussian one, which remains UV repulsive. The situation with $f_y > 0$ is much more interesting. In this case, the beta function for the Yukawa coupling features two FPs,

$$y_\circ^* = 0 \qquad \text{and} \qquad y_\bullet^* = \sqrt{16\pi^2\, f_y/5}\,, \tag{4.4}$$

with the respective critical exponents,

$$\theta_\circ^y = f_y\, > 0 \qquad \text{and} \qquad \theta_\bullet^y = -\,2f_y\, < 0\,. \tag{4.5}$$

As one can see from the critical exponents, in the case where QG fluctuations contribute with $f_y > 0$, the Gaussian FP $y^*_\circ$ becomes UV attractive, while the additional (non-Gaussian) FP $y^*_\bullet$ has UV repulsive nature. The two FPs in (4.4) provide interesting scenarios for UV completion. Due to the positive critical exponent associated with $y^*_\circ$, the RG flow for the Yukawa coupling admits asymptotically free trajectories emanating from a free FP in the UV and flowing towards a range of non-vanishing possible values in the IR. For the non-Gaussian FP $y^*_\bullet$, there is a unique (asymptotically safe) trajectory connecting the UV to the IR. In such a case, the IR values of the Yukawa coupling is completely determined in terms of the fixed structure. Moreover, the IR value predicted by the FP $y^*_\bullet$ works as an upper bound for IR values associated with the asymptotically free trajectories connected to the Gaussian FP $y^*_\circ$.

The previous discussion can be easily transported to the case of couplings associated to (non-)Abelian gauge fields[2] [100, 101]. Typically, the leading order gravitational contribution to the running of (non-)Abelian gauge couplings is parameterized as

$$\Delta\beta^{\text{Grav}}_{e^2} = -f_{e^2}\, e^2\,, \tag{4.6}$$

where e is the (non-)Abelian gauge coupling and f_{e^2} encodes the details of the graviton propagator and gravity-matter vertices. In general, f_{e^2} has the same form both for Abelian and non-Abelian gauge fields. Within the SM framework, the most critical case is the one associated with the Abelian $U_{\text{Y}}(1)$ gauge sector due to the existence of a Landau pole in the UV regime[3]. If $f_{e^2} > 0$, gravity acts with anti-screening contributions, which compensate the screening effects from other matter fields and possibly generate UV complete trajectories in the Abelian gauge sector. In this case, the situation is quite similar to the Yukawa case, namely, gravity induces an interacting FP with $e^*_\bullet \propto \sqrt{f_{e^2}}$, while the Gaussian one at $e^*_\circ = 0$ becomes UV attractive. The trajectory emanating from $e^*_\bullet$ is unique and, therefore, yields predictive values along all the RG flow. On the other hand, for the asymptotically free trajectories connected to the FP $e^*_\circ$, despite of being not predictive, the IR values of the Abelian gauge coupling become bounded by the safe trajectory associated with $e^*_\bullet$ [101].

Besides the Yukawa and (non-)Abelian gauge interactions, the SM also features quartic self-interactions in the Higgs sector. If we consider only the Higgs self-interaction, then, the leading order contribution to the running of the quartic coupling, here denoted as λ, is proportional to λ^2 (with positive coefficient). In this case, the RG flow of λ features a Landau-pole/triviality problem [150–152]. The situation becomes qualitatively different once we switch-on the Yukawa interactions. In particular, the fermionic

[2]For the sake of simplicity, we use the short nomenclature "(non-)Abelian gauge coupling" to denote the coupling associated with interactions involving (non-)Abelian gauge fields.

[3]The non-Abelian gauge sector do the SM already features UV completion due to anti-screening contributions resulting from self-interactions of the gauge field. For this reason, our primary interest is the effect of graviton fluctuations on the running of Abelian gauge couplings.

loop induces a contribution of the form $-y^4$ to the running of λ (at 1-loop). In such a case, the negative sign in $-y^4$ pushes the quartic potential towards regions of instability [272, 273], another indication that extra d.o.f. might be necessary to circumvent the problems of the SM [274]. Within the ASQG scenario, there are indications that the inclusion of QG effects might induce UV complete and predictive RG trajectories for the quartic coupling λ [97]. In order to understand the underlying mechanism, let us consider a toy model involving interactions of the form $\frac{\lambda}{4!}\phi^4 + iy\phi\,\bar{\psi}\psi$. Including possible QG effects to the running of λ, the 1-loop beta function takes the form

$$\beta_\lambda^{\text{1-Loop+Grav}} = \frac{3}{16\pi^2}\lambda^2 + \frac{1}{2\pi^2}\lambda\, y^2 - \frac{3}{\pi^2}y^4 + f_\lambda \lambda\,, \tag{4.7}$$

where f_λ parameterizes the leading order graviton contributions.

The physically appealing case is the one characterized by $f_\lambda \geq 0$ (combined with $f_y > 0$ in Eq. (4.2)). For simplicity, we first consider the class of asymptotically free RG trajectories for the Yukawa coupling, such that y approaches the Gaussian FP $y_\circ^* = 0$ in the UV. In this case, the beta function (4.7) supports a UV repulsive Gaussian FP $\lambda_\circ^* = 0$. We note that despite of being UV repulsive, this FP does not imply trivial trajectories for λ, since, once one flow towards the IR, the $-y^4$ contribution drives λ to positive values. The UV repulsive nature of such FPs makes the corresponding RG trajectories predictive along the flow. The situation described here remains basically the same for safe trajectories in the Yukawa coupling approaching the interacting FP $y_\bullet^*$. The main difference in this case is that the Gaussian FP $\lambda_\circ^*$ is shifted to a non-Gaussian one with $\lambda_\bullet^* \sim y_\bullet^{*2}$, however, the qualitative discussion remains the same as in the Gaussian case. Finally, it is interesting mentioning that in the case $f_\lambda < 0$, the RG trajectories for λ are no longer predictive. Yet, the beta function for λ admits safe trajectories associated with an attractive UV FP.

The mechanism discussed here has an interesting consequence to the realistic SM of particle physics. As we know, in this case, the Higgs mass is determined by $m_{\rm H}^2 \sim \lambda_{\rm H}\, v^2$, where v^2 sets the electroweak scale and $\lambda_{\rm H}$ denotes the Higgs quartic coupling. In the pure SM (without gravitational d.o.f.), the quartic coupling $\lambda_{\rm H}$ is a free parameter and has to be fixed by experiments. Within the ASQG scenario, there are indications (based on approximations) that the mechanism discussed in the previous paragraph is actually realized, leading to a predictive flow for $\lambda_{\rm H}$ and, as consequence, allowing to compute the Higgs mass from first principles [97].

In this chapter, we explore the mechanisms discussed in this section as a first step to constrain the FP structure in the unimodular theory space from phenomenological considerations. In particular, we focus on the viability of induced UV complete and predictive RG trajectories for SM-like couplings. In this sense, we set out a truncation for UG minimally coupled to matter fields, involving SM-like interactions. Within this setting, we evaluate the gravitational contribution to the beta functions of y, g and λ. As it will be shown, such an analysis allows us to determine constraints on possible FP values appearing in the gravitational part of our truncation. The investigation presented here is complemented by a comparative analysis including the corresponding results from the standard (non-unimodular) ASQG setting. The content reported in the remaining of this chapter is based on [223].

4.2 Gravitational contribution to the RG-flow of SM-like couplings

4.2.1 Setting up a truncation for gravity-matter systems

As already discussed in the previous chapters, the use of FRG techniques to access the RG flow of running couplings relies on truncation methods. In the present chapter, our goal is to investigate the impact of graviton fluctuations in the RG flow of SM-like couplings, in the unimodular setting. In this sense, the truncated EAA is supposed to include both gravitational and matter degrees of field. The starting point for our analysis is a truncation of the form

$$\Gamma_k = \Gamma_k^{\mathrm{UG}} + \Gamma_k^{\mathrm{SM}} + \Gamma_k^{\mathrm{g.f.}} \,, \tag{4.8}$$

where Γ_k^{UG} denotes the pure-gravity sector, Γ_k^{SM} encodes gravity-matter interactions and $\Gamma_k^{\mathrm{g.f.}}$ stands for the gauge-fixing contributions. For the gravitational sector, Γ_k^{UG}, we include a complete basis of canonically relevant and marginal operators in the unimodular theory space, namely

$$\Gamma_k^{\mathrm{UG}} = \frac{1}{16\pi G_{\mathrm{N}}} \int_x \omega \, \left(-R + \bar{a}\, R^2 + \bar{w}\, C_{\mu\nu\alpha\beta} C^{\mu\nu\alpha\beta} \right) \,, \tag{4.9}$$

where $\bar{a}$ and $\bar{w}$ represent dimensionful couplings. The corresponding dimensionless couplings are defined as $a_k = \bar{a}\, k^2$ and $b_k = \bar{b}\, k^2$. In principle, we can also include an additional curvature squared operator composed by appropriated contractions of the Riemann tensor, however, in $d = 4$ such contribution can be cast as a surface term due to the Gauss-Bonnet theorem. In the gravity-matter sector, Γ_{SM}, we consider a scalar field (ϕ), an Abelian gauge field (A_μ) and a Dirac spinor[4] (ψ). Our truncation includes

[4] In this thesis, the Dirac spinor is coupled to gravity by means of the vielbein formalism. Here, we take as assumption the absence of torsion. In such a case, the spin-connection appearing in the fermionic covariant derivative can be expressed in terms of the vielbein. For a discussion on discussion on how to relate the vielbein fluctuation with metric fluctuation, see the App. B.

SM-like interactions minimally coupled to (unimodular) gravity,

$$\Gamma_k^{\mathrm{SM}} = \int_x \omega \left(\frac{1}{2} g^{\mu\nu} \partial_\mu \phi \partial_\nu \phi + V(\phi^2) + \frac{1}{4\,e^2} g^{\mu\alpha} g^{\nu\beta} F_{\mu\nu} F_{\alpha\beta} + i\bar{\psi} \not{D} \psi + iy\, \phi\, \bar{\psi}\psi \right) , \quad (4.10)$$

where $V(\phi^2)$ denotes a scalar potential and $F_{\mu\nu} = \partial_\mu A_\nu - \partial_\nu A_\mu$ is the field strength associated with the Abelian gauge sector. Since our analysis is not constrained by the requirement of perturbative renormalizability, we shall keep an arbitrary scalar potential $V(\phi^2)$ (invariant under $\phi \mapsto -\phi$). An explicit mass term for the fermion is incompatible with the discrete "chiral" symmetry transformation $\psi \mapsto \mathrm{e}^{i\pi\gamma_5/2}\psi$ and $\bar{\psi} \mapsto \bar{\psi}\mathrm{e}^{i\pi\gamma_5/2}$, combined with $\phi \mapsto -\phi$. It is interesting to observe that, due to the unimodularity condition, both the scalar potential and the Yukawa sector do not interact directly with QG fluctuations.

Finally, the gauge-fixing part of our truncation is chosen according to

$$\Gamma_k^{\mathrm{g.f.}} = \frac{1}{2\alpha} \int_x \omega\, \bar{g}^{\mu\nu} F_\mu^{\mathrm{T}}[h;\bar{g}] F_\nu^{\mathrm{T}}[h;\bar{g}] + \frac{1}{2\zeta} \int_x \omega\, (\bar{g}^{\mu\nu} \bar{\nabla}_\mu A_\nu)^2 \,, \quad (4.11)$$

where α and ζ denote gauge parameters. In both cases we consider the Landau gauge limit $\alpha \to 0$ and $\zeta \to 0$. The gauge-fixing function $F_\mu^{\mathrm{T}}[h;\bar{g}]$ was defined in (A.6). We observe the absence of Faddeev-Popov ghosts and Lautrup-Nakanishi fields, which are not necessary for the investigation performed here.

Despite the fact that we are dealing with perturbatively non-renormalizable theories, in setting up our truncation we follow the power-counting criteria as a guiding principle. This strategy relies on the assumption of near-canonical scaling (see the discussion in Sect. 2.2.5). If such behavior is actually realized, we might expect that canonically irrelevant operator would remain as UV irrelevant direction at in interacting FP. In additional, there are indications based on FRG calculations showing that the backreaction of irrelavant operators is subleading with respect to relevant ones at the FP [73, 89, 90]. Ultimately, such an assumption has to be confronted with further calculations based on more sophisticated truncations.

A class of higher-order (canonically irrelevant) operators, selected according to their global symmetries as discussed in [100, 204–207, 209, 212, 217, 219], features non-vanishing values at an interacting gravitational FP. Such a property appears as a consequence of QG-induced effects. This class of induced interactions includes the $(F_{\mu\nu}F^{\mu\nu})^2$ for (non-)Abelian gauge fields [100, 219], the derivative scalar-fermion interactions $\bar{\psi}\not{D}\psi\, \partial_\mu\phi\partial^\mu\phi$ [207, 209] and non-minimal operators involving gravity-matter interactions [212, 217].. This class of operators has been systematically explored in the framework of standard ASQG. An important outcome of such an investigation is that higher-order operators produce sub-leading impact on the FP values of couplings associated with canonically relevant/marginal operators [100, 209, 219]. This result holds as long as gravity remains sufficiently weakly coupled such that the induced FP stay at real values [100,207,209,212,217]. While a similar analysis is not currently available for UG, it opens an interesting avenue for future investigations. In fact, a systematic study concerning the fate of induced operators is a relevant step towards the validation of canonical power-counting as a trustful guiding principle for the choice of truncation. Furthermore, the search of qualitative differences concerning gravity-matter interactions might be an interesting way to probe the equivalence between UG and GR at the quantum level.

The building blocks to compute the gravitational contribution to the running of matter couplings are the dressed propagators and the proper-vertices involving gravity-matter interactions, both extracted from the truncation we are dealing with. For the analysis performed here, the flat background $\bar{g}_{\mu\nu} = \delta_{\mu\nu}$ is sufficient to capture all the relevant features that we are interested. The relevant (dressed-)propagators are given by[5]

$$\mathbf{G}^{\mu\nu\alpha\beta}_{k,hh}(p) = \frac{\mathcal{P}^{\mu\nu\alpha\beta}_{\mathrm{TT}}(p)}{Z_{k,\mathrm{TT}}\left(1 + 2\,\bar{w}_k P_k(p^2)\right) P_k(p^2)} - \frac{2\,\mathcal{P}^{\mu\nu\alpha\beta}_{\sigma}(p)}{Z_{k,\sigma}\left(1 - 6\,\bar{a}_k P_k(p^2)\right) P_k(p^2)}\,, \tag{4.12a}$$

$$\mathbf{G}^{\mu\nu}_{k,AA}(p) = \frac{\mathcal{P}^{\mu\nu}_{\mathrm{T}}(p)}{Z_{k,A}\, P_k(p^2)}\,, \tag{4.12b}$$

$$\mathbf{G}_{k,\phi\phi}(p) = \frac{1}{Z_{k,\phi}\, P_k(p^2)}\,, \tag{4.12c}$$

$$\mathbf{G}_{k,\psi\bar{\psi}}(p) = -\frac{1}{Z_{k,\psi}\, P_k(p^2)^{1/2}} \frac{\not{p}}{\sqrt{p^2}}\,, \tag{4.12d}$$

where we have defined $P_k(p^2) = (1 + r_k(p^2))p^2$. The relevant gravity-matter vertices can be directly computed by taking functional derivatives of Γ_k, after expansion up to second order in the fluctuation field $h_{\mu\nu}$. In the present sector we shall not compute the running of the couplings associated with the gravitational sector. For this reason, there is not need to expand the truncation up to order higher than two in the fluctuation field. The expressions for the gravity-matter vertices are quite lengthy, and therefore, we do not report them here (for the explicit expressions, see App. C of Ref. [223]).

Before we proceed with our investigation, let us add some comments concerning the graviton propagator $\mathbf{G}_{k,hh}$. If we remove the FRG regulator ($k \to 0$), $P_k(p^2)$ reduces

[5] Note that there is an implicit introduction of wave function renormalization factors ($Z_{k,\mathrm{TT}}$ and $Z_{k,\sigma}$) associated with the different "York-projections of the fluctuation field". For further details, see the prescription discussed in Chap. 3.

to p^2 and, therefore, the graviton propagator gives rise to structures of the form

$$\frac{1}{\left(1+2\,\bar{w}\,p^2\right)p^2} \qquad \text{and} \qquad \frac{1}{\left(1-6\,\bar{a}\,p^2\right)p^2}\,, \tag{4.13}$$

which is precisely the type of pole structure arising in curvature-squared gravity [20]. In the perturbative setting, the pole at $p^2 = -(2\bar{w})^{-1}$ is typically viewed as a problem, since it corresponds to a massive ghost-like state (or a tachyon, depending on the sign of $\bar{w}$), resulting in unitarity (causality) issues.

From the FRG perspective, on the other hand, the association of such poles with ghost/tachyons is not straightforward. In this setting, questions involving unitarity and instabilities in the physical spectrum requires the full effective action $\Gamma = \Gamma_{k=0}$. In principle, we do not expect that the full effective action should correspond to the naive limit $k \to 0$ within a truncation based on power-counting criteria. The appropriate limit corresponding to the full effective action has to be done by properly integrating Γ_k down to $k = 0$. In general, this procedure might generate involved interactions that are not captured by simple polynomials as those appearing in the denominators of the expressions in (4.13). In this sense, truncations of the form that we are considering here are not suitable to address questions such as unitary/stability violation.

4.2.2 Yukawa and Abelian gauge couplings

Starting from the Yukawa sector, the gravitational contribution[6] to the beta function associated with the Yukawa coupling can be cast in the form [207, 209]

$$\Delta\beta_y^{\text{Grav}} = \left(\frac{1}{2}\eta_\phi^{\text{Grav}} + \eta_\psi^{\text{Grav}}\right) y_k + \mathcal{D}_y\, y_k\,, \tag{4.14}$$

where η_ϕ^{Grav} and η_ψ^{Grav} represent the gravitational contribution to the scalar and fermion anomalous dimensions, respectively. Generically, η_ϕ^{Grav} and η_ψ^{Grav} can be computed in terms of the diagrams represented in Figs. 4.1 and 4.1. The last term, $\mathcal{D}_y$, denotes the contributions coming from the diagrams depicted in 4.3. In UG, due to the absence of direct gravity-matter vertices in the Yukawa sector, only the triangle diagrams in the last column produce non-vanishing results. This is in contrast with the situation in standard ASQG, where all the diagrams represented in Fig. 4.3 contribute to $\mathcal{D}_y$. To extract η_ϕ^{Grav}, η_ψ^{Grav} and $\mathcal{D}_y$, we apply the following projection rules

$$\eta_\phi^{\text{Grav}} = -\frac{1}{Z_{k,\phi}}\left[\frac{\partial}{\partial p^2}\left(\sum \text{Diagrams}\Big|_{\text{Fig.4.1}}\right)\right]_{p^2=0}, \tag{4.15a}$$

[6] It is important to emphasize that by "gravitational contribution" we mean the contributions coming from all the diagrams involving at least one graviton-propagator.

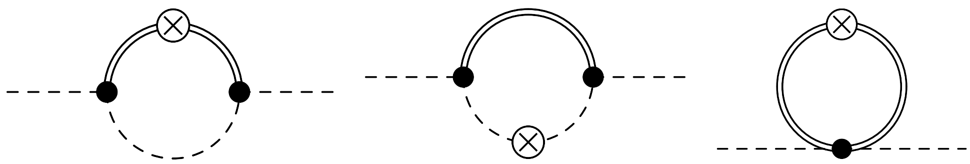

Figure 4.1: Diagrams contributing to the anomalous dimension η_ϕ. The dashed line denotes the scalar field dressed propagator and the double line represents the graviton propagator.

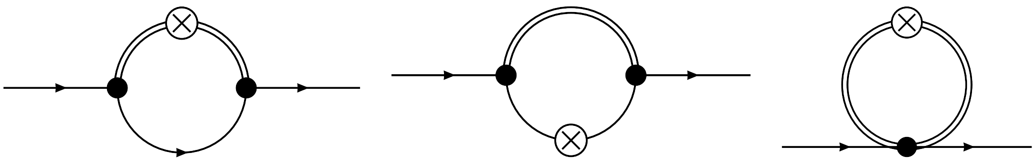

Figure 4.2: Diagrams contributing to the anomalous dimension η_ψ. The solid line with an arrow denotes the fermionic field propagator and the double line represents the graviton propagator.

$$\eta_\psi^{\text{Grav}} = \frac{1}{4\, Z_{k,\psi}} \left[\frac{\partial}{\partial p^2} \left(\not{p} \sum \text{Diagrams}\Big|_{\text{Fig.4.2}} \right) \right]_{p^2=0}, \tag{4.15b}$$

$$\mathcal{D}_y\, y_k = -\frac{i}{4\, Z_{k,\phi}^{1/2}\, Z_{k,\psi}} \left(\sum \text{Diagrams}\Big|_{\text{Fig.4.3}} \right)_{|p|=0}. \tag{4.15c}$$

For the Abelian gauge sector, there are multiple ways in which we can extract the flow of the gauge coupling. For example, it can be extracted from the 3-vertex involving charged fermionic fields. Alternatively, the running of the gauge coupling can be obtained from the 3- or 4-vertex involving charged scalar fields. Here, we take a simple route by observing that the beta function for the Abelian gauge coupling, denoted as e, is related to the gauge field anomalous dimension, $\eta_A = -Z_{k,A}^{-1}\partial_t Z_{k,A}$, according to the following equation [100, 101]

$$\beta_{e^2} = \eta_A\, e_k^2\,. \tag{4.16}$$

It is interesting to observe that, in the FRG setting, the different possibilities to compute β_{e^2} are related by modified Ward identities [176]. Taking into account Eq. (4.16), the gravitational contribution to the running of the gauge coupling can be easily isolated as

$$\Delta\beta_{e^2}^{\text{Grav}} = \eta_A^{\text{Grav}}\, e_k^2\,, \tag{4.17}$$

where η_A^{Grav} denotes the gravitational contribution to the gauge field anomalous dimension. The diagrams contributing to η_A^{Grav} are represented in Fig. 4.4. To evaluate η_A^{Grav}

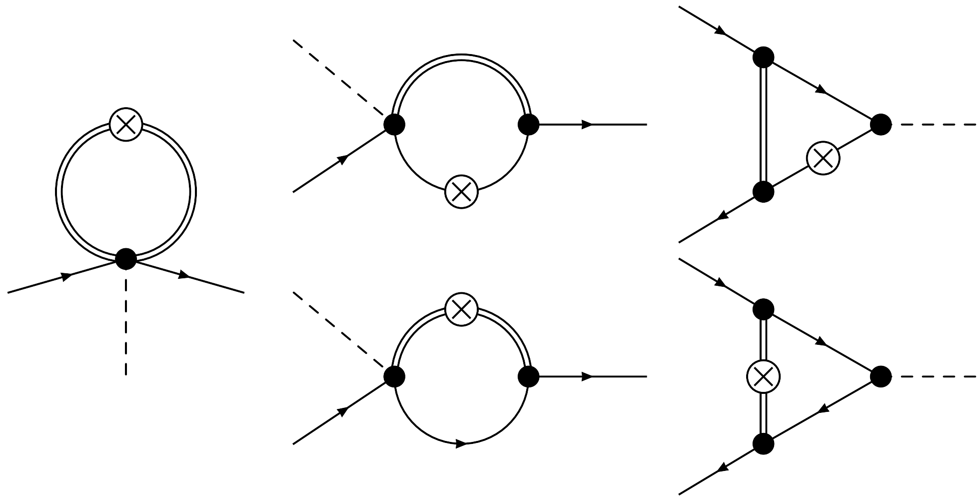

Figure 4.3: Diagrams contribution to the RG flow of the Yukawa coupling. The solid line with an arrow denotes the fermionic field propagator and the double line represents the graviton propagator. In the unimodular setting, only the triangle diagrams in the third column give non-vanishing results. In the standard (non-unimodular) framework, all the diagrams contributes to β_y.

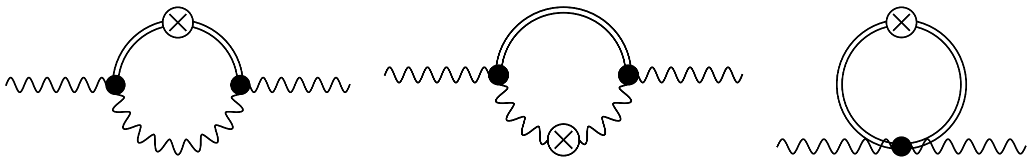

Figure 4.4: Diagrams contributing to the anomalous dimension η_A. The wiggly line correspond to the propagator associated with the Abelian gauge field and the double line represents the graviton propagator.

we apply the projection rule

$$\eta_A^{\rm Grav} = -\frac{1}{3\,Z_{k,A}}\left[\frac{\partial}{\partial p^2}\left(\mathcal{P}_{\rm T}(p)\circ\sum \text{Diagrams}\Big|_{\rm Fig.4.4}\right)\right]_{p^2=0}. \tag{4.18}$$

Note that we are using the notation $\mathcal{P}_{\rm T}(p)\circ(\cdots)$ to the denote the full contraction of the transverse projector $\mathcal{P}_{\rm T}^{\mu\nu}(p)$ with the free indices resulting from the diagrams depicted in Fig. 4.4.

Since gravity is universal w.r.t. internal symmetries, the direct QG contribution to the flow of gauge couplings does not dependent on the specific choice of gauge group. In this sense, the resulting expressions for $\eta_A^{\rm Grav}$, introduced as the gravitational contribution to the Abelian gauge field, is also valid for the non-Abelian sector. Similarly, there is no flavor dependence on $\beta_y^{\rm Grav}$. As a consequence, the gravitational contributions to the running of a simple Yukawa interaction of the form $\phi\,\bar{\psi}\psi$ can be easily extended to more complicated situations with Yukawa terms involving flavor indices. From the FRG perspective, such considerations are valid as long as we stay in the semi-perturbative approximation, i.e., neglecting the anomalous dimensions arising from the regulator insertions $\partial_t\mathbf{R}_k$ (see Chap. 3).

4.2.3 The flow of the scalar potential

In the standard ASQG setting, the gravitational contribution to the flow of the scalar potential $V_k(\phi^2)$ drives it towards irrelevance at the free FP[7] $V^*(\phi)^2 = 0$ [97, 208, 213, 214, 218, 275]. This implies that[8] QG effects tend to flatten the scalar potential in an IR predictive way. Under the assumption that this scenario is realized in more realistic models, this could have important phenomenological consequences, such as the prediction of the Higgs mass in the vicinity of the observed value [97, 218, 274], the decoupling of the Higgs portal to scalar dark matter [213] and a possible criteria to rule out certain grand unified theories [221].

In the UG, the gravitational contribution to the flow of a scalar potential $V_k(\phi^2)$ comes exclusively through the scalar field anomalous dimension η_ϕ. This feature appears as a consequence of the absence of direct gravity-matter interactions in the scalar potential sector. This is very different from the standard case, where the scalar potential couples to gravity via metric-determinant fluctuations. In the standard setting, the main contribution to the flow of the scalar potential comes from tadpole diagrams involving scalar-graviton vertices derived from $\sqrt{g}\, V_k(\phi^2)$. Such a difference on the structure of the interactions strongly motivates the investigation of QG-effects on the scalar potential in the unimodular setting.

To make clear the difference discussed in the previous paragraph, let us focus on the simple truncation where the scalar potential is parameterized by a single quartic interaction, namely.

$$V_k(\phi^2) = \frac{1}{4!} Z_\phi^2 \,\lambda_k \,\phi^4 \tag{4.19}$$

In such a case, the RG of the potential is translated to the beta function β_λ. In the unimodular setting, the graviton contribution to the beta function of the quartic coupling takes the form

$$\Delta\beta_\lambda^{\mathrm{Grav}}|_{\mathrm{UG}} = 2\,\eta_\phi^{\mathrm{Grav}} \lambda_k \,, \tag{4.20}$$

where $\eta_\phi^{\mathrm{Grav}}$ is obtained according to the projection rule given by Eq. (4.15a) (see Fig. 4.1 for the diagrams contributing to $\eta_\phi^{\mathrm{Grav}}$). In contrast, the corresponding contribution in the standard setting of ASQG is given by the following expression[9]

$$\Delta\beta_\lambda^{\mathrm{Grav}}|_{\mathrm{Std.}} = 2\,\eta_\phi^{\mathrm{Grav}} \lambda_k \,+\, \mathcal{D}_\lambda \,\lambda_k \,, \tag{4.21}$$

[7]More precisely, $V^*(\phi)^2$ correspond to a "fixed function" defined as a solution of the equation $\partial_t V^*(\phi^2) = 0$.

[8]With possible exception of the mass term, which might remain UV relevant

[9]Note that we are using the "Std." as a reference to the standard ASQG setting.

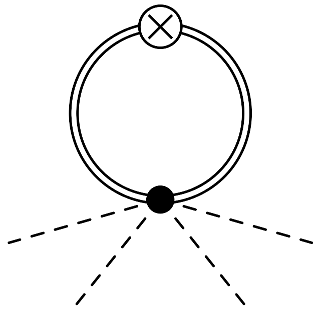

Figure 4.5: Tadpole diagrams contributing to the flow of the quartic scalar coupling. The dashed line denotes the scalar field dressed propagator and the double line represents the graviton propagator. Note that this diagrams is not present in the unimodular case.

where $\mathcal{D}_\lambda \lambda_k$ encodes gravitational effects resulting from the tadpole diagram depicted in Fig. 4.5. Comparing Eqs. (4.20) and (4.21), we can easily observe that $\Delta\beta_\lambda^{\mathrm{Grav}}|_{\mathrm{UG}}$ and $\Delta\beta_\lambda^{\mathrm{Grav}}|_{\mathrm{Std.}}$ receive contributions from considerably different diagrams, involving unrelated gravity-matter vertices. As a consequence, there is no *a priori* reason to expect that both settings lead to the same qualitative picture.

4.3 Towards phenomenological constraints in the unimodular theory space

In the present section we explore the ideas discussed in Sect. 4.1 as a possible way to impose constraints in the (truncated) theory space of UQG. Basically, we are interested in two types of phenomenologically motivated viability tests: i) induced UV completion in the Yukawa and Abelian gauge sectors; ii) predictivity of the Higgs mass due to QG effects. As we have discussed in Sect. 4.1, this set of viability tests basically depends on the sign of f_y, f_{e^2} and f_λ, which can translated in terms of $\eta_\phi^{\mathrm{Grav}}$, $\eta_\psi^{\mathrm{Grav}}$, η_A^{Grav} and $\mathcal{D}_y$, namely

$$f_y = -\left(\frac{1}{2}\eta_\phi^{\mathrm{Grav}} + \eta_\psi^{\mathrm{Grav}} + \mathcal{D}_y\right) , \tag{4.22a}$$

$$f_{e^2} = -\,\eta_A^{\mathrm{Grav}} , \tag{4.22b}$$

$$f_\lambda = 2\,\eta_\phi^{\mathrm{Grav}} . \tag{4.22c}$$

Within the truncation defined by Eq. (4.8), we can readily compute the relevant diagrams depicted in Figs. 4.1, 4.1, 4.3 and 4.4. Applying the corresponding projection rules (Eqs. (4.15a), (4.15b), (4.15c) and (4.18)), we obtain the following results

$$\eta_{\phi}^{\text{Grav}} = \frac{G_k}{20\pi}\left[\frac{25\,(1+3w_k)}{(1+2w_k)^2} + \frac{2\,(5-33a_k)}{(1-6a_k)^2}\right], \tag{4.23a}$$

$$\eta_{\psi}^{\text{Grav}} = \frac{G_k}{80\pi}\left[\frac{25\,(1+3w_k)}{(1+2w_k)^2} - \frac{31-246a_k}{(1-6a_k)^2}\right], \tag{4.23b}$$

$$\eta_{A}^{\text{Grav}} = -\frac{G_k}{45\pi}\left[\frac{5(5+7w_k)}{(1+2w_k)^2} - \frac{2\,(5-21a_k)}{(1-6a_k)^2}\right], \tag{4.23c}$$

and

$$\mathcal{D}_y = \frac{G_k}{20\pi}\frac{5-39a_k}{(1-6a_k)^2}\,. \tag{4.24}$$

Note that these results correspond to the semi-perturbative approximation, i.e., we are not taking into account the anomalous dimensions coming from the regulator insertion. Plugging $\eta_{\phi}^{\text{Grav}}$, $\eta_{\psi}^{\text{Grav}}$, η_{A}^{Grav} and $\mathcal{D}_y$ into (4.22a), (4.22b) and (4.22c), we find

$$f_y = -\frac{3\,G_k}{80\pi}\left[\frac{25\,(3w_k+1)}{(1+2w_k)^2} + \frac{3-14a_k}{(1-6a_k)^2}\right], \tag{4.25a}$$

$$f_{e^2} = \frac{G_k}{45\pi}\left[\frac{5\,(5+7w_k)}{(1+2w_k)^2} - \frac{2\,(5-21a_k)}{(1-6a_k)^2}\right], \tag{4.25b}$$

$$f_{\lambda} = \frac{G_k}{10\pi}\left[\frac{25\,(1+3w_k)}{(1+2w_k)^2} + \frac{2\,(5-33a_k)}{(1-6a_k)^2}\right]. \tag{4.25c}$$

With this result in mind, we can constrain regions in the space of gravitational parameters (G_k, a_k and w_k) according with the requirements f_y, f_{e^2}, $f_\lambda > 0$. In general, we are going to set $G_k > 0$ as a consistency requirement. In this sense, our analysis reduces to a systematic investigation on the sign of f_y, f_{e^2} and f_λ in terms of the curvature squared couplings a_k and w_k.

Let us start our investigation with the Yukawa sector. In this case, the relevant condition for the viability of induced UV completion corresponds to the following inequality ($f_y > 0$)

$$\frac{25\,(3w_k+1)}{(1+2w_k)^2} + \frac{3-14a_k}{(1-6a_k)^2} \;<\; 0\,. \tag{4.26}$$

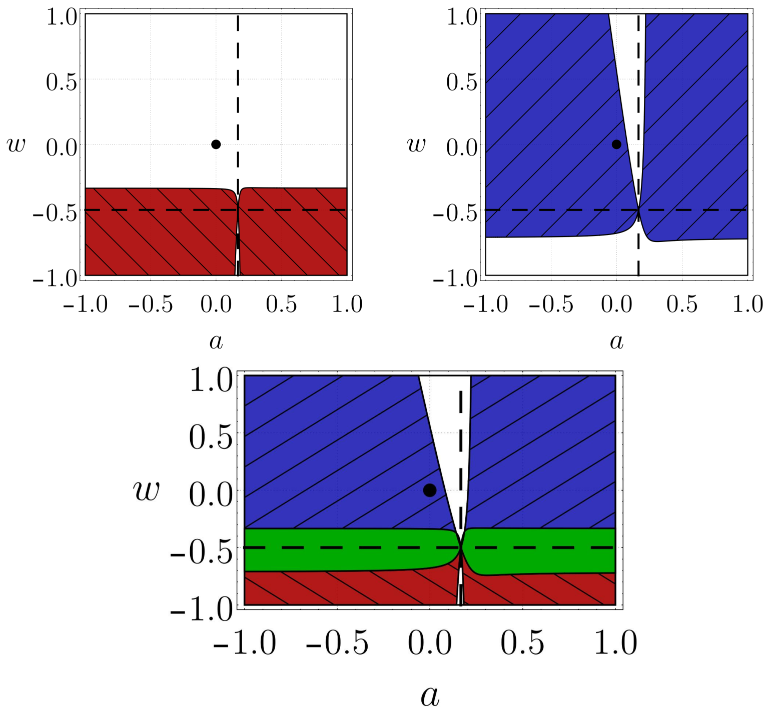

Figure 4.6: Left panel: viable region for UV completion in the Yukawa sector (in red); Center panel: viable region for UV completion in the Abelian gauge sector (in blue); Right panel: combined plot showing the viable region for UV completion in the Yukawa and the Abelian gauge sector. The green part (without diagonal lines) indicates the region with overlap of the viability conditions $f_y > 0$ and $f_{e^2} > 0$. In all plots the dashed lines indicated the poles lines $1 + 2w_k = 0$ and $1 - 6a_k = 0$.

In Fig. 4.6 (left) we plot the region where this inequality holds. A gravitational FP in that region would generate an antiscreening contribution to the beta function for the Yukawa coupling. As we can see, such a region occurs at negative values of w_k, with only a sub-leading dependence on the coupling a_k. Except for the vicinity of the pole $a_k = 1/6$, the viable region can be roughly approximated by $w_k \lesssim -1/3$.

As one can observe in Fig. 4.6, the point corresponding to the Einstein-Hilbert truncation ($a_k = w_k = 0$) does not belong to the viable region for induced UV completion. One might have expected this result from the analogous result in the standard ASQG, since, in that case, the presence of the cosmological constant is crucial in the absence of higher-order couplings. At vanishing cosmological constant (along with $a_k = w_k = 0$), the transverse traceless contribution to β_y dominates, yielding $f_y < 0$. At sufficiently negative value for the dimensionless cosmological constant, a reweighing of contributions to β_y occurs, such that the transverse traceless contribution is actually subdominant and $f_y > 0$ can be achieved, see [209] for a comprehensive discussion. In the unimodular case, the cosmological constant no longer appears in the graviton propagator. Accordingly, the results can be expected to be similar to those in the standard ASQG at vanishing cosmological constant (of course, the correspondence is not exact).

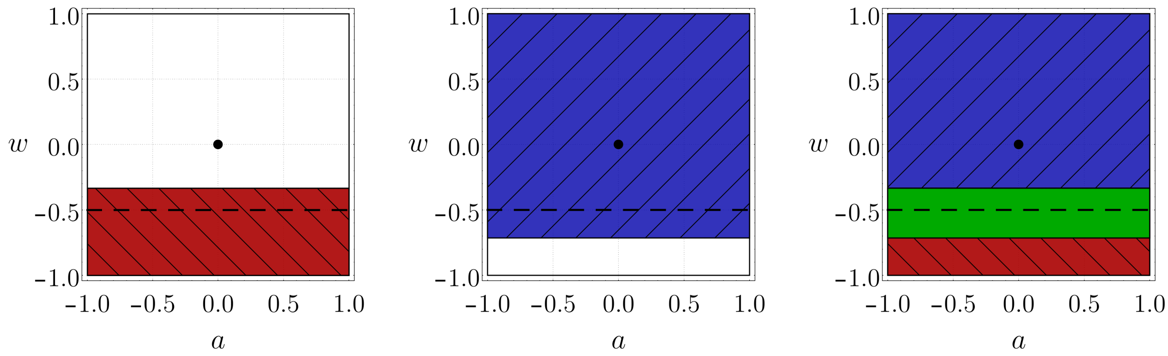

Figure 4.7: Viability regions for QG induced UV completion in the Yukawa and Abelian gauge sectors in the TT-approximation. Left panel: viable region for UV completion in the Yukawa sector (in red). Center panel: viable region for UV completion in the Abelian gauge sector (in blue). Right panel: combined plot showing the viable region for UV completion in the Yukawa and the Abelian gauge sector. The green part (without diagonal lines) indicates the region with overlap of the viability conditions $f_y > 0$ and $f_{e^2} > 0$. In all plots the dashed line indicated the pole line $1 + 2w_k = 0$.

Turning our attention to the Abelian gauge sector, the viability condition for UV completion induced by QG-effects is characterized by the inequality,

$$\frac{5\,(5 + 7w_k)}{(1 + 2w_k)^2} - \frac{2\,(5 - 21a_k)}{(1 - 6a_k)^2} > 0\,, \tag{4.27}$$

which follows from $f_{e^2} > 0$. The corresponding region in the $a_k \times w_k$ plane is exhibited in Fig. 4.6 (center). Similarly to what happens in the Yukawa coupling, the sign of f_{e^2} is mostly dictated by the coupling w_k. In the present case, the viable region for UV completion can be approximated by $w_k \gtrsim -5/7$, except for the neighborhood of the pole line at $a_k = 1/6$. In contrast to the Yukawa sector, the Einstein-Hilbert point ($a_k = w_k = 0$) belongs to the viable region for a UV completion of the gauge sector. Once again, this is similar to the results obtained in the standard ASQG, where $f_{e^2} > 0$ holds at vanishing cosmological constant, see, e.g., [101, 196, 203].

In Fig. 4.6 (right) we present the combined constraints on the gravitational parameter space arising from $f_{e^2} > 0$ and $f_y > 0$. Far away from the pole line $a_k = 1/6$, the combined viable region for UV completion can be approximated by $-5/7 \lesssim w_k \lesssim -1/3$. This approximated behavior reflects the dominance of the transverse and traceless mode, i.e., the "TT-dominance". Fig. 4.7 shows the viable region in the TT-approximation, which is obtained by neglecting contributions the σ-sector in the graviton propagator.

The third phenomenologically motivated constraint on the (truncated) unimodular theory space comes from the scalar potential. In this case, a positive gravitational contribution anomalous dimension η_ϕ drives the scalar potential towards UV irrelevance at the FP $V^*(\phi^2) = 0$. This effect is particularly interesting for the quartic self-coupling, which is canonically marginal and might become UV irrelevant due to QG-effects. The

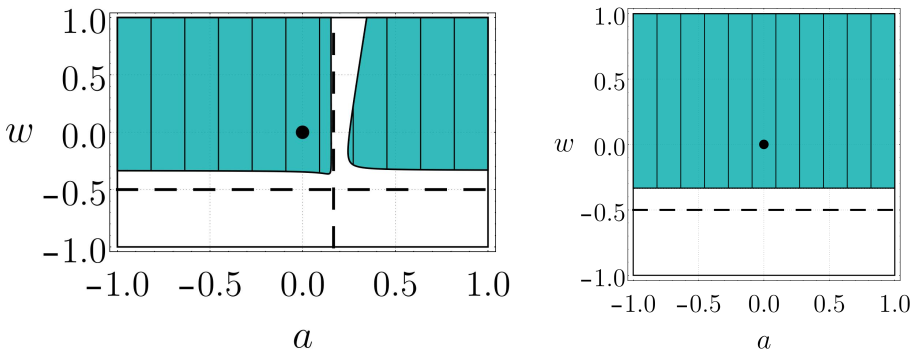

Figure 4.8: Viable region (cyan) for a predictive scalar potential ($\eta_\phi^{\text{Grav}} > 0$). The left panel show the full result and the right panel corresponds to the TT-approximation. The dashed lines indicated the poles lines $1 + 2w_k = 0$ and $1 - 6a_k = 0$.

positive contribution to the anomalous dimension translates to $f_\lambda > 0$. In such a case, the relevant condition for a predictive scalar potential is encoded in the following inequality ($f_\lambda > 0$ or $\eta_\phi^{\text{Grav}} > 0$)

$$\frac{25\,(1+3w_k)}{(1+2w_k)^2} + \frac{2\,(5-33a_k)}{(1-6a_k)^2} > 0\,. \tag{4.28}$$

Fig. 4.8 (left) shows the region in the $a_k \times w_k$ plane where the above condition is satisfied. In a similar way to what was observed in the Yukawa and Abelian gauge coupling, the viable region for a predictive scalar potential basically depends on the coupling associated with the $C^2_{\mu\nu\alpha\beta}$ contribution. Once again, this result reflects the dominance of the TT-mode (see Fig. 4.8 (right)). Except for the vicinity of the pole $a_k = 1/6$, the viability condition for a predictive scalar potential can be approximated as $w_k \gtrsim -1/3$.

It is interesting to understand whether the conditions $f_y > 0$ and $f_{e^2} > 0$, necessary for UV completion of Yukawa and Abelian gauge sectors, can be coexist with the requirement $\eta_\phi^{\text{Grav}} > 0$ ($f_\lambda > 0$), which renders a predictive scalar potential. Within our approximation, such a combined region imposes a significant restriction on the space of curvature squared couplings, see Fig. 4.9. The origin of this severe restriction can be seen in the TT-approximation, where the gravitational contribution to the running of the Yukawa coupling takes the form

$$f_y|_{\text{TT}} = -\left(\frac{1}{2}\eta_\phi|_{\text{TT}} + \eta_\psi|_{\text{TT}} + \mathcal{D}_y|_{\text{TT}}\right) = -\frac{3}{4}\eta_\phi|_{\text{TT}}\, y\,, \tag{4.29}$$

where we have used $\eta_\psi|_{\text{TT}} = \eta_\phi|_{\text{TT}}/4$ and $\mathcal{D}_y|_{\text{TT}} = 0$. As a consequence, the viability condition for a UV completion of the Yukawa coupling becomes $\eta_\phi|_{\text{TT}} < 0$, which is in conflict with the requirement for a calculable Higgs mass. Beyond the TT-approximation, scalar fluctuations generate a region which features the combined

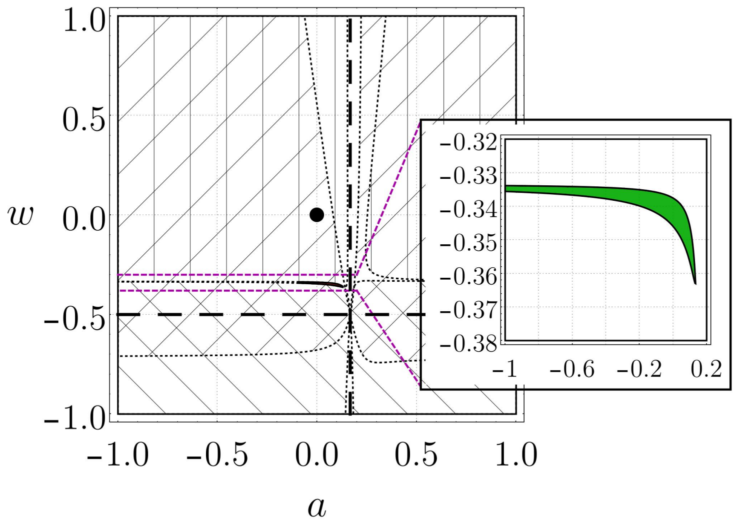

Figure 4.9: Combined plot showing the boundaries of the "viability regions" corresponding to each one of the sectors discussed here. The small portrait zooms in the overlapping regions where the three conditions, $f_y > 0$, $f_{e^2} > 0$ and $\eta_\phi^{\rm Grav} > 0$, hold simultaneously.

inequalities $f_y > 0$ and $\eta_\phi^{\rm Grav} > 0$, showing that fluctuations of scalar modes can play an important role in parts of the gravitational parameter space. It is important to emphasize that the UV completion of the scalar sector is also consistent with $\eta_\phi^{\rm Grav} < 0$, since the scalar quartic coupling is then asymptotically free. Nevertheless, in such a case, the quartic scalar coupling is no longer predictive as a consequence of the FP structure, but remains as a free parameter to be fixed by experiments.

4.4 Comparison with the standard ASQG setting

In this section, we contrast the phenomenologically motivated constraints in the unimodular theory space, discussed in the previous section, with the corresponding ones in the standard ASQG, i.e., within the framework where the theory space is defined by the full *Diff* symmetry. In this setting, we consider the following truncation

$$\Gamma_k^{\rm Std.} = \Gamma_k^{\rm Grav} + \Gamma_k^{\rm SM} + \Gamma_k^{\rm g.f.}\,, \tag{4.30}$$

where

$$\Gamma_k^{\rm Grav} = \frac{1}{16\pi G_{\rm N}} \int_x \sqrt{g}\,\left(2\Lambda_{{\rm cc},k} - R + \bar{a}\,R^2 + \bar{w}\,C_{\mu\nu\alpha\beta}C^{\mu\nu\alpha\beta}\right)\,, \tag{4.31a}$$

$$\Gamma_k^{\rm SM} = \int_x \sqrt{g}\left(\frac{1}{2}g^{\mu\nu}\partial_\mu\phi\partial_\nu\phi + V(\phi^2) + \frac{1}{4\,e^2}g^{\mu\alpha}g^{\nu\beta}F_{\mu\nu}F_{\alpha\beta} + i\bar{\psi}\not{D}\psi + iy\,\phi\,\bar{\psi}\psi\right)\,, \tag{4.31b}$$

$$\Gamma_k^{\text{g.f.}} = \frac{1}{2\alpha} \int_x \sqrt{\bar{g}}\, \bar{g}^{\mu\nu} F_\mu[h;\bar{g}] F_\nu[h;\bar{g}] + \frac{1}{2\zeta} \int_x \sqrt{\bar{g}}\, (\bar{g}^{\mu\nu} \bar{\nabla}_\mu A_\nu)^2 \,. \tag{4.31c}$$

In the standard ASQG setting, since the metric determinant is not constrained by the unimodularity condition, the cosmological constant term $\int_x \sqrt{g}\, \Lambda_{\text{cc}}$ enters as part of the theory space. Furthermore, the metric determinant generates contributions to the gravity-matter vertices that are not present in the unimodular case. In the gauge-fixing sector we use

$$F_\mu[h;\bar{g}] = \bar{\nabla}^\nu h_{\mu\nu} - \frac{1+\beta}{4} \bar{\nabla}_\mu h^{\text{tr}} \,, \tag{4.32}$$

instead of the transverse gauge condition $F_\mu^{\text{T}}[h;\bar{g}]$ adopted in UG. In contrast to the unimodular case, in standard ASQG the metric splitting is taken to be the linear one, namely $g_{\mu\nu} = \bar{g}_{\mu\nu} + \sqrt{32\pi G_{\text{N}}}\, h_{\mu\nu}$. Note that in this case the metric fluctuation $h_{\mu\nu}$ is not restricted by the tracelessness condition. Here, we are going to set the gauge parameter β to zero, which decouples the σ-mode from our computations.

To compute the gravitational contribution to the RG flow of matter couplings we follow the same procedure already discussed in the unimodular case. It is important to note that, in the standard ASQG framework, all the diagrams exhibited in Fig. 4.3 are relevant to the flow of the Yukawa couplings. Moreover, the tadpole represented in Fig. 4.5, which is not present in the unimodular setting, is the dominant contribution to the running of the quartic scalar coupling. The gravitational contribution to the anomalous dimensions of matter fields is encoded in the following expressions

$$\eta_\phi^{\text{Grav}}|_{\text{Std.}} = \frac{G_k}{15\pi} \frac{15 - 117\, a_k - 10\, \Lambda_k}{(3 - 18\, a_k - 4\, \Lambda_k)^2} \,, \tag{4.33a}$$

$$\eta_\psi^{\text{Grav}}|_{\text{Std.}} = -\frac{G_k}{80\pi} \left[\frac{125\,(1+3w_k)}{(1+2\,w_k - 2\,\Lambda_k)^2} - \frac{9\,(41 - 346\, a_k - 16\, \Lambda_k)}{(3 - 18\, a_k - 4\, \Lambda_k)^2} \right] , \tag{4.33b}$$

$$\eta_A^{\text{Grav}}|_{\text{Std.}} = -\frac{G_k}{9\pi} \frac{5 + 7\, w_k - 20\, \Lambda_k}{(1 - 2\,\Lambda_k + 2\, w_k)^2} \,. \tag{4.33c}$$

The diagrams in Figs. 4.3 and 4.5 lead to the following results

$$\mathcal{D}_y|_{\text{Std.}} = \frac{G_k}{20\pi} \left[\frac{50\,(1+3w_k)}{(1+2\,w_k - 2\,\Lambda_k)^2} - \frac{3\,(37 - 295\, a_k - 22\, \Lambda_k)}{(3 - 18\, a_k - 4\, \Lambda_k)^2} \right] , \tag{4.34a}$$

$$\mathcal{D}_\lambda|_{\text{Std.}} = \frac{G_k}{2\pi} \left[\frac{5\,(1+3\,w_k)}{(1+2\,w_k - 2\,\Lambda_k)^2} + \frac{6\,(1 - 9\, a_k)}{(3 - 18\, a_k - 4\, \Lambda_k)^2} \right] . \tag{4.34b}$$

This result can easily converted into the parameterized gravitational contributions f_y, f_{e^2} and f_λ, namely

$$f_y|_{\text{Std.}} = -\frac{G_k}{240\pi}\left[\frac{225\,(1+3\,w_k)}{(1+2w_k-2\,\Lambda_k)^2} - \frac{105-342\,a_k-280\,\Lambda_k}{(3-18\,a_k+4\,\Lambda_k)^2}\right], \tag{4.35a}$$

$$f_{e^2}|_{\text{Std.}} = \frac{G_k}{9\pi}\frac{5+7\,w_k-20\,\Lambda_k}{(1-2\,\Lambda_k+2\,w_k)^2}, \tag{4.35b}$$

$$f_\lambda|_{\text{Std.}} = \frac{G_k}{30\pi}\left[\frac{75\,(1+3\,w_k)}{(1+2\,w_k-2\,\Lambda_k)^2} + \frac{2\,(75-639\,a_k-20\,\Lambda_k)}{(3-18\,a_k+4\,\Lambda_k)^2}\right]. \tag{4.35c}$$

The possibility of a UV completion for the Yukawa sector ($f_y > 0$), within standard ASQG setting, was studied in [207, 209, 210, 215]. In Fig. 4.10 we show the viable region for a QG induced FP for the Yukawa coupling in the $a_k \times w_k$ plane, for several values of the dimensionless cosmological constant ($\Lambda_k = k^{-2}\Lambda_{\text{cc},k}$). In the particular case of vanishing cosmological constant ($\Lambda_k = 0$), we observe a coincidence between the unimodular and the standard setting. This result follows from the dominance of the TT-mode. In fact, if we restrict ourselves to the TT-approximation (with $\Lambda_k = 0$), both settings give the same results for the gravitational contribution to the Yukawa coupling, namely

$$f_y|^{\text{TT}}_{\text{Std.}} = f_y|^{\text{TT}}_{\text{UG}} = -\frac{G_k}{16\pi}\frac{15\,(1+3\,w_k)}{(1+2w_k-2\,\Lambda_k)^2}. \tag{4.36}$$

Note that this equality is rather nontrivial, since the various diagrams that contribute to these results differ in the two settings. In the vicinity of the pole line associated with the scalar mode ($a_k = 1/6$ for $\Lambda_k = 0$), on the other hand, the dominant contribution comes from the scalar sector of the fluctuation field $h_{\mu\nu}$. In the unimodular setup, the scalar sector corresponds to the σ-mode, while in the standard gravity framework the scalar sector by a combination of σ and h^{tr}. Within the gauge choice $\beta = 0$, only the trace mode contributes to the results. Since these different setups receive contributions from different graviton modes, we observe a quantitative disagreement in the neighborhood of the scalar-mode pole.

For non-vanishing cosmological constant, the scalar fluctuations become more relevant. For positive values of Λ_k, we observe a screening behavior of metric fluctuations for values of a_k and w_k close to the scalar pole. This leads to the reduction of viable regions for UV completion in the regime $\Lambda_k > 0$, cf. Fig. 4.10. For negative values of Λ_k, the mechanism works in the opposite direction. In this regime, scalar fluctuations contribute in an anti-screening manner to the Yukawa beta function and, as a conse-

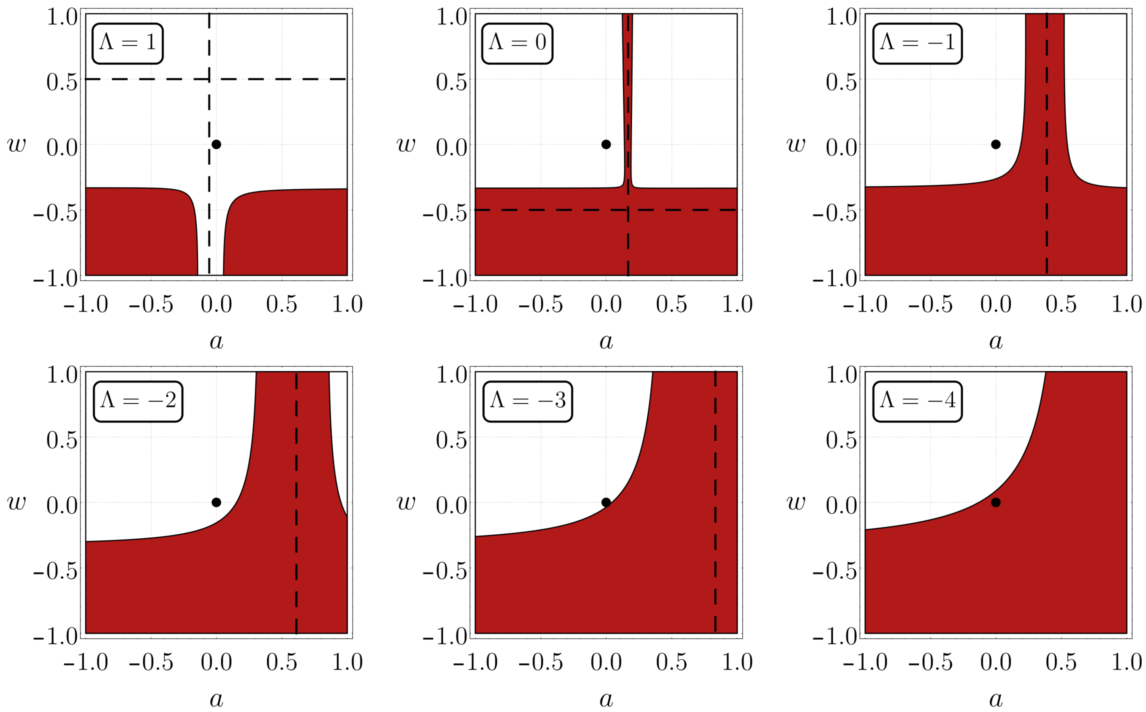

Figure 4.10: Viable region for UV completion in the Yukawa sector ($f_y > 0$) within the standard ASQG framework. The different plots correspond to different values of the dimensionless cosmological constant. The dashed lines indicate the pole lines $1 + 2w_k - 2\,\Lambda_k = 0$ and $3 - 18\,a_k + 4\,\Lambda_k = 0$.

quence, this results in the enlargement of the viable region. In particular, we note that if Λ_k is sufficiently negative, the point corresponding to the Einstein-Hilbert truncation ($a_k = w_k = 0$) becomes part of the viable region for UV completion.

Concerning the Abelian gauge sector, the relevant condition for UV completion induced QG effects ($f_{e^2} > 0$) reduces to the simple inequality

$$5 + 7\,w_k - 20\,\Lambda_k > 0\,. \tag{4.37}$$

In this case, as a consequence of the gauge choice $\beta = 0$, the impact of gravitational fluctuations comes exclusively from the transverse and traceless contributions. For this reason, the inequality (4.37) does not depend on the coupling associated with the R^2 term. At vanishing cosmological constant, the result for the standard setting generates the same "viability region" as that was obtained in the within the TT-approximation in the unimodular case. For non-vanishing Λ_k, we observe a similar behavior in comparison with the Yukawa coupling, namely, negative values of Λ_k enlarge the viable region for induced UV completion in the Abelian gauge sector (see Fig. 4.11).

Finally, let us discuss the gravitational contribution to the flow of the scalar potential. More precisely, the impact of QG effects on the running of the quartic coupling. In Fig. 4.12, we show the region where graviton fluctuations induce predictive trajectories for the quartic coupling (for several values of the dimensionless cosmological

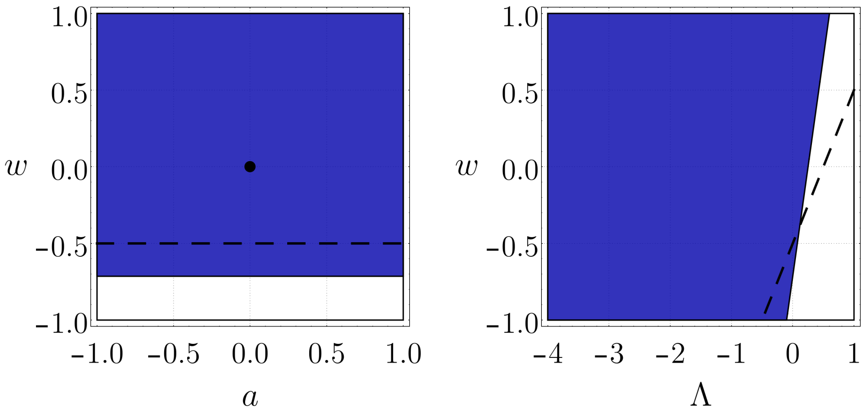

Figure 4.11: Viable region for UV completion in the Abelian gauge sector ($f_{e^2} > 0$) within the standard ASQG framework. The left panel shows the viability region in the $a \times w$ plane with $\Lambda_k = 0$. Since the result is independent of the parameter a, in the right panel we show the viability region in the $\Lambda \times w$ plane. The dashed lines indicate the pole lines $1 + 2w_k - 2 = 0$ and $1 + 2w_k - 2\,\Lambda_k = 0$.

constant). In the case with $\Lambda_k = 0$, we observe the same qualitative behavior as in UG. Once again, this fact can be explained in terms of the dominance of the TT-mode. For non-vanishing Λ_k the results change considerably. In particular, for negative values of the cosmological constant, the region with predictive quartic coupling is deformed in such a way that we observe that the overlap with the region allowing UV FPs in the Yukawa and Abelian gauge couplings becomes larger.

4.5 Extended unimodular theory space: regulator induced mass parameters

In Chap. 3 we motivated the introduction of mass parameters as a consequence of a symmetry breaking effect induced by the FRG regulator. In unimodular QG, this is a first step towards the investigation of theory spaces properly defined in terms of coarse-grained symmetry identities. The results reported in Chap. 3 indicate that the symmetric breaking masses mimic the impact of the cosmological constant. To some extent, this is expected by noting that the cosmological constant acts as a mass-like parameter in the graviton propagator. It is intriguing to understand whether the introduction of symmetry-breaking masses could produce similar effects, in comparison with the cosmological constant, on the viable regions for induced UV completion and predictive quartic coupling.

In the present section we address this question by extending our truncation (Eq. (4.8)) with the inclusion of an additional sector involving a symmetry-breaking mass

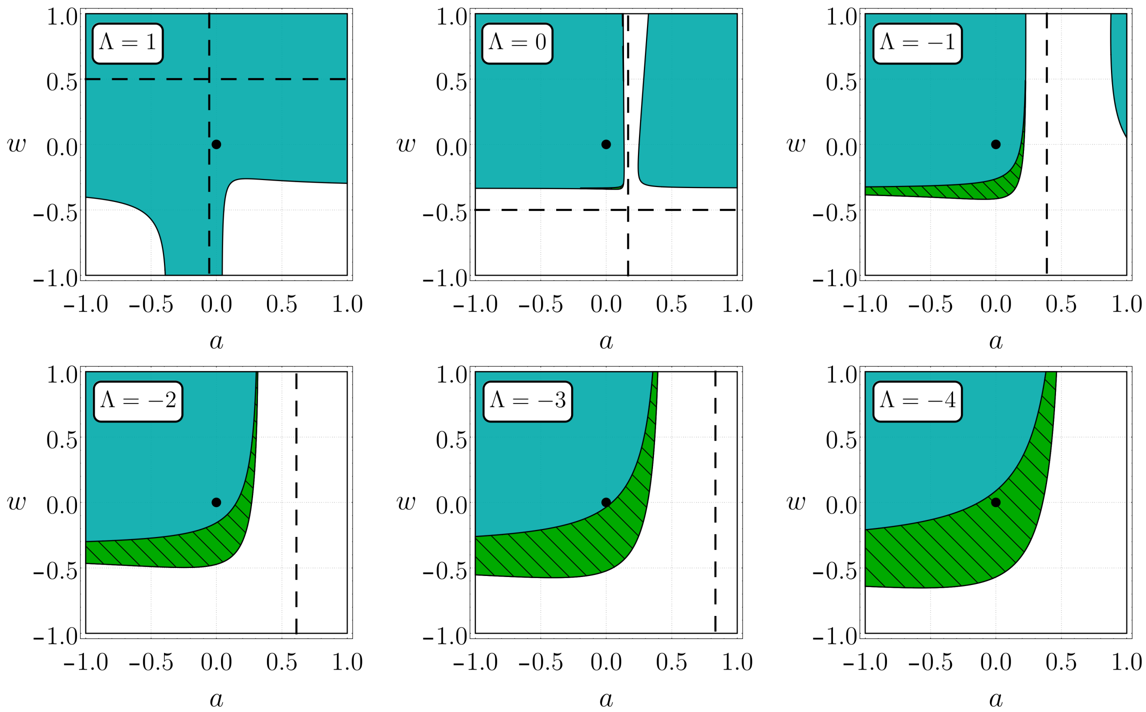

Figure 4.12: Viable region (cyan) for a predictive quartic scalar coupling ($f_\lambda > 0$) within the standard ASQG framework. The different plots correspond to different values of the dimensionless cosmological constant. The dashed lines indicate the pole lines $1+2w_k-2\,\Lambda_k = 0$ and $3-18\,a_k+4\,\Lambda_k = 0$. The green part (with diagonal lines) indicate the overlapping region where $f_y > 0$, $f_{e^2} > 0$ and $f_\lambda > 0$ are simultaneously verified.

parameter, namely

$$\Gamma_k^{m_h^2} = \frac{m_{k,h}^2}{2} \int_x \omega\, \bar{g}^{\mu\alpha} \bar{g}^{\nu\beta} h_{\mu\nu} h_{\alpha\beta}\,. \tag{4.38}$$

With the inclusion of symmetry-breaking masses, we redefine the relevant parts of the graviton propagator according to the following rules

$$\frac{1}{\big(1+2\,\bar{w}_k P_k(p^2)\big) P_k(p^2)} \mapsto \frac{1}{\big(1+2\,\bar{w}_k P_k(p^2)\big) P_k(p^2) + m_{k,\mathrm{TT}}^2}\,, \tag{4.39a}$$

$$\frac{1}{\big(1-6\,\bar{a}_k P_k(p^2)\big) P_k(p^2)} \mapsto \frac{1}{\big(1-6\,\bar{a}_k P_k(p^2)\big) P_k(p^2) + m_{k,\sigma}^2}\,. \tag{4.39b}$$

Note that we are also redefining the single mass parameter $m_{k,h}^2$ according to $m_{k,h}^2 \mapsto m_{k,\mathrm{TT}}^2$ and $m_{k,h}^2 \mapsto -\frac{1}{2} m_{k,\sigma}^2$, respectively, for the TT- and σ-modes. The inclusion of symmetry breaking masses modifies the explicit results for the diagrams contributing to the flow of couplings in the matter sector. In terms of the parameterized contributions

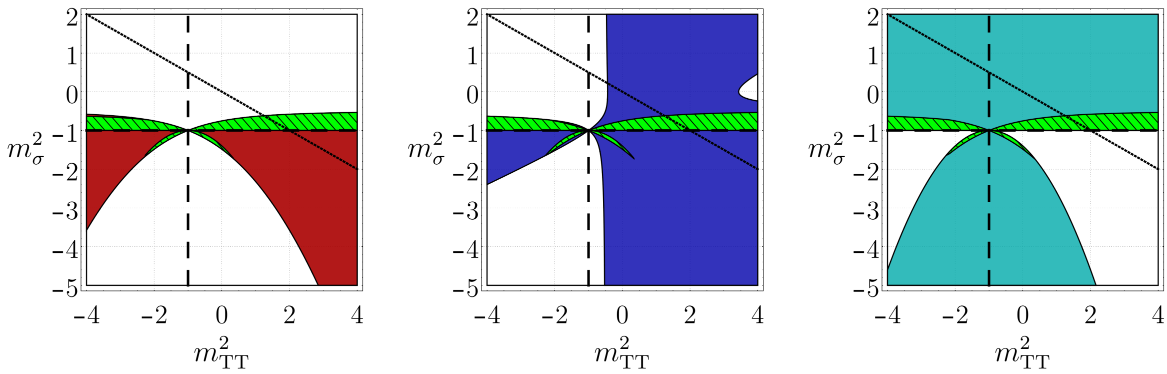

Figure 4.13: Viability regions in the space of symmetry-breaking masses (with vanishing curvature squared couplings). Left panel: viable region for UV completion in the Yukawa sector ($f_y > 0$). Center panel: viable region for UV completion in the Abelian gauge sector ($f_{e^2} > 0$). Right panel: viable region for a predictive scalar potential ($\eta_\phi^{\rm Grav} > 0$). In all cases the dashed lines indicate the poles lines $1 + m^2_{\rm TT} = 0$ and $1 + m^2_\sigma = 0$. The diagonal (dotted) line correspond to the single mass approximation $m^2_{\rm TT} = -2m^2_\sigma = m^2_k$. The green regions (with diagonal lines) indicates the overlap of the tree viability conditions $f_y > 0$, f_{e^2} and $\eta_\phi^{\rm Grav} > 0$.

f_y, f_{e^2} and f_λ, the main results can be summarized with following expressions

$$f_y = -\frac{3\,G_k}{80\pi}\left[\frac{25\,(1+3\,w_k)}{(1+2\,w_k+m^2_{k,\rm TT})^2} + \frac{3-14\,a_k+6\,m^2_{k,\sigma}}{(1-6\,a_k+m^2_{k,\sigma})^2}\right], \tag{4.40a}$$

$$f_{e^2} = -\frac{G_k}{45\pi}\left[\frac{5\,(5+7\,w_k+10\,m^2_{k,\rm TT})}{(1+2\,w_k+m^2_{k,\rm TT})^2} - \frac{10-42\,a_k+20\,m^2_{k,\sigma}}{(1-6\,a_k+m^2_{k,\sigma})^2}\right], \tag{4.40b}$$

$$f_\lambda = \frac{G_k}{10\pi}\left[\frac{25\,(1+3\,w_k)}{(1+2\,w_k+m^2_{k,\rm TT})^2} + \frac{2\,(5-33\,a_k+5\,m^2_{k,\sigma})}{(1-6\,a_k+m^2_{k,\sigma})^2}\right]. \tag{4.40c}$$

In Fig. 4.13 we show the viable region for induced UV completion ($f_y > 0$ and $f_{e^2} > 0$) and predictive quartic couplings ($f_\lambda > 0$) in the $m^2_{k,\rm TT} \times m^2_{k,\sigma}$ plane (with $a_k = w_k = 0$). As one can observe, even in the absence of couplings associated with R^2 and $C^2_{\mu\nu\alpha\beta}$, the symmetry breaking masses induce viable regions for simultaneous UV completion in the Yukawa and Abelian gauge sectors and predictive quartic coupling in the scalar sector. This result is in contrast with the case without symmetry breaking masses, where, in particular, the viable region for UV completion in the Yukawa sector requires the inclusion of higher-order couplings. The appearance (and enlargement) of overlapping regions lies on the enhancement of the σ-mode contribution due to the mass parameter $m^2_{k,\sigma}$.

Concluding Remarks

In this thesis, the AS program for QG was analyzed. This approach relies in the possibility of UV completion based on the (conjectured) existence of FPs in the RG flow. Usually, the ASQG approach is constructed as a quantum theory for GR, meaning that the theory space is defined in terms of general covariance (*Diff* symmetry). In the present thesis, we have considered a different version of ASQG with theory space defined on top of the unimodular setting for QG, where the metric determinant is fixed to be non-dynamical. In this case, the underlying symmetry corresponds to the *TDiff* group, a special type of *Diff* transformations with transverse generators. At the classical level UG is equivalent to GR provided that we impose covariant conservation of the energy-momentum tensor. At the quantum level, however, the equivalence between the two settings remains unsettled.

In the past two decades, the research program of ASQG went through substantial progress. By now, there is an extensive collection of works, based on FRG techniques, pointing towards the existence of suitable gravitational FPs. Moreover, in the recent years some effort has been done to connect the FP regime with low energy phenomenology. Except for a few works in the literature [125,126,128,129], the unimodular theory space has been much less explored than the standard version based on GR. Nevertheless, since both settings are classically equivalent, there is no *a priori* reason to consider one or the other as the starting point. The analysis performed in this thesis aims to (partially) fill this gap in the ASQG literature.

In the search for UV completion in the unimodular setting, we have employed two different strategies within the FRG framework: i) background field approximation; ii) vertex expansion approach. In the first case, reported in Chap. 2, our results extend previous analysis based on the unimodular version of the $f(R)$-truncation for UG [126]. Our investigation collects further indications for the existence of a suitable UV FP, with two relevant directions, in the unimodular theory space. Moreover, our analysis includes an addition contribution to the flow equation which arises from an appropriated treatment of the volume factor associated with the *TDiff* group. The results for the $f(R)$-approximation show certain similarities in comparison to the standard (non-unimodular) framework for ASQG [73, 90]. In particular, the appearance of two relevant directions in the unimodular setting seems to be in agreement with the indications of three-dimensional UV critical surfaces in the standard case (recall that the cosmological constant - which is absent in the unimodular setting - corresponds to one of the relevant directions in the standard setting). Moreover, our results for the critical exponents in the unimodular $f(R)$-approximation provide further indications for the near-canonical behavior already observed in [126]. As an attempt to include effects beyond the Ricci scalar sector, we also have considered an approximation involving $R_{\mu\nu}^2$-contributions, denominated as FZ-truncation. This type of approximation was first considered in the standard ASQG framework, resulting in a faster "convergence" in comparison with the $f(R)$-truncation [89]. Our results indicate a different qualitative behavior in the unimodular setting. As we have seen in Chap. 2, the FP structure associated with the unimodular FZ-truncation exhibits unstable results in comparison with the $f(R)$-approximation. The source for such a bad behavior remains unclear and deserves further investigation in the future.

Within the vertex expansion approach, discussed in Chap. 3, we performed some steps towards the introduction of effects that are not captured in the background approximation. In particular, we introduced symmetry-breaking effects motivated by regulator induced modifications in the Slavnov-Taylor and Nielsen identities. Furthermore, the anomalous dimensions for the graviton and Faddeev-Popov ghosts were computed by studying the flow of the 2-point functions. Our results provide further information concerning the FP structure in the unimodular theory space. In particular, we found indications for the persistence of FP solutions even after the inclusion of symmetry-breaking terms. Notably, the symmetry-mass parameter acquires a non-vanishing value at the FP.

The quantum (in)equivalence between UG and GR is an intriguing open question that deserves further investigation. On the one hand, if both settings are not equivalent at the quantum level, this triggers the search for elements that might physically distinguish them and select one (if any) of these options as the most adequate one. On the other hand, if the physical equivalence is settled, this would inspire interesting questions concerning the differences at the level of theory space. In particular, it is intriguing to understand the role of the cosmological constant - which is not part of the unimodular theory space - and how it would fit within a setup where both settings are physically equivalent.

Connected to this point, in Chap. 3, we have performed a systematic comparison between UG and the so-called unimodular gauge. The latter corresponds to a type of unimodularity condition as an specific gauge-fixing in full *Diff*-invariant theories (on top of the exponential metric parameterization). Within the truncations we have considered, our investigation reveals the equivalence of both setting at the level of n-point (with $n > 1$) connected correlation functions. From the viewpoint of the standard ASQG, the cosmological constant appears as a essential coupling in full *Diff*-invariant theories and, therefore, requires a FP to define a UV-complete theory. However, in the unimodular gauge, the cosmological constant decouples from the beta functions associated with other couplings and from the n-point correlation functions. In this sense, in the unimodular gauge, the cosmological constant might be interpreted as an inessential coupling. It is important to emphasize that this result should not be interpreted as the physical equivalence between the standard and unimodular versions of ASQG. In particular, the use of the exponential metric parameterization plays an important role on the equivalence between UG and unimodular gauge. In the standard setting, however, one usually considers the linear split and it is not clear whether or not both choices of field parameterization should correspond to the same physical description. In particular, the space of metrics covered by the exponential parameterization is not the same as in the linear split [258].

Despite the importance of theoretical self-consistency, ultimately any physical theory must be confronted with experiments. This is a great challenge in any approach to QG, in particular, due to the strong suppression of direct quantum gravitational effects. In the framework of ASQG, an interesting approach to connect QG effects with experimental observations utilizes the interplay between gravity and matter. This promising route has been explored in the literature, leading to very attractive features such as the possibility of predict (or post-dict) SM free-parameters and the resolution of certain problems of the SM (e.g., Laudau poles in the Abelian sector). These results, of course, rely on approximation methods and deserve further investigation to be confirmed on more solid grounds. In this thesis (see Chap. 4), we have explored the gravity-matter interplay as a way to impose phenomenologically motivated constraints on the truncated unimodular theory space. Our findings indicate that, despite significant differences on the structure of gravity-matter interactions, the unimodular setting leads to very similar results in comparison with the standard ASQG, provided we neglect the impact of the cosmological constant in the latter. This result reinforces previous analysis concerning the importance of non-vanishing cosmological constant for phenomenological viability in standard ASQG [209]. In this sense, the investigation performed here points towards more severe constraints in the unimodular case.

The developments presented in this thesis open several routes for new investigations. An interesting approach, still unexplored in the unimodular setting, combines the vertex expansion with momentum-dependent approximation schemes in the FRG (see Ref. [190] for more details). This approach has been explored in the standard ASQG framework, providing further non-trivial indications for a gravitational FP. "Momentum-dependent" calculations are usually advocated to produce more reliable results in comparison with other approximation schemes [190], therefore, this would be an interesting line for future explorations in the unimodular theory space, not only for pure gravity, but also in gravity-matter systems.

Another point that deserves further attention from the AS perspective is related the implementation of the unimodularity condition on practical calculations. In the present thesis, the unimodularity condition was implemented by means of the exponential parameterization. However, as we have discussed in Chap. 2, this is not the only possibility. In this sense, it would be interesting to explore the possibility of other formulations of UQG, based on different implementations of the unimodularity condition.

Appendix **A**

The Faddeev-Popov Method in QG

A.1 Functional integral of UQG

In this appendix we explore some details concerning the definition of a path integral formalism in UG. In particular, we explore certain subtleties associated with the Faddeev-Popov procedure. The starting point for our discussion is the Euclidean path integral for QG, which can be formally written in the following way

$$Z_{\mathrm{UQG}}[\bar{g}] = \int \frac{\mathcal{D}h_{\mu\nu}}{V_{TDiff}} e^{-S_{\mathrm{UQG}}[h;\bar{g}]} \,, \tag{A.1}$$

where the integration domain is restricted to traceless configurations ($h^{\mathrm{tr}} = 0$) as a way to implement the unimodularity condition. Note that, as it was discussed in Chap. 2, in the present thesis we focused in a formulation for UQG based on the exponential parameterization (see Eq. (2.27)). The factor V_{TDiff} corresponds to the volume of the *TDiff* group.

The action of UG is invariant under *TDiff* transformations, that is, a special class of *Diff* transformations acting on the space-time metric according to

$$\delta_{\epsilon_{\mathrm{T}}} g_{\mu\nu} = g_{\mu\alpha}\nabla_\nu \epsilon^\alpha_{\mathrm{T}} + g_{\nu\alpha}\nabla_\mu \epsilon^\alpha_{\mathrm{T}} \,, \tag{A.2}$$

with generators $\epsilon^\mu_{\mathrm{T}}$ constrained by the transversality condition $\nabla_\mu \epsilon^\mu_{\mathrm{T}} = 0$. It is interesting to note that, for unimodular metrics, one can recast the transversality condition in terms of the background covariant derivative, namely

$$0 = \nabla_\mu \epsilon^\mu_{\mathrm{T}} = \frac{1}{\sqrt{g}}\partial_\mu(\sqrt{g}\,\epsilon^\mu_{\mathrm{T}}) = \frac{1}{\sqrt{\bar{g}}}\partial_\mu(\sqrt{\bar{g}}\,\epsilon^\mu_{\mathrm{T}}) = \bar{\nabla}_\mu \epsilon^\mu_{\mathrm{T}} \,, \tag{A.3}$$

where we have used $\sqrt{g} = \omega = \sqrt{\bar{g}}$ (valid in the unimodular configuration space). Since the path integral (A.1) was defined by means of the background field method, it is helpful to express the *TDiff* transformation directly in terms of the background and fluctuation fields. For the purposes considered here, it is convenient to adopt a decomposition known as "quantum transformation", defined in such a way the gauge transformation is completely encoded in the fluctuation field, namely

$$g_{\mu\nu} \mapsto g_{\mu\nu} + \delta_{\epsilon_{\rm T}} g_{\mu\nu} \quad \longrightarrow \quad \begin{cases} \bar{g}_{\mu\nu} \mapsto \bar{g}_{\mu\nu} \\ h_{\mu\nu} \mapsto h_{\mu\nu} + \delta^{\rm Q}_{\epsilon_{\rm T}} h_{\mu\nu} \end{cases} , \tag{A.4}$$

where $\delta^{\rm Q}_{\epsilon_{\rm T}} h_{\mu\nu}$ corresponds to *TDiff* transformations acting on the fluctuation field (see App. B for more details concerning this point). The action for UQG remains invariant under this transformation,

$$S_{\rm UQG}[h;\bar{g}] \mapsto S_{\rm UQG}[h + \delta^{\rm Q}_{\epsilon_{\rm T}} h;\bar{g}] = S_{\rm UQG}[h;\bar{g}] \,. \tag{A.5}$$

A.2 Faddeev-Popov quantization in UQG

As in the case of standard gauge theories, the existence of a local symmetry causes a redundancy in the definition of the path integral. To eliminate such redundancy one has to impose a gauge-fixing condition. In the present thesis we restricted ourselves to a transverse gauge condition defined according to

$$F^{\rm T}_{\mu}[h\,;\bar{g}] = \sqrt{2}\,(\mathcal{P}_{\rm T})_{\mu}{}^{\nu}\,\bar{\nabla}^{\alpha} h_{\nu\alpha} \,, \tag{A.6}$$

where $(\mathcal{P}_{\rm T})_{\mu}{}^{\nu} = \delta^{\nu}_{\mu} - \bar{\nabla}_{\mu}(\bar{\nabla}^2)^{-1}\bar{\nabla}^{\nu}$ denotes the transverse projector (in configuration space). Since $\epsilon^{\mu}_{\rm T}$ is transverse, we only have the freedom to impose $d-1$ independent gauge conditions (in a d-dimensional space-time). For this reason, we choose to work with a transverse gauge-fixing condition.

In what follows we apply the Faddeev-Popov method to perform the gauge-fixing procedure in UQG. For a discussion in the the non-unimodular case, see [8, 38, 184]. Following the usual strategy from the Faddeev-Popov method, the basic idea is to define a formal "identity" as

$$1 = \Delta_{\rm FP}[h;\bar{g}] \int \mathcal{D}\epsilon^{\mu}_{\rm T}\, \delta(F^{\rm T}[h^{\epsilon};\bar{g}]) \,, \tag{A.7}$$

Rewriting "1" for a gauge transformed configuration $h^{\epsilon'}$, we have

$$1 = \Delta_{\rm FP}[h^{\epsilon'};\bar{g}] \int \mathcal{D}\epsilon^{\mu}_{\rm T}\, \delta(F^{\rm T}[h^{\epsilon'+\epsilon};\bar{g}]) \,. \tag{A.8}$$

Assuming the invariance of the measure $\mathcal{D}\epsilon^{\mu}_{\rm T} = \mathcal{D}(\epsilon^{\mu}_{\rm T} + \epsilon'^{\mu}_{\rm T})$ and relabeling the dummy combination $\epsilon^\mu_{\rm T} + \epsilon'^\mu_{\rm T}$ by $\epsilon^\mu_{\rm T}$, yields

$$1 = \Delta_{\rm FP}[h^{\epsilon'};\bar g] \int \mathcal{D}\epsilon^\mu_{\rm T}\, \delta(F^{\rm T}[h^\epsilon;\bar g])\,. \tag{A.9}$$

By comparing (A.8) and (A.9) we can conclude that $\Delta_{\rm FP}[h;\bar g]$ is invariant under *TDiff* transformations, namely

$$\Delta_{\rm FP}[h;\bar g] = \Delta_{\rm FP}[h^\epsilon;\bar g]. \tag{A.10}$$

Inserting the identity into the functional integral $Z_{\rm UQG}[\bar g]$, we can write

$$\begin{aligned} Z_{\rm UQG}[\bar g] &= \int \frac{\mathcal{D}h_{\mu\nu}}{V_{TDiff}} \times \left(\Delta_{\rm FP}[h;\bar g] \int \mathcal{D}\epsilon^\mu_{\rm T}\, \delta(F^{\rm T}[h^\epsilon;\bar g])\right) \times e^{-S_{\rm UQG}[h;\bar g]} \\ &= \int \frac{\mathcal{D}\epsilon^\mu_{\rm T}}{V_{TDiff}} \left(\int \mathcal{D}h_{\mu\nu}\, \Delta_{\rm FP}[h;\bar g]\, \delta(F^{\rm T}[h^\epsilon;\bar g])\, e^{-S_{\rm UQG}[h;\bar g]}\right) \\ &= \int \frac{\mathcal{D}\epsilon^\mu_{\rm T}}{V_{TDiff}} \left(\int \mathcal{D}h^\epsilon_{\mu\nu}\, \Delta_{\rm FP}[h^\epsilon;\bar g]\, \delta(F^{\rm T}[h^\epsilon;\bar g])\, e^{-S_{\rm UQG}[h^\epsilon;\bar g]}\right) \\ &= \int \frac{\mathcal{D}\epsilon^\mu_{\rm T}}{V_{TDiff}} \times \int \mathcal{D}h_{\mu\nu}\, \Delta_{\rm FP}[h;\bar g]\, \delta(F^{\rm T}[h;\bar g])\, e^{-S_{\rm UQG}[h;\bar g]}\,, \end{aligned} \tag{A.11}$$

where we have used the following properties: $S_{\rm UQG}[h^\epsilon;\bar g] = S_{\rm UQG}[h;\bar g]$, $\mathcal{D}h^\epsilon_{\mu\nu} = \mathcal{D}h_{\mu\nu}$ and $\Delta_{\rm FP}[h;\bar g] = \Delta_{\rm FP}[h^\epsilon;\bar g]$. Note that the invariance of the functional measure, which was defined on top of the exponential parameterization, is a non-trivial assumption and deserves further investigation. However, this is beyond the scope of this thesis.

From the discussion of Sect. 2.1.2 we have seen that the appropriated definition of the volume factor V_{TDiff} takes the form [115, 122]

$$V_{TDiff} = \int \mathcal{D}\epsilon^\mu_{\rm T}\, {\rm Det}^{-1/2}(\Delta)\,, \tag{A.12}$$

where $\Delta = -\bar\nabla^2$. With this definition we can properly cancel out the volume factor in (A.11), leading to the following result

$$Z_{\rm UQG}[\bar g] = \int \mathcal{D}h_{\mu\nu}\, {\rm Det}^{1/2}(\Delta)\ \Delta_{\rm FP}[h;\bar g]\ \delta(F^{\rm T}[h;\bar g])\, e^{-S_{\rm UQG}[h;\bar g]}. \tag{A.13}$$

The remaining part of the calculation can be done by following the standard steps of the Faddeev-Popov procedure. In such a case, we can express $\Delta_{\rm FP}[h;\bar g]$ as a functional integral over anti-commuting vector fields (Faddeev-Popov ghosts), namely

$$\Delta_{\rm FP}[h;\bar g] = \int \mathcal{D}c^\mu\, \mathcal{D}\bar c_\mu \exp\left(-\int_x \omega\, \bar c_\mu\, \mathcal{M}^\mu{}_\nu[h;\bar g]\, c^\nu\right)\,, \tag{A.14}$$

where the Faddeev-Popov operator $\mathcal{M}^\mu{}_\nu[h;\bar g]$ is defined according to the following relation

$$\mathcal{M}^{\mu}{}_{\nu}[h;\bar{g}]\,c^{\nu} = \frac{\delta F^{\mu}[h]}{\delta h_{\alpha\beta}}\,\delta_c^Q h_{\alpha\beta}\,. \tag{A.15}$$

It is interesting to emphasize that the Faddeev-Popov ghost inherits the transverse nature of the generator $\epsilon^{\mu}_{\mathrm{T}}$, that is $\bar{\nabla}_{\mu}c^{\mu} = 0$. Moreover, the functional delta associated with the gauge responsible to impose the gauge condition admits a representation of the form

$$\delta(F^{\mathrm{T}}[h;\bar{g}]) = \lim_{\alpha\to 0} \exp\left(-\frac{1}{2\alpha}\int_x \omega\,\bar{g}^{\mu\nu}F^{\mathrm{T}}_{\mu}[h;\bar{g}]F^{\mathrm{T}}_{\nu}[h;\bar{g}]\right)\,. \tag{A.16}$$

Returning to the functional integral $Z_{\mathrm{UQG}}[\bar{g}]$, we find

$$Z_{\mathrm{UQG}}[\bar{g}] = \int \mathcal{D}h_{\mu\nu}\mathcal{D}c^{\mu}\mathcal{D}\bar{c}_{\mu}\ \mathrm{Det}^{1/2}(\Delta)\,\mathrm{e}^{-S_{\mathrm{UQG}}[h;\bar{g}]-S_{\mathrm{g.f.}}[h,c,\bar{c};\bar{g}]}\,, \tag{A.17}$$

with gauge-fixing action defined as

$$S_{\mathrm{g.f.}}[h,c,\bar{c};\bar{g}] = \frac{1}{2\alpha}\int_x \omega\,\bar{g}^{\mu\nu}F^{\mathrm{T}}_{\mu}[h;\bar{g}]F^{\mathrm{T}}_{\nu}[h;\bar{g}] + \int_x \omega\,\bar{c}_{\mu}\,\mathcal{M}^{\mu}{}_{\nu}[h;\bar{g}]\,c^{\nu}\,. \tag{A.18}$$

The limit $\alpha \to 0$ is understood to be implicit. Very often this limit is relaxed, meaning that the gauge-condition is implemented with the form $F^{\mathrm{T}}_{\mu}[h;\bar{g}] = \alpha\,b_{\mu}$ (where b_{μ} is the Lautrup-Nakanishi[1]) instead of $F^{\mathrm{T}}_{\mu}[h;\bar{g}] = 0$. In such a case, $Z_{\mathrm{UQG}}[\bar{g}]$ also entails a functional integral over the b_{μ}-field, namely

$$Z_{\mathrm{UQG}}[\bar{g}] = \int \mathcal{D}h_{\mu\nu}\mathcal{D}c^{\mu}\mathcal{D}\bar{c}_{\mu}\mathcal{D}b_{\mu}\ \mathrm{Det}^{1/2}(\Delta)\,\mathrm{e}^{-S_{\mathrm{UQG}}[h;\bar{g}]-S_{\mathrm{g.f.}}[h,c,\bar{c},b;\bar{g}]}\,, \tag{A.19}$$

with gauge-fixing action

$$S_{\mathrm{g.f.}}[h,c,\bar{c},b\,;\bar{g}] = \int_x \omega\,\bar{g}^{\mu\nu}\left(b_{\mu}F^{\mathrm{T}}_{\nu}[h\,;\bar{g}] - \frac{\alpha}{2}b_{\mu}b_{\nu}\right) + \int_x \omega\,\bar{c}_{\mu}\,\mathcal{M}^{\mu}{}_{\nu}[h\,;\bar{g}]\,c^{\nu}\,. \tag{A.20}$$

A.3 Faddeev-Popov method in the standard setting

For completeness, let us briefly add some comments concerning the Faddeev-Popov method in the standard (non-unimodular) setting, i.e., based on the quantization of full *Diff*-invariant theories. In general terms, the gauge-fixing procedure follows the same ideas that we have discussed in the unimodular setting, however, with some modification that we are going to point out here. Without diving into the details of

[1]Since $F^{\mathrm{T}}_{\mu}[h;\bar{g}]$ is transverse, we can easily conclude that the b_{μ}-field also satisfies the transversality condition $\bar{\nabla}_{\mu}b^{\mu} = 0$.

the derivation of the Faddeev-Popov procedure[2], the gauge-fixed path integral for QG can be formally expressed in the form[3]

$$
Z_{\mathrm{QG}}[\bar{g}] = \int \mathcal{D}h_{\mu\nu}\mathcal{D}c^{\mu}\mathcal{D}\bar{c}_{\mu}\ \mathrm{e}^{-S_{\mathrm{QGR}}[h;\bar{g}]-S_{\mathrm{g.f.}}[h,c,\bar{c}\,;\bar{g}]}\,, \tag{A.21}
$$

with gauge-fixing action defined according to

$$
S_{\mathrm{g.f.}}[h,c,\bar{c}\,;\bar{g}] = \frac{1}{2\alpha}\int_x \sqrt{\bar{g}}\,\bar{g}^{\mu\nu}F_{\mu}[h;\bar{g}]F_{\nu}[h;\bar{g}] + \int_x \sqrt{\bar{g}}\,\bar{c}_{\mu}\,\mathcal{M}^{\mu}{}_{\nu}[h;\bar{g}]\,c^{\nu}\,, \tag{A.22}
$$

where c^{μ} and $\bar{c}_{\mu}$ denote the Faddeev-Popov ghosts. It is important to emphasize that, in the present case, the ghost fields are not constrained by a transversality condition. The typical choice for the gauge fixing condition is given by

$$
F_{\mu}[h;\bar{g}] = \bar{\nabla}^{\nu}h_{\mu\nu} - \frac{1+\beta}{d}\,\bar{\nabla}_{\mu}h^{\mathrm{tr}}\,, \tag{A.23}
$$

where β is a gauge parameter. Within this gauge choice, the Faddeev-Popov operator can be expressed in the form

$$
\mathcal{M}_{\mu\nu}[h;\bar{g}] = \bar{\nabla}^{\alpha}\big(g_{\mu\nu}\nabla_{\alpha} + g_{\alpha\nu}\nabla_{\mu}\big) - 2\,\frac{\beta+1}{d}\bar{g}^{\alpha\beta}\left(\bar{\nabla}_{\mu}g_{\nu\beta}\nabla_{\alpha}\right). \tag{A.24}
$$

Alternatively, we can also express the gauge-fixing sector in terms of the Lautrup-Nakanishi field, namely

$$
S_{\mathrm{g.f.}}[h,c,\bar{c},b\,;\bar{g}] = \int_x \sqrt{\bar{g}}\,\bar{g}^{\mu\nu}\left(b_{\mu}F_{\nu}[h\,;\bar{g}] - \frac{\alpha}{2}b_{\mu}b_{\nu}\right) + \int_x \sqrt{\bar{g}}\,\bar{c}_{\mu}\,\mathcal{M}^{\mu}{}_{\nu}[h\,;\bar{g}]\,c^{\nu}\,. \tag{A.25}
$$

In this case, $Z_{\mathrm{QG}}[\bar{g}]$ also entails a functional integral over the b_{μ}-field.

[2]For a detailed discussion in the standard framework see [8, 38, 184].

[3]Note that, in this case, the path integral does not involve the extra determinant originating from the volume factor associated with the gauge group. This is a consequence of the direct identification of $\int \mathcal{D}\epsilon^{\mu}$ as the volume of the the *Diff* group.

Appendix B

Aspects of Exponential parameterization

B.1 Local field transformations and the exponential parameterization

B.1.1 General considerations

One elementary task once applying the background field method to QG calculations is to determine the appropriate conversion of gauge transformations acting in the full metric $g_{\mu\nu}$ in terms of transformations acting on the background and fluctuation fields, respectively represented as $\bar{g}_{\mu\nu}$ and $h_{\mu\nu}$. This task is reasonably simple in the case of linear split $g_{\mu\nu} = \bar{g}_{\mu\nu} + \kappa h_{\mu\nu}$, however, the situation becomes more complicated for non-linear splits such as the exponential parameterization used in our calculations for UQG. In this section, we address some details concerning this point. For practical calculations we expand the exponential parameterization in terms of powers of the fluctuation field[1],

$$g_{\mu\nu} = \bar{g}_{\mu\alpha}\left[\exp(\kappa\, h^{\cdot}_{\ \cdot})\right]^{\alpha}_{\ \ \nu} = \bar{g}_{\mu\nu} + \kappa\, h_{\mu\nu} + \sum_{n=2}^{\infty} \frac{\kappa^n}{n!} h_{\mu\alpha_1} \cdots h^{\alpha_{n-1}}_{\ \ \nu}\,. \tag{B.1}$$

It is convenient to express in a more compact notation,

$$g_{\mu\nu} = \sum_{n=0}^{\infty} X^{(n)}_{\mu\nu}\,, \tag{B.2}$$

where

$$X^{(0)}_{\mu\nu} = \bar{g}_{\mu\nu}\,, \qquad X^{(1)}_{\mu\nu} = h_{\mu\nu} \qquad \text{and} \qquad X^{(n)}_{\mu\nu} = \frac{\kappa^n}{n!} h_{\mu\alpha_1} h^{\alpha_1}_{\ \ \alpha_2} \cdots h^{\alpha_{n-1}}_{\ \ \nu}\,. \tag{B.3}$$

As it was mentioned before, our central goal is to determine the gauge transforma-

[1] The discussion presented here was inspired in [212].

tion $\delta_\epsilon h_{\mu\nu}$ as a function of $\delta_\epsilon g_{\mu\nu}$. In order to compute an expression for $\delta_\epsilon h_{\mu\nu}$, we start from the *ansatz*

$$\delta_\epsilon h_{\mu\nu} = \sum_{n=0}^{\infty} Y^{(n)}_{\mu\nu} \,, \tag{B.4}$$

with $Y^{(n)}_{\mu\nu} = [\mathcal{O}(h^n)]_{\mu\nu}$. The basic idea is to compute $Y^{(n)}_{\mu\nu}$ by a recursive method. Let us start by expressing $\delta_\epsilon g_{\mu\nu}$ in terms of $Y^{(n)}_{\mu\nu}$. Using the chain rule for functional variations, we find

$$\begin{aligned} \delta_\epsilon g_{\mu\nu}(x) &= \delta_\epsilon \bar{g}_{\mu\nu} + \sum_{n=1}^{\infty} \int_y \omega \, \frac{\delta X^{(n)}_{\mu\nu}(x)}{\delta h_{\alpha\beta}(y)} \delta_\epsilon h_{\alpha\beta}(y) \\ &= \delta_\epsilon \bar{g}_{\mu\nu} + \sum_{n=0}^{\infty}\sum_{m=0}^{\infty} \int_y \omega \, \frac{\delta X^{(n+1)}_{\mu\nu}(x)}{\delta h_{\alpha\beta}(y)} Y^{(m)}_{\alpha\beta}(y) \,. \end{aligned} \tag{B.5}$$

Taking into account the property $\sum_{n,m=0}^{\infty} c_{n,m} = \sum_{n=0}^{\infty}\sum_{m=0}^{n} c_{n-m,m}$, we can cast

$$\delta_\epsilon g_{\mu\nu} = \delta_\epsilon \bar{g}_{\mu\nu} + \sum_{n=0}^{\infty}\sum_{m=0}^{n} \frac{\delta X^{(n-m+1)}_{\mu\nu}}{\delta h_{\alpha\beta}} \cdot Y^{(m)}_{\alpha\beta} \,, \tag{B.6}$$

where we have used the compact notation

$$\frac{\delta X^{(n+1)}_{\mu\nu}(x)}{\delta h_{\alpha\beta}} \cdot Y^{(m)}_{\mu\nu} = \int_y \omega \, \frac{\delta X^{(n+1)}_{\mu\nu}(x)}{\delta h_{\alpha\beta}(y)} Y^{(m)}_{\alpha\beta}(y) \,. \tag{B.7}$$

Moreover, it is important to observe that

$$\sum_{m=0}^{n} \frac{\delta X^{(n-m+1)}_{\mu\nu}}{\delta h_{\alpha\beta}} \cdot Y^{(m)}_{\alpha\beta} = [\mathcal{O}(h^n)]_{\mu\nu} \,. \tag{B.8}$$

Finally, it is useful to write

$$\delta_\epsilon g_{\mu\nu} = \sum_{n=0}^{\infty} \left(\delta_{n,0}\, \delta_\epsilon \bar{g}_{\mu\nu} + \sum_{m=0}^{n} \frac{\delta X^{(n-m+1)}_{\mu\nu}}{\delta h_{\alpha\beta}} \cdot Y^{(m)}_{\alpha\beta} \right) . \tag{B.9}$$

B.1.2 *TDiff* transformations

Let us focus on the particular case of *TDiff* transformations, which are of primary interest in the framework of UG. In this case, the gauge transformation acting on the full metric takes the form

$$\delta_{\epsilon_{\mathrm{T}}} g_{\mu\nu} = g_{\mu\alpha} \nabla_\nu \epsilon^\alpha_{\mathrm{T}} + g_{\nu\alpha} \nabla_\mu \epsilon^\alpha_{\mathrm{T}} \,, \tag{B.10}$$

which can be rewritten as the Lie derivative along the vector field $\epsilon_{\mathrm{T}}^{\mu}$,

$$\delta_{\epsilon_{\mathrm{T}}} g_{\mu\nu} = \mathcal{L}_{\epsilon_{\mathrm{T}}} g_{\mu\nu} \,. \tag{B.11}$$

Since the action of $\mathcal{L}_{\epsilon}$ is linear, we have

$$\delta_{\epsilon_{\mathrm{T}}} g_{\mu\nu} = \sum_{n=0}^{\infty} \mathcal{L}_{\epsilon_{\mathrm{T}}} X_{\mu\nu}^{(n)} \,. \tag{B.12}$$

Comparing (B.9) and (B.12) order by order in the fluctuation field, we arrive at the following result

$$\delta_{n,0}\, \delta_{\epsilon_{\mathrm{T}}} \bar{g}_{\mu\nu} + \sum_{m=0}^{n} \frac{\delta X_{\mu\nu}^{(n-m+1)}}{\delta h_{\alpha\beta}} \cdot Y_{\mu\nu}^{(m)} = \mathcal{L}_{\epsilon_{\mathrm{T}}} X_{\mu\nu}^{(n)} \,. \tag{B.13}$$

Splitting the sum on the l.h.s., we can write

$$\frac{\delta X_{\mu\nu}^{(1)}}{\delta h_{\alpha\beta}} \cdot Y_{\alpha\beta}^{(n)} = \mathcal{L}_{\epsilon_{\mathrm{T}}} X_{\mu\nu}^{(n)} - \sum_{m=0}^{n-1} \frac{\delta X_{\mu\nu}^{(n-m+1)}}{\delta h_{\alpha\beta}} \cdot Y_{\alpha\beta}^{(m)} - \delta_{n,0}\, \delta_{\epsilon_{\mathrm{T}}} \bar{g}_{\mu\nu} \,. \tag{B.14}$$

Since, as we have seen, $\frac{\delta X_{\mu\nu}^{(1)}(x)}{\delta h_{\alpha\beta}(y)}$ is non-singular (and ultra-local), we can solve the last equation for $Y_{\alpha\beta}^{(n)}$, resulting in

$$Y_{\mu\nu}^{(n)}(x) = \frac{\delta h_{\mu\nu}(x)}{\delta X_{\alpha\beta}^{(1)}} \cdot \left(\mathcal{L}_{\epsilon_{\mathrm{T}}} X_{\alpha\beta}^{(n)} - \sum_{m=0}^{n-1} \frac{\delta X_{\alpha\beta}^{(n-m+1)}}{\delta h_{\lambda\rho}} \cdot Y_{\lambda\rho}^{(m)} - \delta_{n,0}\, \delta_{\epsilon_{\mathrm{T}}} \bar{g}_{\alpha\beta} \right) . \tag{B.15}$$

The "quantum" *TDiff* transformation, used in the Faddeev-Popov procedure, is a particular type of decomposition where the background metric remains unchanged

$$\delta_{\epsilon_{\mathrm{T}}}^{\mathrm{Q}} \bar{g}_{\mu\nu} = 0 \,. \tag{B.16}$$

In such a case, the transformation of the fluctuation field can be written as

$$\delta_{\epsilon_{\mathrm{T}}}^{\mathrm{Q}} h_{\mu\nu} = \sum_{n=0}^{\infty} Y_{\mathrm{Q},\,\mu\nu}^{(n)}, \tag{B.17}$$

with recursive relations

$$Y_{\mathrm{Q},\,\mu\nu}^{(n)}(x) = \frac{\delta h_{\mu\nu}(x)}{\delta X_{\alpha\beta}^{(1)}} \cdot \left(\mathcal{L}_{\epsilon_{\mathrm{T}}} X_{\alpha\beta}^{(n)} - \sum_{m=0}^{n-1} \frac{\delta X_{\alpha\beta}^{(n-m+1)}}{\delta h_{\lambda\rho}} \cdot Y_{\mathrm{Q},\,\lambda\rho}^{(m)} \right) . \tag{B.18}$$

"Background" *TDiff* transformations, on the other hand, is defined by a split of the transformation where the background metric transforms as tensor field, namely

$$\delta^{\mathrm{B}}_{\epsilon_{\mathrm{T}}} \bar{g}_{\mu\nu} = \mathcal{L}_{\epsilon_{\mathrm{T}}} \bar{g}_{\mu\nu} \,. \tag{B.19}$$

Combining this definition with (B.15), the background transformation $\delta^{\mathrm{B}}_{\epsilon_{\mathrm{T}}}$ acting on the fluctuation field results in

$$\delta^{\mathrm{B}}_{\epsilon_{\mathrm{T}}} h_{\mu\nu} = \mathcal{L}_{\epsilon_{\mathrm{T}}} h_{\mu\nu} \,, \tag{B.20}$$

which can be verified through an inductive process.

B.1.3 Split symmetry

As we have discussed in Chap. 3, split symmetry is characterized by a joint transformation $\bar{g}_{\mu\nu} \mapsto \bar{g}_{\mu\nu} + \delta_{\mathrm{split}} \bar{g}_{\mu\nu}$ and $h_{\mu\nu} \mapsto h_{\mu\nu} + \delta_{\mathrm{split}} h_{\mu\nu}$ that keeps the full metric invariant, i.e., $\delta_{\mathrm{split}} g_{\mu\nu} = 0$. Let us define the action of δ_{split} on the background metric according to

$$\delta_{\mathrm{split}} \bar{g}_{\mu\nu} = -\chi_{\mu\nu} \,, \tag{B.21}$$

where $\chi_{\mu\nu} = \chi_{\mu\nu}(x)$ is a local transformation parameter. This definition is inspired in the linear parameterization, where $\delta^{\mathrm{lin.}}_{\mathrm{split}} \bar{g}_{\mu\nu} = -\chi_{\mu\nu}$ and $\delta^{\mathrm{lin.}}_{\mathrm{split}} h_{\mu\nu} = \kappa^{-1} \chi_{\mu\nu}$. For the exponential parameterization, Eq. (B.9) leads to the following result

$$-\delta_{n,0}\, \chi_{\mu\nu} + \sum_{m=0}^{n} \frac{\delta X^{(n-m+1)}_{\mu\nu}}{\delta h_{\alpha\beta}} \cdot Y^{(m)}_{\alpha\beta} = 0 \,. \tag{B.22}$$

Once again we can solve for $Y^{(n)}_{\mu\nu}$, which results in the following recursive formula

$$Y^{(n)}_{\mu\nu}(x) = \frac{\delta h_{\mu\nu}(x)}{\delta X^{(1)}_{\alpha\beta}} \cdot \left(\delta_{n,0}\, \chi_{\alpha\beta} - \sum_{m=0}^{n-1} \frac{\delta X^{(n-m+1)}_{\alpha\beta}}{\delta h_{\lambda\rho}} \cdot Y^{(m)}_{\lambda\rho} \right) . \tag{B.23}$$

B.2 Fermions and the exponential parameterization

The coupling of fermions to gravity, used in Chap. 4, in a setting without torsion, occurs through the vielbein and the spin-connection. Since our formulation is based on functional quantization of the fluctuation field $h_{\mu\nu}$, we have to express both the vielbein and spin-connection in terms of $h_{\mu\nu}$ in accordance with the exponential parameterization.

We start with the vielbein, denoted as e^{a}_{μ}. For our purposes it is sufficient to expand

e_μ^a up to second order around a flat background, namely

$$e_\mu^a = \delta_\mu^a + \delta e_\mu^a + \frac{1}{2}\delta^2 e_\mu^a + \mathcal{O}(\delta^3 e), \tag{B.24}$$

where δ_μ^a is the (trivial) flat space vielbein. In order to gauge fix the local $O(d)$ symmetry which follows from the definition of the vielbein, we adopt the Lorentz symmetric gauge-fixing given by [276, 277]

$$e_{\mu a}\delta_b^\mu - e_{\mu b}\delta_a^\mu = 0\,. \tag{B.25}$$

This condition allows us to obtain the expressions

$$\delta e_\mu^a = \frac{1}{2}\delta^{\nu a}\delta g_{\mu\nu}, \tag{B.26a}$$

$$\delta^2 e_\mu^a = \frac{1}{2}\delta^{\nu a}\delta^2 g_{\mu\nu} - \frac{1}{4}\delta^{\nu a}\delta^{\alpha\beta}\delta g_{\mu\alpha}\delta g_{\nu\beta}. \tag{B.26b}$$

For the exponential parameterization, we have $\delta g_{\mu\nu} = h_{\mu\nu}$ and $\delta^2 g_{\mu\nu} = h_{\mu\alpha}h_\nu{}^\alpha$, resulting in the following expansion for the vielbein

$$e_\mu^a = \delta_\mu^a + \frac{1}{2}\delta^{\nu a}h_{\mu\nu} + \frac{1}{8}\delta^{\nu a}h_{\mu\alpha}h_\nu{}^\alpha + \mathcal{O}(h^3). \tag{B.27}$$

Now, let us turn our attention to the spin-connection, denoted as ω_μ. In our setting, the spin-connection is not taken as an independent variable. Assuming metric compatibility ($\nabla_\mu e_\nu^a = 0$) along with the absence of torsion, one can express ω_μ according to the expression

$$\omega_\mu = [\gamma^a, \gamma^b]\left(\delta_{ac}e_\nu^c\partial_\mu e_b^\nu + \delta_{ac}\Gamma^\lambda_{\mu\alpha}e_\lambda^c e_b^\alpha\right), \tag{B.28}$$

Expanding e_μ^a and $\Gamma^\alpha_{\mu\nu}$ up to the second order in the fluctuation field $h_{\mu\nu}$, leads to

$$\begin{aligned}\omega_\mu = [\gamma^\alpha, \gamma^\beta]\partial_\beta h_{\mu\alpha} + \frac{1}{2}[\gamma^\alpha, \gamma^\beta]\bigg(&-\frac{1}{2}h_\alpha{}^\lambda\partial_\mu h_{\beta\lambda} + \\ &- h_\beta{}^\lambda\partial_\lambda h_{\mu\alpha} - h_\alpha{}^\lambda\partial_\beta h_{\mu\lambda} + \partial_\beta h_{\mu\rho}\, h_\alpha{}^\rho + h_{\mu\rho}\partial_\beta h_\alpha{}^\rho\bigg) + \mathcal{O}(h^3).\end{aligned} \tag{B.29}$$

An alternative to the use of vielbein in the description of fermion-systems is the spin-base formalism [278–280]. At the level of our computations both formalisms render the same results.

Appendix C

Some explicit expressions

C.1 Results from Chap. 3

In this appendix we present some explicit expressions corresponding to the calculations described in Chap. 3.

Graviton anomalous dimensions:

$$\begin{aligned}\eta_{\rm TT} = &- \frac{5\,G_k\,(468 - 120\,\tilde{m}^2_{k,\rm TT} - 696\,\tilde{m}^4_{k,\rm TT} + (-43 + 73\,\tilde{m}^2_{k,\rm TT} + 116\,\tilde{m}^4_{k,\rm TT})\,\eta_{\rm TT})}{2592\pi(1+\tilde{m}^2_{k,\rm TT})^4} \\ &+ \frac{G_k\,(-441 - 816\,\tilde{m}^2_{k,\sigma} - 348\,\tilde{m}^4_{k,\sigma} + (73 + 131\,\tilde{m}^2_{k,\sigma} + 58\,\tilde{m}^4_{k,\sigma})\,\eta_\sigma)}{648\pi(1+\tilde{m}^2_{k,\sigma})^4} \\ &- \frac{25\,G_k\,(-16 - 8\,\tilde{m}^2_{k,\rm TT} - 8\,\tilde{m}^2_{k,\sigma} + (1+\,\tilde{m}^2_{k,\sigma})\,\eta_{\rm TT} + (1+\,\tilde{m}^2_{k,\rm TT})\,\eta_\sigma)}{576\pi\,(1+\tilde{m}^2_{k,\rm TT})^2(1+\tilde{m}^2_{k,\sigma})^2} \\ &+ \frac{G_k\,(12 - 7\eta_c)}{96\pi}\,, \end{aligned} \tag{C.1}$$

$$\begin{aligned}\eta_\sigma = &- \frac{5\,G_k\,(-252 - 816\,\tilde{m}^2_{k,\rm TT} - 132\,\tilde{m}^4_{k,\rm TT} + (91 + 113\,\tilde{m}^2_{k,\rm TT} + 22\,\tilde{m}^4_{k,\rm TT})\,\eta_{\rm TT})}{1296\pi\,(1+\tilde{m}^2_{k,\rm TT})^4} \\ &+ \frac{G_k\,(144 + 312\,\tilde{m}^2_{k,\sigma} - 264\,\tilde{m}^4_{k,\sigma} + (-61 - 17\,\tilde{m}^2_{k,\sigma} + 44\,\tilde{m}^4_{k,\sigma})\,\eta_\sigma)}{1296\pi\,(1+\tilde{m}^2_{k,\sigma})^4} \\ &+ \frac{5\,G_k\,(-16 - 8\,\tilde{m}^2_{k,\rm TT} - 8\,\tilde{m}^2_{k,\sigma} + (1+\tilde{m}^2_{k,\sigma})\,\eta_{\rm TT} + (1+\tilde{m}^2_{k,\rm TT})\,\eta_\sigma)}{144\pi\,(1+\tilde{m}^2_{k,\rm TT})^2(1+\tilde{m}^2_{k,\sigma})^2} \\ &- \frac{7\,G_k\,(4-\eta_c)}{24\pi}\,, \end{aligned} \tag{C.2}$$

Ghost anomalous dimensions:

$$\eta_c = \frac{5\,G_k\,(-24\,\tilde{m}^2_{k,\mathrm{TT}} - 5\,\eta_{\mathrm{TT}} + 3\,(1+\tilde{m}^2_{k,\mathrm{TT}})\,\eta_c)}{648\pi\,(1+\tilde{m}^2_{k,\mathrm{TT}})^2} - \frac{G_k\,(-36 - 24\,\tilde{m}^2_{k,\sigma} + \eta_\sigma + 3\,(1+\tilde{m}^2_{k,\sigma})\,\eta_c)}{81\pi\,(1+\tilde{m}^2_{k,\sigma})^2}\,, \tag{C.3}$$

Flow of symmetry-breaking masses:

$$\partial_t \tilde{m}^2_{k,\mathrm{TT}} = -\,(2-\eta_{\mathrm{TT}})\,\tilde{m}^2_{k,\mathrm{TT}} + \frac{G_k\,(-620 - 1160\,\tilde{m}^2_{k,\mathrm{TT}} + (91 + 145\,\tilde{m}^2_{k,\mathrm{TT}})\,\eta_{\mathrm{TT}})}{1296\pi\,(1+\tilde{m}^2_{k,\mathrm{TT}})^3} + \frac{G_k\,(100 - 440\,\tilde{m}^2_{k,\sigma} + (1+55\,\tilde{m}^2_{k,\sigma})\,\eta_\sigma)}{6480\pi\,(1+\tilde{m}^2_{k,\sigma})^3} - \frac{G_k\,(110 - 7\eta_c)}{540\pi}\,, \tag{C.4}$$

$$\partial_t \tilde{m}^2_{k,\sigma} = -\,(2-\eta_\sigma)\,\tilde{m}^2_{k,\sigma} - \frac{G_k\,(-620 - 1160\,\tilde{m}^2_{k,\mathrm{TT}} + (91 + 145\,\tilde{m}^2_{k,\mathrm{TT}})\,\eta_{\mathrm{TT}})}{648\pi\,(1+\tilde{m}^2_{k,\mathrm{TT}})^3} - \frac{G_k\,(100 - 440\,\tilde{m}^2_{k,\sigma} + (1+55\,\tilde{m}^2_{k,\sigma})\,\eta_\sigma)}{3240\pi\,(1+\tilde{m}^2_{k,\sigma})^3} + \frac{G_k\,(110 - 7\eta_c)}{270\pi}\,. \tag{C.5}$$

C.2 Projectors on flat background

The transverse and longitudinal projectors (on vector fields) are defined, around flat background, in the standard way

$$\mathcal{P}^{\mu\nu}_{\mathrm{T}}(p) = \delta^{\mu\nu} - \frac{p^\mu p^\nu}{p^2} \qquad \text{and} \qquad \mathcal{P}^{\mu\nu}_{\mathrm{L}}(p) = \frac{p^\mu p^\nu}{p^2}\,. \tag{C.6}$$

For rank-2 symmetric tensors, we define the projection operators

$$\mathcal{P}^{\mu\nu\alpha\beta}_{\mathrm{TT}}(p) = \frac{1}{2}\Big(\mathcal{P}^{\mu\alpha}_{\mathrm{T}}(p)\mathcal{P}^{\nu\beta}_{\mathrm{T}}(p) + \mathcal{P}^{\mu\beta}_{\mathrm{T}}(p)\mathcal{P}^{\nu\alpha}_{\mathrm{T}}(p)\Big) - \frac{1}{3}\mathcal{P}^{\mu\nu}_{\mathrm{T}}(p)\mathcal{P}^{\alpha\beta}_{\mathrm{T}}(p)\,, \tag{C.7a}$$

$$\mathcal{P}^{\mu\nu\alpha\beta}_{\xi}(p) = \frac{1}{2}\Big(\mathcal{P}^{\mu\alpha}_{\mathrm{T}}(p)\mathcal{P}^{\nu\beta}_{\mathrm{L}}(p) + \mathcal{P}^{\mu\beta}_{\mathrm{T}}(p)\mathcal{P}^{\nu\alpha}_{\mathrm{L}}(p) + \mathcal{P}^{\nu\beta}_{\mathrm{T}}(p)\mathcal{P}^{\mu\alpha}_{\mathrm{L}}(p) + \mathcal{P}^{\nu\alpha}_{\mathrm{T}}(p)\mathcal{P}^{\mu\beta}_{\mathrm{L}}(p)\Big)\,, \tag{C.7b}$$

$$\mathcal{P}^{\mu\nu\alpha\beta}_{\sigma}(p) = \frac{1}{12}\mathcal{P}^{\mu\nu}_{\mathrm{T}}(p)\mathcal{P}^{\alpha\beta}_{\mathrm{T}}(p) - \frac{1}{4}\mathcal{P}^{\mu\nu}_{\mathrm{T}}(p)\mathcal{P}^{\alpha\beta}_{\mathrm{L}}(p) - \frac{1}{4}\mathcal{P}^{\mu\nu}_{\mathrm{L}}(p)\mathcal{P}^{\alpha\beta}_{\mathrm{T}}(p) + \frac{3}{4}\mathcal{P}^{\mu\nu}_{\mathrm{L}}(p)\mathcal{P}^{\alpha\beta}_{\mathrm{L}}(p)\,, \tag{C.7c}$$

$$\mathcal{P}_{\mathrm{tr}}^{\mu\nu\alpha\beta} = \frac{1}{4}\bar{g}^{\mu\nu}\bar{g}^{\alpha\beta}\,. \tag{C.7d}$$

These projectors select the different components of the usual York decomposition [265]. For the purpose of the discussion presented in Sect. 3.4, it is also useful to define the traceless projector

$$\mathcal{P}_{1-\mathrm{tr}}^{\mu\nu\alpha\beta} = \frac{1}{2}(\bar{g}^{\mu\alpha}\bar{g}^{\nu\beta} + \bar{g}^{\mu\beta}\bar{g}^{\nu\alpha}) - \frac{1}{4}\bar{g}^{\mu\nu}\bar{g}^{\alpha\beta}\,. \tag{C.8}$$

Bibliography

[1] M. Tanabashi et al. Review of particle physics. *Phys. Rev. D*, 98:030001, 2018.

[2] C.M. Will. The confrontation between general relativity and experiment. *Living Rev. Rel.*, 17:4, 2014.

[3] B.P. Abbott et al. Observation of Gravitational Waves from a Binary Black Hole Merger. *Phys. Rev. Lett.*, 116(6):061102, 2016.

[4] K. Akiyama et al. First M87 Event Horizon Telescope Results. I. The Shadow of the Supermassive Black Hole. *Astrophys. J.*, 875(1):L1, 2019.

[5] S.W. Hawking and G.F.R. Ellis. *The large scale structure of space-time*. Cambridge Monographs on Mathematical Physics. Cambridge University Press, 1975.

[6] D.J.W. Giulini, C. Kiefer, and C. Lammerzahl. *Quantum gravity: from theory to experimental search*. LNP0731. Springer, 1 edition, 2003.

[7] D. Oriti. *Approaches to quantum gravity: toward a new understanding of space, time and matter*. Osborne. Cambridge University Press, 2009.

[8] C. Kiefer. *Quantum gravity*. International Series of Monographs on Physics. Oxford University Press, USA, 2 edition, 2007.

[9] A. Ashtekar. New Variables for Classical and Quantum Gravity. *Phys. Rev. Lett.*, 57:2244–2247, 1986.

[10] A. Ashtekar and J. Lewandowski. Background independent quantum gravity: A Status report. *Class. Quant. Grav.*, 21:R53, 2004.

[11] H.W. Hamber. *Quantum Gravitation: The Feynman Path Integral Approach*. Springer, 1 edition, 2008.

[12] G. 't Hooft and M.J.G. Veltman. One loop divergencies in the theory of gravitation. *Ann. Inst. H. Poincare Phys. Theor. A*, 20:69–94, 1974.

[13] S. Deser and P. van Nieuwenhuizen. Nonrenormalizability of the Quantized Dirac-Einstein System. *Phys. Rev. D*, 10:411, 1974.

[14] S. Deser, H.-S. Tsao, and P. van Nieuwenhuizen. Nonrenormalizability of Einstein Yang-Mills Interactions at the One Loop Level. *Phys. Lett. B*, 50:491–493, 1974.

[15] S. Deser and P. van Nieuwenhuizen. Nonrenormalizability of the Quantized Einstein-Maxwell System. *Phys. Rev. Lett.*, 32:245–247, 1974.

[16] S.M. Christensen and M.J. Duff. Quantizing Gravity with a Cosmological Constant. *Nucl. Phys. B*, 170:480–506, 1980.

[17] M.H. Goroff and A. Sagnotti. Quantum Gravity at Two Loops. *Phys. Lett. B*, 160:81–86, 1985.

[18] M.H. Goroff and A. Sagnotti. The Ultraviolet Behavior of Einstein Gravity. *Nucl. Phys. B*, 266:709–736, 1986.

[19] A.E.M. van de Ven. Two loop quantum gravity. *Nucl. Phys. B*, 378:309–366, 1992.

[20] K.S. Stelle. Renormalization of Higher Derivative Quantum Gravity. *Phys. Rev. D*, 16:953–969, 1977.

[21] J.F. Donoghue and G. Menezes. Gauge Assisted Quadratic Gravity: A Framework for UV Complete Quantum Gravity. *Phys. Rev. D*, 97(12):126005, 2018.

[22] J.F. Donoghue and G. Menezes. Massive poles in Lee-Wick quantum field theory. *Phys. Rev. D*, 99(6):065017, 2019.

[23] J.F. Donoghue and G. Menezes. Arrow of Causality and Quantum Gravity. *Phys. Rev. Lett.*, 123(17):171601, 2019.

[24] J.F. Donoghue and G. Menezes. Unitarity, stability and loops of unstable ghosts. *Phys. Rev. D*, 100(10):105006, 2019.

[25] D. Anselmi. Fakeons, Microcausality And The Classical Limit Of Quantum Gravity. *Class. Quant. Grav.*, 36:065010, 2019.

[26] D. Anselmi. Fakeons And Lee-Wick Models. *JHEP*, 02:141, 2018.

[27] D. Anselmi and M. Piva. Quantum Gravity, Fakeons And Microcausality. *JHEP*, 11:021, 2018.

[28] D. Anselmi. Fakeons and the classicization of quantum gravity: the FLRW metric. *JHEP*, 04:061, 2019.

[29] J.F. Donoghue. Introduction to the effective field theory description of gravity. In *Advanced School on Effective Theories*, 6 1995.

[30] C.P. Burgess. Quantum gravity in everyday life: General relativity as an effective field theory. *Living Rev. Rel.*, 7:5–56, 2004.

[31] J.F. Donoghue. The effective field theory treatment of quantum gravity. *AIP Conf. Proc.*, 1483(1):73–94, 2012.

[32] H. Georgi. Effective field theory. *Ann. Rev. Nucl. Part. Sci.*, 43:209–252, 1993.

[33] J.F. Donoghue. Leading quantum correction to the Newtonian potential. *Phys. Rev. Lett.*, 72:2996–2999, 1994.

[34] J.F. Donoghue. General relativity as an effective field theory: The leading quantum corrections. *Phys. Rev. D*, 50:3874–3888, 1994.

[35] John F. Donoghue and Tibor Torma. Infrared behavior of graviton-graviton scattering. *Phys. Rev. D*, 60:024003, 1999.

[36] N.E.J Bjerrum-Bohr, John F. Donoghue, and Barry R. Holstein. Quantum gravitational corrections to the nonrelativistic scattering potential of two masses. *Phys. Rev. D*, 67:084033, 2003. [Erratum: Phys.Rev.D 71, 069903 (2005)].

[37] N.E.J. Bjerrum-Bohr, John F. Donoghue, Barry R. Holstein, Ludovic Planté, and Pierre Vanhove. Bending of Light in Quantum Gravity. *Phys. Rev. Lett.*, 114(6):061301, 2015.

[38] R. Percacci. *An Introduction to Covariant Quantum Gravity and Asymptotic Safety*, volume 3 of *100 Years of General Relativity*. World Scientific, 2017.

[39] M. Reuter and F. Saueressig. *Quantum Gravity and the Functional Renormalization Group: The Road towards Asymptotic Safety*. Cambridge University Press, 1 2019.

[40] G. Parisi. The Theory of Nonrenormalizable Interactions. 1. The Large N Expansion. *Nucl. Phys. B*, 100:368–388, 1975.

[41] S. Weinberg. Critical Phenomena for Field Theorists. In *14th International School of Subnuclear Physics: Understanding the Fundamental Constitutents of Matter*, page 1, 8 1976.

[42] S. Weinberg. Ultraviolet divergences in quantum theories of gravitation. *Chap. 16 in General Relativity ed. by Hawking, S.W. and Israel, W.*, 1979.

[43] H.D. Politzer. Reliable Perturbative Results for Strong Interactions? *Phys. Rev. Lett.*, 30:1346–1349, 1973.

[44] D.J. Gross and F. Wilczek. Ultraviolet Behavior of Nonabelian Gauge Theories. *Phys. Rev. Lett.*, 30:1343–1346, 1973.

[45] H.D. Politzer. Asymptotic Freedom: An Approach to Strong Interactions. *Phys. Rept.*, 14:129–180, 1974.

[46] S.M. Christensen and M.J. Duff. Quantum Gravity in Two + ϵ Dimensions. *Phys. Lett. B*, 79:213–216, 1978.

[47] R. Gastmans, R. Kallosh, and C. Truffin. Quantum Gravity Near Two-Dimensions. *Nucl. Phys. B*, 133:417–434, 1978.

[48] H. Kawai and M. Ninomiya. Renormalization Group and Quantum Gravity. *Nucl. Phys. B*, 336:115–145, 1990.

[49] I. Jack and D.R.T. Jones. The Epsilon expansion of two-dimensional quantum gravity. *Nucl. Phys. B*, 358:695–712, 1991.

[50] M. Reuter. Nonperturbative evolution equation for quantum gravity. *Phys. Rev. D*, 57:971–985, 1998.

[51] C. Wetterich. Exact evolution equation for the effective potential. *Phys. Lett. B*, 301:90–94, 1993.

[52] N. Dupuis, L. Canet, A. Eichhorn, W. Metzner, J.M. Pawlowski, M. Tissier, and N. Wschebor. The nonperturbative functional renormalization group and its applications. 6 2020.

[53] W. Souma. Nontrivial ultraviolet fixed point in quantum gravity. *Prog. Theor. Phys.*, 102:181–195, 1999.

[54] M. Reuter and F. Saueressig. Renormalization group flow of quantum gravity in the Einstein-Hilbert truncation. *Phys. Rev.*, D65:065016, 2002.

[55] O. Lauscher and M. Reuter. Flow equation of quantum Einstein gravity in a higher derivative truncation. *Phys. Rev. D*, 66:025026, 2002.

[56] D.F. Litim. Fixed points of quantum gravity. *Phys. Rev. Lett.*, 92:201301, 2004.

[57] A. Codello and R. Percacci. Fixed points of higher derivative gravity. *Phys. Rev. Lett.*, 97:221301, 2006.

[58] Alessandro Codello, Roberto Percacci, and Christoph Rahmede. Ultraviolet properties of f(R)-gravity. *Int. J. Mod. Phys. A*, 23:143–150, 2008.

[59] P.F. Machado and F. Saueressig. On the renormalization group flow of $f(R)$-gravity. *Phys. Rev. D*, 77:124045, 2008.

[60] A. Codello, R. Percacci, and C. Rahmede. Investigating the Ultraviolet Properties of Gravity with a Wilsonian Renormalization Group Equation. *Annals Phys.*, 324:414–469, 2009.

[61] A. Eichhorn, H. Gies, and M.M. Scherer. Asymptotically free scalar curvature-ghost coupling in Quantum Einstein Gravity. *Phys. Rev. D*, 80:104003, 2009.

[62] D. Benedetti, P.F. Machado, and F. Saueressig. Asymptotic safety in higher-derivative gravity. *Mod. Phys. Lett.*, A24:2233–2241, 2009.

[63] D. Benedetti, P.F. Machado, and F. Saueressig. Taming perturbative divergences in asymptotically safe gravity. *Nucl. Phys.*, B824:168–191, 2010.

[64] A. Eichhorn and H. Gies. Ghost anomalous dimension in asymptotically safe quantum gravity. *Phys. Rev. D*, 81:104010, 2010.

[65] E. Manrique, M. Reuter, and F. Saueressig. Bimetric Renormalization Group Flows in Quantum Einstein Gravity. *Annals Phys.*, 326:463–485, 2011.

[66] E. Manrique, S. Rechenberger, and F. Saueressig. Asymptotically Safe Lorentzian Gravity. *Phys. Rev. Lett.*, 106:251302, 2011.

[67] N. Christiansen, D.F. Litim, J.M. Pawlowski, and A. Rodigast. Fixed points and infrared completion of quantum gravity. *Phys. Lett.*, B728:114–117, 2014.

[68] D. Benedetti and F. Caravelli. The Local potential approximation in quantum gravity. *JHEP*, 06:017, 2012. [Erratum: JHEP 10, 157 (2012)].

[69] J.A. Dietz and T.R. Morris. Asymptotic safety in the f(R) approximation. *JHEP*, 01:108, 2013.

[70] K. Falls, D.F. Litim, K. Nikolakopoulos, and C. Rahmede. A bootstrap towards asymptotic safety. 2013.

[71] D. Benedetti. On the number of relevant operators in asymptotically safe gravity. *EPL*, 102(2):20007, 2013.

[72] N. Ohta and R. Percacci. Higher Derivative Gravity and Asymptotic Safety in Diverse Dimensions. *Class. Quant. Grav.*, 31:015024, 2014.

[73] K. Falls, D.F. Litim, K. Nikolakopoulos, and C. Rahmede. Further evidence for asymptotic safety of quantum gravity. *Phys. Rev.*, D93(10):104022, 2016.

[74] A. Codello, G. D'Odorico, and C. Pagani. Consistent closure of renormalization group flow equations in quantum gravity. *Phys. Rev. D*, 89(8):081701, 2014.

[75] N. Christiansen, B. Knorr, J.M. Pawlowski, and A. Rodigast. Global Flows in Quantum Gravity. *Phys. Rev.*, D93(4):044036, 2016.

[76] K. Falls. Asymptotic safety and the cosmological constant. *JHEP*, 01:069, 2016.

[77] K. Falls. Renormalization of Newton's constant. *Phys. Rev. D*, 92(12):124057, 2015.

[78] N. Christiansen, B. Knorr, J. Meibohm, J.M. Pawlowski, and M. Reichert. Local Quantum Gravity. *Phys. Rev.*, D92(12):121501, 2015.

[79] Maximilian Demmel, Frank Saueressig, and Omar Zanusso. A proper fixed functional for four-dimensional Quantum Einstein Gravity. *JHEP*, 08:113, 2015.

[80] N. Ohta, R. Percacci, and G.P. Vacca. Flow equation for $f(R)$ gravity and some of its exact solutions. *Phys. Rev. D*, 92(6):061501, 2015.

[81] N. Ohta, R. Percacci, and G.P. Vacca. Renormalization Group Equation and scaling solutions for $f(R)$ gravity in exponential parametrization. *Eur. Phys. J. C*, 76(2):46, 2016.

[82] B. Knorr. Infinite order quantum-gravitational correlations. *Class. Quant. Grav.*, 35(11):115005, 2018.

[83] N. Christiansen, K. Falls, J.M. Pawlowski, and M. Reichert. Curvature dependence of quantum gravity. *Phys. Rev.*, D97(4):046007, 2018.

[84] H. Gies, B. Knorr, and S. Lippoldt. Generalized Parametrization Dependence in Quantum Gravity. *Phys. Rev.*, D92(8):084020, 2015.

[85] H. Gies, B. Knorr, S. Lippoldt, and F. Saueressig. Gravitational Two-Loop Counterterm Is Asymptotically Safe. *Phys. Rev. Lett.*, 116(21):211302, 2016.

[86] J. Biemans, A. Platania, and F. Saueressig. Quantum gravity on foliated spacetimes: Asymptotically safe and sound. *Phys. Rev.*, D95(8):086013, 2017.

[87] T. Denz, J.M. Pawlowski, and M. Reichert. Towards apparent convergence in asymptotically safe quantum gravity. *Eur. Phys. J.*, C78(4):336, 2018.

[88] K. Falls and N. Ohta. Renormalization Group Equation for $f(R)$ gravity on hyperbolic spaces. *Phys. Rev. D*, 94(8):084005, 2016.

[89] K. Falls, C.R. King, D.F. Litim, K. Nikolakopoulos, and C. Rahmede. Asymptotic safety of quantum gravity beyond Ricci scalars. *Phys. Rev.*, D97(8):086006, 2018.

[90] K.G. Falls, D.F. Litim, and J. Schroder. Aspects of asymptotic safety for quantum gravity. *Phys. Rev. D*, 99(12):126015, 2019.

[91] G.P. de Brito, N. Ohta, A.D. Pereira, A.A. Tomaz, and M. Yamada. Asymptotic safety and field parametrization dependence in the $f(R)$ truncation. *Phys. Rev. D*, 98(2):026027, 2018.

[92] B. Knorr, C. Ripken, and F. Saueressig. Form Factors in Asymptotic Safety: conceptual ideas and computational toolbox. *Class. Quant. Grav.*, 36(23):234001, 2019.

[93] B. Burger, J.M. Pawlowski, M. Reichert, and B.-J. Schaefer. Curvature dependence of quantum gravity with scalars. 12 2019.

[94] K. Falls, N. Ohta, and R. Percacci. Towards the determination of the dimension of the critical surface in asymptotically safe gravity. 4 2020.

[95] A. Eichhorn. An asymptotically safe guide to quantum gravity and matter. *Front. Astron. Space Sci.*, 5:47, 2019.

[96] A. Eichhorn and A. Held. Towards implications of asymptotically safe gravity for particle physics. In *An Alpine LHC Physics Summit 2019*, 7 2019.

[97] M. Shaposhnikov and C. Wetterich. Asymptotic safety of gravity and the Higgs boson mass. *Phys. Lett. B*, 683:196–200, 2010.

[98] G. Aad et al. Observation of a new particle in the search for the Standard Model Higgs boson with the ATLAS detector at the LHC. *Phys. Lett. B*, 716:1–29, 2012.

[99] S. Chatrchyan et al. Observation of a New Boson at a Mass of 125 GeV with the CMS Experiment at the LHC. *Phys. Lett. B*, 716:30–61, 2012.

[100] N. Christiansen and A. Eichhorn. An asymptotically safe solution to the U(1) triviality problem. *Phys. Lett. B*, 770:154–160, 2017.

[101] A. Eichhorn and F. Versteegen. Upper bound on the Abelian gauge coupling from asymptotic safety. *JHEP*, 01:030, 2018.

[102] J.L. Anderson and D. Finkelstein. Cosmological constant and fundamental length. *Am. J. Phys.*, 39:901–904, 1971.

[103] J.J. van der Bij, H. van Dam, and Y.J. Ng. The Exchange of Massless Spin Two Particles. *Physica A*, 116:307–320, 1982.

[104] W. Buchmuller and N. Dragon. Gauge Fixing and the Cosmological Constant. *Phys. Lett. B*, 223:313–317, 1989.

[105] W. Buchmuller and N. Dragon. Einstein Gravity From Restricted Coordinate Invariance. *Phys. Lett. B*, 207:292–294, 1988.

[106] W.G. Unruh. A Unimodular Theory of Canonical Quantum Gravity. *Phys. Rev. D*, 40:1048, 1989.

[107] M. Henneaux and C. Teitelboim. The Cosmological Constant and General Covariance. *Phys. Lett. B*, 222:195–199, 1989.

[108] G.F.R. Ellis, H. van Elst, J. Murugan, and J.-P. Uzan. On the Trace-Free Einstein Equations as a Viable Alternative to General Relativity. *Class. Quant. Grav.*, 28:225007, 2011.

[109] S. Weinberg. The Cosmological Constant Problem. *Rev. Mod. Phys.*, 61:1–23, 1989.

[110] A. Einstein. The Foundation of the General Theory of Relativity. *Annalen Phys.*, 49(7):769–822, 1916.

[111] F. Wilczek. Foundations and Working Pictures in Microphysical Cosmology. *Phys. Rept.*, 104:143, 1984.

[112] A. Zee. REMARKS ON THE COSMOLOGICAL CONSTANT PROBLEM. *Stud. Nat. Sci.*, 20:211–230, 1985.

[113] E. Alvarez. Can one tell Einstein's unimodular theory from Einstein's general relativity? *JHEP*, 03:002, 2005.

[114] E. Alvarez and A.F. Faedo. Unimodular cosmology and the weight of energy. *Phys. Rev. D*, 76:064013, 2007.

[115] R. Percacci. Unimodular quantum gravity and the cosmological constant. *Found. Phys.*, 48(10):1364–1379, 2018.

[116] A. Padilla and I.D. Saltas. A note on classical and quantum unimodular gravity. *Eur. Phys. J. C*, 75(11):561, 2015.

[117] A. Padilla. Lectures on the Cosmological Constant Problem. 2 2015.

[118] L. Smolin. The Quantization of unimodular gravity and the cosmological constant problems. *Phys. Rev. D*, 80:084003, 2009.

[119] L. Smolin. Unimodular loop quantum gravity and the problems of time. *Phys. Rev. D*, 84:044047, 2011.

[120] E. Álvarez, S. González-Martín, M. Herrero-Valea, and C.P. Martín. Quantum Corrections to Unimodular Gravity. *JHEP*, 08:078, 2015.

[121] E. Alvarez, S. Gonzalez-Martin, and C.P. Martin. Unimodular Trees versus Einstein Trees. *Eur. Phys. J. C*, 76(10):554, 2016.

[122] R. de León Ardón, N. Ohta, and R. Percacci. Path integral of unimodular gravity. *Phys. Rev. D*, 97(2):026007, 2018.

[123] R. Bufalo, M. Oksanen, and A. Tureanu. How unimodular gravity theories differ from general relativity at quantum level. *Eur. Phys. J. C*, 75(10):477, 2015.

[124] S. Upadhyay, M. Oksanen, and R. Bufalo. BRST Quantization of Unimodular Gravity. *Braz. J. Phys.*, 47(3):350–365, 2017.

[125] A. Eichhorn. On unimodular quantum gravity. *Class. Quant. Grav.*, 30:115016, 2013.

[126] A. Eichhorn. The Renormalization Group flow of unimodular $f(R)$ gravity. *JHEP*, 04:096, 2015.

[127] M. Herrero-Valea and R. Santos-Garcia. Non-minimal Tinges of Unimodular Gravity. 6 2020.

[128] D. Benedetti. Essential nature of Newton's constant in unimodular gravity. *Gen. Rel. Grav.*, 48(5):68, 2016.

[129] I.D. Saltas. UV structure of quantum unimodular gravity. *Phys. Rev. D*, 90(12):124052, 2014.

[130] R. Penrose. Gravitational collapse and space-time singularities. *Phys. Rev. Lett.*, 14:57–59, 1965.

[131] A. Tilloy. Does gravity have to be quantized? Lessons from non-relativistic toy models. *J. Phys. Conf. Ser.*, 1275(1):012006, 2019.

[132] M. Srednicki. *Quantum field theory.* Cambridge University Press, 1 edition, 2007.

[133] M.D. Schwartz. *Quantum Field Theory and the Standard Model.* Quantum Field Theory and the Standard Model. Cambridge University Press, illustrated edition, 2013.

[134] J. Beringer et al. Review of particle physics. *Phys. Rev. D*, 86:010001, Jul 2012.

[135] P.J. Mohr, B.N. Taylor, and D.B. Newell. Codata recommended values of the fundamental physical constants: 2010. *Rev. Mod. Phys.*, 84:1527–1605, Nov 2012.

[136] A. Deur, S.J. Brodsky, and G.F. de Teramond. The QCD Running Coupling. *Prog. Part. Nucl. Phys.*, 90:1–74, 2016.

[137] M. Gell-Mann and F.E. Low. Quantum electrodynamics at small distances. *Phys. Rev.*, 95:1300–1312, 1954.

[138] M. Gockeler, R. Horsley, V. Linke, P.E.L. Rakow, G. Schierholz, and H. Stuben. Is there a Landau pole problem in QED? *Phys. Rev. Lett.*, 80:4119–4122, 1998.

[139] M. Gockeler, R. Horsley, V. Linke, Paul E.L. Rakow, G. Schierholz, and H. Stuben. Resolution of the Landau pole problem in QED. *Nucl. Phys. B Proc. Suppl.*, 63:694–696, 1998.

[140] Holger Gies and Joerg Jaeckel. Renormalization flow of QED. *Phys. Rev. Lett.*, 93:110405, 2004.

[141] S. Kim, J.B. Kogut, and M.-P. Lombardo. On the triviality of textbook quantum electrodynamics. *Phys. Lett. B*, 502:345–349, 2001.

[142] L. Maiani, G. Parisi, and R. Petronzio. Bounds on the Number and Masses of Quarks and Leptons. *Nucl. Phys.*, B136:115–124, 1978.

[143] N. Cabibbo, L. Maiani, G. Parisi, and R. Petronzio. Bounds on the Fermions and Higgs Boson Masses in Grand Unified Theories. *Nucl. Phys.*, B158:295–305, 1979.

[144] R.F. Dashen and H. Neuberger. How to Get an Upper Bound on the Higgs Mass. *Phys. Rev. Lett.*, 50:1897, 1983.

[145] D.J.E. Callaway. Nontriviality of Gauge Theories With Elementary Scalars and Upper Bounds on Higgs Masses. *Nucl. Phys.*, B233:189–203, 1984.

[146] M. A. B. Beg, C. Panagiotakopoulos, and A. Sirlin. Mass of the Higgs Boson in the Canonical Realization of the Weinberg-Salam Theory. *Phys. Rev. Lett.*, 52:883, 1984.

[147] M. Lindner. Implications of Triviality for the Standard Model. *Z. Phys.*, C31:295, 1986.

[148] J. Kuti, L. Lin, and Y. Shen. Upper Bound on the Higgs Mass in the Standard Model. *Phys. Rev. Lett.*, 61:678, 1988.

[149] T. Hambye and K. Riesselmann. Matching conditions and Higgs mass upper bounds revisited. *Phys. Rev.*, D55:7255–7262, 1997.

[150] B. Freedman, P. Smolensky, and D. Weingarten. Monte Carlo Evaluation of the Continuum Limit of (phi**4) in Four-Dimensions and (phi**4) in Three-Dimensions. *Phys. Lett.*, 113B:481–486, 1982.

[151] M. Aizenman. Proof of the Triviality of phi**4 in D-Dimensions Field Theory and Some Mean Field Features of Ising Models for D>4. *Phys. Rev. Lett.*, 47:1–4, 1981.

[152] J. Frohlich. On the Triviality of Lambda (phi**4) in D-Dimensions Theories and the Approach to the Critical Point in D >= Four-Dimensions. *Nucl. Phys.*, B200:281–296, 1982.

[153] R.P. Feynman, F.B. Morinigo, W.G. Wagner, and D. Pines. *Feynman lectures on gravitation*. Frontiers in Physics. Addison-Wesley, 1st edition, 1995.

[154] I.L. Buchbinder, S. Odintsov, and I. L. Shapiro. *Effective Action in Quantum Gravity*. CRC Press, first edition, 1992.

[155] E. Alvarez, D. Blas, J. Garriga, and E. Verdaguer. Transverse Fierz-Pauli symmetry. *Nucl. Phys. B*, 756:148–170, 2006.

[156] M. Herrero-Valea. What do gravitons say about (unimodular) gravity? *JHEP*, 12:106, 2018.

[157] D. Blas. Gauge Symmetry and Consistent Spin-Two Theories. *J. Phys. A*, 40:6965–6972, 2007.

[158] S. Weinberg. Photons and gravitons in perturbation theory: Derivation of Maxwell's and Einstein's equations. *Phys. Rev.*, 138:B988–B1002, 1965.

[159] S. Deser. Selfinteraction and gauge invariance. *Gen. Rel. Grav.*, 1:9–18, 1970.

[160] J.F. Donoghue, M.M. Ivanov, and A. Shkerin. EPFL Lectures on General Relativity as a Quantum Field Theory. 2 2017.

[161] D.G. Boulware and S. Deser. Classical General Relativity Derived from Quantum Gravity. *Annals Phys.*, 89:193, 1975.

[162] A. Accioly, M. Dias, B. Giacchini, and W. Herdy. Interesting features of semi-classical gravitational deflection. *Class. Quant. Grav.*, 32(17):175020, 2015.

[163] K.G. Wilson. The Renormalization Group: Critical Phenomena and the Kondo Problem. *Rev. Mod. Phys.*, 47:773, 1975.

[164] M.E. Peskin and D.V. Schroeder. *An introduction to quantum field theory.* Frontiers in Physics. Addison-Wesley Pub. Co, 1995.

[165] S. Weinberg. *Quantum theory of fields. Foundations*, volume Volume 1. Cambridge University Press, 1 edition, 1995.

[166] S. Weinberg. *Quantum theory of fields. Modern applications*, volume Volume 2. Cambridge University Press, 1 edition, 1996.

[167] J. Polchinski. Renormalization and Effective Lagrangians. *Nucl. Phys. B*, 231:269–295, 1984.

[168] C. Bagnuls and C. Bervillier. Exact renormalization group equations. An Introductory review. *Phys. Rept.*, 348:91, 2001.

[169] O.J. Rosten. Fundamentals of the Exact Renormalization Group. *Phys. Rept.*, 511:177–272, 2012.

[170] P. Kopietz, L. Bartosch, and F. Schutz. *Introduction to the Functional Renormalization Group.* Lecture Notes in Physics 798. Springer-Verlag Berlin Heidelberg, 1 edition, 2010.

[171] D. Delamotte. An Introduction to the nonperturbative renormalization group. *Lect. Notes Phys.*, 852:49–132, 2012.

[172] U. Ellwanger. FLow equations for N point functions and bound states. pages 206–211, 9 1993.

[173] T.R. Morris. The Exact renormalization group and approximate solutions. *Int. J. Mod. Phys. A*, 9:2411–2450, 1994.

[174] J.M. Pawlowski. Aspects of the functional renormalisation group. *Annals Phys.*, 322:2831–2915, 2007.

[175] J. Berges, J. Tetradis, and C. Wetterich. Nonperturbative renormalization flow in quantum field theory and statistical physics. *Phys. Rept.*, 363:223–386, 2002.

[176] H. Gies. Introduction to the functional RG and applications to gauge theories. *Lect. Notes Phys.*, 852:287–348, 2012.

[177] Stefan Floerchinger. Analytic Continuation of Functional Renormalization Group Equations. *JHEP*, 05:021, 2012.

[178] S. Bornholdt and C. Wetterich. Average action for models with fermions. *Z. Phys. C*, 58:585–594, 1993.

[179] M. Reuter and C. Wetterich. Average action for the Higgs model with Abelian gauge symmetry. *Nucl. Phys. B*, 391:147–175, 1993.

[180] M. Reuter and C. Wetterich. Effective average action for gauge theories and exact evolution equations. *Nucl. Phys. B*, 417:181–214, 1994.

[181] Daniel F. Litim. Optimization of the exact renormalization group. *Phys. Lett. B*, 486:92–99, 2000.

[182] D.F. Litim. Optimized renormalization group flows. *Phys. Rev. D*, 64:105007, 2001.

[183] C. Wetterich. Average Action and the Renormalization Group Equations. *Nucl. Phys. B*, 352:529–584, 1991.

[184] A. Codello. *A novel functional renormalization group framework for gauge theories and gravity*. PhD thesis, Mainz U., Inst. Phys., 2010.

[185] Astrid Eichhorn, David MesterhÃ¡zy, and Michael M. Scherer. Multicritical behavior in models with two competing order parameters. *Phys. Rev. E*, 88:042141, 2013.

[186] I. Balog, Hugues Chaté, B. Delamotte, M. Marohnic, and N. Wschebor. Convergence of Nonperturbative Approximations to the Renormalization Group. *Phys. Rev. Lett.*, 123(24):240604, 2019.

[187] G. De Polsi, I. Balog, M. Tissier, and N. Wschebor. Precision calculation of critical exponents in the $O(N)$ universality classes with the nonperturbative renormalization group. *Phys. Rev. E*, 101(4):042113, 2020.

[188] M. Reichert. Lecture notes: Functional Renormalisation Group and Asymptotically Safe Quantum Gravity. *PoS*, 384:005, 2020.

[189] A. Eichhorn. Asymptotically safe gravity. In *57th International School of Subnuclear Physics: In Search for the Unexpected*, 2 2020.

[190] J.M. Pawlowski and M. Reichert. Quantum gravity: a fluctuating point of view. 7 2020.

[191] D. Dou and R. Percacci. The running gravitational couplings. *Class. Quant. Grav.*, 15:3449–3468, 1998.

[192] R. Percacci and D. Perini. Constraints on matter from asymptotic safety. *Phys. Rev. D*, 67:081503, 2003.

[193] P. Dona, A. Eichhorn, and R. Percacci. Matter matters in asymptotically safe quantum gravity. *Phys. Rev. D*, 89(8):084035, 2014.

[194] P. Dona, A. Eichhorn, P. Labus, and R. Percacci. Asymptotic safety in an interacting system of gravity and scalar matter. *Phys. Rev. D*, 93(4):044049, 2016. [Erratum: Phys.Rev.D 93, 129904 (2016)].

[195] J. Meibohm, J.M. Pawlowski, and M. Reichert. Asymptotic safety of gravity-matter systems. *Phys. Rev. D*, 93(8):084035, 2016.

[196] N. Christiansen, D.F. Litim, J.M. Pawlowski, and M. Reichert. Asymptotic safety of gravity with matter. *Phys. Rev. D*, 97(10):106012, 2018.

[197] J. Biemans, A. Platania, and F. Saueressig. Renormalization group fixed points of foliated gravity-matter systems. *JHEP*, 05:093, 2017.

[198] N. Alkofer and F. Saueressig. Asymptotically safe $f(R)$-gravity coupled to matter I: the polynomial case. *Annals Phys.*, 396:173–201, 2018.

[199] N. Alkofer. Asymptotically safe $f(R)$-gravity coupled to matter II: Global solutions. *Phys. Lett. B*, 789:480–487, 2019.

[200] A. Eichhorn, P. Labus, J.M. Pawlowski, and M. Reichert. Effective universality in quantum gravity. *SciPost Phys.*, 5(4):031, 2018.

[201] A. Eichhorn, S. Lippoldt, J.M. Pawlowski, M. Reichert, and M. Schiffer. How perturbative is quantum gravity? *Phys. Lett. B*, 792:310–314, 2019.

[202] U. Harst and M. Reuter. QED coupled to QEG. *JHEP*, 05:119, 2011.

[203] Sarah Folkerts, Daniel F. Litim, and Jan M. Pawlowski. Asymptotic freedom of Yang-Mills theory with gravity. *Phys. Lett. B*, 709:234–241, 2012.

[204] A. Eichhorn and H. Gies. Light fermions in quantum gravity. *New J. Phys.*, 13:125012, 2011.

[205] A. Eichhorn. Quantum-gravity-induced matter self-interactions in the asymptotic-safety scenario. *Phys. Rev.*, D86:105021, 2012.

[206] J. Meibohm and J.M. Pawlowski. Chiral fermions in asymptotically safe quantum gravity. *Eur. Phys. J.*, C76(5):285, 2016.

[207] A. Eichhorn, A. Held, and J.M. Pawlowski. Quantum-gravity effects on a Higgs-Yukawa model. *Phys. Rev.*, D94(10):104027, 2016.

[208] K.-y. Oda and M. Yamada. Non-minimal coupling in Higgs-Yukawa model with asymptotically safe gravity. *Class. Quant. Grav.*, 33(12):125011, 2016.

[209] A. Eichhorn and A. Held. Viability of quantum-gravity induced ultraviolet completions for matter. *Phys. Rev.*, D96(8):086025, 2017.

[210] A. Eichhorn and A. Held. Top mass from asymptotic safety. *Phys. Lett. B*, 777:217–221, 2018.

[211] A. Eichhorn, A. Held, and C. Wetterich. Quantum-gravity predictions for the fine-structure constant. *Phys. Lett.*, B782:198–201, 2018.

[212] A. Eichhorn, S. Lippoldt, and V. Skrinjar. Nonminimal hints for asymptotic safety. *Phys. Rev.*, D97(2):026002, 2018.

[213] A. Eichhorn, Y. Hamada, J. Lumma, and M. Yamada. Quantum gravity fluctuations flatten the Planck-scale Higgs potential. *Phys. Rev.*, D97(8):086004, 2018.

[214] Y. Hamada and M. Yamada. Asymptotic safety of higher derivative quantum gravity non-minimally coupled with a matter system. *JHEP*, 08:070, 2017.

[215] A. Eichhorn and A. Held. Mass difference for charged quarks from asymptotically safe quantum gravity. *Phys. Rev. Lett.*, 121(15):151302, 2018.

[216] H. Gies and R. Martini. Curvature bound from gravitational catalysis. *Phys. Rev.*, D97(8):085017, 2018.

[217] A. Eichhorn, S. Lippoldt, and M. Schiffer. Zooming in on fermions and quantum gravity. *Phys. Rev.*, D99(8):086002, 2019.

[218] J.M. Pawlowski, M. Reichert, C. Wetterich, and M. Yamada. Higgs scalar potential in asymptotically safe quantum gravity. *Phys. Rev.*, D99(8):086010, 2019.

[219] A. Eichhorn and M. Schiffer. $d = 4$ as the critical dimensionality of asymptotically safe interactions. *Phys. Lett.*, B793:383–389, 2019.

[220] G.P. de Brito, Y. Hamada, A.D. Pereira, and M. Yamada. On the impact of Majorana masses in gravity-matter systems. 2019.

[221] A. Eichhorn, A. Held, and C. Wetterich. Predictive power of grand unification from quantum gravity. 9 2019.

[222] C. Wetterich and M. Yamada. Variable Planck mass from gauge invariant flow equation. 2019.

[223] G.P. De Brito, A. Eichhorn, and A.D. Pereira. A link that matters: Towards phenomenological tests of unimodular asymptotic safety. *JHEP*, 09:100, 2019.

[224] A. Eichhorn, A. Platania, and M. Schiffer. Lorentz invariance violations in the interplay of quantum gravity with matter. *Phys. Rev. D*, 102(2):026007, 2020.

[225] M. Reichert and J. Smirnov. Dark Matter meets Quantum Gravity. *Phys. Rev. D*, 101(6):063015, 2020.

[226] A. Eichhorn and M. Pauly. Safety in darkness: Higgs portal to simple Yukawa systems. 5 2020.

[227] J.F. Donoghue. A Critique of the Asymptotic Safety Program. *Front. in Phys.*, 8:56, 2020.

[228] A. Bonanno, A. Eichhorn, H. Gies, J.M. Pawlowski, R. Percacci, M. Reuter, F. Saueressig, and G.P. Vacca. Critical reflections on asymptotically safe gravity. 4 2020.

[229] D.F. Litim and J.M. Pawlowski. Wilsonian flows and background fields. *Phys. Lett. B*, 546:279–286, 2002.

[230] I.H. Bridle, J.A. Dietz, and T.R. Morris. The local potential approximation in the background field formalism. *JHEP*, 03:093, 2014.

[231] M. Safari. Splitting Ward identity. *Eur. Phys. J. C*, 76(4):201, 2016.

[232] E. Manrique and M. Reuter. Bimetric Truncations for Quantum Einstein Gravity and Asymptotic Safety. *Annals Phys.*, 325:785–815, 2010.

[233] D. Becker and M. Reuter. En route to Background Independence: Broken split-symmetry, and how to restore it with bi-metric average actions. *Annals Phys.*, 350:225–301, 2014.

[234] J.A. Dietz and T.R. Morris. Background independent exact renormalization group for conformally reduced gravity. *JHEP*, 04:118, 2015.

[235] P. Labus, T.R. Morris, and Z.H. Slade. Background independence in a background dependent renormalization group. *Phys. Rev. D*, 94(2):024007, 2016.

[236] R. Percacci and G.P. Vacca. The background scale Ward identity in quantum gravity. *Eur. Phys. J. C*, 77(1):52, 2017.

[237] C.M. Nieto, R. Percacci, and V. Skrinjar. Split Weyl transformations in quantum gravity. *Phys. Rev. D*, 96(10):106019, 2017.

[238] N. Ohta. Background Scale Independence in Quantum Gravity. *PTEP*, 2017(3):033E02, 2017.

[239] L. Bosma, B. Knorr, and F. Saueressig. Resolving Spacetime Singularities within Asymptotic Safety. *Phys. Rev. Lett.*, 123(10):101301, 2019.

[240] J. Ambjorn, A. Goerlich, J. Jurkiewicz, and R. Loll. Nonperturbative Quantum Gravity. *Phys. Rept.*, 519:127–210, 2012.

[241] J. Ambjorn, J. Gizbert-Studnicki, A. Goerlich, J. Jurkiewicz, and D. Nemeth. Towards an UV fixed point in CDT gravity. *JHEP*, 07:166, 2019.

[242] J. Laiho and D. Coumbe. Evidence for Asymptotic Safety from Lattice Quantum Gravity. *Phys. Rev. Lett.*, 107:161301, 2011.

[243] J. Laiho, S. Bassler, D. Coumbe, D. Du, and J.T. Neelakanta. Lattice Quantum Gravity and Asymptotic Safety. *Phys. Rev. D*, 96(6):064015, 2017.

[244] A. Eichhorn, T. Koslowski, and A.D. Pereira. Status of background-independent coarse-graining in tensor models for quantum gravity. *Universe*, 5(2):53, 2019.

[245] C. Rovelli. What Is Observable in Classical and Quantum Gravity? *Class. Quant. Grav.*, 8:297–316, 1991.

[246] H. Westman and S. Sonego. Coordinates, observables and symmetry in relativity. *Annals Phys.*, 324:1585–1611, 2009.

[247] R. Brunetti, K. Fredenhagen, and K. Rejzner. Quantum gravity from the point of view of locally covariant quantum field theory. *Commun. Math. Phys.*, 345(3):741–779, 2016.

[248] J.J. Lopez-Villarejo. TransverseDiff gravity is to scalar-tensor as unimodular gravity is to General Relativity. *JCAP*, 11:002, 2011.

[249] J.J. Lopez-Villarejo. A theorem of equivalence between TransverseDiff theories and scalar-tensor gravity. *J. Phys. Conf. Ser.*, 314:012046, 2011.

[250] S. Gielen, R. de Leon Ardon, and R. Percacci. Gravity with more or less gauging. *Class. Quant. Grav.*, 35(19):195009, 2018.

[251] T. Josset, A. Perez, and D. Sudarsky. Dark Energy from Violation of Energy Conservation. *Phys. Rev. Lett.*, 118(2):021102, 2017.

[252] J.A. Astorga-Moreno, J. Chagoya, J.C. Flores-Urbina, and M.A. Garcia-Aspeitia. Compact objects in unimodular gravity. *JCAP*, 09:005, 2019.

[253] C. Corral, N. Cruz, and E. Gonzalez. Diffusion in unimodular gravity: Analytical solutions, late-time acceleration, and cosmological constraints. *Phys. Rev. D*, 102(2):023508, 2020.

[254] A. Perez, D. Sudarsky, and E. Wilson-Ewing. Resolving the H_0 tension with diffusion. 1 2020.

[255] H. Kawai, Y. Kitazawa, and M. Ninomiya. Scaling exponents in quantum gravity near two-dimensions. *Nucl. Phys.*, B393:280–300, 1993.

[256] H. Kawai, Y. Kitazawa, and M. Ninomiya. Quantum gravity in (2+epsilon)-dimensions. *Prog. Theor. Phys. Suppl.*, 114:149–174, 1993.

[257] H. Kawai, Y. Kitazawa, and M. Ninomiya. Ultraviolet stable fixed point and scaling relations in (2+epsilon)-dimensional quantum gravity. *Nucl. Phys.*, B404:684–716, 1993.

[258] A. Nink. Field Parametrization Dependence in Asymptotically Safe Quantum Gravity. *Phys. Rev.*, D91(4):044030, 2015.

[259] R. Percacci and G.P. Vacca. Search of scaling solutions in scalar-tensor gravity. *Eur. Phys. J.*, C75(5):188, 2015.

[260] P. Labus, R. Percacci, and G.P. Vacca. Asymptotic safety in $O(N)$ scalar models coupled to gravity. *Phys. Lett.*, B753:274–281, 2016.

[261] N. Ohta, R. Percacci, and A.D. Pereira. Gauges and functional measures in quantum gravity I: Einstein theory. *JHEP*, 06:115, 2016.

[262] N. Ohta, R. Percacci, and A.D. Pereira. Gauges and functional measures in quantum gravity II: Higher derivative gravity. *Eur. Phys. J.*, C77(9):611, 2017.

[263] N. Ohta, R. Percacci, and A.D. Pereira. $f(R, R^2_{\mu\nu})$ at one loop. *Phys. Rev. D*, 97(10):104039, 2018.

[264] D. Benedetti, K. Groh, P.F. Machado, and F. Saueressig. The Universal RG Machine. *JHEP*, 06:079, 2011.

[265] J.W. York. Conformatlly invariant orthogonal decomposition of symmetric tensors on Riemannian manifolds and the initial value problem of general relativity. *J. Math. Phys.*, 14:456–464, 1973.

[266] I.G. Avramidi. *Heat Kernel and Quantum Gravity.* Lecture notes in physics m64. Springer, 1 edition, 2000.

[267] A.O. Barvinsky and G.A. Vilkovisky. The Generalized Schwinger-Dewitt Technique in Gauge Theories and Quantum Gravity. *Phys. Rept.*, 119:1–74, 1985.

[268] I.G. Avramidi. *Heat kernel and quantum gravity*, volume 64. Springer, New York, 2000.

[269] D.V. Vassilevich. Heat kernel expansion: User's manual. *Phys. Rept.*, 388:279–360, 2003.

[270] G.P. de Brito and A.D. Pereira. Unimodular quantum gravity: Steps beyond perturbation theory. 7 2020.

[271] B. Knorr and S. Lippoldt. Correlation functions on a curved background. *Phys. Rev. D*, 96(6):065020, 2017.

[272] R. Sondenheimer. *Renormalization group flow of the Higgs sector.* PhD thesis, Jena U., TPI, 2016.

[273] A.V. Bednyakov, B.A. Kniehl, A.F. Pikelner, and O.L. Veretin. Stability of the Electroweak Vacuum: Gauge Independence and Advanced Precision. *Phys. Rev. Lett.*, 115(20):201802, 2015.

[274] F. Bezrukov, M.Y. Kalmykov, B.A. Kniehl, and M. Shaposhnikov. Higgs Boson Mass and New Physics. *JHEP*, 10:140, 2012.

[275] G. Narain and R. Percacci. Renormalization Group Flow in Scalar-Tensor Theories. I. *Class. Quant. Grav.*, 27:075001, 2010.

[276] R. P. Woodard. The Vierbein Is Irrelevant in Perturbation Theory. *Phys. Lett.*, 148B:440–444, 1984.

[277] P. van Nieuwenhuizen. Classical Gauge Fixing in Quantum Field Theory. *Phys. Rev.*, D24:3315, 1981.

[278] Holger Gies and Stefan Lippoldt. Fermions in gravity with local spin-base invariance. *Phys. Rev.*, D89(6):064040, 2014.

[279] Holger Gies and Stefan Lippoldt. Global surpluses of spin-base invariant fermions. *Phys. Lett.*, B743:415–419, 2015.

[280] Stefan Lippoldt. Spin-base invariance of Fermions in arbitrary dimensions. *Phys. Rev.*, D91(10):104006, 2015.